# Development of a continuous process for the telomerization of butadiene with methanol

# Entwicklung eines kontinuierlichen Prozesses für die Telomerisation von Butadien mit Methanol

Der Technischen Fakultät der

Friedrich-Alexander-Universität Erlangen-Nürnberg

zur Erlangung des Grades

DOKTOR – INGENIEUR

vorgelegt von

**Dipl.-Ing. Lisa Hopf**

aus Schweinfurt

*Für Johannes und meine Eltern*

## Vorwort

**Conference contributions**

Parts of this work have been previously presented at the conferences listed.

- L. Hopf, J. Coetzee, D.J. Cole-Hamilton, M. Haumann, P. Wasserscheid: *Use of ionic liquids for catalyst immobilisation in the telomerisation reaction of butadiene with methanol,* EUCHEM, Tallinn, Estonia (2014), oral presentation.

- L. Hopf, J. Coetzee, D.J. Cole-Hamilton, M. Haumann, P. Wasserscheid: *From batch to conti: telomerisation of butadiene with methanol in biphasic reaction system with ILs,* Jahrestreffen Reaktionstechnik, Würzburg (2014), oral presentation.

- L. Hopf, A. Chartoire, S.P. Nolan, M. Haumann, P. Wasserscheid: *Unusual dependency of butadiene telomerisation with methanol on catalyst type and substrate composition,* 47. Jahrestreffen Deutscher Katalytiker, Weimar (2014), poster presentation.

- L. Hopf, R. Wölfel, P. Wasserscheid: *Von Batch zu Konti: Entwicklung eines flexiblen Reaktorkonzepts zur Charakterisierung einphasiger sowie mehrphasiger Reaktionen,* Jahrestreffen Reaktionstechnik, Würzburg (2013), poster presentation.

- L. Hopf, R. Wölfel, P. Wasserscheid: *Screening of ILs with COSMO-RS for the application in biphasic telomerisation reaction system,* Green Solvents for Synthesis, Boppard (2012), poster presentation.

# Table of contents

# List of symbols, indices and abbreviations

## *Latin symbols*

| | | |
|---|---|---|
| $A$ | peak area | - |
| $a$ | specific phase boundary area | $m^2 \cdot m^{-3}$ |
| $C$ | correction factor | - |
| $c$ | concentration | $mol \cdot m^{-3}$ |
| $E$ | exit age distribution | - |
| $F$ | residence time summation function | - |
| $f$ | function of | - |
| $G$ | Gibbs free energy | $J \cdot mol^{-1}$ |
| $K$ | distribution coefficient | - |
| $K$ | rate constant | |
| $k$ | mass transfer coefficient | $m \cdot s^{-1}$ |
| $L$ | length of the tubular reactor | m |
| $m$ | mass | kg |
| $n$ | molar amount | mol |
| $\dot{n}$ | molar flow | $mol \cdot h^{-1}$ |
| $p$ | pressure | bar |
| $r$ | reaction rate | $mol \cdot s^{-1}$ |
| $S$ | selectivity | - |
| $T$ | temperature | °C |
| $t$ | time | h |
| $\bar{t}$ | effective residence time | h |
| $u$ | flow velocity | $m \cdot h^{-1}$ |
| $\dot{V}$ | volume flow | $m^3 \cdot h^{-1}$ |

| | | |
|---|---|---|
| *V* | reaction volume | $m^3$ |
| *X* | conversion | - |
| *x* | molar fraction | - |
| *Y* | yield | - |

### Greek symbols

| | | |
|---|---|---|
| $\alpha$ | phase $\alpha$ | - |
| $\beta$ | phase $\beta$ | - |
| $\gamma$ | activity coefficient | - |
| $\Delta$ | difference | |
| $\mu$ | chemical potential | $J \cdot mol^{-1}$ |
| $\sigma$ | screening charge density | $e \cdot m^{-2}$ |
| $\tau$ | hydrodynamic residence time | h |
| $\theta$ | dimensionless time | - |
| $\vartheta$ | stoichiometric coefficient | - |

### Indices

| | |
|---|---|
| B | butadiene |
| *c* | chemo |
| circ | circulation |
| *i* | component *i* |
| *j* | component *j* |
| L | liquid |
| p | product |
| Pd_ionic liquid | amount of Pd in the ionic liquid phase |
| Pd_org | amount of Pd in the organic phase |

| Pd_tot | total amount of Pd |
|--------|--------------------|
| Pd,pre | Pd precursor |
| STD | internal standard |
| sol | solubility |
| 0 | at $t = 0$ |

### *Abbreviations*

| 1-Mode | 1-methoxy-2,7-octadiene |
|--------|--------------------------|
| 3-Mode | 3-methoxy-1,7-octadiene |
| AC | autoclave |
| acac | acetylacetonate |
| AES | atom emission spectroscopy |
| Ar | 2,4,5-tri-*iso*-propylphenyl |
| cin | cinnamyl |
| COSMO-RS | conductor like screening model for real solvents |
| CSTR | continuous stirred tank reactor |
| DBE | di-*n*-butylether |
| DFT | density functional theory |
| DPPP | bis(diphenylphosphine)propane |
| DPPM | bis(diphenylphosphine)methane |
| dvds | 1,1,3,3-tetramethyl-1,3-divinyl-disiloxane |
| dba | dibenzylideneactone |
| EU | European Union |
| FID | flame ionization detector |
| GC | gas chromatography |
| HPLC | high pressure liquid chromatography |

| | |
|---|---|
| ICP | inductively coupled plasma |
| IL | ionic liquid |
| IFP | Institute Francais du Pétrole |
| IMes | 1,3-dimesitylimidazol-2-ylidene |
| iPr | 1,3-bis(2,6-bis(diisopropylphenyl)-imidazol-2-ylidene) |
| iPr* | 1,3-bis(2,6-bis(diphenylmethyl)-4-methylphenyl)-imidazol-2-ylidene) |
| IR | infrared |
| KOMe | potassium methoxide |
| LAO | linear $\alpha$-olefin |
| LDH | layered double hydroxide |
| Lig | ligand |
| LiOMe | lithium methoxide |
| LLDPE | linear low density polyethylene |
| LR | loop reactor |
| Ma | macrocycle |
| MeOH | methanol |
| $MeSO_3$ | methanesulfonate |
| MIM | methylimidazole |
| monospanphos | 4,4,4',4',6,6'-hexamethyl-2,2'-spirobi[chroman]-8-yl-diphenylphosphine |
| monoxantphos | 2,7-di-tert-butyl-9,9-dimethylxanthene-4-yl-diphenylphosphine |
| MS | mass spectrometry |
| MSC | multiplicative scatter correction |
| NaOH | sodium hydroxide |
| NaOMe | sodium methoxide |
| $HNEt_2$ | diethylamine |

| | |
|---|---|
| NEt$_3$ | triethylamine |
| NHC | N-heterocyclic carbene |
| NIR | near infrared |
| NMR | nuclear magnetic resonance |
| OAc | acetate |
| OTEN | octatriene |
| PCA | principal component analysis |
| PCR | principal component regression |
| PFTR | plug flow tubular reactor |
| PLS | partial least-squares |
| rpm | revolutions per minute |
| RWTH | Rheinisch-Westfälische Technische Hochschule |
| sCC$_4$ | synthetic crack-C$_4$ |
| SHOP | Shell Higher Olefin Process |
| STY | space time yield |
| TOF | turn over frequency |
| TON | turn over number |
| TOS | time on stream |
| TPP | triphenylphosphine |
| TPPDS | triphenylphosphine disulfonate |
| TPPMS | triphenylphosphine monosulfonate |
| TPPTS | triphenylphosphine trisulfonate |
| VCHEN | vinylcyclohexene |

## Abbreviations of ionic liquids

| | |
|---|---|
| [BETI]<sup>-</sup> | bis[(pentafluoroethyl)sulfonyl]imide |
| [BMIM][BF$_4$] | 1-butyl-3-methylimidazolium tetrafluoroborate |
| [BMMIM][BF$_4$] | 1-butyl-2,3-dimethylimidazolium tetrafluoroborate |
| [BMMIM]Cl | 1-butyl-2,3-dimethylimidazolium chloride |
| [BMMIM][NTf$_2$] | 1-butyl-2,3-dimethylimidazolium bis(trifluoromethylsulfonyl)imide |
| [BMMIM][OcSO$_4$] | 1-butyl-2,3-dimethylimidazolium octylsulfate |
| [BMMIM][TOS] | 1-butyl-2,3-dimethylimidazolium *p*-toluolsulfonate |
| [BuPy][PF$_6$] | 1-butylpyridinium hexafluorophosphate |
| [EMMIM][BF$_4$] | 1-ethyl-2,3-dimethylimidazolium tetrafluoroborate |
| [EMMIM]Cl | 1-butyl-2,3-dimethylimidazolium chloride |
| [EMMIM][MeSO$_4$] | 1-butyl-2,3-dimethylimidazolium methylsulfate |
| [EMIM][NTf$_2$] | 1-ethyl-3-methylimidazolium bis(trifluoromethylsulfonyl)imide |
| [EMMIM][NTf$_2$] | 1-ethyl-2,3-dimethylimidazolium bis(trifluoromethylsulfonyl)imide |
| [EMMIM][TOS] | 1-ethyl-2,3-dimethylimidazolium *p*-toluolsulfonate |
| [FAP]<sup>-</sup> | tris(pentafluoroethyl)trifluorophosphate |

# 1 Introduction

Catalysis saves raw materials and energy, prevents waste production and is consequently considered as the key technology for sustainable production of chemicals [1]. Around 90 % of all chemical processes are supposed to be catalyzed by at least one catalyst [1]. Catalysts are defined to accelerate chemical reactions without being consumed during reaction. In industry, catalysts are mainly applied as either homogeneous or heterogeneous catalysts whereas the latter comprises around 80 % of all processes. Around 15 % are catalyzed by homogeneous catalysts. The remaining 5 % can be related to biocatalysis [1].

The reason for this superiority of heterogeneous catalysis is the better processing due to easy catalyst separation and recycling which is an important factor for industrial applications. In contrast, homogeneous catalysis which takes place in the bulk of a solvent suffers often from catalyst separation problems. The catalyst recycling is very elaborate and complex and consequently time as well as cost-intensive. Nevertheless, homogeneous catalysis exhibits several advantages especially with respect to activity and, even more important, selectivity. Furthermore, homogeneous catalysts work at rather mild conditions ($T < 200$ °C).

In the recent two decades, research focused on combining the advantages of homogeneous and heterogeneous catalysis [2]. Mainly two approaches became apparent, namely the heterogenization of a catalyst by immobilization on a support and liquid-liquid biphasic catalysis in which only one phase contains the catalyst and the product phase can be easily separated by decantation. For the latter approach, different liquid-liquid combinations such as organic/organic or organic/aqueous are possible [3]. Also combinations with fluorous [4-7], supercritical solvents [8-10] or ionic liquids [11-14] are known. Industrial examples applying the biphasic reaction concept are the oligomerization of ethylene in the Shell Higher Olefin Process (SHOP) [3; 15], the hydroformylation of alkenes in the Ruhrchemie/Rhône-Poulenc Process [16-20] or the Difasol Process for the dimerization of short chain alkenes into branched, longer chain alkenes [11; 12].

Despite the successful application of heterogenized catalysts or biphasic reaction systems, still a lot of the homogeneously catalyzed industrial processes are carried out batch-wise or with the disposal of the catalyst after each catalytic run. One

example is the Dow Chemical Process for producing 1-octene via the telomerization of butadiene with methanol [21-23]. In general, the telomerization describes a dimerization of 1,3-dienes, e.g. 1,3-butadiene, with simultaneous addition of a nucleophile, e.g. methanol. The main products of the telomerization of butadiene with methanol are a linear as well as a branched form of methoxyoctadienes, namely 1-methoxy-2,7-octadiene (1-Mode) and 3-methoxy-1,7-octadiene (3-Mode). In the Dow Chemical Process, the palladium catalyzed telomerization reaction is followed by complete hydrogenation to the corresponding methoxyoctanes. In the last step of the reaction cascade, methanol is split off thermally forming the desired 1-octene. However, the telomerization step in this process is operated without direct catalyst recycling. The palladium is destroyed and regenerated after reaction. This is a limitation of the technical process not only due to the high price of palladium but also because of the product contamination and a more complicated downstream processing required for the recovery of palladium.

Besides the well-known triphenylphosphine (TPP) ligand, the telomerization of butadiene with methanol can also be catalyzed in combination with more steric phosphine ligands [24-26] or N-heterocyclic carbene (NHC)-ligands [27-29].

For the telomerization of butadiene with methanol, a few attempts for the recycling of the Pd catalyst can be found in the literature [30-40]. Two very interesting approaches were studied by Dehn [30] and by Magna *et al.* [33]. While Dehn focused on a three-phase approach with water as catalyst phase and gaseous butadiene in a continuously running loop reactor, Magna *et al.* studied the ability of ionic liquids as catalyst phase. They succeeded to recycle the catalyst phase for 4 times without an obvious drop in the activity of the system. However, they did not follow up their studies by implementing this attempt in a continuous process.

The aim of this thesis is to develop a continuous process for the telomerization of butadiene with methanol based on a biphasic reaction system with ionic liquids. The work is part of the SYNFLOW project. The latter is a large-scale collaborative research project within the 7th European Framework Programme for Research and Technological Development. The goal of SYNFLOW is to transfer batch-wise processes to continuous flow processing. This should be achieved by combining molecular understanding of synthesis and catalysis with engineering science in process design and plant concepts. One of in sum six case studies within SYNFLOW

deals with the telomerization of butadiene with methanol which is the topic of this thesis.

Based on preliminary batch experiments without ionic liquids, dependencies on process parameters and differences between phosphine based ligands and NHC-ligands should be figured out.

For the development of the continuous process based on a liquid-liquid biphasic reaction system with ionic liquids, ionic liquid as well as ligand screenings were intended to be carried out in a batch autoclave. Attention should be focused on the influence of anion and cation of the ionic liquid on the activity as well as stability of the catalyst. The latter should be tested by recycling experiments. With the knowledge from the preliminary batch experiments, the transfer to the continuous process was intended. The target was to meet the criteria of longterm stability, high selectivity and high activity by a stepwise optimization of the continuous process.

Besides the development of a continuous process for the telomerization of butadiene with methanol, the feasibility of inline process control by NIR spectroscopy for a homogeneously catalyzed reaction should be exemplarily shown. In addition, the ability of NIR spectroscopy in ionic liquid mixtures should be tested.

# 2   General part

## 2.1   Introduction to the telomerization reaction

In general, telomerization represents a dimerization reaction of 1,3-dienes (taxogen) with simultaneous addition of a nucleophile (telogen) [23; 41-43]. The products of this reaction are called telomers. This reaction type was independently discovered by Takahashi *et al.* [44] and Smutny *et al.* [45] in the year 1967 and is schematically shown for 1,3-butadiene in Scheme 1. An excellent review concerning advances and applications of the telomerization reaction was published in 2009 by Behr *et al.* [23].
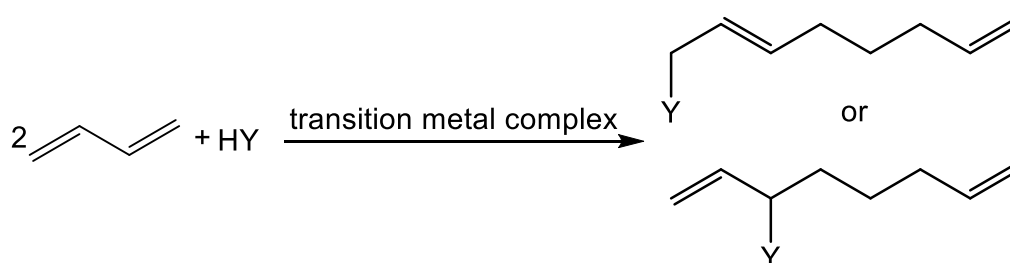


**Scheme 1: General reaction scheme of the telomerization of 1,3-butadiene with a nucleophile HY according to [23; 44; 45].**

The telomerization is catalyzed by transition metal complexes containing for example nickel, palladium or platinum whereas palladium is the most frequently used one [23; 42]. The variety of possible taxogens and telogens results in a wide product spectrum [23; 43]. Since 1967, different research groups reported successful telomerization of 1,3-dienes with e.g. alcohols [44-49], water [34; 50-54], $CO_2$ [55-57], acids [44; 58-60], amines [61-65] and carbohydrate derivatives [66-69]. The resulting products can be used in different application fields, e.g., as surfactants or emulsifiers, fragrances or intermediates for pharmaceuticals, as well as intermediates in the production of plasticizers or copolymers [23; 43]. The latter is realized by the telomerization of 1,3-butadiene with water and methanol leading to 1-octanol and 1-octene, two industrially implemented processes.

## 2.1.1 Industrial application of the telomerization reaction

Despite the wide range of possible products, only two telomerization reactions are performed on industrial scale. The Kuraray Process is based on the telomerization of butadiene with water, also called hydrodimerization, forming 1-octanol. The process was implemented on industrial scale (5,000 t/a) by Kuraray in 1991 [23; 70]

The second industrial application is the telomerization of butadiene with methanol producing 1-octene by Dow Chemical [21-23]. The industrial intermediate 1-octene is mainly used as comonomer for the production of linear low density polyethylene (LLDPE) [71-73] and its total world demand amounted to $5.8 \cdot 10^5$ t/a in 2006 [74].

One highly selective process for the production of 1-octene is the synthesis route via the telomerization of butadiene with methanol which was implemented on industrial scale in Tarragona, Spain, by Dow Chemical in 2008 [21-23]. This process is based on a patented reaction cascade to form 1-octene starting with butadiene and methanol. The reaction cascade is shown in Scheme 2.
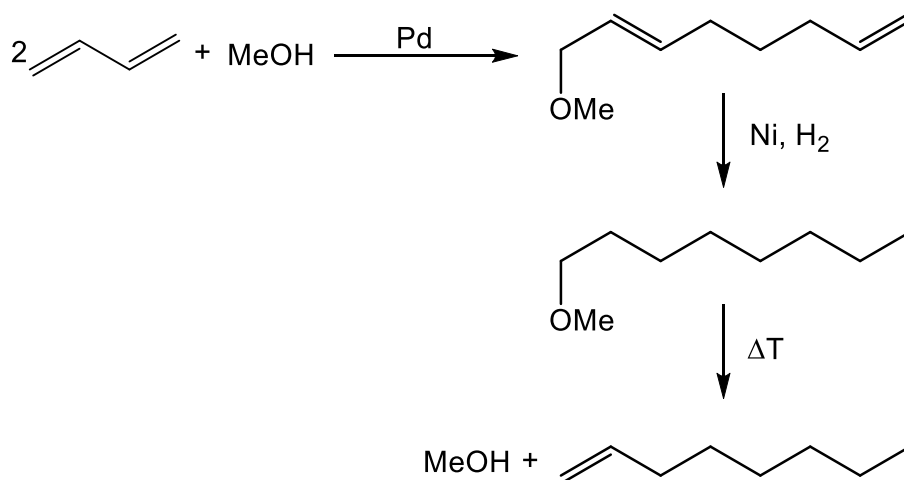


**Scheme 2: Reaction cascade to form 1-octene via telomerization of butadiene with methanol according to [21; 23].**

The catalyst system for the telomerization step consists of Pd and a phosphine based ligand [21-23; 25; 75]. The reaction cascade toward 1-octene starts with the highly selective telomerization of butadiene with methanol forming mainly the *n*-telomer, namely 1-methoxy-2,7-octadiene (1-Mode). The next step is the hydrogenation of the telomers toward the corresponding methoxyoctanes. In the final step, methanol is split off thermally from the methoxyoctanes forming the desired 1-

octene and methanol which is then recycled. The process flow scheme is depicted in Scheme 3 according to Behr [76].
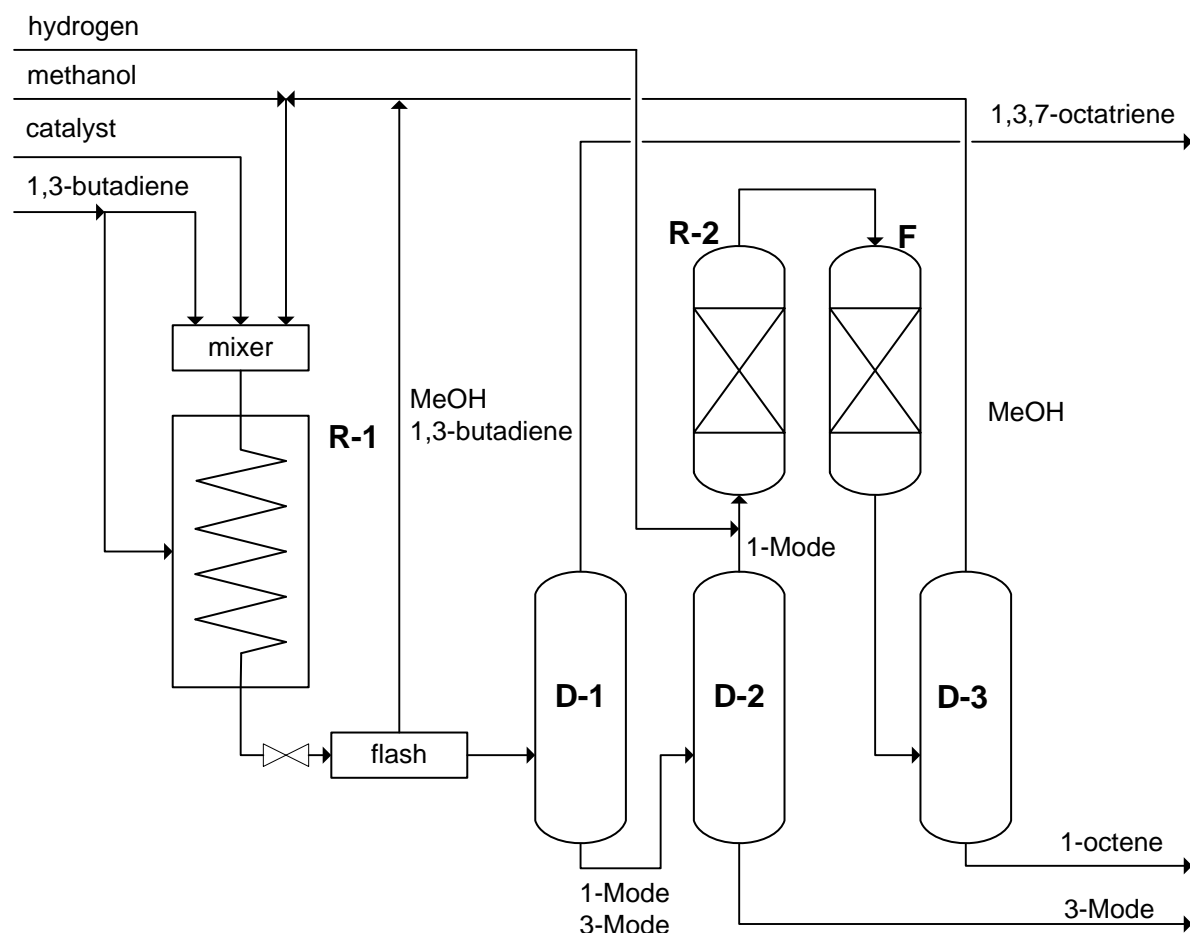


**Scheme 3: Process scheme of the Dow Chemical Process to produce 1-octene [76].**

After passing a mixer, the reactants enter the tubular reactor **R-1** at 90 °C with a catalyst concentration of 0.0025 mol% using crude $C_4$ as butadiene source. After the telomerization reaction step, the pressure is released and the low boiling reactants butadiene and methanol are separated in a flash and recycled into the tubular reactor. The product mixture and the dissolved homogeneous catalyst pass two distillation steps (**D-1** and **D-2**) during which the catalyst is destroyed and the desired intermediate product 1-Mode is isolated. The latter passes a heterogeneous Ni-catalyzed hydrogenation step in reactor **R-2** followed by thermal splitting in furnace **F** into methanol and 1-octene. In the last step, methanol is distilled off (**D-3**)

and recycled into the tubular reactor. The desired product 1-octene is received with a purity of up to 99 %.

Despite the low catalyst concentration, the recycling of the transition metal palladium would improve the cost-effectiveness of this industrial process. The lack of the recycling process for the applied homogeneous palladium catalyst encouraged a few research groups to study and develop a possibility for catalyst recycling [30-32; 34-40] and is also the aim of this thesis. The state of the art of this research area is discussed in detail in Chapter 2.1.2.5 and 2.2.2.

Other important industrial routes for the production of 1-octene are the Fischer-Tropsch synthesis and the oligomerization/tetramerization of ethylene.

The Fischer-Tropsch synthesis is a heterogeneously catalyzed conversion of synthesis gas into liquid hydrocarbons [1]. The Fischer-Tropsch synthesis suffers from a mathematical product distribution (Schulz-Flory) resulting in unselective production of linear $\alpha$-olefins (LAOs) with different chain lengths. Besides the purification of the achieved product mixture, another main disadvantage of so called "full range producer" is that only the desired products find further application, the remaining undesired products are often waste products.

The Shell Higher Olefin Process (SHOP) is an example for LAO production via the oligomerization of ethylene [1]. The latter also suffers from a wide product distribution according to Schulz-Flory and the resulting difficult and cost-intensive purification process.

The $\alpha$-SABLIN Process is also based on the oligomerization/tetramerization of ethylene and was commercialized in 2009 by Linde and SABIC [71; 77]. A product distribution containing around 80 % 1-butene, 1-hexene and 1-octene resulting in a necessary product purification unit is produced.

In the recent decade, a lot of effort was spent in the development of highly selective on-purpose 1-octene production [78]. Sasol introduced two new routes based on the tetramerization of ethylene [78-86] and hydroformylation of 1-heptene [78; 87]. In order to produce 1-octene from 1-heptene, a reaction cascade of three reactions has to be passed: first, the hydroformylation of 1-heptene to octanal followed by the hydrogenation of octanal to 1-octanol and the dehydration of 1-octanol to 1-octene. This process was commercialized in 2007 whereas the commercialization of the tetramerization process was planned for 2013 [1; 24; 74; 78].

### 2.1.2 Telomerization of butadiene with methanol

The telomerization of 1,3-butadiene with methanol was first reported by Takahashi *et al.* [44]. They discovered this reaction type while they were working on investigations regarding the dimerization of 1,3-butadiene. The reaction with the resulting products and byproducts is depicted in Scheme 4.
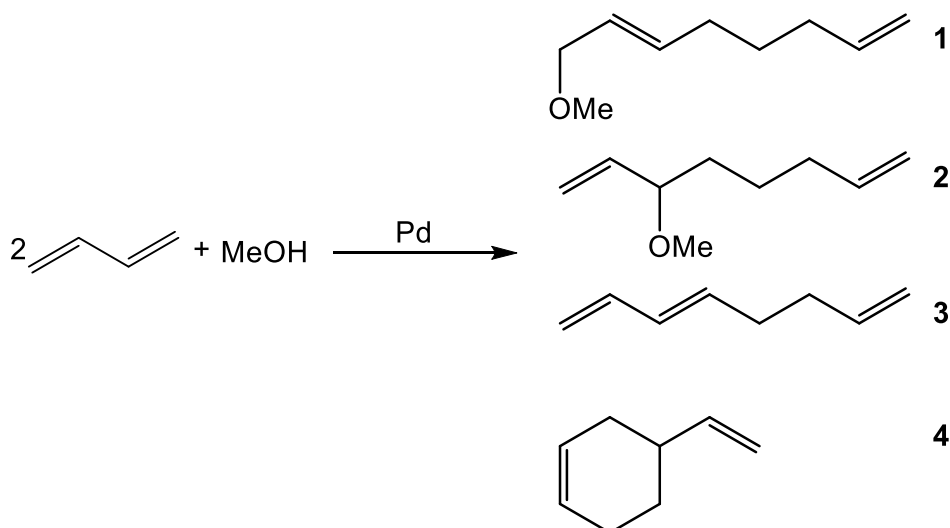


**Scheme 4: Reaction scheme of the telomerization of 1,3-butadiene with methanol according to [44].**

The telomerization of 1,3-butadiene with methanol results in a linear as well as branched form of methoxyoctadiene as products, namely 1-methoxy-2,7-octadiene (1-Mode, **1**) and 3-methoxy-1,7-octadiene (3-Mode, **2**), whereas 1-Mode is the main product. Further, but undesired byproducts of this reaction are linear or cyclic dimers of 1,3-butadiene, namely 1,3,7-octatriene **3** and 4-vinylcyclohexene **4**. The latter is formed by the Diels-Alder reaction of two molecules of 1,3-butadiene and is described in detail in Chapter 2.1.2.1.3 [88].

Usually, the telomerization is carried out with phosphine ligands such as triphenylphosphine (TPP). However, within the research of the last decade, also alternative ligands for the telomerization of 1,3-butadiene with methanol were tested (see Chapter 2.1.2.4).

## 2.1.2.1   Reaction mechanism

For the palladium-catalyzed telomerization of 1,3-butadiene with methanol, two different reaction mechanisms are proposed in the literature, the monopalladium- and the dipalladium-bisallyl mechanism. Both mechanisms are discussed in detail in the following chapters, starting with the dipalladium-bisallyl mechanism.

2.1.2.1.1   Dipalladium-bisallyl mechanism

In 1968 Keim *et al.* [89; 90] proposed the dipalladium-bisallyl mechanism for the telomerization reaction of 1,3-butadiene with phenol and acetic acid. The mechanism is depicted in Scheme 5 but is not restricted to these two nucleophiles.

**Scheme 5: Dipalladium-bisallyl mechanism according to [89; 90].**

The reaction mechanism starts with complex **5**, the catalytically active species. The latter is a dipalladium core with two or more coordinating ligands and stabilized by two bridging nucleophiles. The ligands are dissociated and two molecules of 1,3-butadiene coordinate at the stabilized dipalladium species (complex **6**). In the following step, the dipalladium-bisallylic species (complex **7**) is formed by an oxidative C-C coupling. In 1986, complex **7** was isolated and studied by Behr *et al.* [90]. Depending on whether the nucleophile attacks at the C1 or C3 atom (complex **8** or **9**), the telomerization products 1-Mode **1** or 3-Mode **2** are formed by the substitution of further ligands. After the dissociation of the products, the active species (complex **5**) is formed again closing the catalytic cycle. Without nucleophilic attack at the bisallylic intermediate (complex **7**), the byproduct 1,3,7-octatriene **3** is formed by addition of two or more ligands.

### 2.1.2.1.2   Monopalladium-bisallyl mechanism

In 1985 Jolly *et al.* [91-94] proposed the monopalladium-bisallyl mechanism for the telomerization of 1,3-butadiene using methanol as nucleophile. They succeeded to isolate and identify several intermediates of this mechanism. In the literature, the monopalladium-bisallyl mechanism is the most applied one for the telomerization of 1,3-butadiene and methanol. The mechanism is depicted in Scheme 6.

Starting with a palladium-ligand complex $PdL_n$, two molecules of 1,3-butadiene coordinate at the palladium under removal of $n$ ligands. Oxidative coupling of complex **10** results in the $\eta^1$, $\eta^3$-octadiendiyl species (complex **11**). The next step is the nucleophilic addition of methanol resulting in complex **12** via intermediate state **11\***. Intermediate **11** was crystallized and identified by X-ray diffraction analysis [91]. Furthermore, tetrafluoroborate analogues of this complex as well as of complex **12** were isolated and analyzed by Vollmüller *et al.* [95]. However, complex **10** could not be isolated or characterized up to now.

If the methoxide anion attacks at the C1 atom, the chelate complex **13**, $\eta^2$, $\eta^2$-1-methoxy-2,7-octadienpalladium, is formed resulting in the linear telomer 1-Mode. This step was verified with ^{31}P-NMR studies by Jolly *et al.* [92]. The branched telomer 3-Mode is formed in a similar way. Nucleophilic attack at the C3

atom of complex **12** leads to complex **14**. The olefin exchange at complexes **13** and **14** results in the products 1-Mode and 3-Mode and complex **10** closing the catalytic cycle. The nucleophilic attack at complex **12** is the determining step for the regioselectivity. In general, the nucleophilic attack at the C1 atom leading to 1-Mode is preferred due to steric reasons whereas the C3 attack is the electronically favored one [96; 97]. Furthermore, the formation of 1-Mode is favored as it is thermodynamically more stable due to its internal double bond and the intermediate step via the chelate complex **13** [98].

If no nucleophilic attack takes place, the linear dimerization product 1,3,7-octatriene **3** is formed by β-H-elimination.
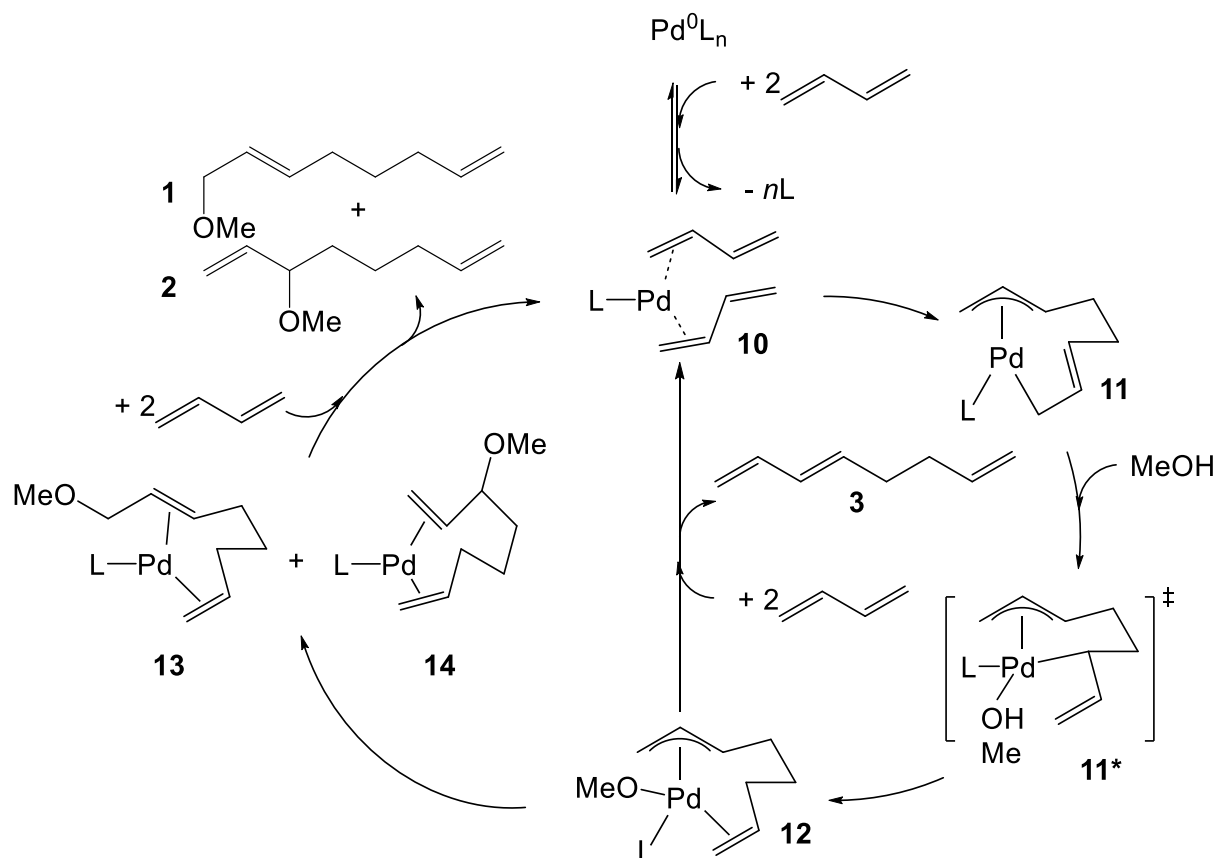


**Scheme 6: Monopalladium-bisallyl mechanism according to [91-94].**

2.1.2.1.3  Formation of 4-vinylcyclohexene

According to Scheme 4, the byproduct 4-vinylcyclohexene results also from the telomerization of butadiene with methanol. The cyclic dimerization product is formed uncatalyzed by the Diels-Alder reaction of two molecules of butadiene. The Diels-Alder reaction was first reported by Otto Paul Hermann Diels and Kurt Alder [88] in 1928 and describes the thermally induced cyclization of a conjugated diene and a dienophilic compound. The reaction for two butadiene molecules, including a pericyclic 4+2-π-electron transition state, is shown in Scheme 7.
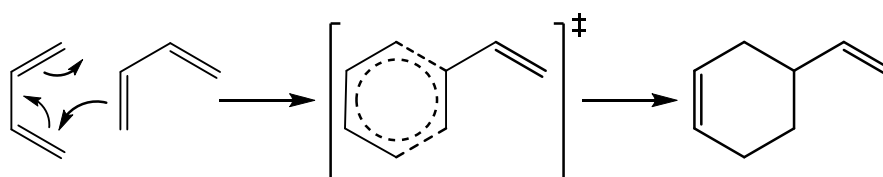


**Scheme 7: Formation of 4-vinylcyclohexene via the Diels-Alder reaction of butadiene.**

Within the telomerization reaction studied in this thesis, butadiene acts as diene and dienophile. Due to the poor dienophilic character of 1,3-butadiene, the cyclization should take place slowly. Thus, only small quantities of the cyclic byproduct are expected within the telomerization reaction.

**2.1.2.2  Influence of base, temperature, ligands and reactants on the catalytic performance**

It is well-known that bases such as amines or methoxides facilitate and accelerate the reduction of Pd(II) precursors, e.g. Pd(acac)$_2$ or Pd(OAc)$_2$, to Pd(0) complexes [99-101]. Also in the telomerization reaction, bases seem to influence the reaction positively [102-104]. Vollmüller *et al.* [102] observed that the base triethylamine (NEt$_3$) accelerated the reaction rate at the start of reaction whereas it did not affect the overall selectivity or productivity. This effect was more pronounced with lower phosphine to palladium ratios and at lower temperatures. This observation was further studied by calorimetry experiments which showed that the induction period of

the reaction was reduced when using NEt$_3$. Thus, the base NEt$_3$ facilitates the reduction of Pd(II) to Pd(0).

In addition, Jolly *et al.* [92; 93] stated that the base supports the nucleophilic attack to form $\eta^2$, $\eta^2$-1-methoxy-2,7-octadienpalladium (complex **13**).

Based on the monopalladium-bisallyl mechanism, continuative investigations regarding the control of chemo- and regioselectivity were carried out by Vollmüller *et al.* [95; 102]. Temperature increase causes higher catalytic activity but decreases the chemoselectivity, while the regioselectivity remains almost unaffected. Above 50 °C, the byproduct 1,3,7-octatriene is formed to a higher extend. At temperatures above 90 to 100 °C, obviously more butadiene undergoes the Diels-Alder reaction forming the cyclic byproduct 4-vinylcyclohexene.

In addition, the ligand to palladium ratio has a strong influence especially on the regioselectivity of the telomerization reaction [95; 102]. With increasing phosphine concentration, the amount of branched telomer increases while the regioselectivity decreases. With this observation, Vollmüller *et al.* [95] postulated an expansion of the monopalladium-bisallyl mechanism involving the influence of phosphine ligands such as TPP on the regioselectivity. The reaction step is depicted in Scheme 8.
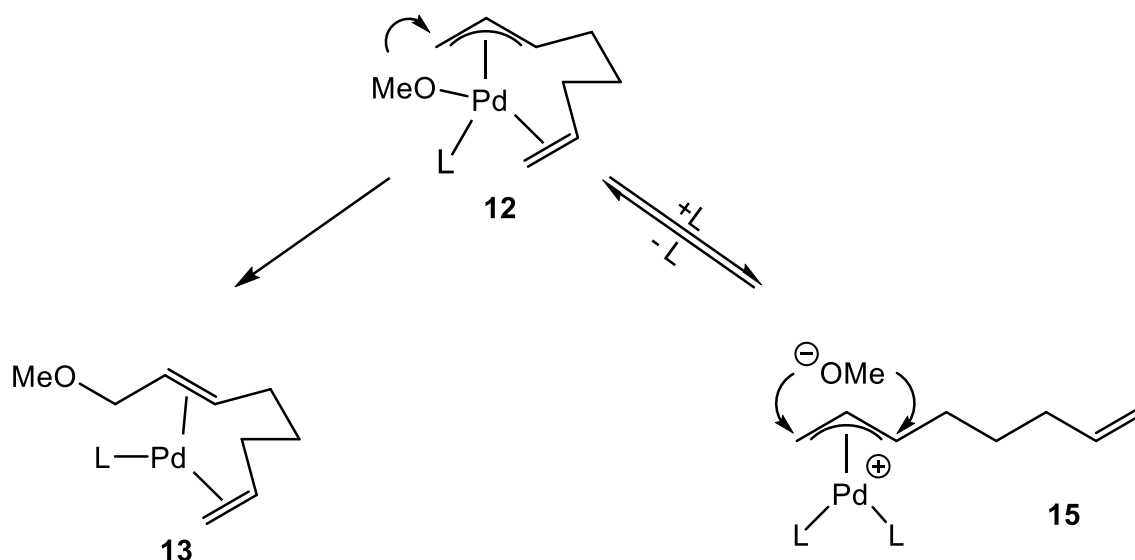


**Scheme 8: Influence of the ligand concentration on the regioselectivity according to [95].**

They stated that with increasing concentration of TPP, a second TPP molecule competes for the coordination site at the palladium atom. Due to the P$_2$Pd(0) moiety

of complex **15**, the energetically favored chelating $\eta^2, \eta^2$-1-methoxy-2,7-octa-dienpalladium complex **13** cannot be formed anymore as the coordination of both double bonds is not possible. The attack of the methoxide ion at the C1 atom of complex **15** is less preferred than the attack at the C1 atom of complex **12**. However, the methoxide anion prefers the attack at the C3 atom of complex **15**. In consequence, the regioselectivity decreases with increasing concentration of TPP.

Besides the decrease in regioselectivity, an increase in catalyst productivity was observed probably due to the better stabilization of the catalyst present at higher ligand concentration [95].

When using ligands with a larger steric demand, the probability of the coordination of a second ligand should be reduced. Based on this knowledge, alternative ligands were investigated in the literature which are discussed in detail in Chapter 2.1.2.4.

The postulations regarding the influence of phosphine concentration on the regioselectivity were further verified by experiments with varying butadiene to methanol ratio. Vollmüller *et al.* [95] observed a decrease in regioselectivity with increasing butadiene concentration. This behavior was already reported by Beger *et al.* [48] in 1973, but Vollmüller *et al.* [95] tried to explain this behavior first by stating that an excess of butadiene has a similar effect as an excess of TPP. The proposed effect is shown in Scheme 9.
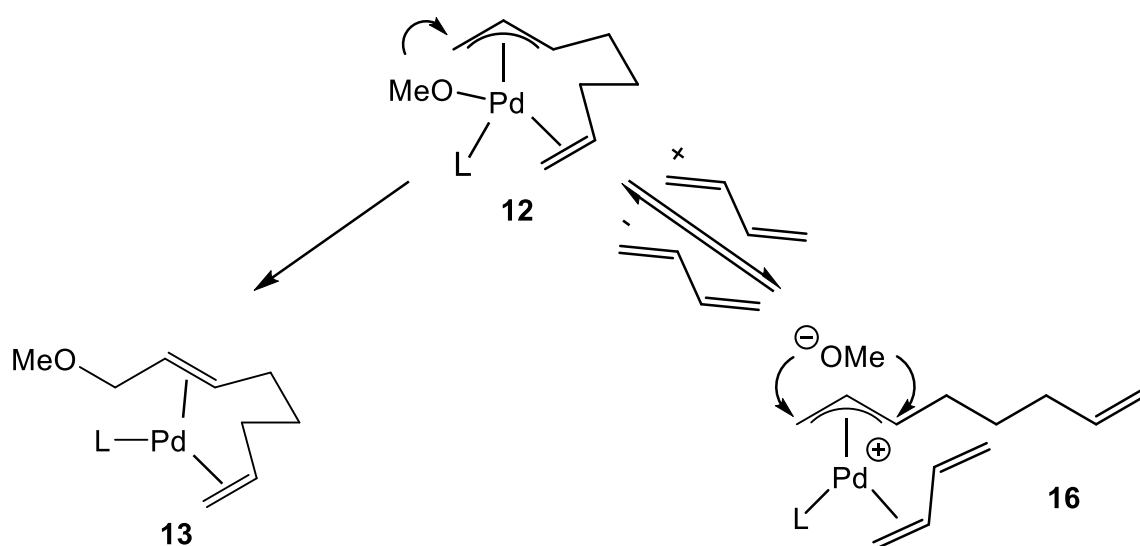


**Scheme 9: Influence of the butadiene concentration on the regioselectivity according to [95].**

The excess of butadiene results in the loss of the second coordination site of the palladium atom by coordinating a butadiene molecule. Thus, the nucleophilic attack does not result in the chelating $\eta^2$, $\eta^2$-1-methoxy-2,7-octadienpalladium complex, but yields complex **16**. Similar to the behavior with an excess of TPP, the nucleophilic attack at the C1 atom of complex **16** is no longer favored in the same extent as the C1-attack of complex **12**. In consequence, also an excess of butadiene leads to a decrease in regioselectivity.

Besides the regioselectivity, the ratio of butadiene to methanol also affects the chemoselectivity [95]. The influence of methanol on the chemoselectivity of the telomerization reaction is presented in Scheme 10.



**12**
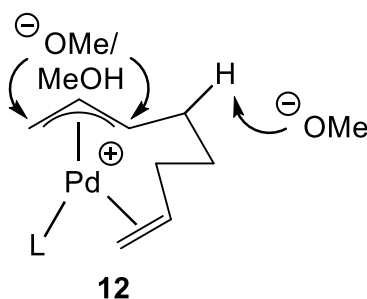
**Scheme 10: Influence of the methanol concentration on the chemoselectivity according to [95].**

A decrease of chemoselectivity with decreasing methanol concentration was observed [95]. Instead of the telomers, the byproduct 1,3,7-octatriene is formed to a larger extent. They proposed that the methoxide anion does not undergo only the nucleophilic attack towards the telomers, but also reacts intermolecular with complex **12** to deprotonate it. The effect of the methoxide anion is less pronounced at higher methanol concentrations resulting in lower formation of 1,3,7-octatriene and consequently in a higher chemoselectivity.

**2.1.2.3   DFT calculations for verifying the proposed mechanism**

For the monopalladium-bisallyl mechanism, some computational studies exist [105; 106]. Huo [105] computed the most stable isomers of each intermediate of the mechanism. However, only the transition states of the oxidative C-C coupling step were studied in detail. For the remaining steps, no energy profiles were calculated.

Based on this work [105], Jabri *et al.* [106] focused on the steps 2 and 3 involving charged species and presented the first complete energy profile for the monopalladium-bisallyl mechanism. According to Huo *et al.* [105], the first step of oxidative C-C coupling was found to have low energy barriers and is expected not to be the rate determining step. The second step, the protonation of complex **11**, was experimentally proven to have low energy barriers as complex **11** acts as a base able to deprotonate acidic proton donors [91; 92]. In accordance with these experimental observations, the calculations of Jabri *et al.* [106] at neutral pH using $NMe_3$ as co-catalyst showed that this step has low energy barriers and is highly exergonic. Thus, it is not the rate determining step. The next step of the reaction mechanism is the nucleophilic attack at complex **12** to form complex **13**. The nucleophilic attack was calculated to have the highest energy barriers of all steps within the mechanism and seems to be the rate determining step. Furthermore, the nucleophilic attack at C3 atom to form the branched isomer via complex **14** has a significantly higher energy barrier than the nucleophilic attack at C1 atom. This means that the chelating complex **13** forms favorably the linear product, 1-Mode, according to the experimental observations by Vollmüller *et al.* [95]. They stated that higher concentrations of ligand and butadiene result in complex **15** and **16** forming favorably the branched product, 3-Mode. Jabri *et al.* [106] calculated this reaction step and were able to support the statements of Vollmüller *et al.* [95]. The last step is the olefin exchange of the coordinating 1-Mode with two molecules of butadiene forming the desired linear telomer. The dissociative exchange was calculated to show a very low energy barrier being probably not the rate determining step. Furthermore, also the formation of the byproduct octatriene was computed [106], which is favorably formed at higher temperatures [95]. They considered two possible formation pathways, namely the commonly proposed direct deprotonation of the octadienyl group of complex **12** and the β-H-elimination. Due to the calculated energy barriers of these two pathways at neutral pH, it seems to be more likely that the β-H-

elimination is the reaction step forming 1,3,7-ocatriene. This result is in accordance with the experimentally observed increase of 1,3,7-ocatriene formation with increasing temperature.

Also the effect of bases was studied by Jabri *et al.* [106]. They calculated the energy profile of the reaction mechanism using a high concentration of LiOMe. The obtained results show that the protonation step has a higher energy barrier compared to the results computed at neutral pH. The step of nucleophilic attack is facilitated by using LiOMe as co-catalyst resulting in an increased reaction rate for telomerization reactions where the nucleophilic attack is the rate determining step. The energy barriers of the protonation step and nucleophilic attack are rather similar. They proposed the step of protonation to be the rate determining step when working at high pH [106]. The obtained complete energy profile for the reaction mechanism at neutral as well as at high pH is shown in Figure 1.
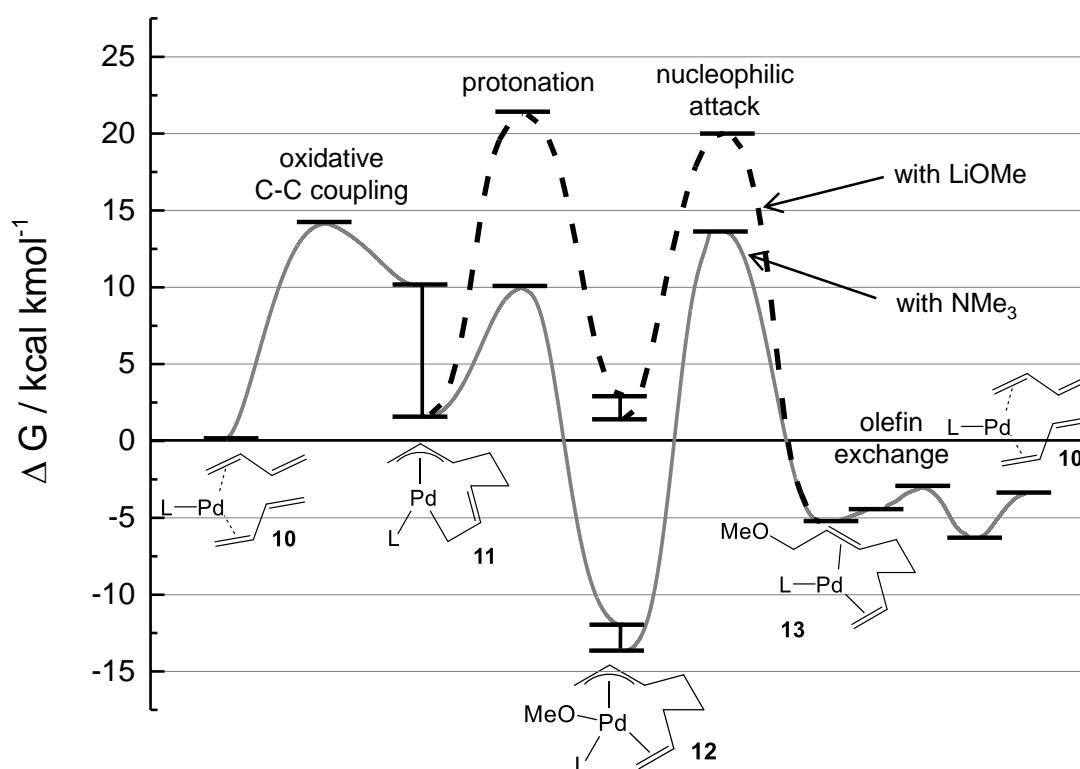


**Figure 1: Calculated energy profile for the Jolly mechanism of the telomerization reaction according to [71].**

## 2.1.2.4 Alternative ligands in the telomerization of butadiene with methanol

As discussed in Chapter 2.1.2.2, the ligand concentration has a strong influence on the regioselectivity. If the concentration is too high, the regioselectivity decreases due to the coordination of a second ligand. In consequence, the coordinating ligand should not be present in excess. However, phosphine ligands have to be added in excess in order to stabilize the catalyst which is present, in general, at very low concentration [24; 28]. Furthermore, phosphine is lost due to its catalytic oxidation during the reaction [24; 107; 108]. In order to overcome this problem of required ligand excess, the possibility of a strongly bound ligand with large steric demand was discussed and studied in the literature especially by Jackstell *et al.* [27-29] and Tschan *et al.* [24; 25; 75; 109]. Further research groups were engaged in the development of bidentate [110; 111] or chelate ligands [112; 113], macrocyclic components [35; 36; 40], cyclopalladated complexes [114] or allylic compounds [115]. This thesis focuses on the application of N-heterocyclic carbene (NHC)-ligands and bulky phosphines being discussed in detail in the following. More details concerning the other studied ligands can be found in the corresponding literature [40; 110-115].

2.1.2.4.1 N-heterocyclic carbene (NHC)-ligands

N-heterocyclic carbenes (NHC) are an interesting class of ligands which were discovered in the early 1960s [116-118]. According to Viciu and Nolan [107] this class of ligands has several advantages compared to the commonly used phosphines. They are stable at higher temperatures and do not seem to dissociate easily from the metal center due to the strong bond with the metal. In consequence, no ligand excess is required in order to avoid clustering of the metal or formation of elemental metal.

NHC-ligands are applied in a various number of transition metal catalysis, e.g., hydrosilylation [119], ruthenium-catalyzed furan synthesis [120], iridium-catalyzed hydrogenation [121; 122]. Detailed information about the application of NHC-ligands

in the transition metal catalysis can be found for example in the reviews provided by the Nolan group [107; 123].

NHC-ligands were also successfully tested in the palladium-catalyzed telomerization of butadiene with methanol, especially by Jackstell *et al.* [27-29]. The main achievements of their work are introduced in the following.

One first step was the application of the [Pd(0)(dvds)(IMes)] complex ((1,3-di-mesitylimidazol-2-ylidene)-palladium(0)-1,1,3,3-tetramethyl-1,3-divinyl-disiloxane) in the telomerization of butadiene with methanol [27; 28]. The synthesized complex is depicted in Figure 2. The complex should mimic the 1,6-chelating intermediate species in the mechanism proposed by Jolly *et al.* [91-94] (see Chapter 2.1.2.1.2).



**17**
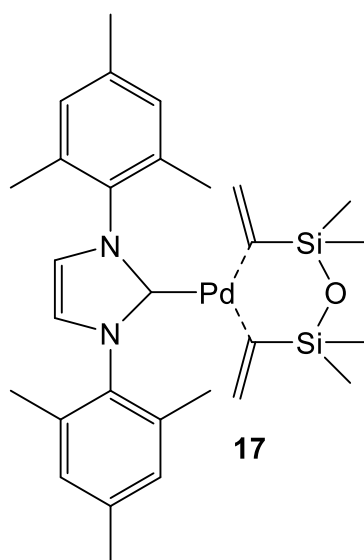
**Figure 2: Chemical structure of the synthesized [Pd(0)(dvds)(IMes)] complex according to [27; 28].**

The experiments were carried out with a ratio of methanol to butadiene of 2:1 and the addition of 1 mol% NaOH. Compared to the commonly used $Pd(OAc)_2$/TPP system, the complex catalyzes the reaction already at 50 °C with excellent chemo- and regioselectivities. Also at 90 °C, the chemo- and regioselectivities of the carbene-complex are very high and comparable to those achieved at 50 °C. The fact that the selectivity of the IMes system seems to be independent of the temperature is one important advantage compared to the TPP system. In general, the IMes system works more selectively toward the telomers than the TPP system. When using the corresponding imidazolium salt for in-situ preparation of the ligand-catalyst-complex,

as well as the free carbene, similar results compared to the ex-situ prepared, well-defined complex [Pd(0)(dvds)(IMes)] were achieved.

Jackstell *et al.* [28] also tested some ferrocenyl-based carbene ligands in the telomerization of butadiene with methanol, but they all showed worse results compared to the IMes system.

In order to study the influence of different substituents on the carbene backbone (4- or 5-position), Jackstell *et al.* [29] synthesized different [Pd(0)(dvds)(NHC)] complexes and tested them in the telomerization of butadiene with methanol. The chemical structures of these complexes are shown in Figure 3 and the results are presented in Table 1.

**Table 1: Results of catalyst complex screening according to [29].**

| Complex | $Y_{1+2}$ / % | *n*:*iso* / - | $S_{1+2}$ / % | TON (**1+2**) / - | TOF (**1+2**) / $h^{-1}$ |
|:---:|:---:|:---:|:---:|:---:|:---:|
| **17** | 96 | 98:2 | > 99 | 96,000 | 6,000 |
| **18** | 93 | 98:2 | 99 | 93,000 | 5,813 |
| **19** | 96 | 98:2 | > 99 | 96,000 | 6,000 |
| **20** | 90 | 92:8 | 97 | 90 | 5,625 |
| **21** | 2 | 91:9 | - | 2,000 | 125 |

*Reaction conditions: 70 °C, 16 h, 1 mol% NaOMe, MeOH:butadiene = 2:1.*

The Pd(0) complexes **17** and **19** showed excellent results regarding yield of the telomers (96 %), chemo- and regioselectivity (> 99 % and *n*:*iso* = 98:2) whereas a yield of only 26 % was found for the commonly used Pd(OAc)$_2$/TPP (TPP:Pd = 3). Also the selectivities were observed to be significantly higher for the studied complexes. Interestingly, the IPr-complex **20** (Pd(0)(dvds)IPr, 1,3-bis-(2,6-diisopropylphenyl)imidazole-2-ylidene-palladium(0)-1,1,3,3-tetramethyl-1,3-divinyl-disiloxane) gave worse results regarding yield, chemo- and regioselectivity compared to the IMes-complex **17** meaning that an increase in steric demand lowers the catalytic performance. Complex **21** was hardly active showing a yield of only 2 %.

A substitution at the IMes backbone in 4- and 5-position (complex **18**) does not seem to significantly influence the catalyst performance. Also in-situ generated catalyst complexes starting with IMes HCl and Pd(OAc)$_2$ as precursors probably form the same catalytic active species as the catalytic performance was almost similar to that of the corresponding ex-situ prepared complex.
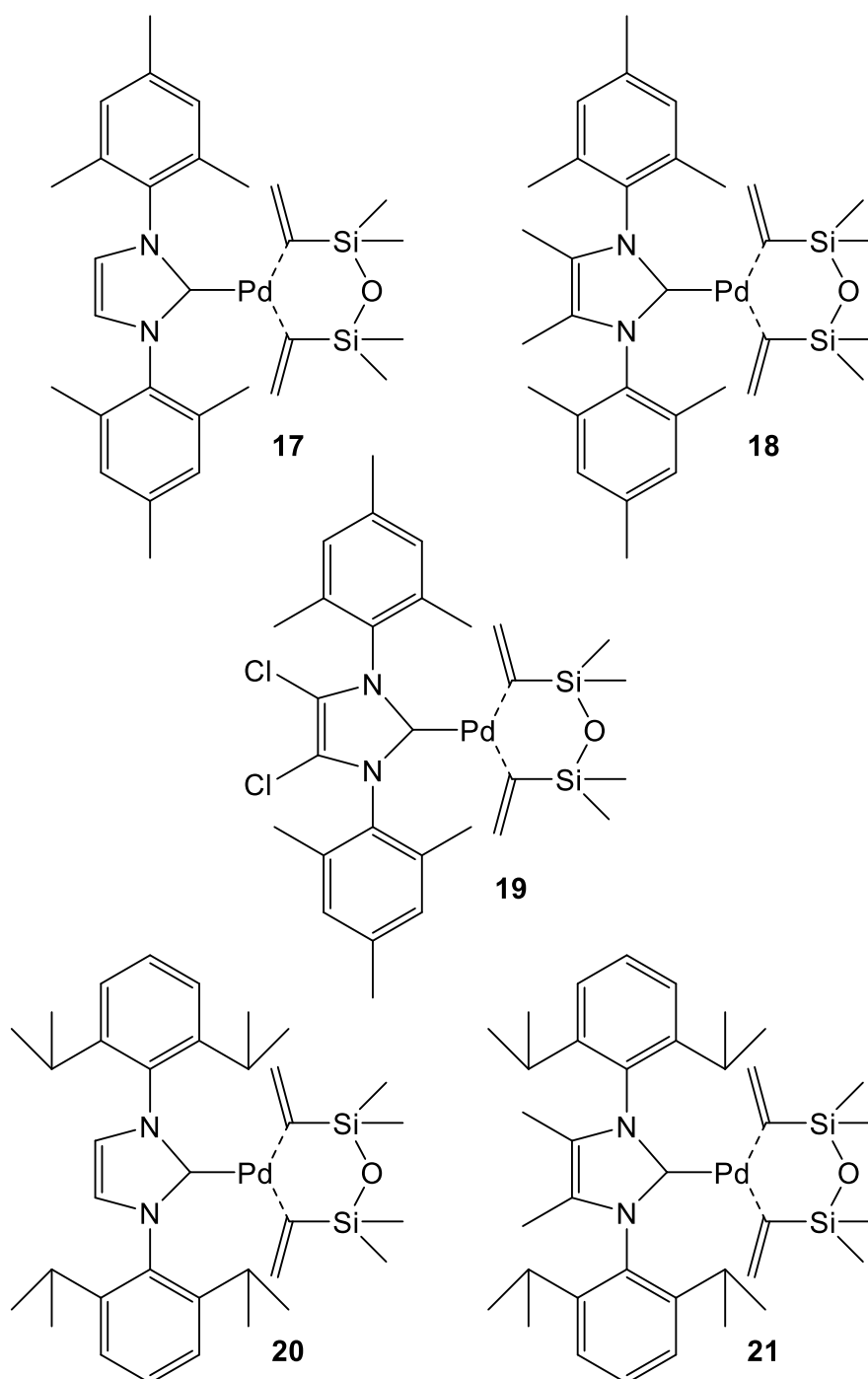
**Figure 3: Chemical structures of the synthesized [Pd(0)(dvds)(NHC)] complexes according to [29].**

In order to test the catalyst activity especially at reaction start, samples were taken frequently during reaction. An influence of the substitution at the backbone (4- and 5-position) of the IMes ligand was observed [29]. The substitution of electron withdrawing chlorine seems to destabilize the catalyst complex resulting in a better catalytic activity whereas substitution of electron donating methyl groups stabilizes

the catalyst complex resulting in worse catalytic activity. This assumption was supported by some DFT calculations mimicking the model of the ligand exchange reaction at the Pd(0) complexes representing the 1,6-chelating intermediate species in the Jolly mechanism.

To further optimize the catalyst productivity, some excess ligand (IMes HCl as precursor) was added to the IMes complex **17** [29]. With a concentration of only 0.5 ppm of complex **17** and an excess of IMes HCl of 4 ppm, Jackstell *et al.* achieved the highest catalyst productivity (TON = 1,540,000, after 16 h reaction time) reported at that time for any telomerization reaction. Similar high chemo- and regioselectivities were obtained compared to the experiments without ligand excess. This observation is in contradiction to the behavior found for TPP as ligand [95]. The steric hindered and strongly bound IMes seems to prevent the coordination of a second ligand at complex **12** in the Jolly mechanism. Thus, the 1,6-chelating intermediate species **13** results which prefers the nucleophilic attack at the C1 atom forming 1-Mode.

## 2.1.2.4.2 Phosphine ligands

Tschan *et al.* [24; 25] focused on the study of bulky phosphines and compared them to the benchmark system using TPP. In a first publication [24], they reported similar productivity and selectivity when using ex-situ prepared phosphine-palladium-dvds complexes compared to the in-situ prepared ones with the same ligands. They did not observe a trend regarding the properties of the used ligands and the productivity and selectivity of the catalytic systems. The most promising ligand was the literature known monoxantphos. The chemical structure of the latter is shown in Figure 4.

The catalytic system with monoxantphos **22** is more selective and active compared to TPP. Also at 100 °C and in the presence of crude $C_4$, the monoxantphos system remains selective and highly active with a TOF of 140,000 $h^{-1}$ after 5 minutes compared to 41,600 $h^{-1}$ when using TPP. At a reaction temperature of 90 °C, they observed that the loss of palladium due to precipitation is lower for monoxantphos (6 %) than for TPP (17 %). Thus, monoxantphos seems to stabilize the catalytic active species.
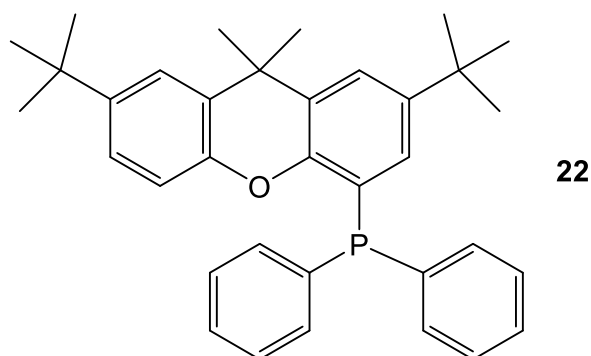
**Figure 4: Chemical structure of monoxantphos.**

Based on the promising results described for monoxantphos, Tschan *et al.* [25] continuatively studied the electronic and steric effects of further bulky phosphines based on the structure of monoxantphos. All phosphines were tested under the commercial conditions of the Dow Chemical Process (90 °C, NaOMe:Pd = 5 (molar), Pd:butadiene = 0.0025 mol%, crude $C_4$) with varying temperature and methanol to butadiene ratio. Compared to TPP, all studied ligands showed a better performance regarding selectivity and productivity. Tschan *et al.* [25] found that ligands which are less basic than monoxantphos are less productive and less selective. A higher palladium loss was observed for ligands possessing a less bulky backbone.

Concerning conversion, chemoselectivity and palladium loss monoxantphos and monospanphos were the best of the studied ligands. The structure of the latter is shown in Figure 5.
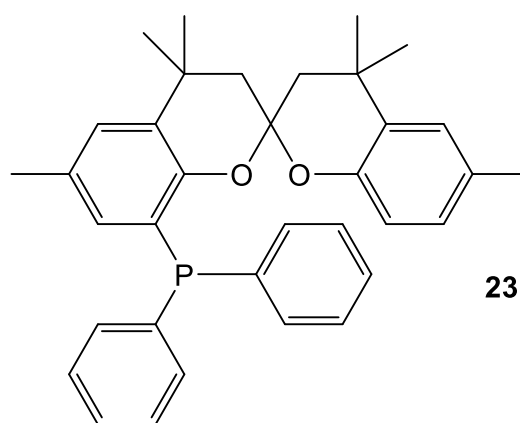


**Figure 5: Chemical structure of monospanphos.**

The two ligands showed almost similar performance except at lower temperatures. At 60 °C monospanphos **23** showed a higher reaction rate than monoxantphos. The

selectivities, however, were the same. For both ligands, the selectivity decreased with increasing temperature.

Tschan *et al.* [25] focused on further investigation of these two ligands by comparing their catalytic performance under commercial conditions with the best working NHC-ligand, IMes. Both, monoxantphos and monospanphos, showed better performance under commercial conditions than IMes. The reason is the low concentration of base (NaOMe:Pd = 5 (molar)). The formation of the catalytic active species of the IMes ligand seems to require higher base concentration. With molar ratios of NaOMe to palladium of 100 to 1,000 for IMes, performances similar to those of monoxantphos and monospanphos at a molar ratio of NaOMe:Pd of 5 were observed [25]. The discussed studies resulted from collaboration with Dow Chemical who patented the novel, high performing phosphine based catalysts [75].

A further, interesting study concerning phosphine based ligands was published by Briggs *et al.* [26] in 2011. Their work focused on the performance study of newly developed monodentate triarylphosphine ligands, see Figure 6.

In a first series of experiments (**24** to **32**) using high throughput methodology and slightly different reaction conditions compared to the commercially applied ones, they observed a dependence on the basicity of the ligand. With more basic ligands, the selectivity as well as the productivity of the catalytic system increased. When working under conditions more similar to the commercially applied one, this trend could not be observed anymore. Instead, an optimum at moderate basicity was obtained. This behavior probably is the result of two opposing trends, the decreasing stability and the increasing activity with increasing basicity of the ligand. They proposed that the phosphine decomposition is the reason for catalyst deactivation in phosphine-promoted telomerization reaction. Further improvement of the triarylphosphine ligands (**34** to **38**) were achieved by lowering the basicity of the ligand moderately, e.g. by the substitution of one arene ring with electron-withdrawing groups.

**24** X = NMe$_2$
**25** X = OMe
**26** X = Me
**27** X = H
**28** X = F
**29** X = Cl
**30** X = CF$_3$

**31** X = H
**32** X = OMe

**33** X = H, Y = H
**34** X = H, Y = CF$_3$
**35** X = Cl, Y = H
**36** X = F, Y = H
**37** X = CF$_3$, Y = H
**38** X = H, Y = F
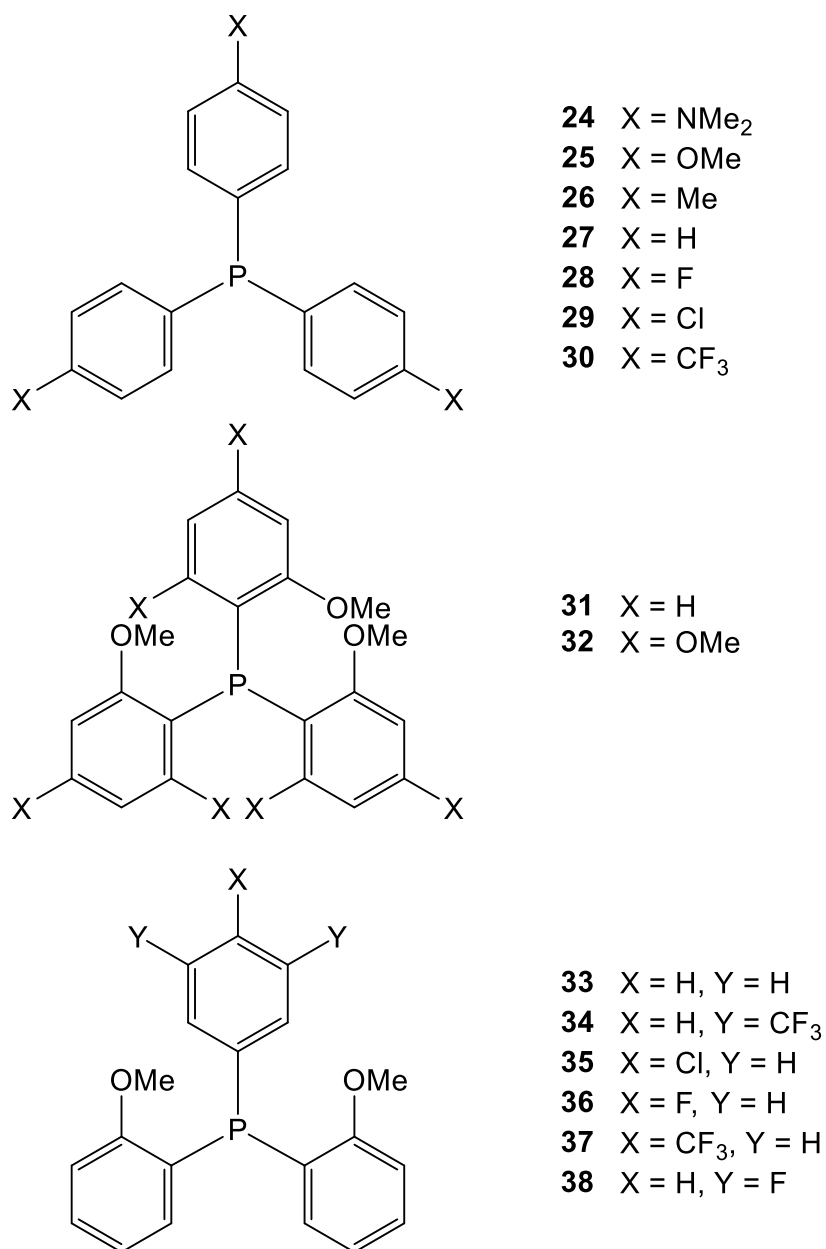
**Figure 6: Chemical structure of substituted triarylphosphines according to [26].**

### 2.1.2.5 Immobilization strategies for the telomerization

The telomerization reaction is an interesting and versatile example for a homogeneously catalyzed reaction exhibiting high selectivities and activities at moderate reaction conditions. However, as almost every homogeneously catalyzed reaction, the telomerization reaction suffers from the product/catalyst separation problem. Without the recycling of the often very expensive catalyst, homogeneously

catalyzed reactions become inefficient and cost-intensive. Heterogeneously catalyzed reactions might offer the solution for the separation problem but they often exhibit much lower activities and selectivities as their homogeneous analogues. The mentioned facts prompted high research attention on combining the advantages of homogeneous and heterogeneous catalysis. Mainly two approaches can be distinguished, namely the heterogenization of a catalyst by immobilization on a support and the use of a biphasic catalytic system where the phase which contains the catalyst has to be immiscible with the formed product phase. An excellent review on the extensive research in this field was published 2002 by Tzschucke *et al.* [2].

As already mentioned in Chapter 2.1.1, a possibility of catalyst recycling in the industrially implemented telomerization of butadiene with methanol would also improve the cost-effectiveness of this process. A possibility for catalyst recycling would be the above mentioned combination of homogeneous and heterogeneous catalysis. However, only a few research groups are engaged in this problem. Some literature publications report catalyst immobilization by applying multiphasic reaction systems [30-33]. This immobilization strategy and its application in the telomerization reaction are introduced in detail in Chapter 2.2.

Further studies focused on the heterogenization of the palladium catalyst [34-39] as well as on the recovery of macrocyclic-palladium complexes [40]. The latter was an attempt to recycle a soluble catalyst with a macrocyclic structure by distillation under reduced pressure. The applied macrocyclic-palladium complex **39** and the pure macrocyclic ligand **40** are depicted in Figure 7.
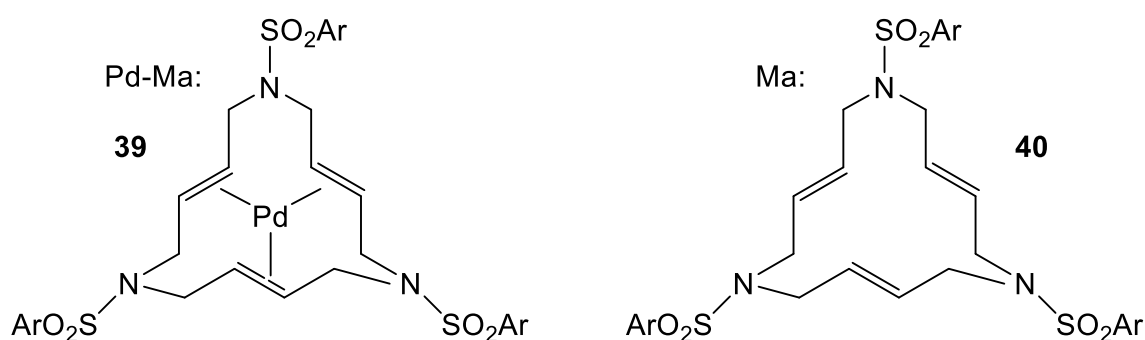


Ar = 2,4,5-tri-*iso*-propylphenyl

**Figure 7: Chemical structures of macrocyclic-Pd-complex and macrocyclic ligand according to [40].**

The recovery of the homogeneously dissolved catalyst was possible when using the macrocyclic-Pd-complex with additional phosphine (TPP). Also activity and selectivity of this catalyst system was regained. For the used benchmark catalyst systems, Pd-dba and Pd(OAc)$_2$ with TPP, the catalyst recycling was not successful with both decreasing activity and selectivity. However, when adding the free macrocyclic ligand to the benchmark systems, for Pd-dba, the catalytic activity as well as the selectivity of the recycle runs were even higher compared to the first run without free macrocycle. The system with Pd(OAc)$_2$ as catalyst precursor was also recyclable with additional macrocyclic ligand, but the results of the initial run could not be regained.

In a further study the role of the macrocyclic ligand in the presence of phosphines was studied [124]. They found that the macrocyclic-Pd-complex provides palladium to the phosphines forming catalytic active species. When the phosphine is then decomposed due to oxidation, the palladium is reincorporated in the macrocyclic structure. Thus, agglomeration or formation of palladium-black is prevented.

With this knowledge Blanco *et al.* [35] investigated the catalytic performance in telomerization reaction when the macrocyclic-Pd-complex is covalently bonded to a silica matrix, mimicking a heterogeneously catalyzed reaction. However, the activity of this catalytic system was poor, the recyclability was soon depleted and the formation of palladium-black was observed.

In 1999, Benvenuti *et al.* [38; 39] studied anchored palladium on silica, functionalized styrene/divinylbenzene and linear polystyrene in the telomerization of butadiene with methanol. They found that palladium bound on activated silica did not show any activity. Pd(II) complexes heterogenized on crosslinked styrene/divinylbenzene functionalized with acetylacetonate moieties were not stably anchored and leached into the liquid reaction mixture. However, palladium anchored to crosslinked styrene/divinylbenzene by 1,3-diphosphine chelating ligands, e.g. bis(diphenylphosphine)propane (DPPP) or bis(diphenylphosphine)methane (DPPM), showed high activity and selectivity when using NaOMe as cocatalyst comparable to the results obtained with its homogeneous analogues. Also recycling was successful with this heterogenized catalyst complex meaning that the anchoring on this polymer matrix by 1,3-diphosphine chelating ligands is very stable. For the recycling experiments no further addition of cocatalyst was required. With this attempt

Benvenuti *et al.* [38; 39] introduced a heterogenized palladium catalyst being stable in the liquid phase also in the presence of a strong base.

Lee *et al.* [34] tested montmorillonite, a swelling-type layered silicate clay, as support for palladium catalysts. For testing their performance in telomerization reactions, they applied these heterogenized catalysts to the telomerization of butadiene with water. Furthermore, they investigated the catalytic performance of palladium supported on alumina and on activated carbon in the same reaction. The commonly used homogeneous $Pd(OAc)_2$/TPP-system was introduced as benchmark system. Compared to the results of the latter, all studied heterogenized catalyst systems showed a similar product distribution. Palladium supported on alumina and on activated carbon showed lower activity compared to the homogenous system and do not seem to be stably anchored. Recycling experiments showed less activity probably due to deactivation and leaching of the catalyst. For palladium on silica, the activity could be regained after the treatment with oxygen at 300 °C. Supported on montmorillonite, the catalyst showed similar activity compared to the homogeneous system. In recycling experiments, the catalyst was recovered by filtration and added with fresh reactants resulting in similar activity and selectivity compared to the initial experiment. Thus, it can be assumed that palladium is stably anchored to montmorillonite without considerable leaching.

Estrine *et al.* [36] tested the recyclability of catalysts in the telomerization of butadiene with methanol and phenol using different catalyst supports, namely silica, montmorillonite and $KF/Al_2O_3$. They worked with a catalytic system consisting of $Pd(acac)_2$ as catalyst precursor and the threefold sulfonated triphenylphosphine TPPTS as ligand which was immobilized on the different supports. In recycling experiments, the solid catalyst was dried under vacuum without any further treatment. Palladium heterogenized on montmorillonite showed the highest activity and selectivity in the initial experiment. However, in the recycling experiments this system lost its activity and selectivity continuously. A similar behavior was observed for Pd/TPPTS immobilized on silica showing no activity in the second recycling experiment. The use of $KF/Al_2O_3$ as support showed the best recycling results but only low activity. Even the third recycling experiment showed similar results concerning activity and selectivity compared to the initial experiment reaching a TON of about 400.

The difference in the recyclability of montmorillonite supported palladium obtained by Lee *et al.* [34] and Estrine *et al.* [36] probably is caused by the different treatment of the recycled solid catalyst before introducing it again to the reaction. Estrine *et al.* [36] dried the catalyst under vacuum without further treatment whereas Lee *et al.* [34] additionally treated the catalyst with oxygen at 300 °C.

Parvulescu *et al.* [37] studied the heterogenization of the Pd/TPPTS-system on a layered double hydroxide (LDH) support material via ion-exchange and their performance in the telomerization of butadiene with methanol. They developed pseudo-heterogeneous complexes where either the ligand or the catalyst is bound to LDH as well as heterogeneous complexes where both, ligand and catalyst, in the form of preformed complexes are bound to LDH. With the pseudo-heterogeneous complexes the achieved TON was comparable to that obtained with the same catalytic system heterogenized on $KF/Al_2O_3$ [36]. The heterogeneous systems showed TONs comparable to the homogenous analogues when using the same, low catalyst concentration. However, using LDH as catalyst support has a drastic effect on the product distribution. For both, heterogeneous and pseudo-heterogeneous, higher telomers, in particular C16 telomers, were formed with selectivities higher than 50 %. In addition, the recyclability of both LDH-supported complexes was poor as the activity distinctly decreased with each further recycling experiment.

Summing up the introduced attempts to recycle the catalyst, the most interesting and most promising approaches are the application of $KF/Al_2O_3$ as support, macrocyclic-Pd-complexes and Pd anchored to crosslinked styrene/divinylbenzene by 1,3-diphosphine chelating ligands. However, none of these attempts were followed up successfully and implemented in a continuous process. Apart from these studies, further promising attempts to immobilize the palladium catalyst were realized by the application of biphasic or multiphase reaction systems. These approaches are introduced in detail in Chapter 2.2.

## 2.2 Biphasic or multiphase reaction systems

As already mentioned, one major problem in homogeneous catalysis is the challenging separation and recovery of products and catalyst. In consequence, efficient catalyst recycling is required for economically and ecologically effective homogeneously catalyzed industrial processes. In Chapter 2.1.2.5 different immobilization strategies applied for the telomerization reaction have already been introduced. In the following, especially the immobilization by biphasic reaction systems and its application for telomerization reactions is described as this is the main concept of this thesis.

Catalyst recycling can be realized by using a biphasic reaction system where one phase is the catalyst phase and the other one is the product phase [15; 125]. The products can separate from the catalyst phase either during the catalyzed reaction with or without additional extraction solvent or the products are extracted after the reaction. The product phase can be removed and the catalyst phase can be recycled. This approach is based on the proper choice of the catalyst phase. The latter must possess the following characteristics:

- Exhibiting proper distribution coefficients reflected in the extraction efficiency,
  - o Good solubility for the reactants
  - o Poor solubility for the products
- No or marginal mass transport limitation of the reactants in the catalyst phase,
- Excellent solubility of the catalyst and ligand in the catalyst phase,
- Stabilization of the dissolved catalyst and ligand to prevent leaching.

For biphasic reaction systems, different liquid-liquid combinations such as organic/organic or organic/aqueous are possible [3]. Also catalytic biphasic reactions using fluorous [4-7], supercritical solvents [8-10; 126] or ionic liquids [11-14] are known. The biphasic reaction concept for homogeneous catalysis has already been successfully implemented in the industry. Established processes are the Shell Higher Olefin Process (SHOP) [3; 15] and the Ruhrchemie/Rhône-Poulenc Process [16-20]. A well-known biphasic process with ionic liquids is the Difasol Process which is the biphasic version of the established Dimersol Process of the Institute Francais du Pétrole (IFP) [11; 12].

For the telomerization reaction of butadiene with methanol, two approaches of a biphasic reaction system were studied in the literature up to now and are described in detail in the following.

## 2.2.1  Use of water for three-phase telomerization

For many telomerization reactions, an aqueous biphasic reaction system is a well-known and adequate catalyst immobilization strategy [127-133].

A first attempt for a continuous telomerization of butadiene with methanol using a continuous catalyst recycling by an aqueous biphasic system was carried out by Dietmar Dehn [30-32]. In his PhD thesis, Dehn [30-32] studied the three-phase telomerization of butadiene with methanol. For this he worked with a biphasic organic/aqueous reaction system and added the gaseous butadiene feed. This gas/liquid/liquid reaction was realized in a loop reactor where phase transfer was improved compared to a common stirred tank reactor and separation within the reactor was possible by a separation unit.

Preliminary experiments were carried out in a semibatch autoclave. The threefold sulfonated phosphine ligand TPPTS was used for all experiments. The reaction was mass transport limited with respect to the gaseous butadiene feed. A variation of the reaction temperature showed that an optimum exists due to the increased butadiene solubility at lower temperature and the increased reaction rate at higher temperatures. Within these preliminary experiments, a palladium leaching into the product phase of 50 ppm was determined.

The continuous experiments were carried out in a loop reactor which was constructed especially for gas/liquid/liquid reactions. The phase transfer between the gaseous butadiene and the aqueous methanol/catalyst phase was supported by a sparger. The separation of the product and the aqueous phase was achieved by a gravity settler.

First experiments showed that the mass transport limitations could be reduced by increasing the circulation speed of the reaction mixture resulting in higher butadiene conversion and higher product formation [30-32]. This observation was confirmed by measured $k_L a$-values. However, the circulation speed did not influence the obtained

selectivities. Furthermore, the selectivity results of the preliminary semibatch experiments could be reproduced in the loop reactor. For all experiments, chemoselectivity was above 99 % and the regioselectivity reached values of 93 to 96 %. Experiments with a reaction time of up to 10 h showed only a slight decrease in activity. In order to check the long-term stability of the catalyst system, experiments with a reaction time of 50 h were carried out. A slight palladium leaching was observed (50 ppm of the product phase) resulting in a constant slight decrease of the catalytic activity. In order to counteract this leaching, a small amount of catalyst solution was added to the reaction mixture each hour. Comparing the experiments with and without additional catalyst supply, the activity was similar within the first 20 h. After 40 h reaction time, first distinct differences of the activity could be observed. This behavior was attributed to the slight leaching of palladium [30-32]. At the end, a space time yield (STY) of 160 kg·m$^{-3}$·h$^{-1}$ within a time period of 56 h was achieved.

## 2.2.2  Use of ionic liquids for biphasic telomerization

Ionic liquids are organic salts which are molten at temperatures below 100 °C and consist of an organic cation and either an organic or inorganic anion [14]. If they are in a liquid state at temperatures below about 25 °C, they are also called room temperature ionic liquids.

One noteworthy property of ionic liquids is their negligibly small, hardly measurable vapor pressure lying in the range of the vapor pressure of iron [14]. Furthermore, ionic liquids show other interesting properties such as non-flammability or an excellent dissolving power for many organic and inorganic components. They are used as solvents in separation processes [134; 135] and catalysts in chemical reactions [14], process engineering [13; 136], biotechnology [137; 138], material engineering [139-142] and sensor technology [143]. In addition, ionic liquids are also suitable for applications in electrochemistry [144; 145] due to their ionic structure and the resulting good electric conductivity and electrical stability.

Ionic liquids are also called "designer solvents" as properties such as viscosity, electrical conductivity, or solubility strongly depend on and can be designed by the

combination of cation and anion. For instance, within a biphasic reaction system the ionic liquid can be used as catalyst phase. The ionic liquid can be chosen and synthesized in a way exhibiting a good solubility for the reactants and an extracting effect for the formed products. Furthermore, the ionic liquid/catalyst phase can be easily separated gravimetrically due to its proportionally high density. As already mentioned in Chapter 2.2, the use of ionic liquids in biphasic reaction systems was studied for different reactions.

Also for telomerization reactions, the application of ionic liquids as catalyst phase in biphasic reaction systems was tested. Dullius *et al.* [146] tested the use of the ionic liquid [BMIM][BF$_4$] for the telomerization of butadiene with water. They proved this catalytic system to be active and selective toward the desired telomer. The recovered ionic liquid/catalyst phase was successfully reused with only marginal changes in activity and selectivity. Fonseca *et al.* [147] also applied the ionic liquid [BMIM][BF$_4$] for immobilization of the catalytic system and tested this approach for the telomerization of butadiene with diethylamine (NHEt$_2$). The catalytic performance of this system was found to be strongly dependent on the applied reaction conditions (e.g. temperature, reaction time, composition of catalytic system). Selectivities toward the desired telomers of up to 99 % were achieved. When recycling the ionic liquid/catalyst phase, the selectivities remained constant whereas the conversion decreased slightly with each recycle.

Magna *et al.* [33] adopted the biphasic reaction concept with ionic liquids to the telomerization of butadiene with methanol. The first interesting observation they found was that the addition of 1,3-dialkylimidazolium ionic liquids to the reaction medium led to complete deactivation of the catalytic system as no or only low conversion was observed. They assumed that 1,3-dialkylimidazolium ionic liquids form highly stable palladium imidazolylidene complexes due to the labile proton at the C2 atom. The formation of the proposed 1,3-dialkylimidazol-2-ylidene palladium complexes is shown in Scheme 11.
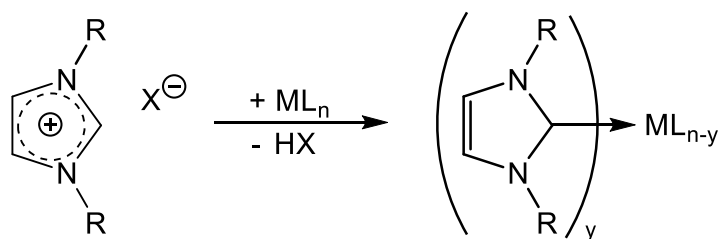
**Scheme 11: General scheme for the formation of 1,3-dialkylimidazol-2-ylidene palladium complexes according to [33].**

Further experiments showed that with increasing ratio of ionic liquid to palladium, the achieved conversion decreases leading to an increased deactivation of the catalyst. The results of these experiments are depicted in Figure 8.
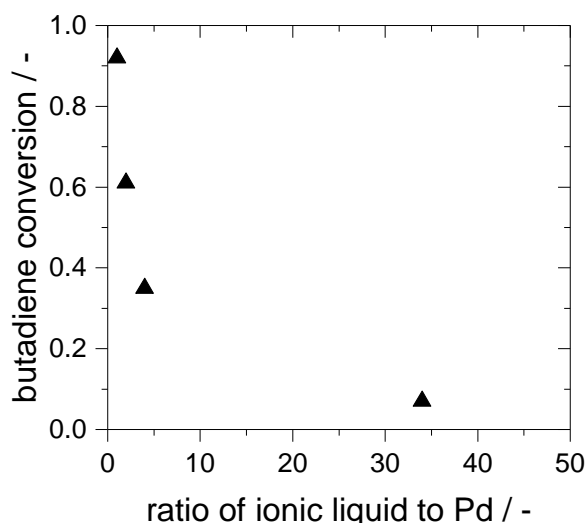


**Figure 8: Deactivation of the palladium catalyst with 1,3-dialkylimidazolium ionic liquids according to [33].**

*Reaction conditions: 85 °C, Pd(OAc)$_2$: 30 mg (0.134 mmol), TPP: 105 mg (0.400 mmol), ionic liquid: varying molar ratio with respect to Pd, MeOH: 15 ml (370 mmol), 1,3-butadiene: 20 g (370 mmol).*

In order to confirm their assumption of imidazolylidene complex formation, they tested imidazolium based ionic liquids protected at the C2 atom. For these, the acidic proton in 2-position was replaced by a methyl group resulting in 1-butyl-2,3-methylimidazolium ([BMMIM]) ionic liquids. In addition, with 1-butylpyridinium hexafluorophosphate [BuPy][PF$_6$] they tested a completely different cation. The obtained results of these experiments are summarized in Table 2. They

34

determined the conversion of butadiene in two different ways. Conversion A was determined by the volume of unreacted butadiene condensed in a cooling trap and conversion B by the mass increase of the liquid solution in the autoclave. The selectivity was determined by GC analysis.

**Table 2: Results for the telomerization of butadiene with methanol using different ionic liquids according to [33].**

| ionic liquid | $X_A$ | $X_B$ | $t$ | $S_{1+2}$ | $S_3$ | $S_4$ | $S_{oligo}$ | $n{:}iso$ | TON |
|---|---|---|---|---|---|---|---|---|---|
| | / % | / % | / h | | | / % | | / - | / - |
| [EMIM][NTf$_2$] | 7 | 0 | 22 | 27.5 | 0.6 | 44.7 | 27.1 | 7 | 271 |
| [BuPy][PF$_6$] | 100 | 81 | 5 | 56.8 | 28.1 | 1.0 | 14.1 | 18 | 2,403 |
| [BMMIM][BF$_4$] | 100 | 92 | 1 | 81.8 | 15.1 | 0.2 | 2.9 | 8 | 2,619 |
| [BMMIM][NTf$_2$] | 100 | 89 | 1 | 84.0 | 13.7 | 0.2 | 2.1 | 9 | 2,537 |

*Reaction conditions: 85 °C, Pd(OAc)$_2$: 30 mg (0.134 mmol), TPP: 105 mg (0.400 mmol), ionic liquid: 4 ml, MeOH: 15 ml (370 mmol), 1,3-butadiene: 20 g (370 mmol).*

For the pyridinium based ionic liquid, full conversion was achieved after 5 h. However, the selectivity toward the telomers exhibited a value of only 56.8 %. The two threefold alkylated imidazolium based ionic liquids showed full conversion already after 1 h reaction time. For both, the selectivity toward the telomers was distinctly higher compared to the pyridinium based ionic liquid while the formation of side products was decreased. However, the *n:iso* ratio was two times smaller compared to the pyridinium based ionic liquid.

The results for the 1,2,3-trialkylimidazolium based ionic liquids were comparable to those obtained with the benchmark system. The used anion did not seem to have an influence on the catalytic performance. At the end of the experiment, a biphasic reaction system was obtained for the 1,2,3-trialkylimidazolium based ionic liquids without any palladium-black. However, the two phases were both yellow in color indicating that the catalyst was dissolved in both phases. This observation was confirmed by titration experiments. The dissolution of the catalyst in the organic phase is not desirable if the catalyst should be recycled. In order to being able to recover 100 % palladium, the catalyst should only be dissolved in the ionic liquid phase. Then the two phases can be separated easily and the ionic liquid phase containing the catalyst can be reintroduced in the reaction. In order to achieve this,

Magna *et al.* tested the use of the monosulfonated phosphine ligand (TPPMS) instead of TPP. Surprisingly, when using TPPMS the reaction medium is a single-phase system at the end of reaction. They assumed that TPPMS acts as surfactant. However, when adding heptane to the reaction medium at the end of reaction a clean separation of organic and ionic liquid phase resulted. This observation was the basis for further experiments. In order to ensure a biphasic system during the reaction, they added heptane prior to the reaction. Furthermore, they worked with a stoichiometric ratio of the reactants (methanol:butadiene = 1:2). In the previous experiments a ratio of methanol to butadiene of 1:1 was applied. In order to study the partition of the palladium catalyst, they used three different phosphine ligands, namely TPP, TPPMS and the twofold alkylated phosphine ligand TPPDS. The obtained results are summarized in Table 3.

**Table 3: Results for the telomerization of butadiene with methanol using different ligands and heptane as additional extraction solvent according to [33].**

| ligand | $X_A$ | $X_B$ | $S_{1+2}$ | $S_3$ | $S_4$ | $S_{oligo}$ | $n{:}iso$ | Pd leaching | TON |
|--------|-------|-------|-----------|-------|-------|-------------|-----------|-------------|-----|
|        | / %   | / %   |           | / %   |       |             | / -       | / %         | / - |
| TPP    | 82    | 71    | 53.3      | 40.6  |       | 6.1         | 14.6      | 14.2        | 2,127 |
| TPPMS  | 74    | 66    | 70.3      | 14.1  | 0.6   | 15.0        | 13.1      | 1.9         | 1,816 |
| TPPDS  | 56    | 51    | 58.6      | 17.5  | 1.2   | 22.8        | 15.0      | 1.8         | 1,373 |

*Reaction conditions: 85 °C, 3 h, Pd(OAc)$_2$ 30 mg (0.134 mmol), ligand:Pd = 3 equiv. (0.400 mmol), [BMMIM][NTf$_2$]: 4 ml, MeOH: 7.5 ml (185 mmol), 1,3-butadiene: 20 g (370 mmol).*

In general, the applied systems were less active than without heptane. This could be caused by either the dilution effect due to the addition of heptane or the mass transfer limitation between the organic and the ionic liquid/catalyst phase. The conversion decreased with increasing grade of sulfonation of the phosphine ligand. However, with TPP the selectivity toward the telomers was distinctly lower compared to TPPMS. Magna *et al.* stated that this might be caused by the partial solubility of the TPP/Pd system in heptane where only a low concentration of methanol is present resulting in a higher formation of the dimerization product octatriene. Interestingly, the *n:iso* ratio is higher than without additional heptane for all applied ligands. For the three experiments, the palladium partition within the two phases was determined by titration. For TPP, the leaching was determined to 14.2 % of the initial palladium

whereas with TPPMS and TPPDS only 1.9 and 1.8 % of the initial palladium leached into the organic phase.

The key question of the biphasic reaction system approach is the recycling of the catalyst. This was also tested by Magna *et al.* for the TPPMS system and the results are depicted in Table 4.

The activity of the system changed slightly with each run. First, the activity and consequently the conversion increased for the first and second recycle and decreased again for the third and fourth recycle reaching the initial conversion again. Interestingly, the selectivity toward the telomers increased with each recycle whereas the formation of oligo products decreased. The improvement of the selectivities and the initial increase of the conversion might be caused by the completion of the formation of the catalytic active species. The slight decrease of conversion in the third and fourth recycle might be caused by the slight palladium leaching of 1 to 4 % per each recycle and the incomplete recovery of the ionic liquid phase after each recycle.

**Table 4: Results for the recycling of the ionic liquid/catalyst phase according to [33].**

| recycle | $X_A$ | $X_B$ | $S_{1+2}$ | $S_3$ | $S_4$ | $S_{oligo}$ | $n{:}iso$ | TON |
|---|---|---|---|---|---|---|---|---|
| | / % | / % | | / % | | | | |
| | 74 | 66 | 70.3 | 14.1 | 0.6 | 15.0 | 13.1 | 1,816 |
| 1 | 82 | 73 | 72.2 | 13.2 | 0.5 | 14.2 | 12.4 | 3,817 |
| 2 | 89 | 81 | 72.4 | 15.9 | 0.4 | 11.3 | 15.4 | 6,066 |
| 3 | 80 | 68 | 75.6 | 16.2 | 0.5 | 7.7 | 16.3 | 7,973 |
| 4 | 70 | 63 | 78.8 | 17.3 | 0.9 | 3.1 | 18.6 | 9,682 |

*Reaction conditions: 85 °C, 3 h, Pd(OAc)$_2$: 30 mg (0.134 mmol), TPPMS: 146 mg (0.401 mmol), [BMMIM][NTf$_2$]: 4 ml, MeOH: 7.5 ml (185 mmol), 1,3-butadiene: 20 g (370 mmol), heptane: 10 ml.*

Summing up the results of these first attempts to apply an ionic liquid biphasic reaction system to the telomerization of butadiene with methanol, it is obvious that this might be a promising approach where further variations of applied ionic liquids, ligands and reaction conditions might improve the reaction performance as well as the recycling of the catalyst. For this a more detailed understanding of the reaction kinetics and influencing parameters is necessary. To obtain the required data, online monitoring would be advantageous. A possible technique might be NIR spectroscopy

which will be introduced in Chapter 2.3. Furthermore, due to the large variety of ionic liquids, a reliable prediction method for ionic liquids would be desirable. A possible method will be introduced in the following chapter.

### 2.2.3  COSMO-RS as screening tool for thermodynamic properties

As already mentioned in Chapter 2.2, for a biphasic reaction system the proper choice of the catalyst phase is crucial. Amongst others, the solubility properties of the reactants and products are important for a good catalyst phase and a good extraction efficiency. From a thermodynamic point of view, the solubility and thus the distribution of a component $i$ between two phases $\alpha$ and $\beta$, e.g. catalyst phase and organic phase, can be described by the phase equilibrium which is defined by Equation (1).

$$x_i^{\alpha} \cdot \gamma_i^{\alpha} = x_i^{\beta} \cdot \gamma_i^{\beta} \qquad\qquad (1)$$

Here, $x_i^{\alpha}$ and $x_i^{\beta}$ are the molar fraction of the component $i$ in phase $\alpha$ and $\beta$ and $\gamma_i^{\alpha}$ and $\gamma_i^{\beta}$ are the activity coefficients of the component $i$ in phase $\alpha$ and $\beta$.

From Equation (1), the distribution coefficient $K_i^{\alpha\beta}$ can be derived according to Equation (2).

$$K_i^{\alpha\beta} = \frac{x_i^{\alpha}}{x_i^{\beta}} = \frac{\gamma_i^{\beta}}{\gamma_i^{\alpha}} \qquad\qquad (2)$$

In order to possess a good solubility in phase $\alpha$, the activity coefficient of component $i$, $\gamma_i^{\alpha}$, has to be small whereas the activity coefficient in phase $\beta$, $\gamma_i^{\beta}$, has to be high.

By varying the combination of anion and cation of the ionic liquid, the activity coefficient and thus the solubility properties can be influenced. Due to the large variety of possible anion-cation combinations, a determination of the solubility properties cannot be based only on experimental work. With the computational tool

COSMO-RS, the activity coefficient can be predicted a priori also for systems containing ionic liquids as shown by Klamt *et al.* [148; 149].

COSMO-RS is a quantum chemical based model that is used to predict chemical potentials in liquids and liquid mixtures in thermodynamic equilibrium [148-151]. For the calculations, only the molecular structure is required as input parameter. Thus, this method is suitable as a priori prediction tool for ionic liquids.

In Figure 9 the steps necessary for the calculation of thermodynamic properties as well as the required computational software are depicted.
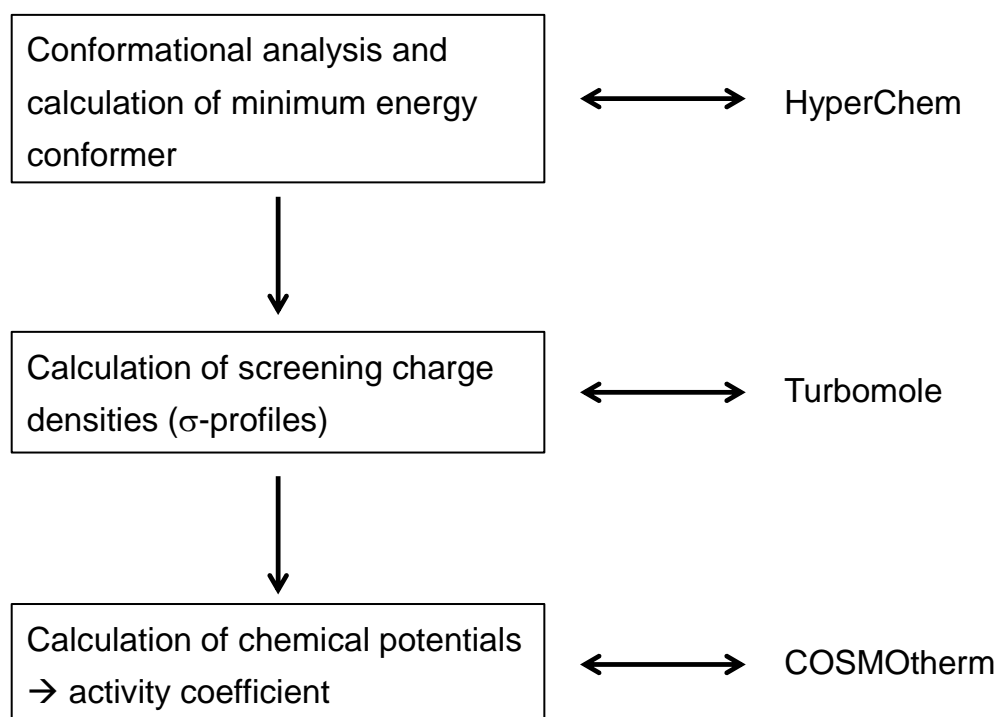


**Figure 9: Necessary steps and required computational software for the prediction of chemical potentials in a liquid mixture [152].**

The first step is the conformational analysis of the ions of the ionic liquid as well as of all substances which should be predicted using the modeling software HyperChem. The goal of the conformational analysis is to find the minimum energy conformer. For this, the molecules are assumed to be in vacuum and are rotated around single bonds. For complex molecules the number of possible conformers must be reduced so that further calculations become less extensive and time consuming. This can be achieved by the adaption of the convergence criteria of the algorithm, e.g. the

parameter which is used to distinguish whether two conformers are regarded as the same or not. This depends on their angle of torsion.

In the next step the so called "COSMO-files" are generated. These files include the $\sigma$-profiles of each conformer which is a statistical description of surface elements exhibiting the same charge density ($\sigma$ - screening charge density). The COSMO model is implemented in the software Turbomole which calculates the molecular energies of each optimized compound using the density functional theory (DFT).

The final step is the prediction of the chemical potential $\mu$ with COSMOtherm by the analysis of the charge density distribution of each component using methods of statistical thermodynamics.

For more detailed information on the approach of COSMO-RS refer to detailed literature [149-151].

## 2.3  NIR spectroscopy

Near infrared (NIR) spectroscopy was already discovered in 1800, but did not attract much interest until the mid of the last century [153; 154]. The near infrared light represents the region between visible spectral light and the mid-infrared region exhibiting a wavelength range of 780 to 2,500 nm, respectively wavenumbers of 12,821 to 4,000 cm$^{-1}$ [155]. In this region, the occurring absorption bands mainly correspond to overtones or combinations of the fundamental vibrations from the mid-infrared region. In contrast, for the application of classical IR-spectroscopy the light of the mid-infrared region is used where the fundamental vibrations are observed [156].

In general, the intensity of the NIR absorption bands is affected by the change in the dipole moment and the anharmonicity of the bond. The largest vibrations and deviations from harmonic behavior are observed for the lightest existent atom, namely the hydrogen atom [153]. This means that in the NIR region absorption bands of hydrogen-bonds or bonds of other light atoms are observed, e.g. C-H, N-H, O-H, S-H. As the absorption bands observed in the NIR region are overtones or combinations of the fundamental vibrations and are induced by only a few functional groups, the absorption bands of NIR light are very weak, broad and tend to overlap. An example for typical NIR spectra with the broad and overlapping peaks is represented in Figure 10.
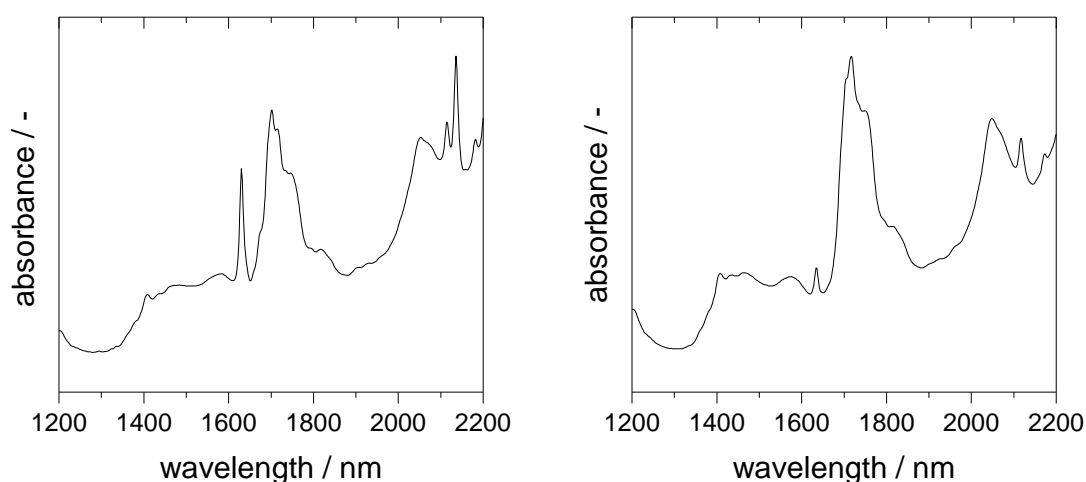


**Figure 10: Example for NIR spectra with its broad and overlapping peaks of the telomerization at the start (left) and the end (right) of reaction.**

Furthermore, the change in absorption caused by varying concentrations is very small. In consequence, NIR spectroscopy suffered from the possibility of extracting exact information out of the observed absorption bands. However, with the increase of computational potentials and the development of new mathematical methods, the data treatment of multivariate data sets became possible. This is the reason why from the mid of the last century the NIR spectroscopy attracted broad interest as a tool for qualitative as well as quantitative analysis.

A spectrum represents many absorbance/transmittance data dependent on the wavelength and can be understood as a multivariate data set. Thus, mathematical and statistical methods are very important for the analysis of NIR data. These methods are called chemometrics. The latter is defined as a discipline using different mathematical and statistical methods for the treatment of multivariate data in order to get as much relevant information as possible from these data sets [157-159].

As within this thesis, NIR spectroscopy was used only for quantitative analysis, the latter will be introduced in the following. For more general information on qualitative as well as quantitative analysis refer to detailed textbooks [159-161].

The quantitative analysis of the recorded spectra starts with a pretreatment of the data to enhance desired information and reduce the influence of undesired information such as e.g. scattering. The removal of undesired information is required in order to get more simple and robust calibration models. Examples of classical pretreatment for NIR spectra are normalization, derivatives, multiplicative scatter correction (MSC).

As the recorded spectra contain a large amount of information, the next step is the reduction of variables. The mostly used method to reduce the dimension of the original data to a few variables exhibiting relevant information is the principal component analysis (PCA). Here, new axes, which are named principal components, are created by looking for the directions with the largest variability of the data. By this, the relevant information of the multivariate data set are filtered and presented by an often drastically reduced number of variables.

With the multivariate analysis method or regression method, a calibration model will be created. Once this model is created, it has to be validated. For this, the data used for the calibration are divided in a calibration set and a test set. In general, within the multivariate analysis non-linear as well as linear methods exist and are used depending on whether the spectral data are related to the target property, e.g.

concentration, in a linear or non-linear fashion. The principal component regression (PCR) and the partial least-squares (PLS) regression are the methods which are mainly used in NIR spectroscopy. Using the PCR method, a link between the principal components and the target property is created. This means that the principal components must not correlate with the target property. In contrast, the PLS regression method creates principal components by linking the spectral information with the target property. The advantage of PLS compared to PCR is that the defined principal components definitely contain strong and relevant information on the target property. Because of this important advantage, the PLS regression method will be used within this thesis.

The NIR spectroscopy is a versatile analysis method but in order to get a robust calibration model every variation, e.g. pressure, temperature, as well as the whole concentration range and every component present in the reaction have to be considered in the model. Although, the effort of developing a good calibration model is high, the fast development of the chemometrical methods shed new light on the NIR spectroscopy due to its convincing characteristics. As every optical measuring technique, NIR spectroscopy is a very fast non-invasive and non-destructive technique. Furthermore, no sample pretreatment is required. Due to the fibre optics and the robustness of NIR equipment at-line, online and inline process control can be realized.

The wide range of applications shows the relevance of NIR spectroscopy as an analytical tool. NIR spectroscopy is used not only in the pharmaceutical [154] or environmental sector, but also in the petrochemical sector [162-170]. NIR spectroscopy is also applied for e.g. kinetic studies of polymerization reactions [171] or in heterogeneous catalysis research [172]. The latter study by Sasol Technology showed the successful application of NIR spectroscopy for kinetic studies. They managed to follow the progress of a heterogeneously catalyzed reaction in real-time and inline using NIR spectroscopy combined with chemometrical methods. However, most applications of NIR spectroscopy in the chemical field concentrate on the petrochemical sector.

## 2.4 Objective of this work

Basic aim of this thesis was the development of a continuous process for the telomerization of butadiene with methanol including preliminary experiments, planning and set-up of a rig and the transfer from a batch to a continuous process. The immobilization of the catalyst should be realized by applying a liquid-liquid biphasic reaction system with ionic liquids. The main challenge of the immobilization is the reactant methanol itself. Methanol acts as good solvent for the catalyst as well as for the product, two contradictory aspects for a successful catalyst immobilization.

In addition, the feasibility of inline process control by NIR spectroscopy for a homogeneously catalyzed reaction should be exemplarily shown for the telomerization of butadiene with methanol. The application of NIR spectroscopy in reaction mixtures with ionic liquid should be tested as well.

For a successful development of a continuously working biphasic reaction system, the behavior of the reaction without ionic liquid should be understood. For this, the reaction performance of two relevant catalyst/ligand systems in combination with two different feeds should be comparatively studied in monophasic experiments. The optimization of reaction conditions should be achieved by investigating the influence of different parameters. The commissioning of the loop reactor should be carried out by the transfer and scale up of the telomerization reaction including reproduction of batch experiments and first continuous experiments without catalyst recycling.

The next part of this thesis focused on the development of the liquid-liquid biphasic reaction system. Preliminary to the experimental work, the extraction efficiency of different anion-cation combinations should be determined using the computational tool COSMO-RS. An ionic liquid screening combined with a ligand screening should be carried out in the batch autoclave. The aim was to find ionic liquid-ligand combinations exhibiting a low Pd-leaching and thus a high immobilization potential. As the catalyst stability is an important factor for continuous processes, the catalyst stability should be tested in recycling experiments.

With the knowledge from the batch experiments, the transfer to the continuously working loop reactor should be carried out. The criteria for a successful continuous process are long catalyst stability, low catalyst leaching, high selectivity and adequate turn over frequencies (TOFs).

# 3 Experimental

In the following, general working techniques, the used experimental set-ups and procedures are described in detail. In addition, the isolation of the main product 1-Mode as well as applied analytical methods and procedures are shown.

## 3.1 General working techniques

The complete experimental work was operated under inert atmosphere as the telomerization reaction is oxygen sensitive (see Chapter 4.2.2.1). The used catalyst and ligand precursors were stored under inert atmosphere in a Plexiglas® Glovebox (GS GLOVEBOX Systemtechnik GmbH, Argon 4.6). For the start of reaction, a defined mass of catalyst and ligand were transferred to a Schlenk flask in the Glovebox and afterwards dissolved in a defined mass of methanol. The methanol solutions of catalyst and ligand, base, dibutylether and all other used solvents were handled and stored using Schlenk technique. The ionic liquids were dried overnight at 80 °C under high vacuum (p < 0.1 mbar). The chemicals used in this thesis are summarized in Appendix 7.1, Table A 3. The ligand [BMMIM]-TPPMS was synthesized according to [173]. The structural analysis by NMR spectroscopy is shown in Appendix 7.2. Applied formula and definitions are listed in Appendix 7.3.

## 3.2 Procedure of telomerization reaction experiments

Within this work, different reactors were used. Preliminary experiments were carried out in a batch autoclave. Based on the knowledge created from these experiments, continuative batch experiments as well as continuous experiments were operated in the loop reactor. The set-up of both reactors and the experimental procedure are described in detail in the following.

### 3.2.1 Batch autoclave

### 3.2.1.1 Experimental set-up

The preliminary batch experiments were carried out in a 250 ml batch autoclave. The flowsheet of this reactor is shown in Figure 11.
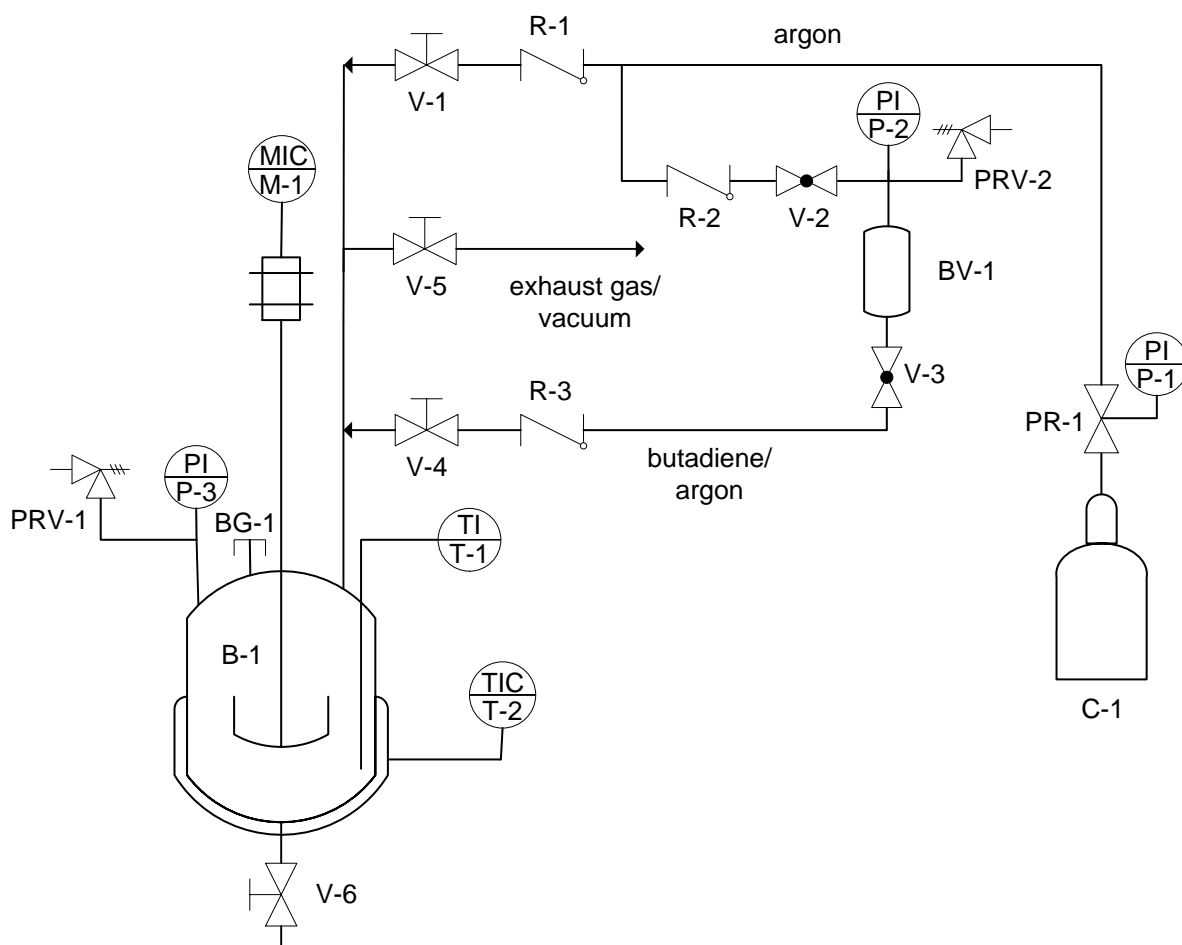


**Figure 11: Flowsheet of the batch autoclave.**

The reaction vessel **B-1** consisted of Hastelloy C and was equipped with a four-blade gas entrainment stirrer **M-1**, a pressure gauge **P-3**, a pressure relief valve **PRV-1** and a heating jacket. The temperature in the vessel was measured with a thermocouple **T-1** and controlled by a temperature regulator **T-2** (Horst GmbH, HT MC1) connected with the heating jacket. Through blind plug **BG-1**, the reagents could be introduced into the reactor under an argon counter flow. All experiments were carried out in a liquid phase. To liquefy 1,3-butadiene, the pressure in the autoclave had to be higher

than the vapor pressure of 1,3-butadiene at reaction temperature. The pressure was adjusted with the inert gas argon. The argon gas cylinder **C-1** was equipped with a pressure reducer **PR-1** and a pressure gauge **P-1** and was connected to the periphery of the reactor. The inert gas could either be directly led to the reactor by passing valve **V-1** or was used to introduce 1,3-butadiene to the reaction vessel by passing the valves **V-2**, **V-3**, **V-4** and the ballast vessel **BV-1** filled with 1,3-butadiene. The latter was equipped with a pressure relief valve **PRV-2** and a pressure gauge **P-2**. To avoid undesired backflow of 1,3-butadiene or other gaseous reagents into the argon cylinder, the inlet lines were equipped with nonreturn valves **R-1**, **R-2** and **R-3**. Samples were taken using fine valve **V-6**. Via valve **V-5**, the exhaust gas was led to the hood. In addition, vacuum could be connected to valve **V-5** for the cleaning procedure.

### 3.2.1.2 Experimental procedure

The batch autoclave was evacuated overnight before every experiment. For reaction start, the reactor was filled with a slight argon flow via valve **V-2**. The required amount of catalyst and ligand solution, methanol, base, dibutylether, hexane, toluene and ionic liquid were filled into syringes and introduced into the autoclave under an argon counter flow through the open fitting of blind plug **BG-1**. After reattachment of the blind plug and closure of valve **V-2**, the stirrer was set to 400 rpm for experiments without ionic liquids and to 800 rpm for biphasic experiments and the reaction mixture was heated to reaction temperature.

During the heating period, the required amount of 1,3-butadiene or the applied diluted feed, synthetic crack-$C_4$ (s$CC_4$), was transferred from the gas cylinder to the ballast vessel by means of a cooled HPLC pump. The ballast vessel was fixed in a metal stand, placed on a scale and connected with a capillary tube to the gas cylinder. After reaching the required mass, the ballast vessel was disconnected from the gas cylinder, reattached to the experimental set-up of the autoclave and pressurized with the reaction pressure. For this, argon was led via valve **V-2** to the gas cylinder whereas valve **V-3** was still closed. The reaction pressure was set to 15 bar except for the experiments at 90 °C where the pressure was set to 18 bar for

liquefaction of butadiene. For the experiments with additional 1-butene, *iso*-butene or *n*-butane, 1,3-butadiene was transferred to the ballast vessel first. Afterwards, the latter was connected to the gas cylinder of the desired second gas which is then added to the ballast vessel already filled with 1,3-butadiene.

As soon as the reaction mixture in the autoclave equilibrated at the desired reaction temperature, the valves **V-3** and **V-4** were opened simultaneously. This moment was defined as reaction start ($t = 0$). The addition of liquefied 1,3-butadiene at room temperature caused a sudden temperature drop of around 15 to 20 °C. The required reaction temperature was restored within maximal 5 minutes with a maximal observed overheating of around 5 °C.

During the reaction time, the first sample was taken after 5 minutes in order to determine the vinylcyclohexene already present in the gas cylinder of 1,3-butadiene or sCC$_4$. All other samples were taken every 30 minutes relative to the reaction start. During the ionic liquid screening experiments and the recycle experiments, no samples were taken during the reaction.

For recycling experiments, a valve was connected to blind plug **BG-1** through which the reaction pressure and the unreacted butadiene were slowly released at the end of the experiment. For the separation of the organic phase, the reactor was cooled down to ambient temperature, detached from the experimental set-up under a continuous flow of argon and the product phase was decanted with a syringe. In order to avoid oxygen contamination, the syringe was purged with argon for at least three times. The reactor was then filled with fresh reactants and reattached to the set-up in order to start the next experiment. After the initial experiment and its first recycle, the catalyst phase had to be stored overnight. For this, the product phase was decanted and only methanol was added to the catalyst phase. The reactor was reattached to the set-up and pressurized with argon for storage overnight.

At the end of each experiment, the heating and the stirrer were switched off and valves **V-2** and **V-3** were closed. The reaction pressure was released to the hood via valve **V-5** and the remaining reaction mixture was discharged via valve **V-6** to a flask. The autoclave was removed and cleaned with ethanol. After reattachment of the autoclave, a pressure test was carried out at 20 bar for 1 hour. If the autoclave was tight, the pressure was released and the autoclave was evacuated for at least 1 hour in preparation of the next experiment.

### 3.2.1.3   Sample treatment

For the experiments without ionic liquids, the samples were diluted with methanol and analyzed immediately by offline GC analysis.

For the experiments with ionic liquids, the samples had to be pretreated before analysis in order to ensure that no ionic liquid was transferred onto the GC column. For further extraction, hexane was added to the samples resulting in a well-defined phase separation. The upper organic phase was taken, diluted with methanol and analyzed by offline GC analysis. In most experiments with ionic liquids, the internal standard dibutylether was not added to the reaction mixture. Instead, dibutylether was used as external standard afterwards.

Due to the instant degassing of butadiene, only the concentration of the products was determined for the batch experiments analyzed with offline GC.

As explained in Chapter 2.1.2.1.3, 4-vinylcyclohexene is formed uncatalyzed in a Diels-Alder reaction. Due to the storage of liquefied butadiene in steel cylinders, 4-vinylcyclohexene was already present in the butadiene feed. This was considered in the analysis of the experimental data by subtracting the initial 4-vinylcyclohexene amount. The latter was determined from a sample which was taken 5 minutes after reaction start.

### 3.2.2   Loop reactor

### 3.2.2.1   Experimental set-up

Within this thesis, a loop reactor was planned and set-up. This type of reactor was, e.g. successfully used by Eichmann [174; 175] for a biphasic dimerization of propene and 1-butene in ionic liquids. The principle of this reactor type is based on the continuous recycling of the catalyst/reactant phase due to the separation of the product phase. The advantage of the loop reactor is that it can approach both ideal reactor concepts, PFTR und CSTR, depending on the circulation flow of the pump. So, a wide range of residence time distributions can be adjusted within the same reactor. The planning of the reactor was based on the condition, that monophasic

and biphasic as well as batch and continuous experiments could be operated. Thus, all experiments became most comparable to each other. Another advantage of the loop reactor is that the analytic devices can be easily integrated into the loop. The flowsheet of the loop reactor is shown in Figure 12.

The feed lines of the loop reactor were equipped with three HPLC pumps (2x Techlab, mini pump; Knauer, Compact HPLC pump) with cooled pump head. The cooling was provided by a cryostat (Huber, minichiller). The feed mixture containing methanol, base, catalyst and ligand for batch experiments and methanol for continuous experiments was pumped to the inlet of the reactor via a filter **F-2** by HPLC pump **HP-2**. The liquefied butadiene was fed to the reactor via a filter **F-3** by HPLC pump **HP-3**. After passing the nonreturn valves **R-2** and **R-3**, both inlet lines were heated to reaction temperature before entering the loop (**T-1** and **T-3**). With HPLC pump **HP-1**, hexane could be added for continuous biphasic experiments as additional extraction solvent. The hexane line was also equipped with a filter **F-1** and a nonreturn valve **R-1**.

The whole loop was electrically heated in order to keep the reaction temperature constant. The heating lines (Horst GmbH) were connected each to a Eurotherm regulator. The static mixer guaranteed mixing of the biphasic as well as of the monophasic reaction system. For safety aspects, the loop reactor was equipped with different pressure release valves (**PRV-1** to **PRV-5**). The reaction system was circulated within the loop by the circulation pump **CP** (Gather Industrie GmbH). The actual flow rate was measured by a turbine flowmeter (**F-1**, Kobold Messring GmbH) mounted directly behind the circulation pump.

Different analytical devices were integrated in the loop by two bypasses which could be disconnected by valves **V-7**, **V-8**, **V-9** and **V-10**. By the use of the throttle valves **THR-1** and **THR-2**, the reaction mixture passed the analytical lines. In reference to SYNFLOW deliverable D4.6, Evonik observed the temporary occurrence of turbidity in the reaction system. They noted a correlation between this turbidity and the activity of the system. In order to further investigate this observation, the analytical line of the new loop reactor was equipped with a turbidity sensor (**TURB**, Optek, product series C4000). The conductivity which seemed to be related to the conversion of methanol was measured by a conductivity sensor (**CON**, ABB, product series AX400).
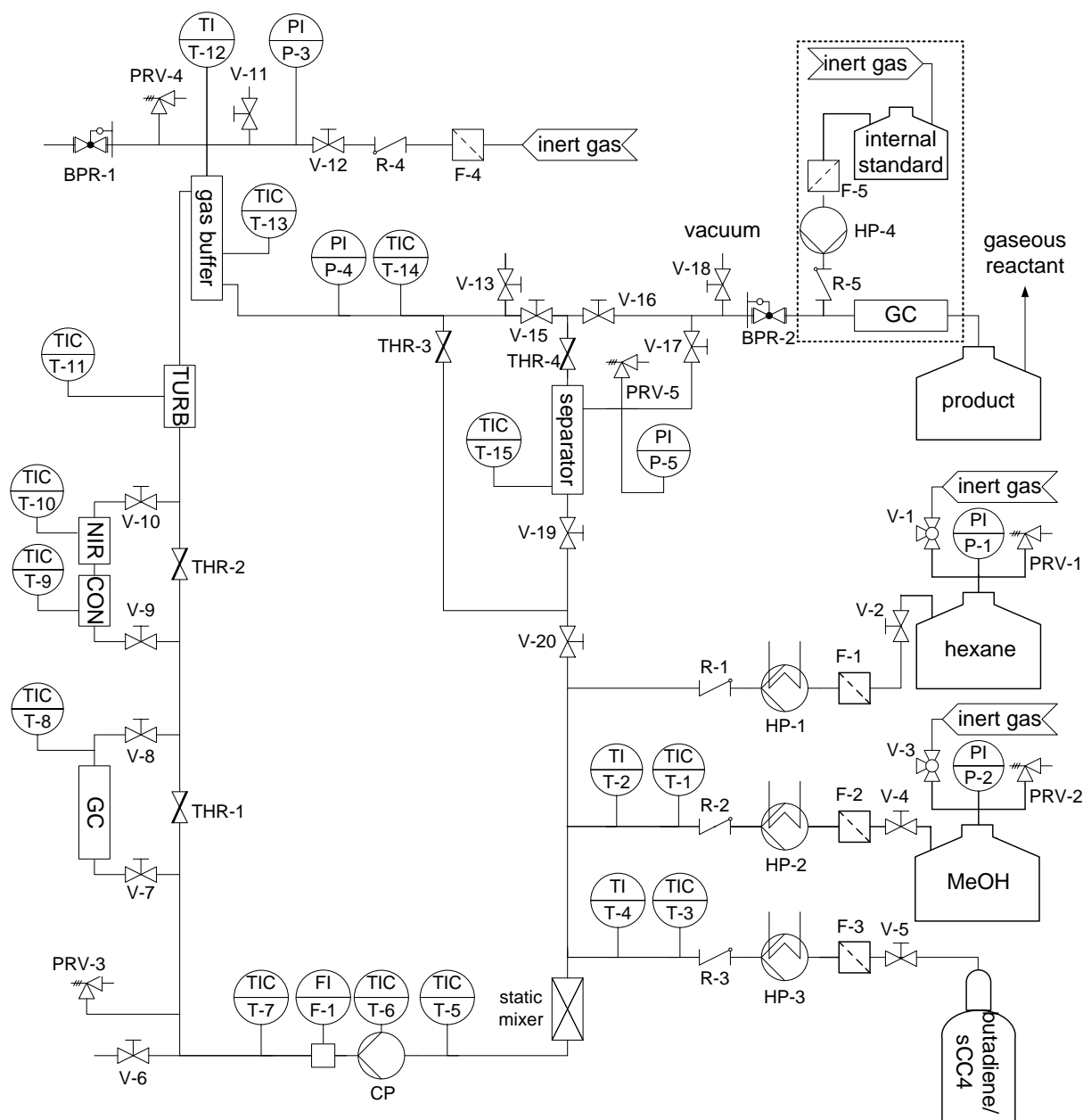
**Figure 12: Flowsheet of the loop reactor.**

For the online analysis of the reactants' composition, an optical measuring cell (Hellma) connected with a NIR spectrometer (**NIR**, Polytec) was integrated. For monophasic experiments without ionic liquids, the online GC (**GC,** Bruker, 450-GC) was installed in the first bypass. For biphasic experiments, the online GC was connected in the outlet stream and additional feeding of an external standard via HPLC pump **HP-4** was used for quantitative determination of the composition in the outlet stream (see area surrounded by dotted lines in the flowsheet).

The loop reactor was equipped with a gas buffer to realize additional dosing of 1,3-butadiene or methanol in batch operation by replacing the inert gas via back pressure regulator **BPR-1**.

The integrated settler enables the separation of the product from the catalyst phase. For batch experiments, the separator was bypassed due to the closing of valves **V-15** and **V-19**. For continuous experiments valves **V-15** and **V-19** were opened allowing the reaction mixture to pass the separator. In the latter, the heavier ionic liquid/catalyst phase settled due to gravity and the product phase could be removed from top. The removing of the product was controlled by the back pressure regulator **BPR-2** via **V-17**. The product stream was separated from the remaining butadiene by pressure release.

For cleaning procedure, the loop reactor could be connected to vacuum via valve **V-18**.

### 3.2.2.2   Experimental procedure for batch experiments

For starting a batch experiment in the loop reactor, the desired reaction temperature was set and the reactor was pressurized with 5 bar argon. The temperature of the cryostat for the cooled HPLC pump was set to -1 °C. Valves **V-15** and **V-19** were closed for bypassing the separator.

The required amounts of catalyst and ligand precursors were dissolved in the required amount of methanol in a Schlenk flask. As soon as the powder was dissolved, the required amount of internal standard and base were added and stirred for 5 minutes followed by the transfer of the solution to a Schott flask. The latter was connected to its fitting and charged with 0.1 bar excess pressure. The flow rates of the two HPLC pumps were adjusted to the desired ratio of butadiene to methanol. The amounts of catalyst and ligand precursors, base and dibutylether dissolved in methanol were calculated based on the desired flow rate of the methanol pump to reach the right reaction conditions. The time required for filling the reactor with a volume of about 350 ml depended on the adjusted flow rates of the HPLC pump and differed between 5 and 10 minutes. It was assumed that the reaction started with the

first contact of butadiene and the catalyst/ligand solution. Thus, the start of the feeding was defined as reaction start ($t = 0$).

As soon as the loop reactor was filled, the HPLC pumps were switched off, the reactor was pressurized to reach the required reaction pressure (15 to 18 bar) and the circulation pump was switch on. The latter was set to, if not mentioned otherwise, 1,000 rpm resulting in a flow rate of 1 l·min$^{-1}$. However, with the closing of the throttle valves **THR-1** and **THR-2** to ensure the flow through the analytical lines, the flow rate was reduced to a value of 0.7 to 0.8 l·min$^{-1}$.

Every 15 to 20 minutes, the online GC injected a sample. With the NIR spectroscopy, it was possible to record a spectrum every second for the analysis of the composition of the reaction mixture.

Most of the batch experiments were run between 15 and 20 hours. At the end of an experiment, the pressure was released via valve **V-11** followed by discharging the remaining reaction mixture via valve **V-6** to a flask. For the cleaning procedure, ethanol was pumped to the loop reactor by the HPLC pump **HP-2** and circulated for 5 to 10 minutes using the circulation pump **CP**. This procedure was repeated two times. For the evacuation of the loop, vacuum was connected to valve **V-18** and the valves **V-15**, **V-17** and **V-19** had to be opened. Vacuum was applied for two hours. Until the next experiment was started, the evacuated reactor was pressurized with argon.

### 3.2.2.3 Experimental procedure for continuous experiments

For starting a continuous experiment, valves **V-15** and **V-19** were opened and **V-16** was closed so that the product phase could be removed from top via **V-17** and **BPR-2**. The latter was set to an opening pressure of 18 bar. The temperature of the cryostat for the cooling of the HPLC pumps was set to -1 °C. Catalyst and ligand were dissolved in the required amount of methanol in a Schlenk flask and the desired amount of ionic liquid and base were added. All components were calculated in a way to adjust the required ratio related to butadiene for the reaction volume of 800 ml. This mixture was filled into the loop with a syringe under a slight flow of

argon via valve **V-13**. The reaction temperature was set and the reactor was pressurized with 5 bar argon.

For completing the filling with butadiene and hexane, the calculated amounts of each were transferred via the HPLC pumps. After filling the reactor with all components in the right ratio, the circulation pump **CP** was switched on and the flow rates of the three HPLC pumps were set in a way to adjust the ratio of butadiene, methanol and hexane and the feeding velocity for the continuous experiments.

The determination of the composition was carried out by NIR spectroscopy directly in the loop reactor and with the online GC in the outlet stream. Quantification was realized by adding an external standard via HPLC pump **HP-4**. In order to control the online measurements, samples were taken as well for offline GC analysis. For ICP analysis, samples were collected for a time period of 1 to 2 hours.

The procedure at the end of an experiment for discharging and cleaning the loop was the same as for batch experiments, see Chapter 3.2.2.2.

## 3.3  Experimental validation of COSMO-RS results

For experimental validation of the COSMO-RS results, a reaction without ionic liquid was carried out using TPP as ligand. The reaction was conducted until full conversion of butadiene was reached. The resulting reaction mixture consisted of unreacted methanol and products. A defined amount, e.g. 2 ml, was transferred into a thin test glass and ionic liquid was added until a second phase was observed. This amount was compared for different ionic liquids. The solid ionic liquids were added to the reaction mixture and dissolved by the methanol present.

## 3.4  Isolation and purification of 1-Mode

For the analysis of the composition of the reaction mixture, a calibration of the used GC with the components was required. As the main product 1-Mode is commercially unavailable, the isolation of pure 1-Mode from the product mixture was necessary.

This was realized by fractional vacuum distillation. The procedure of product isolation will be described in detail in the following.

### 3.4.1 Pretreatment of the product mixture

Before vacuum distillation could be performed, surplus methanol had to be removed from the product mixture in a first preparative distillation step (80 °C, $p = p_{atmosphere}$). During this distillation step, the catalyst precipitated to palladium-black probably due to the lack of solvent, the high temperature and the oxygen present by non-inert treatment.

The residual methanol was removed by high vacuum ($p < 0.1$ mbar) at room temperature overnight. In order to separate the precipitated catalyst from the product mixture, the latter was heated to 60 °C under high vacuum to transfer it to a new, clean flask. The palladium catalyst was left as black precipitate whereas the product mixture was colorless.

### 3.4.2 Fractional vacuum distillation

Fractional vacuum distillation was performed under high vacuum ($p < 0.1$ mbar). All fractions were taken as soon as a temperature change in the gas phase was noticeable resulting in three different fractions. The composition of all fractions was determined by GC and NMR analysis. The last fraction (fraction 3) contained almost pure 1-Mode but was further purified by a second distillation step. As no further change in temperature was remarkable, four fractions were collected in time steps of 20 minutes. The GC analysis showed that from fraction 3-1 to 3-4, the concentration of 3-Mode decreased steadily. However, absolute purity of 1-Mode could not be obtained. This is probably caused by the physicochemical similarity of 1- and 3-Mode leading to almost the same boiling points. Fraction 3-4 was identified as almost pure 1-Mode with trace amounts of 3-Mode (< 0.4 mol%).

## 3.5 Analytical methods

### 3.5.1 Gas chromatography analysis

Quantitative analysis of the reaction mixture was performed using gas chromatography. Offline gas chromatography was used to analyze the samples from the experiments in the batch autoclave and the control samples of the continuous experiments. With online gas chromatography, the composition of the reaction mixture in the loop reactor was determined.

#### 3.5.1.1 Offline gas chromatography

The samples were analyzed with a Varian 3900 gas chromatograph (GC) equipped with a wall-coated open tubular fused silica column (FS-OV-1-PONA, 50 m x 0.2 mm; C-S Chromatographie Service GmbH) or a column manufactured by Agilent Technologies (CP-Sil PONA CB 50 m x 0.21 mm x 0.5 µm). The injector temperature was set to 250 °C. Helium was used as carrier gas with a flow rate of 1 ml·min$^{-1}$. The products were analyzed by a flame ionization detector (FID) with a temperature of 300 °C. The applied temperature profile is shown in Table 5.

**Table 5: Applied temperature profile of the offline GC.**

| temperature / °C | rate / °C·min$^{-1}$ | hold / min | total / min |
|:---:|:---:|:---:|:---:|
| 50 | - | 2 | 2 |
| 204 | 14 | 1 | 14 |
| 250 | 20 | 4.7 | 21 |

#### 3.5.1.2 Online gas chromatography

The reaction mixture within the loop reactor was analyzed online with a Bruker 450 gas chromatograph equipped with a Restek fused silica column (Stabilwax, 30 m x 0.32 mm). The GC was connected to a liquid sample loop and the sample was taken

by a liquid sample injection valve (M.A.T. Mess- und Apparatetechnik) with an injection volume of 0.1 µl. The injector temperature was 77 °C to avoid polymerization in the injection valve. Helium was used as carrier gas with a flow rate of 1 ml·min$^{-1}$. The products were analyzed by a flame ionization detector (FID) with a temperature of 300 °C. The applied temperature profile is shown in Table 6.

**Table 6: Applied temperature profile of the online GC.**

| temperature / °C | rate / °C·min$^{-1}$ | hold / min | total / min |
|---|---|---|---|
| 50 | - | 2 | 2 |
| 200 | 30 | 6 | 13 |

### 3.5.1.3 Gas chromatography – mass spectrometry (GC-MS)

Qualitative analysis and the correlation of the peaks detected in the GC with the corresponding substance were performed using a Varian 450 GC equipped with a Varian VF-5ms column (30 m x 0.25 m) and a Varian 220 MS (ion trap mass spectrometer) with electron ionization.

### 3.5.2 Nuclear magnetic resonance spectroscopy (NMR)

NMR spectra were recorded using a JEOL ECX +400 spectrometer (JEOL Ltd., $^{1}$H: 400 MHz, $^{13}$C: 100 MHz, $^{31}$P: 162 MHz) at room temperature and DMSO-D6, CDCl$_3$ or MeOD as solvents.

### 3.5.3 Inductively coupled plasma – atom emission spectroscopy (ICP-AES)

The Pd content in the organic product mixture was analyzed by ICP-AES to identify catalyst leaching using a SPECTRO CIROS CCD (SPECTRO Analytical Instruments GmbH). The calibration was carried out with plasma standard solutions of Pd.

For batch experiments, the immobilization of the Pd-catalyst in the ionic liquids and the leaching into the organic phase were determined. For continuous experiments, the outlet stream was collected for a defined time (1 to 2 hours) and analyzed in the same way as the organic samples from batch experiments.

As the analysis of organic samples with ICP is more difficult and less exact compared to aqueous solutions, the samples were prepared in a way allowing to work in the end with aqueous solutions.

For the ionic liquid samples, all remaining organic substances were removed under high vacuum. A defined amount of the remaining ionic liquid sample was weighed into a 100 ml volumetric flask.

The organic samples were filled in a flask and the whole organic phase was removed by vacuum distillation under high vacuum. The remaining residues were analyzed.

After this pretreatment, all samples were solubilized in boiling aqua regia with a ratio of concentrated nitric acid to concentrated hydrochloric acid of 1:3. The samples were dissolved in 100 ml of distilled water and immediately analyzed by ICP.

With the determined Pd amount, the leaching of the initial Pd can be calculated according to Equation (3).

$$\text{Pd-leaching} = \frac{m_{Pd\_i}}{m_{Pd\_tot}} = \frac{m_{Pd\_i}}{m_{Pd\_org} + m_{Pd\_ionic\ liquid}} \qquad (3)$$

The total amount of Pd can be determined by the sum of the measured Pd amounts present in the two phases. In addition, the total amount should equal the initial Pd content. Checking the mass balance was possible by comparing the determined total amount with the initial amount of Pd.

### 3.5.4  Near-infrared spectroscopy

NIR spectroscopy was carried out using a Polytec PSS 2220 spectrometer which was connected via optical fiber cables to a pressure-tight optical measuring cell (Hellma 663.501 Durchflusszelle) equipped with sapphire windows. The spectra were recorded in a wavelength range between 1,200 and 2,200 nm. The increment was adjusted to 2 nm. An integration time of 200 µs was applied and the number of accumulations was set to 100.

### 3.5.5  Turbidity measurement

The turbidity measurements were carried out using a pressure-tight optical measuring cell equipped with sapphire windows (Optek TF16-N sensor). The measuring cell was connected to a photometric converter (Optek, C4000 converter) where the incoming light was analyzed.

### 3.5.6  Conductivity measurement

The conductivity measurements were carried out using a conductivity sensor incorporated in a pressure-tight measuring cell (ABB, AC200 2-Elektroden Leitfähigkeitsmesszelle). The sensor was connected to a conductivity analyzer (ABB, AX400 converter).

# 4   Results and discussion

The results presented in this thesis are basically split into three parts. As a first part the development and validation of the NIR calibration model as well as its feasibility in the telomerization reaction will be introduced. Furthermore, the results of the telomerization experiments are divided according to the applied approaches into results of the telomerization reaction without ionic liquids and in biphasic reactions with ionic liquids.

## 4.1   NIR spectroscopy applied on the telomerization reaction

One aim of this thesis was to test the applicability of NIR spectroscopy for determining the amount of components present in a reaction mixture in homogeneously catalyzed reactions. For the determination of concentrations, a calibration of the applied NIR spectrometer was required. In order to check the quality of the developed calibration models, further validation steps were carried out. Furthermore, the applicability of NIR spectroscopy for reaction mixtures containing ionic liquids was studied. This application would be a great advantage as the online determination of the concentration of organic compounds in a reaction mixture with ionic liquids is not possible in the reaction mixture itself due to the non-volatility of ionic liquids and the resulting limitation using gas chromatography.

### 4.1.1   Development of a calibration model

As this was the first application of NIR spectroscopy at the institute of the Wasserscheid group as well as for this reaction, different strategies for the development of calibration models were tested. Regarding the different applied feeds within this thesis, namely butadiene and $sCC_4$, a technical feed of around 45 mol% butadiene and 55 mol% inerts (butenes and butanes), three different calibration models were developed. One calibration model was constructed by using only experiments carried out with $sCC_4$, another one only with experiments carried out

with pure butadiene. The third calibration model was developed using a combination of the experiments with the two feeds.

In order to develop a calibration model, the design of experiments used for the calibration must be carried out in a way to be most representative for all experiments which should be analyzed by applying this NIR calibration model. During the experiments used for calibration, NIR spectra were recorded and reference values were determined by the online GC. The experiments were conducted for around 18 hours and full conversion was reached resulting in around 115 spectra. The whole possible concentration range of all components was covered during these experiments which is very important for a robust calibration model.

The development of the calibration model was then carried out with the calibration wizard of the SensoLogic© software (SensoLogic GmbH, Norderstedt, Germany). As a first step, the recorded spectra had to be divided into a calibration and a test set. A recommended ratio is 70:30. The next step is the application of chemometrics on the calibration set. Here, the data were pretreated by calculation of the first derivative and the amount of data was reduced using principal components analysis (PCA). Finally, the calibration model was constructed by the application of the method of partial least squares (PLS) and is deposited in the software without a direct output of the model. An explicit correlation between spectra and concentration data is not available for the user of the software. After the development of the calibration model, the latter was validated with the retained test set data. The concentration values were determined by applying the calibration model and afterwards compared to the reference values. The comparison is illustrated by true-predicted plots for every component and each of the three calibration strategies, see Figure 13 to 15. In these plots, the reference values, here represented in mass fraction, were plotted versus the predicted mass fractions by NIR. The true-predicted plots for the main product 1-Mode are depicted in Figure 13. Besides the obtained values, a bisecting line representing a 100 % accordance of true and predicted values as well as a deviation of 5 % representing the experimental error are plotted.

By applying the different feeds, different concentration ranges are covered. This is caused by the lower concentration of butadiene in the $sCC_4$ due to the dilution by inerts. The calibration models for each feed exhibited very good correlation of the predicted mass fractions and the reference values as most of the values lay within the 5 % deviation. If the experiments with $sCC_4$ and pure butadiene were combined

to develop a calibration model, the spreading around the bisecting line was larger. This is probably caused by inert components present in the $sCC_4$ feed as the latter also exhibit signals in the spectra. Due to the broad and overlapping peaks, the characteristic signals for the components of interest become more indistinct.



**Figure 13: Validation of the NIR calibration models for 1-Mode with the spectra of the test set presented in true-predicted plots (○ 1-Mode, — bisecting line, --- 5 % deviation).**

In consequence, the principal components found for the spectra with pure butadiene should be slightly different compared to those with $sCC_4$. For the calibration model with $sCC_4$, the signals of the inerts can be understood as a disturbance of the system that had to be filtered off. This was also successfully realized as the correlation for the calibration model with $sCC_4$ was very good. However, when combining the

experiments of both feeds, the software has to combine slightly different principal components resulting in a larger deviation. This problem could be overcome by using more data for the calibration. Furthermore, this observation shows the sensitivity of the NIR calibration model and that every disturbing signal and change of the system has to be considered in the calibration model.

Another limitation of the NIR spectroscopy will be shown by the discussion of the true-predicted plots obtained for 3-Mode which are presented in Figure 14.
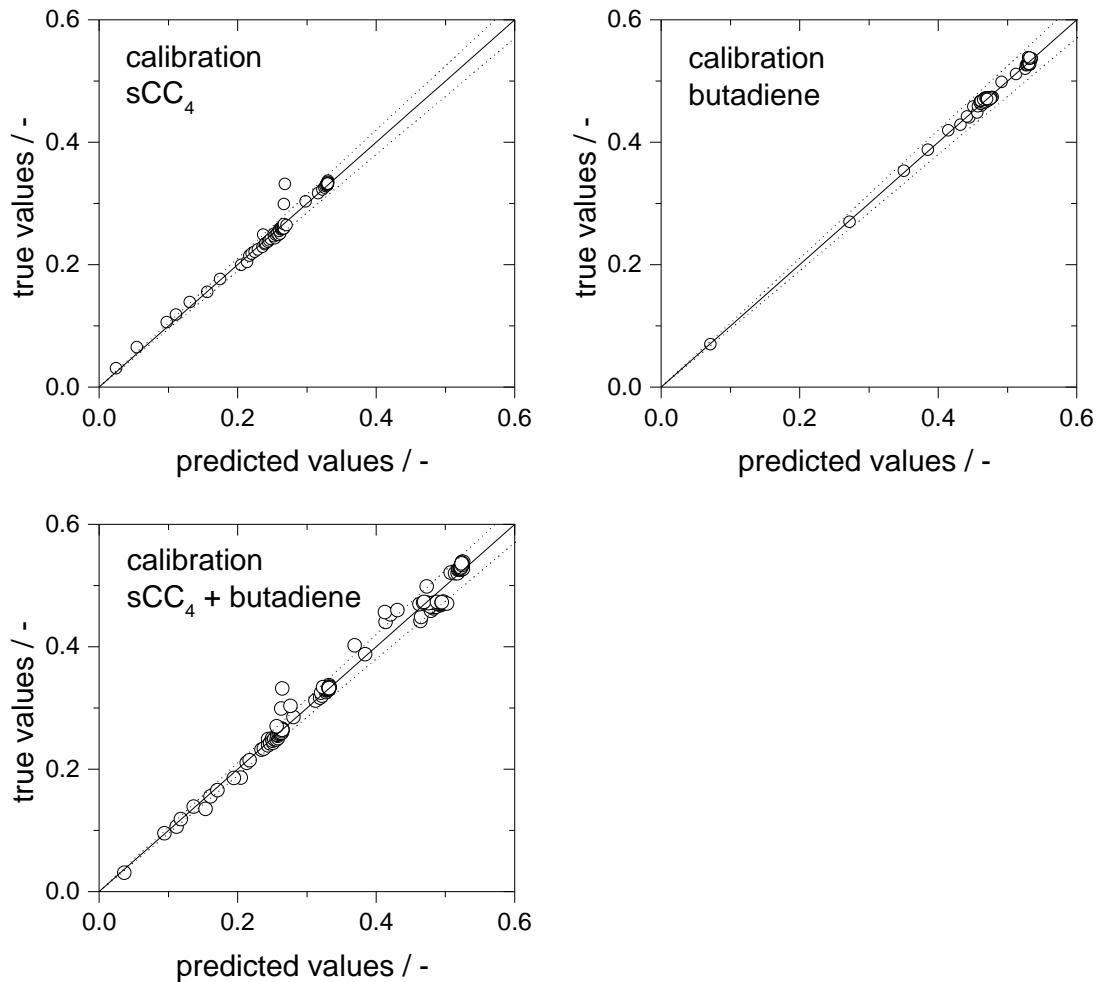


**Figure 14: Validation of the NIR calibration models for 3-Mode with the spectra of the test set presented in true-predicted plots (○ 3-Mode, — bisecting line, --- 5 % deviation).**

Here, the deviation of the predicted mass fraction compared to the reference values was observed to be independent of the calibration model and the spreading was

higher than for 1-Mode. In contrast to 1-Mode, the mass fraction of 3-Mode present in the reaction mixture was distinctly lower as can be seen in the range of the axis. Regarding the experimental error of 5 %, the exact determination of mass fractions in this low range is also difficult when using gas chromatography and might be inaccurate. Thus, also the development of the NIR calibration model was probably based on reference values containing the experimental error of the GC calibration and determination. In addition, the prediction of these low concentrations by the application of NIR spectroscopy is generally difficult due to the low intensity of absorption and the broad and overlapping peaks. Thus, it is difficult to find spectral characteristics for a low concentrated component.

In Figure 15, the true-predicted plots for methanol are depicted. For methanol a very broad range of concentrations was covered. The resulting correlation of all three calibration strategies was very good. As already observed for 1-Mode, the two calibrations where exclusively the experiments with one feed were used showed slightly better results compared to the combined calibration. For butadiene, very similar true-predicted plots were obtained, see Appendix 7.4, Figure A 1.
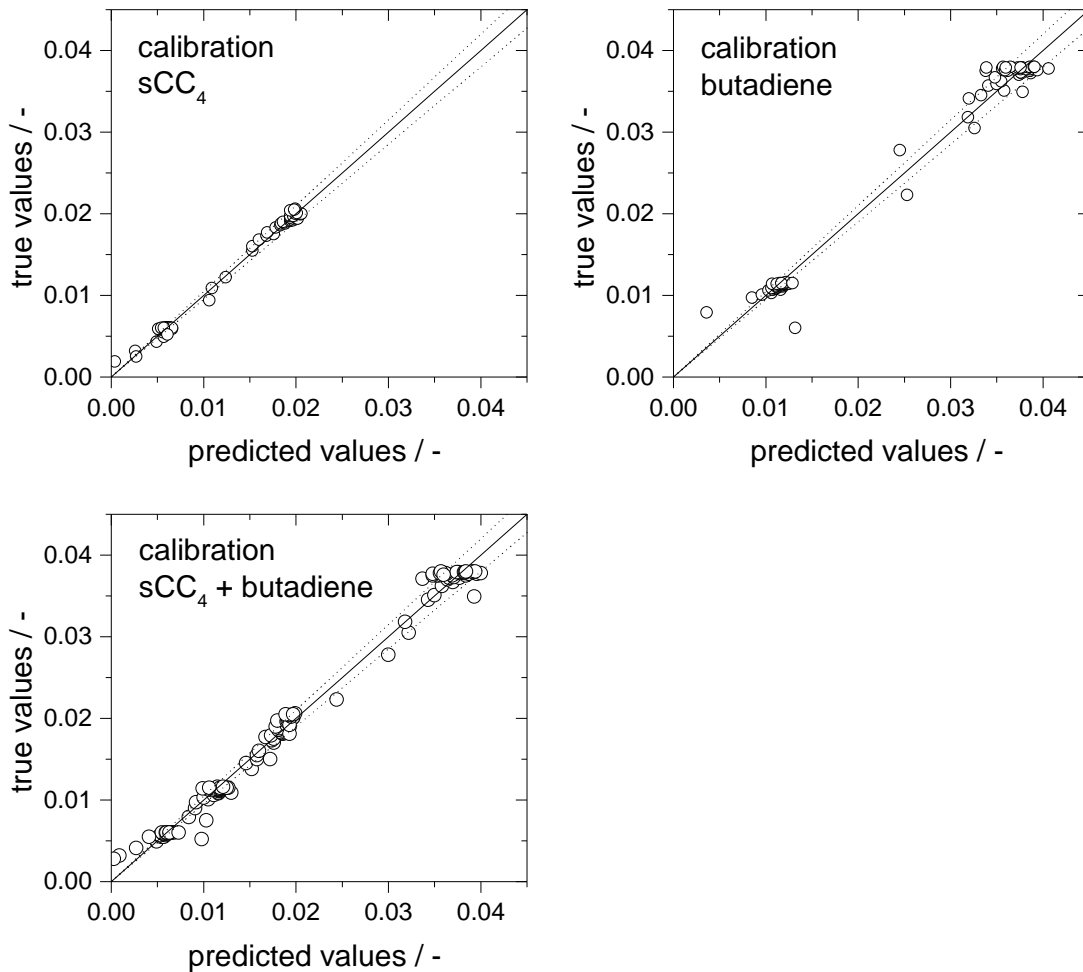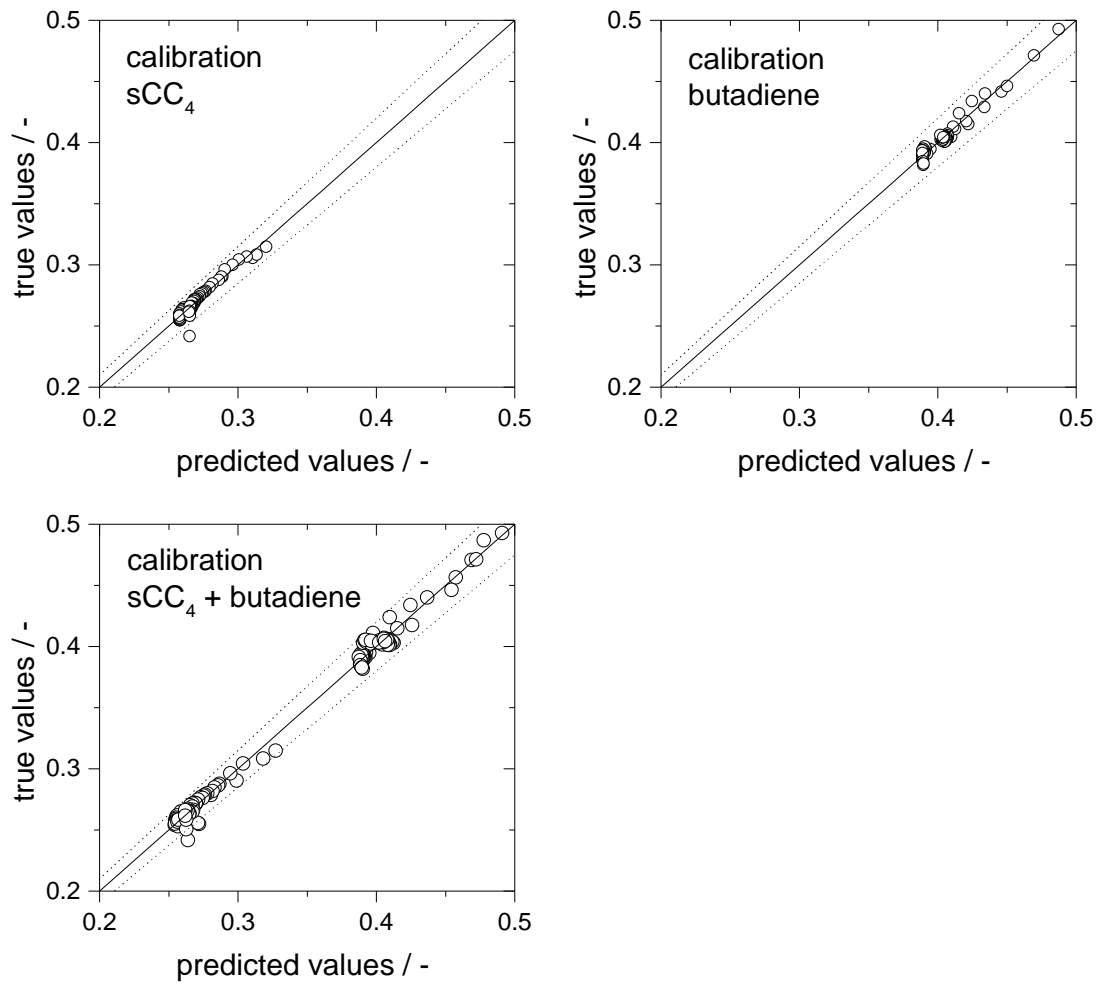
**Figure 15: Validation of the NIR calibration models for methanol with the spectra of the test set presented in true-predicted plots (○ methanol, — bisecting line, --- 5 % deviation).**

### 4.1.2 Additional validation of the developed calibration models

The additional validation of the calibration models was carried out by using independent experiments where NIR spectra were recorded and reference values were determined by gas chromatography. The obtained spectra were analyzed by the developed calibration models. The determined values for the mass fraction were compared to the reference values obtained with the online GC by plotting both over the reaction time, see Figure 16 to 18. The experiment used for the validation shown in this thesis was carried out with $sCC_4$ and the Pd-IMes catalyst. Another example for the Pd-TPP catalyst is shown in Appendix 7.4. The validation was conducted for the three calibration models as well as for each component. The validation of the calibration models for the main product 1-Mode is depicted in Figure 16.

The validation showed that the prediction of the mass fractions by NIR correlated very well with the reference values for the calibration with $sCC_4$ as well as for the combined calibration. With the butadiene calibration, a distinct deviation was observed. However, the reaction progress was described very well. This observation indicates that this deviation is probably induced by a systematic error. The latter could be caused by the already discussed difference of the spectra for experiments with inert components as present in the $sCC_4$ feed and those for pure butadiene. Nevertheless, if these disturbing signals are considered in the calibration model, the prediction can be quite well as can be seen for the combined calibration model.

The prediction of the methanol concentration by NIR was of very similar quality than shown for 1-Mode. Again, the calibration model for $sCC_4$ and the combined one correlated very well whereas the calibration model for pure butadiene showed some deviations but reflecting the progress of reaction. These deviations of the butadiene model can be eliminated by combining the experiments of $sCC_4$ and pure butadiene in one calibration model. The validation plots for methanol are presented in Appendix 7.4, Figure A 2.

**Figure 16: Additional validation of the calibration models determining the mass fraction of 1-Mode using independently conducted experiments for the Pd-IMes system with sCC$_4$ (▲ NIR, ○ GC).**

The validation plots for 3-Mode are depicted in Figure 17. In contrast, the prediction of the mass fractions of 3-Mode was worse for all three calibration models. This is in accordance with the already discussed deviation observed in the true-predicted plots. However, the reaction progress was reflected quite well. In consequence, a quantitative determination of the exact mass fraction for components with very low concentrations is not possible by NIR. Nevertheless, a qualitative statement was possible for 3-Mode.
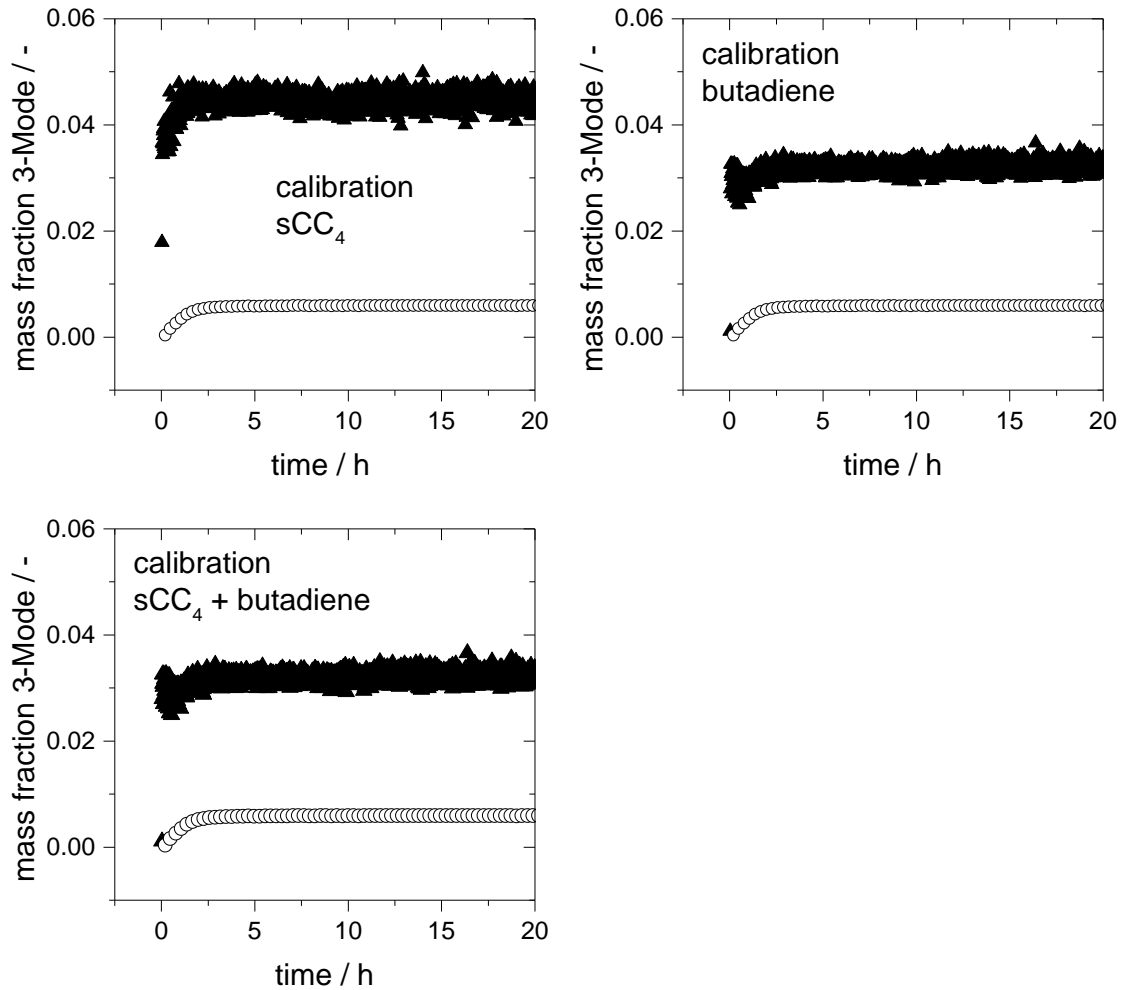
**Figure 17: Additional validation of the calibration models determining the mass fraction of 3-Mode using independently conducted experiments for the Pd-IMes system with sCC$_4$ (▲ NIR, ○ GC).**

The best correlation of predicted data and reference values was observed for butadiene. The results of the validation are presented in Figure 18.

The mass fractions were predicted with high accuracy using the sCC$_4$ as well as the combined calibration model. In addition and in contrast to the other components, the calibration model with pure butadiene exhibited also a good correlation of predicted and reference values. This means that the signals of the inerts in the spectra seem to influence even more the signals exhibited by 1-Mode and methanol than the signals for butadiene.
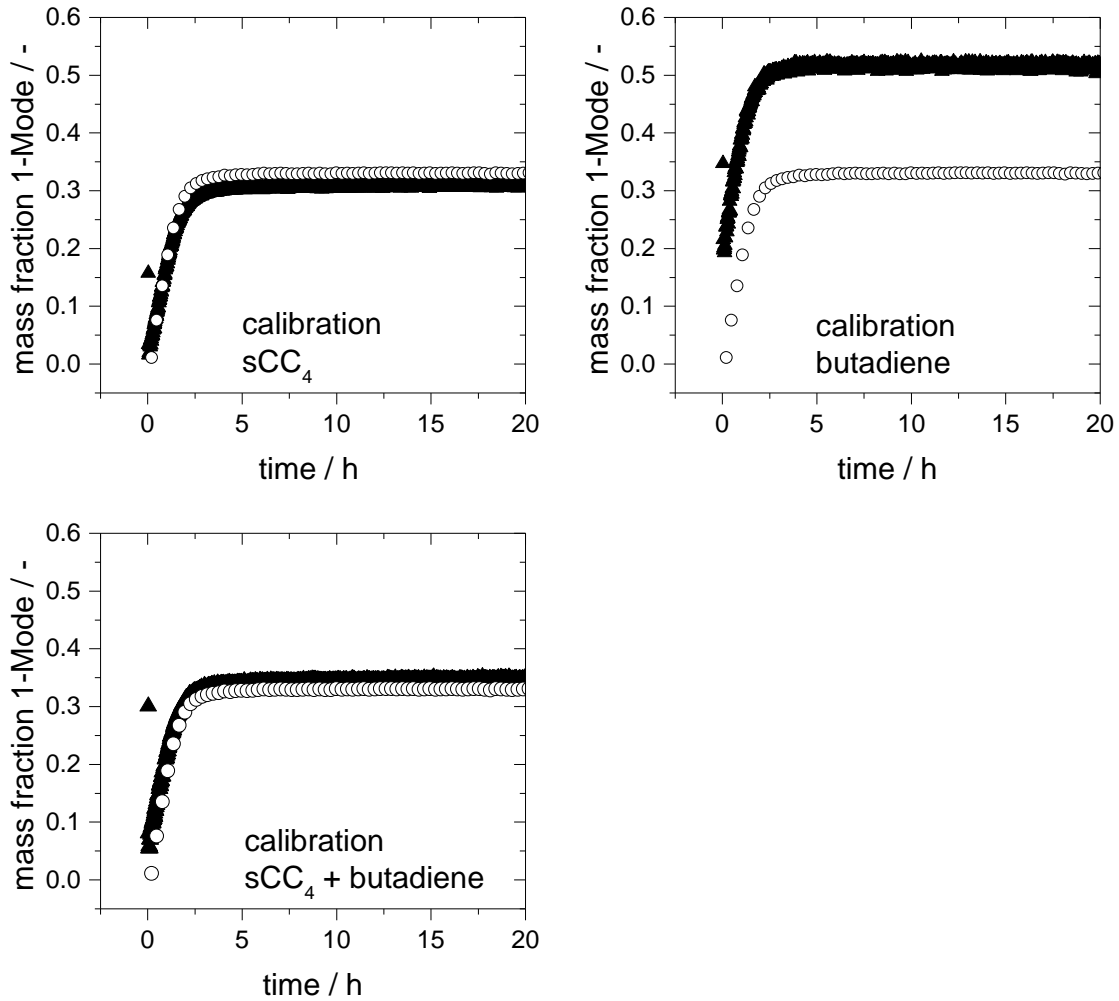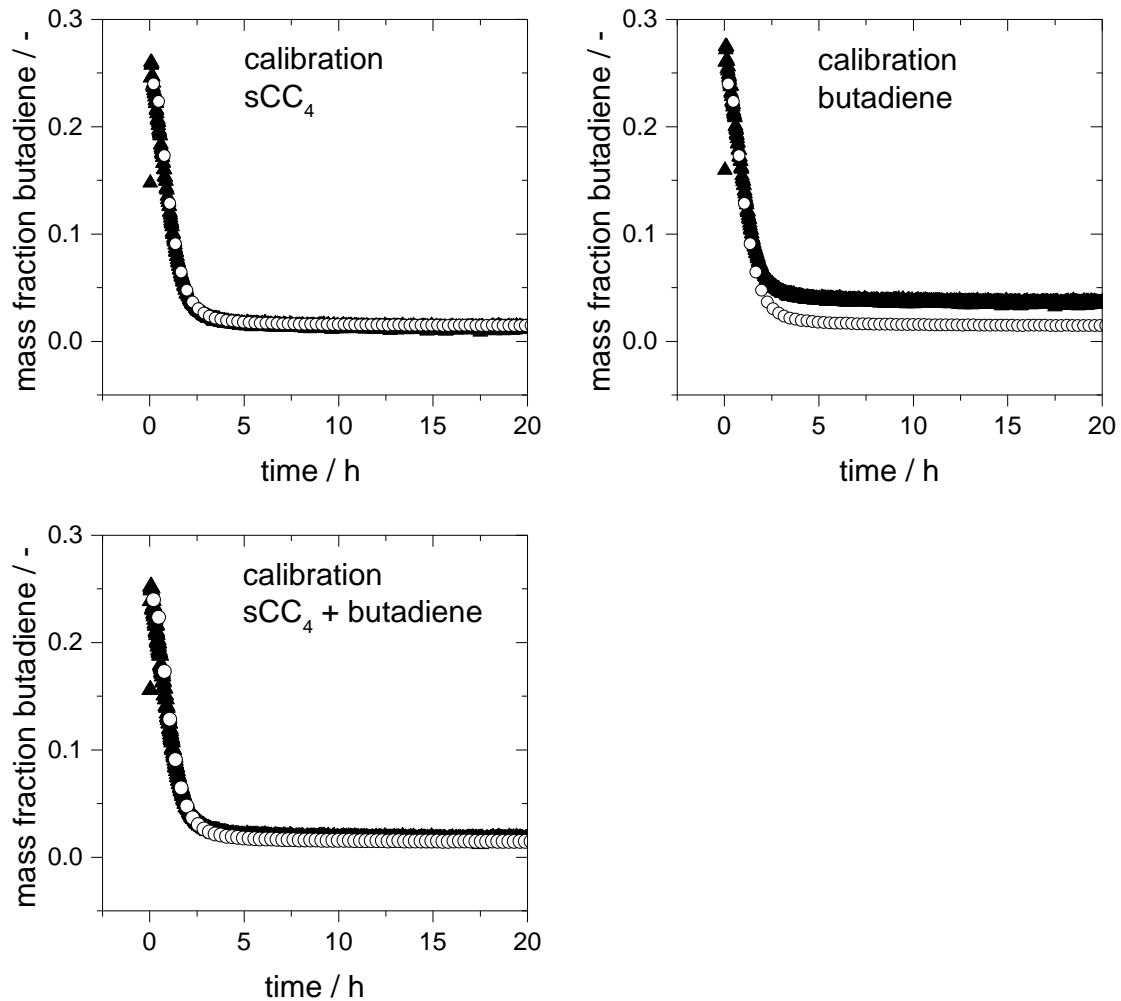
**Figure 18: Additional validation of the calibration models determining the mass fraction of butadiene using independently conducted experiments for the Pd-IMes system with sCC$_4$ (▲ NIR, ○ GC).**

The high accuracy in determination of the butadiene concentration is followed by an excellent determination of the conversion related to butadiene. In consequence, the process control carried out by the observation of the butadiene conversion would be possible by applying NIR. Furthermore, the methanol concentration can be determined quite well. Also the formation of the main product 1-Mode can be recorded by NIR spectroscopy. Due to the limitation concerning the determination of side products with a low concentration, e.g. 3-Mode, it is not possible to receive the exact selectivity of the process. This would be the limitation of NIR spectroscopy for all reactions with very high selectivity toward the desired product. However, for a

continuous process which is performed in a steady state, a change in the selectivity would also be reflected in the mass of formed 1-Mode.

In sum, the feasibility and applicability of NIR spectroscopy for the telomerization reaction was shown. Furthermore, the NIR spectroscopy seems to be very promising for other reactions in the liquid phase, especially for kinetic studies of very fast reactions. The great advantage of NIR spectroscopy in homogeneous catalysis is that it is a non-invasive and non-destructive method. The determination of the reaction composition is not followed by sample removal and thus changing of the reaction volume. But also the limitations of NIR spectroscopy were shown. This study could clearly point out that every parameter change has to be considered in the calibration model to receive a robust and flexible calibration. In addition, NIR spectroscopy struggles with components at very low concentrations due to the low intensity of absorption and the broad and overlapping signals.

Another interesting application of NIR spectroscopy would be the determination of the composition in a reaction mixture with ionic liquids. The feasibility of this was tested in this thesis as well and will be discussed in the following chapter.

### 4.1.3 NIR spectroscopy applied on reaction mixtures with ionic liquids

For the application of quantitative NIR spectroscopy on reaction mixtures with ionic liquids, a separate calibration model based on experiments with ionic liquids was developed. For this, five different compositions of the reactants, the product 1-Mode, the extraction solvent hexane and the ionic liquid were adjusted in the loop reactor and NIR spectra were recorded. The calibration model was built and successfully validated by the test set as described in the previous chapters.

With this calibration model, a continuous biphasic run was analyzed by NIR and compared to the reference values determined by GC analysis. For the ionic liquid experiments, only the composition of the exit stream was analyzed by GC. This composition was assumed to be representative for the whole reaction mixture in the loop reactor. The mass fractions in the loop were calculated based on the obtained conversion in the exit stream and the starting composition of the reactants.

Besides the calibration model with ionic liquid, the calibration models developed for experiments without ionic liquid (see Chapter 4.1.1, "calibration sCC$_4$" and "calibration sCC$_4$ + butadiene") were also applied for the analysis of the recorded spectra. In order to increase the robustness of the calibration model, a fourth model was developed by combining the values of the ionic liquid calibration and the calibration using experiments with sCC$_4$ as feed. The comparison of the four calibration models with the reference values for the mass fractions of 1-Mode is shown in Figure 19.

For 1-Mode, the mass fractions predicted by the two calibration models obtained with experiments without ionic liquids (top) were lower compared to the reference values. Nevertheless, the progress of the continuous experiment was displayed quite well. The increase of the product formation in the first 25 to 50 hours, reaching of the steady state followed by a further increase of the product formation due to an increase of the residence time were represented by the application of NIR spectroscopy. The calibration considering ionic liquids (bottom, left) showed a better alignment of the absolute values while the progress of reaction was not described well. This probably means that the signals and characteristic spectral information for 1-Mode and the ionic liquid occurred in the same wavelength range. A more detailed calibration including a higher number of spectra and reference values might deliver better qualitative results. Compared to the calibration models of the experiments without ionic liquid, the amount of available spectra was reduced due to the effort of mixing the components for calibration measurements. For the prior calibration without ionic liquid, a progressing reaction was recorded. This was of great advantage as with one experiment around 115 different calibration points were easily recorded which cover the full range of compositions.

In order to increase the robustness of the calibration model and the number of available calibration spectra, a combination of the calibration models with ionic liquid and sCC$_4$ were carried out. With this combinatory model, the best results were obtained. The absolute values for the mass fraction were described quite well. Also the progress of the reaction was represented by NIR analysis. This means that an increase in the effort spent for the development of the calibration model increases the quality of the model. All information comprised in the spectra as well as all disturbances have to be considered.

**Figure 19: Comparison of the mass fractions obtained for 1-Mode by GC analysis and four different NIR calibration models for a continuous biphasic experiment with ionic liquid (▲ NIR, ○ GC).**

The results obtained for the determination of the methanol concentration were similar to those for 1-Mode and are shown in Appendix 7.4, Figure A 7. The results for butadiene are different and are depicted in Figure 20.

The determination of butadiene was best when applying the two calibration models without ionic liquid (top). With both models, the absolute values as well as the progress of reaction were predicted in high accuracy. This hints that all information required for the determination of the butadiene concentration were available in the spectra without ionic liquid. For the calibration model with ionic liquid, the progress of the reaction as well as the prediction of the absolute values were not in the same accuracy. The number of spectra used for the calibration with ionic liquid was less

compared to the calibration models without ionic liquid. In addition, the range of calibrated butadiene concentration (0 to 13 wt%) was smaller compared to the previous models (0 to 40 wt%). For a good calibration, the whole range which should be predicted has to be calibrated.

By applying the combinatory model, the accuracy increased slightly supporting the statement of insufficient calibration for the model with ionic liquid.
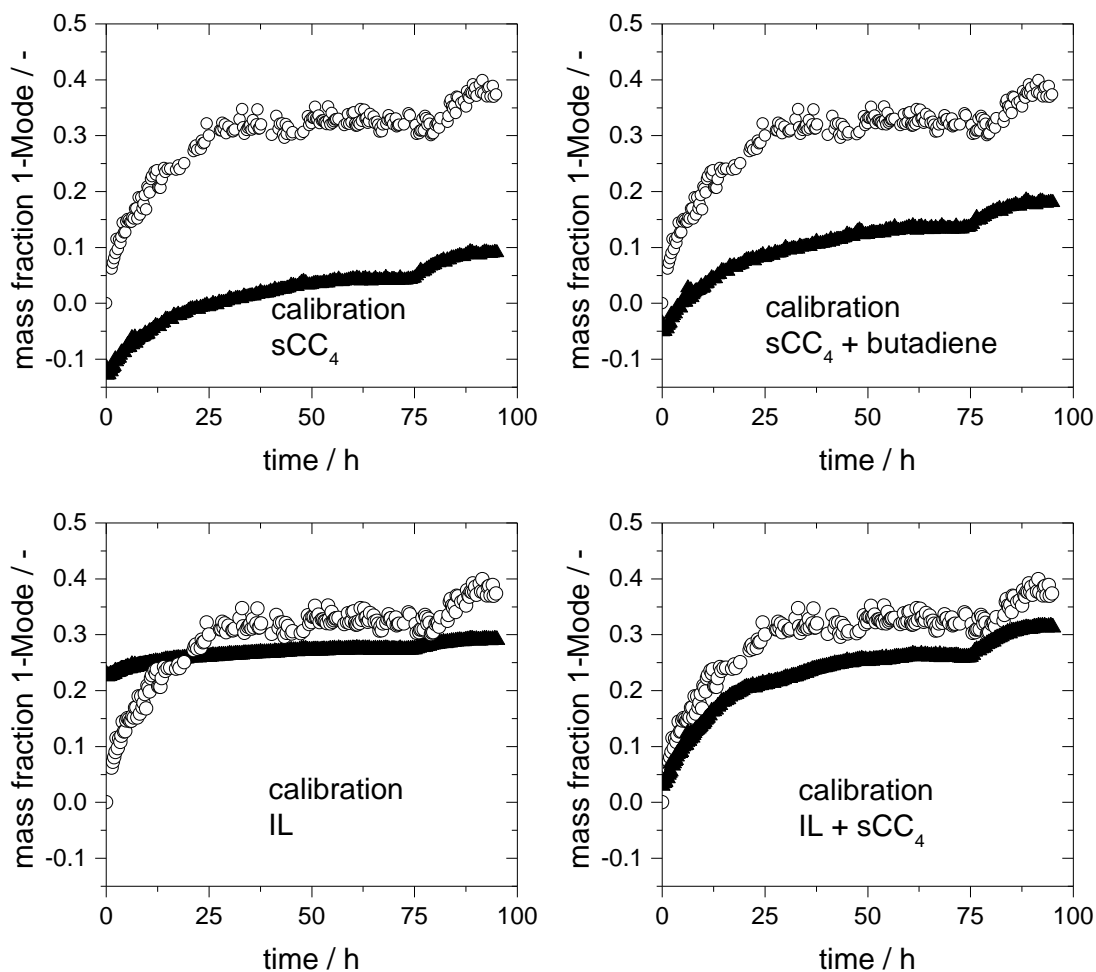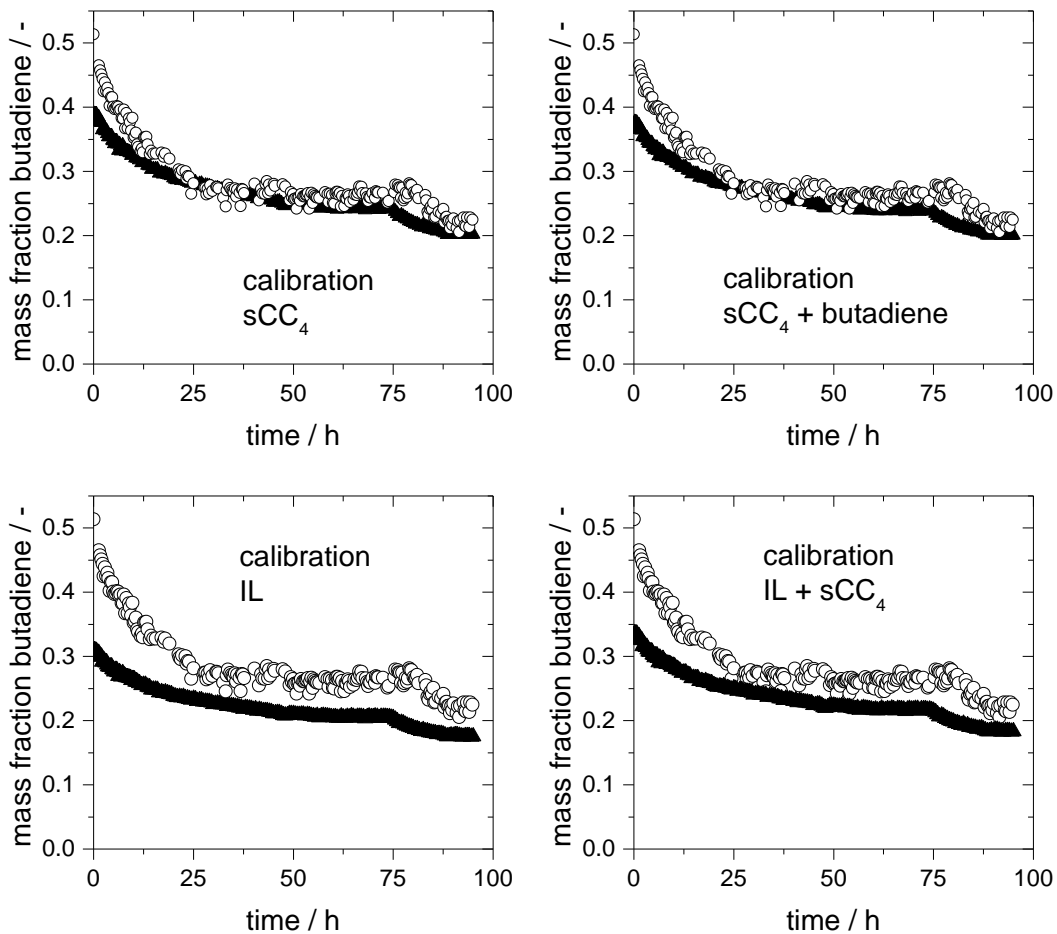


**Figure 20: Comparison of the mass fractions obtained for butadiene by GC analysis and four different NIR calibration models for a continuous biphasic experiment with ionic liquid (▲ NIR, ○ GC).**

The obtained results of this chapter show that the inline determination of the composition in a reaction mixture with ionic liquids is successful. A change in

concentration was determined with high accuracy for all components meaning that an application for process control in continuous operation is possible. Also the prediction of accurate absolute values was possible showing the ability of NIR spectroscopy for kinetic studies. However, for quantitative determination different calibration models showed the best results depending on the component to be predicted. Here, a more sufficient and detailed calibration would probably lead to consistent applicable calibration models. Again, the sensitivity of NIR spectroscopy against disturbances was shown in these investigations.

## 4.2   Telomerization without ionic liquids

This part focuses on investigations of the butadiene telomerization with methanol without ionic liquids. Besides pure butadiene also $sCC_4$, a technical feed consisting of around 45 mol% butadiene and 55 mol% inerts (butenes and butanes) was applied in the telomerization reaction. These two feeds were tested with two literature known ligands, TPP and IMes, resulting in four reaction systems. At the beginning of this chapter, a comparison of the four reaction systems is shown followed by the optimization of the reaction conditions. For a catalyst screening, different palladium precursors for in-situ generation of the catalyst complex as well as ex-situ prepared palladium-NHC-complexes were tested. With the generated knowledge, the transfer and scale-up of the telomerization reaction from the batch autoclave to the specially designed loop reactor was conducted.

### 4.2.1   Telomerization as complex reaction system

In the literature, TPP and IMes are well-known ligands for the telomerization of butadiene with methanol. Also the application of a mixed $C_4$ feed was tested [24; 25; 109]. However, these experiments were carried out by different groups and, to the best of the author's knowledge, a direct comparison of these four reaction systems has never been carried out. Furthermore, most of the published results are not based on complete kinetic studies but only on conversion and selectivity values recorded at the end of reaction. To overcome this lack of information and to get a direct comparison, kinetic studies for the two ligands combined with pure butadiene as well as with $sCC_4$ were carried out.

#### 4.2.1.1   Comparison of the reaction systems

The experiments for the comparative studies were carried out at the same reaction conditions using $Pd(acac)_2$ as catalyst precursor which was modified with either TPP or IMes. The IMes ligand was generated in-situ from the salt [IMes][MeSO$_3$] by

reaction with the strong base KOMe. This is, if not noted otherwise, the general procedure for all experiments with the IMes modified catalyst carried out in this thesis.

The conversion for the two ligands combined with pure butadiene and $sCC_4$ is shown in Figure 21. For all discussed results in this thesis, the conversion was related to butadiene.



**Figure 21: Comparison of the conversion for the TPP (left) and the IMes (right) modified catalysts with pure butadiene (■) and sCC$_4$ (□).**

*Reaction conditions: 70 °C, 15 bar, $n_{butadiene}:n_{MeOH} = 0.5$, $n_{butadiene}:n_{Pd} = 40,000$, $n_{Lig}:n_{Pd} = 4$, $n_{butadiene}:n_{base} = 400$.*

With pure 1,3-butadiene, the initial reaction rate was higher for the TPP modified catalyst compared to the IMes modified one. The final conversion was close to 95 % after 6 hours. At low concentrations of butadiene, the equilibrium in the monopalladium-bisallyl mechanism (see Scheme 6) can be shifted from complex **10** toward the TPP substituted Pd(0) species. This would lower the concentration of active catalyst and decrease the reaction rate.

With the diluted butadiene feed, the reaction started with a lower rate. A further decrease of the activity was observed after 6 hours at a conversion of around 70 %. The decreased reaction rate is probably affected by simple reaction kinetics showing lower activity at lower reactants' concentration due to the dilution effect.

The IMes modified catalyst in combination with pure butadiene exhibited a linear increase in conversion over time. Full conversion was reached after 4.5 hours. In

contrast to the Pd-TPP catalyst system, the reaction rate did not level off strongly before reaching full conversion. This difference could be caused by the steric demand of the IMes ligand which hinders the coordination of a second bulky ligand. Therefore, the equilibrium of the Pd species is in favor of the catalytically active complex **10**.

Interestingly and surprisingly, when using $sCC_4$ as feed, the conversion of the Pd-IMes system was slightly increased reaching full conversion after 4 hours. One possible explanation could be an inhibiting effect of butadiene, e.g. due to a chelating effect of butadiene with the catalyst, thereby reducing the number of active species. Another possible explanation could be a promoting effect by the compounds within the $sCC_4$ or an overall zero order dependency on the reactants.

By comparison of the rate, which can be expressed by plotting the moles of converted butadiene over the reaction time, the dependence on the butadiene concentration can be further exemplified, see Figure 22.
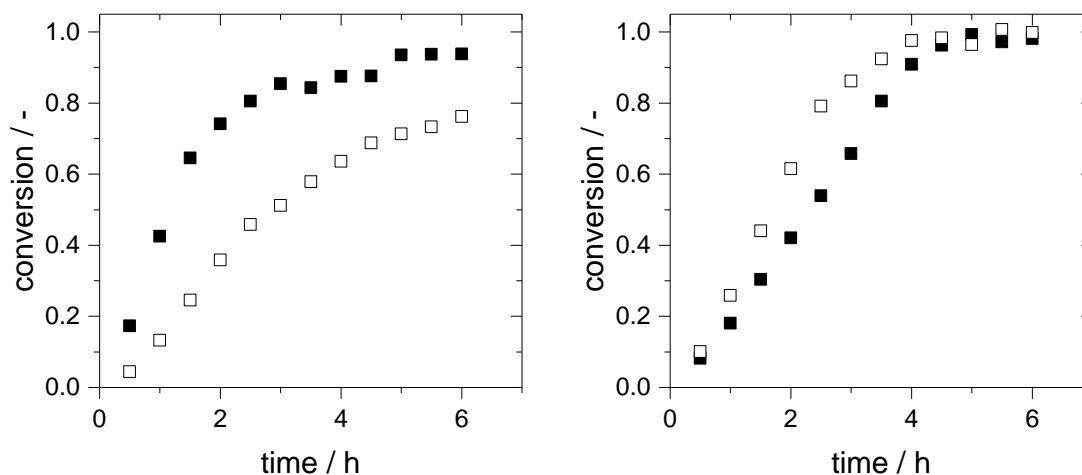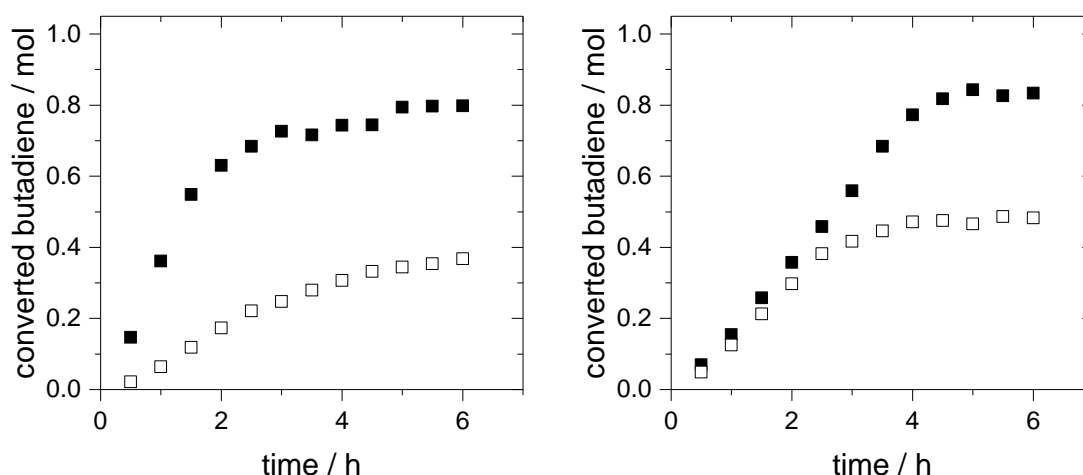


**Figure 22: Comparison of the converted amount of butadiene for the TPP (left) and the IMes (right) modified catalysts with pure butadiene (■) and $sCC_4$ (□).**

*Reaction conditions: 70 °C, 15 bar, $n_{butadiene}{:}n_{MeOH} = 0.5$, $n_{butadiene}{:}n_{Pd} = 40,000$, $n_{Lig}{:}n_{Pd} = 4$, $n_{butadiene}{:}n_{base} = 400$.*

Due to the different starting amount of butadiene depending on the applied feed, a lower end value of converted butadiene is expected when applying $sCC_4$. This behavior was observed for both ligands.

For the Pd-TPP system, the reaction rate was observed to be lower with $sCC_4$ compared to butadiene. This is the expected behavior if the reaction rate depends on the concentration of reactants and thus can be influenced by changing the reactants' concentration.

For the Pd-IMes system, the initial reaction rate with pure butadiene was quite similar to that with $sCC_4$. After 3 hours, the reaction rate with $sCC_4$ levelled off. This is caused by the already obtained full conversion of the system due to the lower amount of butadiene present in the mixture. This means that the Pd-IMes catalyst showed similar reaction rates with both feeds until reaching full conversion. One possible explanation for this observation is an overall zero order dependency in butadiene.

As summarized in Figure 23, the selectivity to 1-Mode was higher for the IMes modified catalyst system and seemed to be independent of the used feed. For TPP, the selectivity to 1-Mode differed slightly dependent on the used feed being higher for pure butadiene.

Compared to the TPP ligand, the IMes modified systems showed a distinctly higher selectivity to the desired product 1-Mode. All byproducts, octatriene (OTEN), vinylcyclohexene (VCHEN) and 3-Mode, were decreased resulting also in a higher *n:iso* ratio. For the TPP modified catalyst, the coordination of a second ligand is facilitated leading to lower 1-Mode selectivity as already shown and discussed by Vollmüller *et al.* [95], see Chapter 2.1.2.2.

The selectivities were observed to be constant over the reaction time and thus over conversion for both ligands and both feeds. Consequently, the selectivity will be discussed by means of comparing end values after the applied reaction time in the following chapters.

The TON reached values between 30,000 and 40,000 according to the Pd inventory and the amount of converted butadiene. As for the investigated systems the catalyst was still active at the end, these TON values do not reflect catalyst performance data and are only dependent on the conversion. Consequently, the TONs are not discussed in detail for every experiment within the following studies as the values are only representing the reached conversion lying always in the same range.
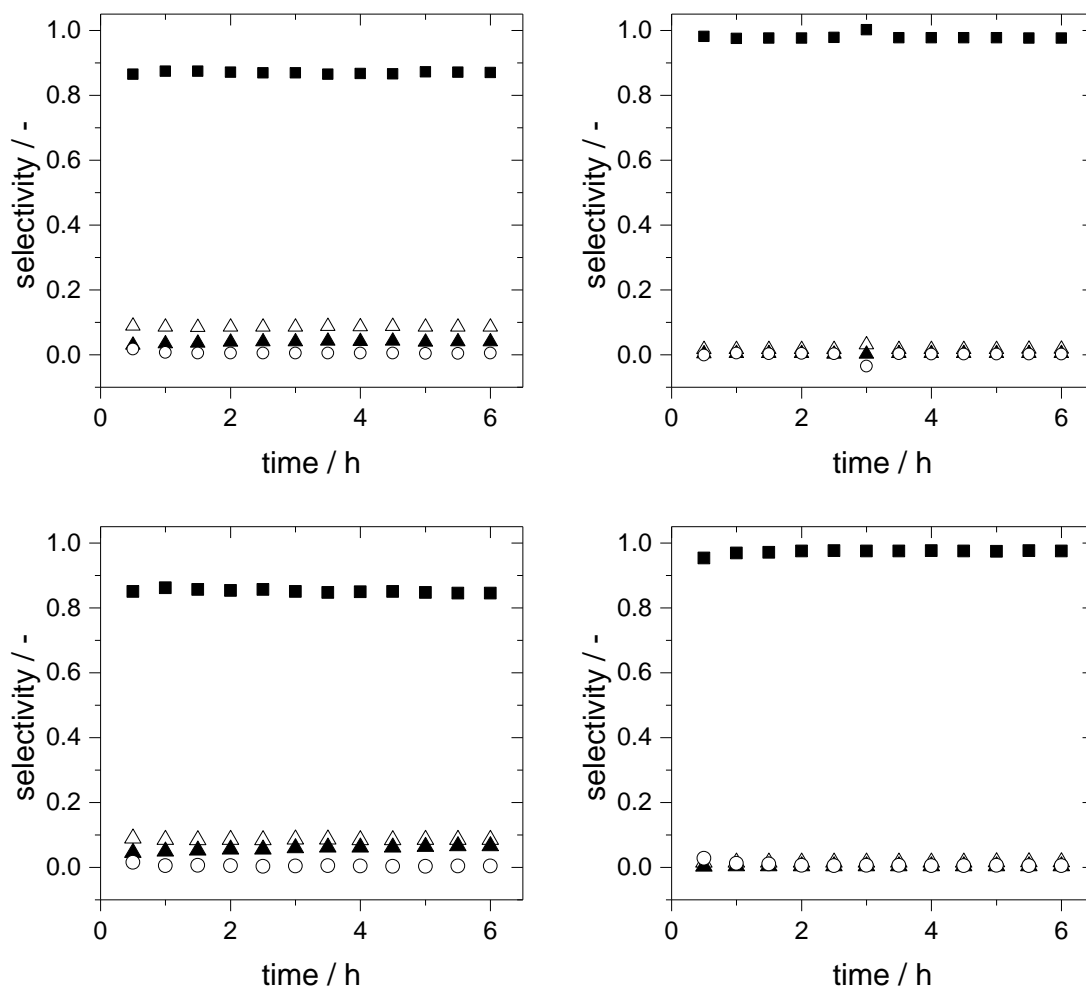
**Figure 23: Comparison of the selectivities for the TPP (left) and the IMes (right) modified catalysts with pure butadiene (top) and sCC$_4$ (bottom) (■ 1-Mode, △ 3-Mode, ▲ octatriene, ○ vinylcyclohexene).**

*Reaction conditions: 70 °C, 15 bar, $n_{butadiene}$:$n_{MeOH} = 0.5$, $n_{butadiene}$:$n_{Pd} = 40,000$, $n_{Lig}$:$n_{Pd} = 4$, $n_{butadiene}$:$n_{base} = 400$.*

### 4.2.1.2  Influence of different solvents

In order to further investigate the behavior of the two ligands when applying sCC$_4$ as feed, pure butadiene was combined with an inert solvent or a component of the sCC$_4$ to mimic the dilution of sCC$_4$ (45 mol% butadiene, 55 mol% inert solvent/sCC$_4$ component). For these experiments, two different solvents were used which should be chemically inert in the telomerization of butadiene with methanol, namely hexane and toluene. Additionally, *iso*-butene which is a component of the sCC$_4$, was tested as well.

For the TPP modified catalyst, these experiments were carried out to prove the dilution effect and the inert character of the sCC$_4$ components. If the lower reaction rate of the Pd-TPP catalyst combined with sCC$_4$ was only caused by the lower concentration of butadiene, the dilution of the butadiene feed by the solvents and C$_4$ components should have the same effect on conversion over time than observed with sCC$_4$. The obtained results are shown in Figure 24 and Table 7.
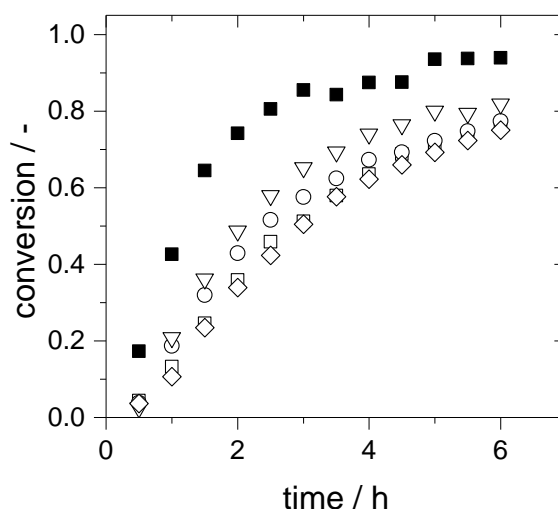


**Figure 24: Comparison of the conversion for the TPP modified catalyst with different diluted feeds (■ pure butadiene, □ sCC$_4$, ○ hexane, ▽ toluene, ◇ *iso*-butene).**

*Reaction conditions: 70 °C, 15 bar, $n_{butadiene}$:$n_{MeOH}$ = 0.5, $n_{butadiene}$:$n_{Pd}$ = 40,000, $n_{Lig}$:$n_{Pd}$ = 4, $n_{butadiene}$:$n_{base}$ = 400; for diluted butadiene (according to inert fraction in sCC$_4$): $n_{butadiene}$ = 45 mol%, $n_{solvent}$ = 55 mol%.*

Pure butadiene showed the highest activity while the activity of all diluted systems was similar to that using $sCC_4$. Only toluene showed a slightly higher reaction rate but this difference lies probably in the experimental error margin.

As summarized in Table 7, the values for the selectivity toward the main product, the chemoselectivity as well as the regioselectivity expressed by the *n:iso* ratio were nearly the same for hexane, toluene and *iso*-butene additions and were again slightly lower compared to pure butadiene.

**Table 7: Results for the TPP modified catalyst with different diluted feeds after 6 h.**

| ligand | feed | $X$ | $S_1$ | $S_2$ | $S_3$ | $S_{1+2}$ | *n:iso* |
|--------|------|-----|-------|-------|-------|-----------|---------|
|        |      | / % | / % | / % | / % | / % | / - |
| TPP | butadiene | 93.8 | 87.0 | 8.6 | 4.0 | 95.5 | 10.2 |
| TPP | $sCC_4$ | 76.2 | 84.5 | 8.6 | 6.5 | 93.1 | 9.9 |
| TPP | hexane | 77.4 | 85.1 | 7.4 | 7.5 | 92.5 | 11.5 |
| TPP | toluene | 81.9 | 84.9 | 7.2 | 7.8 | 92.1 | 11.8 |
| TPP | *iso*-butene | 75.0 | 84.0 | 8.7 | 6.2 | 92.8 | 9.6 |

*Reaction conditions: 70 °C, 15 bar, $n_{butadiene}$:$n_{MeOH} = 0.5$, $n_{butadiene}$:$n_{Pd} = 40,000$, $n_{Lig}$:$n_{Pd} = 4$, $n_{butadiene}$:$n_{base} = 400$; for diluted butadiene (according to inert fraction in $sCC_4$): $n_{butadiene} = 45$ mol%, $n_{solvent} = 55$ mol%.*

As expected all diluted systems showed a similar behavior compared to $sCC_4$. According to the rate law of a chemical reaction, the lower concentration of butadiene causes a lower reaction rate.

The IMes modified catalyst system was investigated using the same conditions and the same inert solvents. In addition to *iso*-butene, also 1-butene and *n*-butane were tested. The obtained results are shown in Figure 25.

For all diluted feeds the conversion was higher than with pure butadiene and comparable to that of $sCC_4$. As all applied $C_4$ components behaved similar to the inert solvents hexane and toluene as well as to $sCC_4$, an accelerating or any other effect of the $C_4$ components can be excluded and the inert character of the latter was confirmed. Instead, the independency of the reaction rate of the butadiene concentration (see Figure 25, bottom) indicates that the catalytic system exhibits an overall reaction rate of zero order in butadiene.

For all investigated diluted feeds, the obtained selectivities were again observed to be unaffected by the dilution of the butadiene feed.
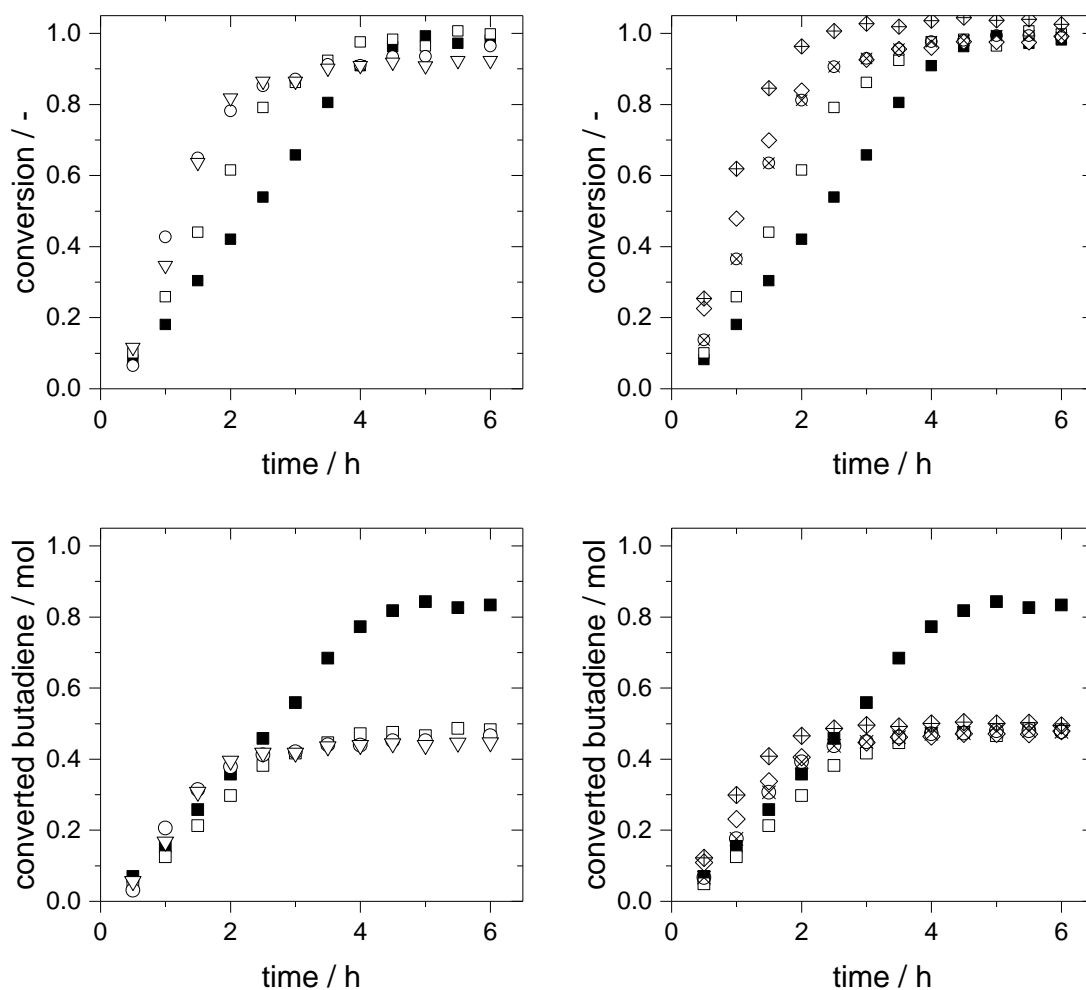
**Figure 25: Comparison of the conversion (top) and of the converted amount of butadiene (bottom) for the IMes modified catalyst with different diluted feeds (■ pure butadiene, □ sCC$_4$, ○ hexane, ▽ toluene, ◇ *iso*-butene, ⊗ 1-butene, ⊕ *n*-butane).**

*Reaction conditions: 70 °C, 15 bar, $n_{butadiene}$:$n_{MeOH} = 0.5$, $n_{butadiene}$:$n_{Pd} = 40,000$, $n_{Lig}$:$n_{Pd} = 4$, $n_{butadiene}$:$n_{base} = 400$; for diluted butadiene (according to inert fraction in sCC$_4$): $n_{butadiene} = 45$ mol%, $n_{solvent} = 55$ mol%.*

### 4.2.2 Influence of reaction conditions

The reaction conditions for the comparison of the four reaction systems were chosen based on literature reports and on the experience of the SYNFLOW partner Evonik. Starting with these conditions, the influence of different parameters, e.g. temperature, ratio of catalyst to ligand or ratio of reactants were studied in order to find the optimum parameter combination for a successful transfer to the later intended continuous process.

### 4.2.2.1 Influence of oxygen and technical methanol

The formation of elemental palladium, so called Pd-black, is known to be an undesired side reaction of the telomerization of butadiene with methanol [25]. In order to define a highly reproducible working procedure for this thesis, the influence of oxygen was tested. Furthermore, the use of technical feeds in an industrial process is important. Besides the application of $sCC_4$ within this thesis, also the effect of technical methanol on the reaction performance was investigated. The influence of both, oxygen and technical methanol, was studied exemplarily for the Pd-TPP system using pure butadiene as feed. The results are depicted in Figure 26. The standard experiment was carried out according to the procedure in Chapter 3.2.1.2. The autoclave was free of oxygen and other impurities due to evacuation for at least 1 hour. The experiment with argon purge was conducted without evacuating the autoclave for at least 1 hour but with application of an altering vacuum-argon purge for three times before filling the reactor. For the experiment with air, the air present after the cleaning procedure remained in the autoclave. Here, the telomerization reaction showed no conversion at all. With the vacuum-argon purge, the obtained performance was similar to the performance using the standard procedure. Also the selectivity toward 1-Mode of around 88 % as well as the chemoselectivity (96 %) were not influenced by the application of the vacuum-argon purge.
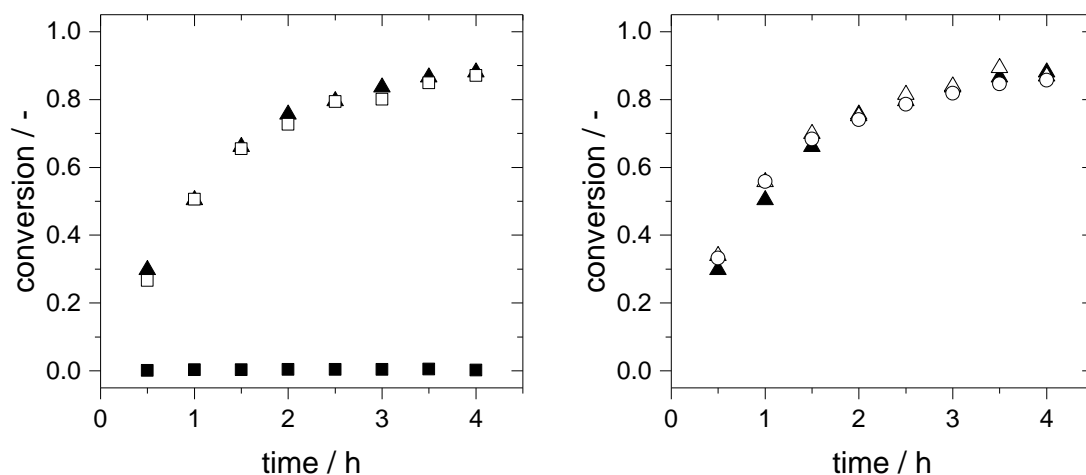
**Figure 26: Influence of oxygen (left) and technical methanol (right) on the Pd-TPP catalyzed telomerization with pure butadiene (▲ standard experiment, ■ with air, □ with argon purge, △ technical methanol, ○ catalyst/ligand dissolved in technical methanol).**

*Reaction conditions: 70 °C, 15 bar, $n_{butadiene}:n_{MeOH} = 0.5$, $n_{butadiene}:n_{Pd} = 40,000$, $n_{Lig}:n_{Pd} = 4$, $n_{butadiene}:n_{base} = 400$.*

Thus, the telomerization reaction seems to be oxygen sensitive but a proper alternation of vacuum-argon purges was sufficient to displace the oxygen. To be sure that no oxygen was present in the reaction and to completely remove the solvents used during the cleaning of the autoclave, the procedure applied in this thesis included evacuation of the autoclave for at least 1 hour.

The main difference between technical and analytical methanol is its water content which is higher in the technical feed. The application of technical methanol did not show any influence on the reaction performance of the telomerization. Also the preparation of the catalyst and ligand solution in technical methanol and the storage of these solutions over night did not affect the reaction performance. For both experiments with technical methanol, the selectivity toward 1-Mode as well as the chemoselectivity and the *n:iso* ratio of 11.5 were not influenced.

In consequence, water does not disturb the butadiene telomerization with methanol and it would be possible to apply a technical methanol feed in an industrial telomerization process as long as it does not contain oxygen impurities.

### 4.2.2.2  Influence of base strength

As already mentioned in Chapter 2.1.2.2, bases such as amines or methoxides facilitate and accelerate the reduction of Pd(II) precursors, e.g. $Pd(acac)_2$ or $Pd(OAc)_2$, to Pd(0) complexes [99-101]. For the telomerization reaction using a Pd-TPP catalyst, Vollmüller *et al.* [102] observed that the base $NEt_3$ accelerated the reaction rate at the start of reaction whereas it did not affect the overall selectivity or productivity. However, the base is not necessary for a Pd-phosphine catalyst system as the phosphine exhibits a basic character itself. In order to test if the base is necessary for the IMes ligand and to study the effect of base type for both ligands, experiments were carried out using different types of base. The obtained results are shown in Figure 27.
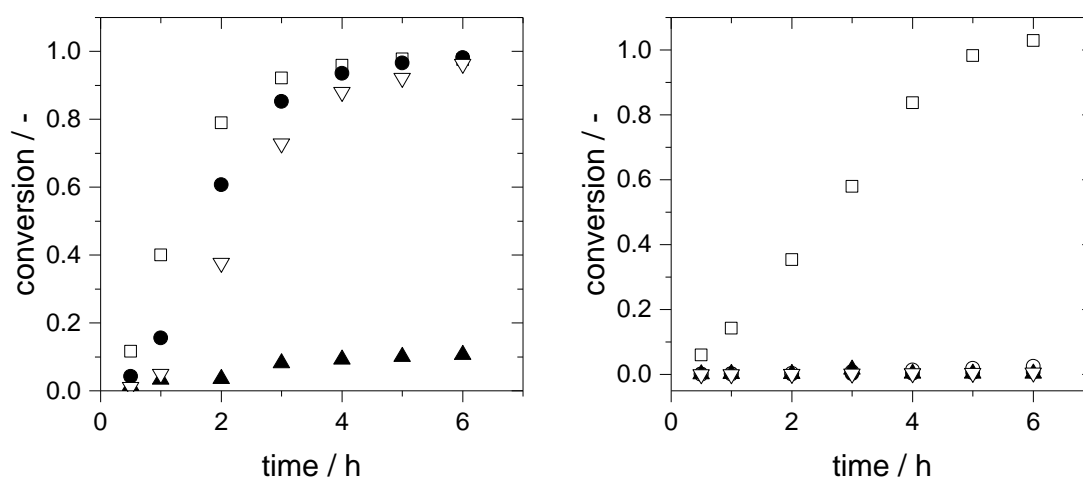


**Figure 27: Conversion with different bases for the TPP (left) and the IMes (right) modified catalysts with pure butadiene ($\square$ KOMe, $\bullet$ NEt$_3$, $\circ$ 10·NEt$_3$, $\blacktriangle$ MIM, $\triangledown$ no base).**

*Reaction conditions: 70 °C, 15 bar, $n_{butadiene}{:}n_{MeOH} = 0.5$, $n_{butadiene}{:}n_{Pd} = 40,000$, $n_{Lig}{:}n_{Pd} = 4$, $n_{butadiene}{:}n_{base} = 400$.*

For the Pd-TPP catalyst, the highest activity was obtained with the strongest base, KOMe, followed by $NEt_3$. The experiment without base exhibited a slight activation phase but showed also a high activity after 2 hours which was only slightly lower than for the experiments with KOMe and $NEt_3$. This is caused by the fact that the TPP ligand is a weak base itself. The application of the weak base methylimidazole (MIM)

led to a very low conversion of around 10 % probably caused by the formation of imidazolyl-Pd-cluster.

The IMes ligand seemed to be only efficiently activated by a strong base such as KOMe as all other experiments showed only very low to no conversion. Even the 10-fold increase of the $NEt_3$ amount exhibited only a conversion of around 2.5 % after 6 hours. The increase of the reaction time from 6 to 18 hours resulted in an increase of conversion to 6 %.

As summarized in Table 8, the strength of the applied base did not influence the selectivity of the Pd-TPP catalyst strongly. For the experiment without base the formation of 3-Mode was decreased by around 2 to 3 %. This is probably due to the fact that the nucleophilic attack is also facilitated at the C3 atom when using an additional base. For MIM the low conversion is likely to be the reason for the lower selectivity toward the main product.

As the achieved conversions for the Pd-IMes catalyst are very low except for the experiment with KOMe, the selectivities of these experiments are not shown and not discussed in detail.

**Table 8: Results with different bases for the TPP modified catalyst with pure butadiene after 6 h.**

| base | ligand | feed | X / % | $S_1$ / % | $S_2$ / % | $S_3$ / % | $S_{1+2}$ / % | n:iso |
|------|--------|------|-------|-----------|-----------|-----------|---------------|-------|
| KOMe | TPP | butadiene | 97.6 | 86.9 | 9.3 | 3.5 | 96.1 | 9.4 |
| $NEt_3$ | TPP | butadiene | 98.1 | 87.8 | 7.4 | 4.5 | 95.2 | 11.9 |
| MIM | TPP | butadiene | 10.6 | 80.4 | 12.1 | 3.2 | 92.5 | 6.7 |
| - | TPP | butadiene | 96.3 | 88.9 | 6.1 | 4.6 | 95.0 | 14.7 |

*Reaction conditions: 70 °C, 15 bar, $n_{butadiene}:n_{MeOH} = 0.5$, $n_{butadiene}:n_{Pd} = 40,000$, $n_{Lig}:n_{Pd} = 4$, $n_{butadiene}:n_{base} = 400$.*

### 4.2.2.3 Variation of the reaction temperature

The influence of the reaction temperature on the telomerization reaction was tested as well. For this, the four reaction systems were studied at three different temperatures. The results of these experiments are depicted in Figure 28.
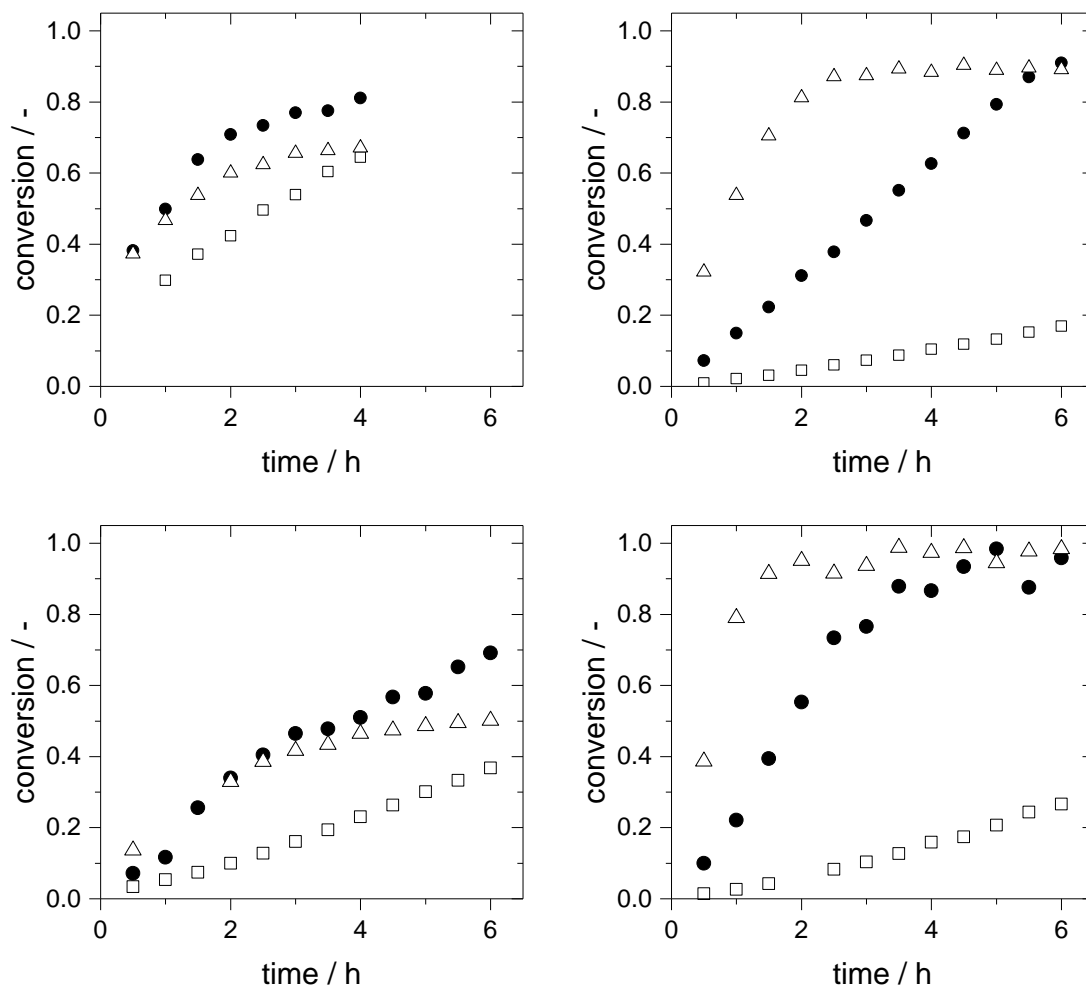
**Figure 28: Influence of the reaction temperature for the TPP (left) and the IMes (right) modified catalysts with pure butadiene (top) and sCC$_4$ (bottom) (□ 50 °C, ● 70 °C, △ 90 °C).**

*Reaction conditions: 15 bar, $n_{butadiene}$:$n_{MeOH}$ = 0.5, $n_{butadiene}$:$n_{Pd}$ = 40,000, $n_{Lig}$:$n_{Pd}$ = 4, $n_{butadiene}$:$n_{base}$ = 400.*

According to the Arrhenius law, an increase in reaction temperature causes an increase in reaction rate. This dependence was observed for both Pd-IMes catalyzed reaction systems (right). For both feeds, the reaction rate was distinctly higher at 90 °C than at 70 °C reaching full conversion after 1.5 to 2 hours. The lowest reaction rate was obtained at 50 °C exhibiting a conversion after 6 hours of around 20 % with pure butadiene and around 25 % with sCC$_4$. For the Pd-IMes catalyst, the zero order dependency in butadiene was independent of the temperature.

In contrast, the Pd-TPP catalyzed telomerization reaction did not correlate with the Arrhenius law. For both feeds, the reaction conducted at 70 °C exhibited the highest activity over reaction time. Within the first 1 to 2 hours, the experiments at 90 °C showed similar reaction rates than those at 70 °C. Afterwards, however, the reaction rates levelled off rapidly exhibiting lower conversions at the end of reaction. This was probably caused by a more pronounced catalyst deactivation at higher temperatures. One indication for this assumption was the presence of a large amount of Pd-black at the end of the experiments conducted at 90 °C. Also for the Pd-IMes catalyzed telomerization reaction a low amount of Pd-black was observed at 90 °C but this was negligible compared to the amount of Pd-black obtained in the Pd-TPP systems.

The Pd-TPP catalyst showed the lowest reaction rate for both feeds at 50 °C. The reaction rates increased linearly reaching a conversion after 4 h of around 60 % with pure butadiene and 25 % with sCC$_4$. The observed dilution effect was not affected by the reaction temperature as the activity for the diluted feed was observed to be always lower compared to the corresponding experiment with pure butadiene.

The influence of the reaction temperature on the selectivities for the different reaction systems is summarized in Table 9.

**Table 9: Results at different temperatures for the TPP modified and the IMes modified catalysts with pure butadiene and sCC$_4$ after 6 h (4 h for Pd-TPP with pure butadiene).**

| $T$ / °C | ligand | feed | $X$ / % | $S_1$ / % | $S_2$ / % | $S_3$ / % | $S_{1+2}$ / % | n:iso / - |
|---|---|---|---|---|---|---|---|---|
| 50 | TPP | butadiene | 64.4 | 91.8 | 6.6 | 1.6 | 98.4 | 14.0 |
| 70 | TPP | butadiene | 81.1 | 89.0 | 7.6 | 3.3 | 96.6 | 11.7 |
| 90 | TPP | butadiene | 67.1 | 84.3 | 7.6 | 8.0 | 91.9 | 11.2 |
| 50 | TPP | sCC$_4$ | 36.8 | 93.0 | 4.1 | 2.7 | 97.0 | 22.9 |
| 70 | TPP | sCC$_4$ | 69.1 | 85.8 | 5.7 | 8.3 | 91.6 | 15.0 |
| 90 | TPP | sCC$_4$ | 50.1 | 75.0 | 6.2 | 18.4 | 81.2 | 12.2 |
| 50 | IMes | butadiene | 16.9 | 98.2 | 1.2 | 0.2 | 99.3 | 85.4 |
| 70 | IMes | butadiene | 91.0 | 97.9 | 1.6 | 0.3 | 99.5 | 61.1 |
| 90 | IMes | butadiene | 89.1 | 96.9 | 2.2 | 0.7 | 99.1 | 44.7 |
| 50 | IMes | sCC$_4$ | 26.7 | 98.6 | 1.0 | 0.1 | 99.6 | 96.3 |
| 70 | IMes | sCC$_4$ | 95.9 | 98.1 | 1.5 | 0.3 | 99.6 | 65.3 |
| 90 | IMes | sCC$_4$ | 98.4 | 97.1 | 2.1 | 0.8 | 99.2 | 46.5 |

*Reaction conditions: 15 bar, $n_{butadiene}$:$n_{MeOH} = 0.5$, $n_{butadiene}$:$n_{Pd} = 40,000$, $n_{Lig}$:$n_{Pd} = 4$, $n_{butadiene}$:$n_{base} = 400$.*

For the Pd-TPP catalyst combined with pure butadiene, the selectivity toward the main product decreased with increasing temperature whereas the formation of 3-Mode remained rather constant. The decrease in 1-Mode was observed to be in favor of the formation of octatriene. Due to the decrease of methoxyoctadiene and the increase of octatriene formation, the chemoselectivity was lowered with increasing temperature. The temperature decrease from 70 °C to 50 °C was followed by a slight increase of regioselectivity whereas the latter remained unaffected by increasing the temperature from 70 °C to 90 °C. These observations are in accordance with the literature reports by Vollmüller *et al.* [95; 102].

Similar behavior was obtained for the Pd-TPP catalyst combined with $sCC_4$ but it was distinctly more pronounced than with butadiene. In contrast to pure butadiene, the formation of 3-Mode was influenced slightly by the temperature variation resulting in a higher variation of the chemoselectivity. However, the decrease of 1-Mode selectivity was mainly followed by a strong rise of octatriene formation. The selectivity toward octatriene increased from 2.7 % at 50 °C to 18.4 % at 90 °C. Thus, also the influence on the regioselectivity was more pronounced.

In contrast to the Pd-TPP catalyst, the Pd-IMes selectivities were only slightly influenced by the temperature variation. For both feeds, the temperature rise of 40 °C caused a decrease of the selectivity toward the main product of around 1.5 % followed by a slight increase of both, 3-Mode and octatriene formation. The chemoselectivity remained unaffected whereas the regioselectivity showed a decrease with increasing temperature.

### 4.2.2.4 Variation of the molar ratio of butadiene to catalyst

In a further set of experiments, the influence of the molar ratio of butadiene to palladium on the reaction rate and selectivity was tested. Again, the experiments were carried out for both catalyst complexes combined with both feeds. The molar ratio of butadiene to palladium was varied between 20,000 and 60,000. All other molar ratios and the reaction volume were kept constant. The results of this study are shown in Figure 29.
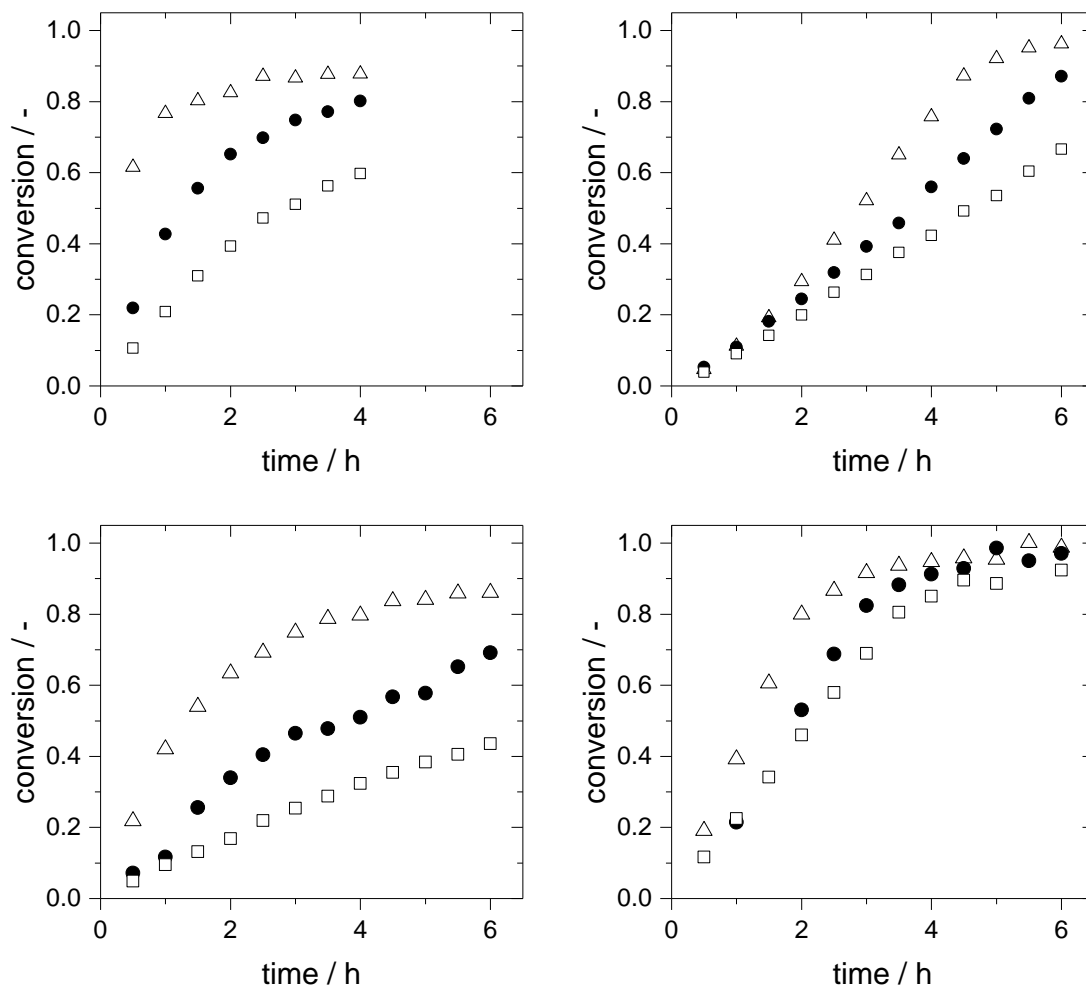
**Figure 29: Influence of the molar ratio of butadiene to Pd for the TPP (left) and the IMes (right) modified catalysts with pure butadiene (top) and sCC$_4$ (bottom) (□ 20,000, ● 40,000, △ 60,000).**

*Reaction conditions: 70 °C, 15 bar, $n_{butadiene}$:$n_{MeOH}$ = 0.5, $n_{Lig}$:$n_{Pd}$ = 4, $n_{butadiene}$:$n_{base}$ = 400.*

With a higher amount of catalyst related to the reactant butadiene, a higher activity of the reaction system would be expected. All investigated systems behaved as expected. The highest activity was achieved with a molar ratio of butadiene to catalyst of 20,000, the lowest activity and as a consequence of the low Pd concentration the highest TON was obtained with a ratio of 60,000. However, the strength of the influence was different depending on the applied system.

The Pd-TPP catalyst showed a strong dependence on the amount of applied catalyst. The reaction resembled a first order dependency on the catalyst

concentration as the reaction rates almost doubled with doubled catalyst amount. The difference in the initial activity led to different conversions at the end of reaction. However, all experiments applying the Pd-TPP catalyst would be expected to reach the same conversion after appropriate chosen reaction times. Indication for this assumption is the observed behavior of the Pd-TPP catalyst with pure butadiene applying a ratio of 20,000 and 40,000. For the highest catalyst concentration, the end conversion was reached after 2 hours. With a ratio of 40,000, the reaction rate over time was observed to be lower but after 4 hours the same end conversion was almost reached.

For the Pd-IMes catalyst, the dependence on butadiene to catalyst ratio was less pronounced but has been found to be a function of the applied feed. For sCC$_4$, the activity was slightly higher at higher catalyst concentration from the start of the reaction. In contrast, pure butadiene exhibited the same activity in the first hour for all tested Pd-concentrations. Afterwards, the activity differs depending on the applied catalyst amount resulting in a distinct activation phase for the highest catalyst amount. This observation indicates that the in-situ generation of the IMes ligand seems to be a rate determining step and is also strongly dependent on the concentration of the base. Also the reaction itself might be dependent on the base. In these experiments, the amount of base was adjusted relative to butadiene not to palladium, with the consequence of a higher ratio of Pd to base for higher Pd concentrations at lower butadiene to Pd ratios.

The influence of the molar ratio of butadiene to palladium on the selectivity of the telomerization reaction is shown in Table 10.

Applying a higher amount of the Pd-TPP catalyst and thus a higher ratio of Pd to base, the telomerization reaction became less selective toward the main product whereas the formation of 3-Mode was increased. With pure butadiene, the octatriene selectivity did not exhibit a clear trend but with sCC$_4$ the formation of octatriene decreased with increasing palladium amount. The chemoselectivity remained rather unaffected whereas the regioselectivity decreased with increasing catalyst amount due to the change of selectivities toward the two methoxyoctadiene products. For this behavior, no explanation can be found in the literature. In general, a lower amount of catalyst should cause a lower selectivity according to Vollmüller *et al.* [95]. The stability of the Pd-TPP complex should not be affected as the ratio of ligand to palladium was kept constant. Another reason for these slight differences in selectivity

might be the higher ratio of Pd to base with lower ratio of butadiene to Pd. The lower amount of base per mol of Pd might lead to a slightly less selective catalyst complex. Compared to the Pd-TPP catalyst, the selectivities obtained with the Pd-IMes catalyst again were observed to be much less affected by the variation of the butadiene to catalyst ratio.

**Table 10: Results at different molar ratios of butadiene to Pd for the TPP modified and the IMes modified catalysts with pure butadiene and sCC$_4$ after 6 h (4 h for Pd-TPP with pure butadiene).**

| ratio butadiene:Pd | ligand | feed | $X$ / % | $S_1$ / % | $S_2$ / % | $S_3$ / % | $S_{1+2}$ / % | $n$:iso / - |
|---|---|---|---|---|---|---|---|---|
| 60,000 | TPP | butadiene | 59.8 | 90.1 | 5.5 | 4.4 | 95.6 | 16.3 |
| 40,000 | TPP | butadiene | 80.2 | 89.6 | 6.5 | 3.9 | 96.0 | 13.9 |
| 20,000 | TPP | butadiene | 87.8 | 86.4 | 8.8 | 4.8 | 95.2 | 9.9 |
| 60,000 | TPP | sCC$_4$ | 43.5 | 87.2 | 5.1 | 7.4 | 92.3 | 17.1 |
| 40,000 | TPP | sCC$_4$ | 69.1 | 85.8 | 5.7 | 8.3 | 91.6 | 15.0 |
| 20,000 | TPP | sCC$_4$ | 86.1 | 85.0 | 8.2 | 6.6 | 93.3 | 10.3 |
| 60,000 | IMes | butadiene | 66.6 | 97.9 | 1.6 | 0.3 | 99.4 | 63.1 |
| 40,000 | IMes | butadiene | 87.1 | 97.8 | 1.6 | 0.3 | 99.4 | 60.3 |
| 20,000 | IMes | butadiene | 96.3 | 97.8 | 1.6 | 0.3 | 99.4 | 59.5 |
| 60,000 | IMes | sCC$_4$ | 92.4 | 98.0 | 1.5 | 0.3 | 99.5 | 64.9 |
| 40,000 | IMes | sCC$_4$ | 97.1 | 98.0 | 1.6 | 0.3 | 99.6 | 62.9 |
| 20,000 | IMes | sCC$_4$ | 98.8 | 97.9 | 1.6 | 0.3 | 99.6 | 60.0 |

*Reaction conditions: 70 °C, 15 bar, $n_{butadiene}$:$n_{MeOH}$ = 0.5, $n_{Lig}$:$n_{Pd}$ = 4, $n_{butadiene}$:$n_{base}$ = 400.*

### 4.2.2.5  Variation of the molar ratio of ligand to catalyst

It is known that the stability of a palladium catalyst is influenced by the ligand [95; 176]. Furthermore, Vollmüller *et al.* [95] reported the dependence of the selectivity on the amount of TPP ligand for the telomerization reaction. In order to compare the influence of TPP and IMes and to investigate their behavior depending on the applied feed, the molar ratio of ligand to palladium was varied. The results for the four reaction systems are depicted in Figure 30.
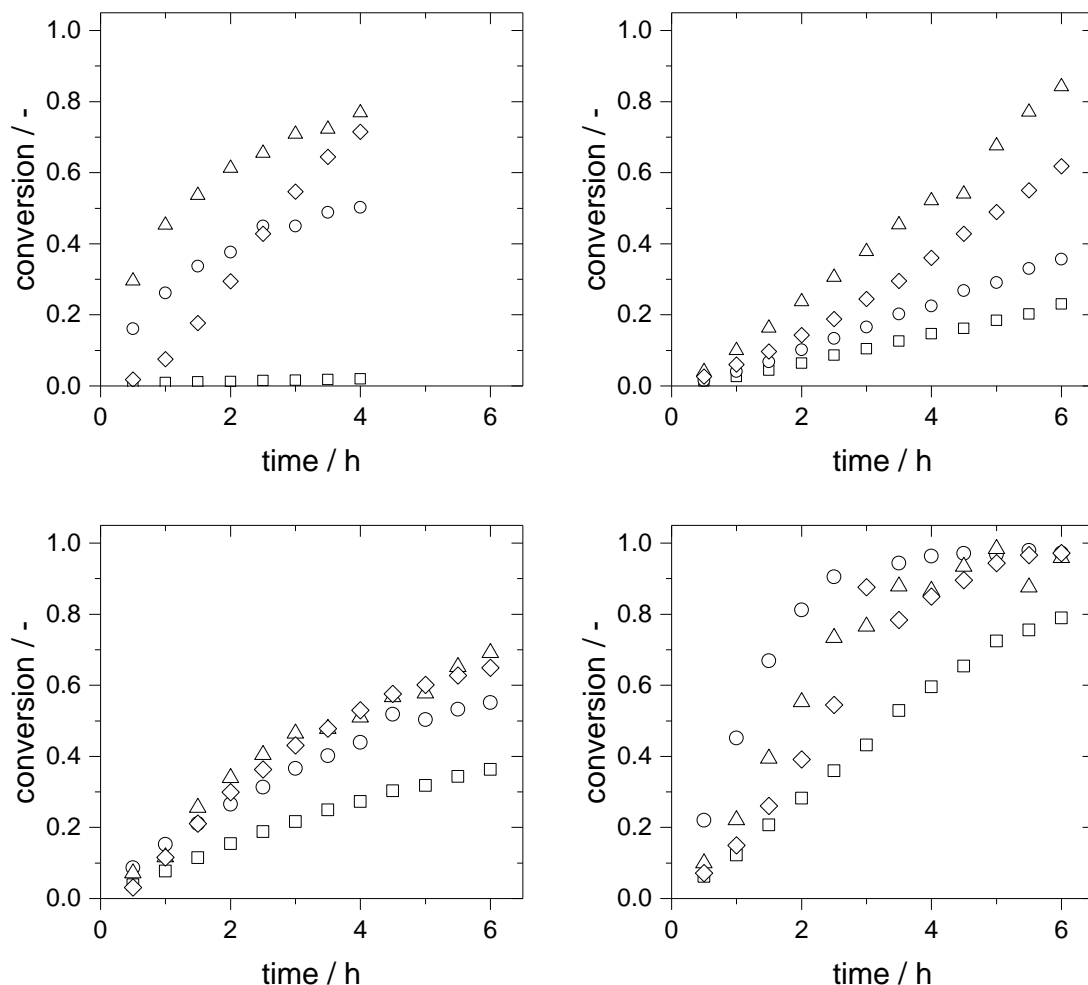
**Figure 30: Influence of the molar ratio of ligand to Pd for the TPP (left) and the IMes (right) modified catalysts with pure butadiene (top) and sCC$_4$ (bottom) (□ 1:5, ○ 1:1, △ 4:1, ◇ 10:1).**

*Reaction conditions: 70 °C, 15 bar, $n_{butadiene}$:$n_{MeOH}$ = 0.5, $n_{butadiene}$:$n_{Pd}$ = 40,000, $n_{butadiene}$:$n_{base}$ = 400.*

For the Pd-TPP catalyst combined with pure butadiene, almost no conversion was achieved when applying an excess of palladium (1:5). This is an indication for the missing stability of the catalyst. The best performance was obtained with a fourfold excess of ligand (4:1). The large excess of TPP (10:1) caused an activation phase. However, the activity increased afterwards and the same conversion was obtained after 4 hours compared to the 4:1 ratio. The excess of ligand seemed to be required in order to stabilize the catalyst. If the excess is too large, however, the excess ligand probably compete for the coordination spots resulting in an activation phase. But

once the active complex is formed, the catalyst is stable and catalyzes the telomerization reaction. With a 1:1 ratio a lower activity was obtained compared to 4:1. It is known that for phosphine ligands, a ligand excess is required to stabilize the catalyst [95].

Interestingly, the dependence of the Pd-TPP catalyst on the ligand to palladium ratio changed when applying the diluted butadiene feed. The use of excess ligand (4:1 and 10:1) led to a similar activity. The negative effect of competing ligand seems to be less pronounced with $sCC_4$ probably because the dilution by the inerts also affects the concentration of palladium and ligand present in the mixture. The reaction rate of the molar ratio of 1:1 was only slightly lower. In contrast to pure butadiene, using an excess of palladium in combination with the diluted butadiene feed, activity was observed but the latter was lower compared to the other applied ratios.

Obviously, the reaction was not only influenced by the ratio of ligand to palladium but also by the concentration of butadiene. An interaction between the active catalyst species which is influenced by the ligand to palladium ratio and butadiene seems to be reasonable for this reaction. As known from the mechanism, a high concentration of butadiene can shift the equilibrium between the inactive $Pd^0L$ species and the active catalyst complex **10**. An explanation could be that the excess of ligand stabilizes and protects the active species against coordination of butadiene. This effect of excess ligand is less pronounced at lower butadiene concentration, e.g. with the application of $sCC_4$, explaining the similar performances of the experiments with the ratios 10:1, 4:1 and 1:1.

Similar to the Pd-TPP catalyst, the worst performance for the Pd-IMes catalyst was obtained with excess of palladium for both feeds. Again, the zero order dependency in butadiene was observed which was more pronounced with excess catalyst. For both feeds, the ratio of 4:1 showed a slightly higher activity compared to the ratio of 10:1. Interestingly, with pure butadiene the reaction rate for the molar ratio of 1:1 is lower than for 4:1 and 10:1 whereas it showed the highest activity with $sCC_4$. This behavior could be caused by a chelating effect of butadiene. The IMes ligand is able to protect the palladium center against the coordination of butadiene. This is important at high concentrations of butadiene. At lower concentrations of butadiene, e.g. with $sCC_4$, this protective function provided by the excess of IMes ligand is not required anymore. This assumption would also correlate with the observation of more

pronounced inhibition when applying excess palladium in combination with pure butadiene.

Regarding the activity of the studied systems, it is obvious that an optimum ratio of ligand to catalyst exists for both catalyst systems. In consequence, the ratio has to be chosen individually depending on the applied system. Furthermore, the activity seems to be an interaction between the ratio of ligand to catalyst and the concentration of butadiene.

As reported by Vollmüller *et al.* [95], the selectivity of the telomerization reaction is influenced by the amount of TPP. By using a ligand with a higher steric demand, this influence can be eliminated [27; 29]. The selectivities obtained for this study are summarized in Table 11.

**Table 11: Results at different molar ratios of ligand to Pd for the TPP modified and the IMes modified catalysts with pure butadiene and sCC$_4$ after 6 h (4 h for Pd-TPP with pure butadiene).**

| ratio ligand:Pd | ligand | feed | $X$ / % | $S_1$ / % | $S_2$ / % | $S_3$ / % | $S_{1+2}$ / % | *n:iso* / - |
|---|---|---|---|---|---|---|---|---|
| 1:5 | TPP | butadiene | 2.0 | 75.4 | 3.0 | 10.0 | 78.5 | 25.1 |
| 1:1 | TPP | butadiene | 50.3 | 90.3 | 4.7 | 4.6 | 95.0 | 19.1 |
| 4:1 | TPP | butadiene | 76.9 | 89.6 | 5.8 | 4.6 | 95.4 | 15.5 |
| 10:1 | TPP | butadiene | 71.5 | 86.3 | 10.5 | 3.2 | 96.8 | 8.2 |
| 1:5 | TPP | sCC$_4$ | 36.3 | 83.7 | 3.8 | 12.1 | 87.5 | 22.3 |
| 1:1 | TPP | sCC$_4$ | 55.2 | 87.0 | 4.3 | 8.6 | 91.3 | 20.3 |
| 4:1 | TPP | sCC$_4$ | 69.1 | 85.8 | 5.7 | 8.3 | 91.6 | 15.0 |
| 10:1 | TPP | sCC$_4$ | 64.9 | 85.5 | 10.2 | 4.2 | 95.7 | 8.4 |
| 1:5 | IMes | butadiene | 23.1 | 97.3 | 1.6 | 1.0 | 98.9 | 61.4 |
| 1:1 | IMes | butadiene | 35.6 | 97.8 | 1.6 | 0.4 | 99.3 | 62.7 |
| 4:1 | IMes | butadiene | 84.2 | 97.8 | 1.6 | 0.4 | 99.4 | 62.3 |
| 10:1 | IMes | butadiene | 61.8 | 97.8 | 1.6 | 0.3 | 99.4 | 62.0 |
| 1:5 | IMes | sCC$_4$ | 78.9 | 97.6 | 1.5 | 0.8 | 99.0 | 67.2 |
| 1:1 | IMes | sCC$_4$ | 97.2 | 98.1 | 1.5 | 0.4 | 99.6 | 64.2 |
| 4:1 | IMes | sCC$_4$ | 95.9 | 98.1 | 1.5 | 0.3 | 99.6 | 65.3 |
| 10:1 | IMes | sCC$_4$ | 97.2 | 98.1 | 1.5 | 0.3 | 99.6 | 63.9 |

*Reaction conditions: 70 °C, 15 bar, $n_{butadiene}{:}n_{MeOH} = 0.5$, $n_{butadiene}{:}n_{Pd} = 40,000$, $n_{butadiene}{:}n_{base} = 400$.*

For the Pd-TPP catalyst, the trends were the same for both feeds. For the molar ratio of ligand to palladium of 1:1, the selectivity toward 1-Mode was the highest. Increasing the amount of ligand, the selectivity toward 1-Mode as well as octatriene

was decreased whereas the formation of 3-Mode was increased. The chemoselectivity remained constant, the regioselectivity decreased due to the 3-Mode formation. This is in accordance with the observations by Vollmüller *et al.* [95]. They reported a favored formation of 3-Mode with excess of ligand due to the coordination of a second ligand to the palladium core as already discussed in detail in Chapter 2.1.2.2.

With catalyst excess, the selectivity toward 1-Mode as well as 3-Mode decreased in favor of the formation of octatriene. This is probably caused by the lack of ligand responsible for the control of selectivity.

In contrast, the selectivity gained with the Pd-IMes catalyst remained completely unaffected by the variation of the amount of ligand. Again, this is in accordance with literature reports [27; 29; 95].

### 4.2.2.6 Variation of the molar ratio of butadiene to methanol

The concentration of butadiene and methanol was reported to influence the selectivity as well [95]. However, no reports on their influence on activity over reaction time as well as no comparative study of the Pd-TPP and the Pd-IMes modified catalyst with the two feeds are found in the literature. Furthermore, the effect of varying methanol concentration is interesting as it acts as solvent and reactant simultaneously. But the latter fact reflects also the problem of this study. By changing the molar ratio of butadiene to methanol, the concentration of butadiene and the concentration of methanol will be changed simultaneously. Without the use of an additional solvent the development of a kinetic rate law will be difficult. However, as the aim of this study was the optimization of reaction conditions and not a classical kinetic study, no additional solvent was applied. Only the ratio of butadiene to methanol was changed, all other ratios, also the ratio of butadiene to catalyst and the reaction volume were kept constant. In collaboration with the SYNFLOW partner RWTH Aachen a reaction kinetic based on the Jolly mechanism was later developed from the obtained data.

Regarding the reaction equation, the first expectation would be that the reaction shows the highest activity when applying a stoichiometric ratio of the reactants.

However, in the literature most often an excess of methanol was used for the Pd-TPP catalyst claiming that a stoichiometric ratio lowers the reaction rate. In this thesis, a more detailed investigation was carried out for the four reaction systems by testing seven different ratios. The butadiene conversion over reaction time is presented in Figure 31.

The influence of varying reactants' ratio differed strongly depending on the applied system. For Pd-TPP with pure butadiene, no large difference was observed within the range of 1:1 to 1:3. The activity behaved very similar over time and no trend was observed so that the variation within this ratio range did not influence the reaction performance. When applying a large excess of methanol (1:5), an activation phase was observed reaching a similar activity after around 1.5 to 2 hours. This was probably caused by the high dilution of the catalyst amount due to the high amount of methanol. With a stoichiometric ratio of 2:1, the reaction rate decreased. Butadiene is known as catalyst inhibitor due to its chelating properties. Possibly, the butadiene concentration at the stoichiometric ratio is too high blocking the catalyst by chelating.

When applying the diluted butadiene feed with the Pd-TPP catalyst, the activity achieved for all ratios was lowered compared to pure butadiene. Interestingly, the highest activity was observed with a large methanol excess. By increasing the butadiene concentration, the activity decreased. This effect was less pronounced in the ratio range of 1:3 to 1:1.5, but strongly pronounced for 1:5, 1:1 and 2:1. This could be again caused by the chelating properties of butadiene. Another explanation of this behavior could be the composition of the $sCC_4$ and thus the whole reaction mixture. By the application of $sCC_4$ the content of hydrocarbons is increased compared to the same ratio of the reactants when using pure butadiene. The solubility of the catalyst species is lower in hydrocarbons than in methanol and is increased with a larger amount of methanol. In addition, the dilution effect caused by excess methanol was less pronounced as the reaction mixture was already highly diluted by the inert compounds of the $sCC_4$ feed.
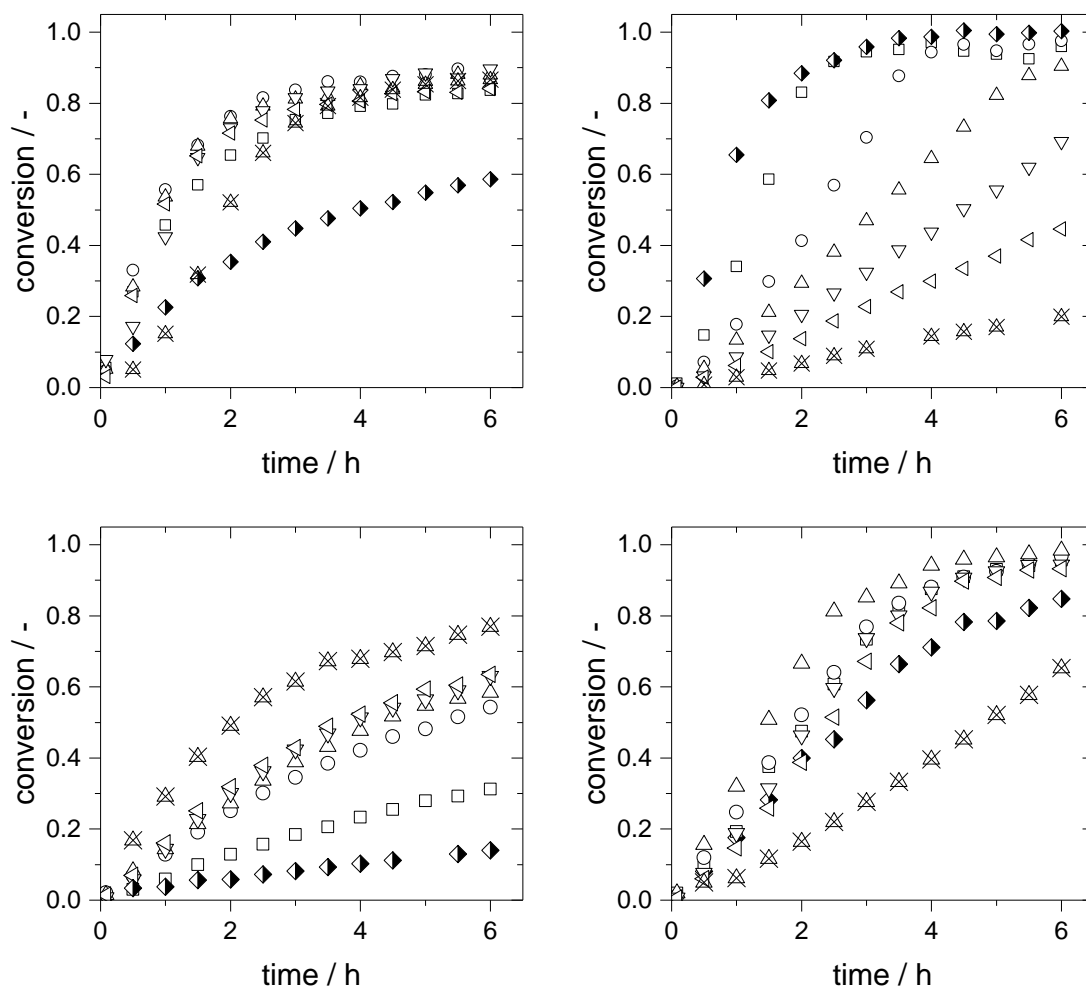
**Figure 31: Influence of the molar ratio of butadiene to methanol on the conversion related to butadiene for the TPP (left) and the IMes (right) modified catalysts with pure butadiene (top) and sCC₄ (bottom) (◆ 2:1, □ 1:1, ○ 1:1.5, △ 1:2, ▽ 1:2.5, ◁ 1:3, ✕ 1:5).**

*Reaction conditions: 70 °C, 15 bar, $n_{butadiene}{:}n_{Pd} = 40{,}000$, $n_{Lig}{:}n_{Pd} = 4$, $n_{butadiene}{:}n_{base} = 400$.*

For the Pd-IMes catalyst a strong dependence on the reactants' ratio was obtained with pure butadiene. A clear trend was observed. The activity of the reaction was increased with increasing concentration of butadiene being in accordance with a literature report dealing with the telomerization of 1,3-pentadiene [177]. However, this observation seems to be in contrast to an assumed zero order dependency in butadiene. Nevertheless, an increase in butadiene is consequently followed by an increase in the catalyst concentration due to the constant ratio of butadiene to

catalyst. Thereby, the reaction rate would probably be also increased due to the already shown dependency on the catalyst concentration. The same explanation would be valid for the base concentration.

With the diluted butadiene feed, the reaction rate first increased with increasing butadiene concentration for the Pd-IMes catalyst reaching an optimum ratio of butadiene to methanol of 1:2. This dependence was found to be similar for pure butadiene. However, after reaching this optimum, the reaction performance decreased with further increasing butadiene. This might be caused by the opposing trend of increasing reaction rate with increasing butadiene concentration and decreasing solubility of the catalyst due to the increasing amount of hydrocarbons.

Interestingly, the influence of the varying reactants' ratio is not pronounced that strongly as with pure butadiene. This might further emphasize a strong dependence on either catalyst or base concentration.

For the Pd-TPP catalyst, the selectivity toward 1-Mode was increased with decreasing butadiene and increasing methanol concentration whereas the formation of 3-Mode and octatriene was lowered. In consequence, the chemoselectivity as well as regioselectivity was increased. This observed trend is in accordance with the literature [95] and is independent of the applied feed.

The Pd-IMes catalyst was again observed to be unaffected by the studied variations exhibiting high selectivities toward the main product of 97 to 98 %. Only at the stoichiometric ratio, the selectivity toward 1-Mode decreased and the formation of 3-Mode and octatriene increased. The exact obtained values for the selectivity are depicted in Appendix 7.5.

### 4.2.3 Kinetic Modeling

In collaboration with the SYNFLOW partner RWTH Aachen, a reaction kinetic based on the two literature known mechanisms and the experiments from the previous Chapter 4.2.2.6 was derived. The reaction kinetics for the Pd-IMes catalyst obviously differ from that for the Pd-TPP catalyst. The results of the kinetic modeling confirmed the observed differences between the two catalysts [178]. Within this thesis, only the relevant results, rate equations and conclusions are shown. For detailed information

on the procedure of the kinetic modeling carried out by Sebastian Recker of the Marquardt group (RWTH Aachen), refer to the collaborative publication [178]. According to Donna Blackmond [179], the experimental results introduced in Chapter 4.2.2.6 were plotted in normed plots confirming that both catalysts follow the Jolly mechanism. In a next step, rate equations were derived based on the Jolly mechanism [180] which fit well with the experimental data for the Pd-TPP catalyst but not for the Pd-IMes catalyst, see Figure 32.

After identifiability analysis, model reduction and parameter estimation [181; 182], the kinetic model for the Pd-TPP catalyst can be described according to Equations (4) - (6).

$$r_{0,TPP} = K_{0,TPP} \cdot c_B{}^2 \cdot c_{Pd,pre} \tag{4}$$

$$r_{1,TPP} = c_{cat} \cdot \frac{K_{1,TPP} \cdot c_B{}^2 \cdot c_{MeOH}}{1 + K_{2,TPP} \cdot c_B{}^2} \tag{5}$$

$$r_{2,TPP} = c_{cat} \cdot K_{3,TPP} \cdot c_B{}^2 \cdot c_{MeOH} \tag{6}$$

The reaction rate for the catalyst activation is described by $r_0$, the reaction rate forming the telomers by $r_1$ and the reaction rate of the side reaction forming octatriene by $r_2$. The concentrations are specified by their corresponding indices. The parameters $K_1$, $K_2$ and $K_3$ compose the rate constants of the different reaction steps within the catalytic mechanism [180]. For the main reaction, the model exhibits a second order in butadiene and first order in methanol at moderate to low butadiene concentrations. This aligns with the slow reaction progress at the end of reaction, especially for the experiments with $sCC_4$. At high butadiene concentration, the reaction rate depends only on the methanol concentration. This confirms quite well the observed behavior of the previously discussed experiments.
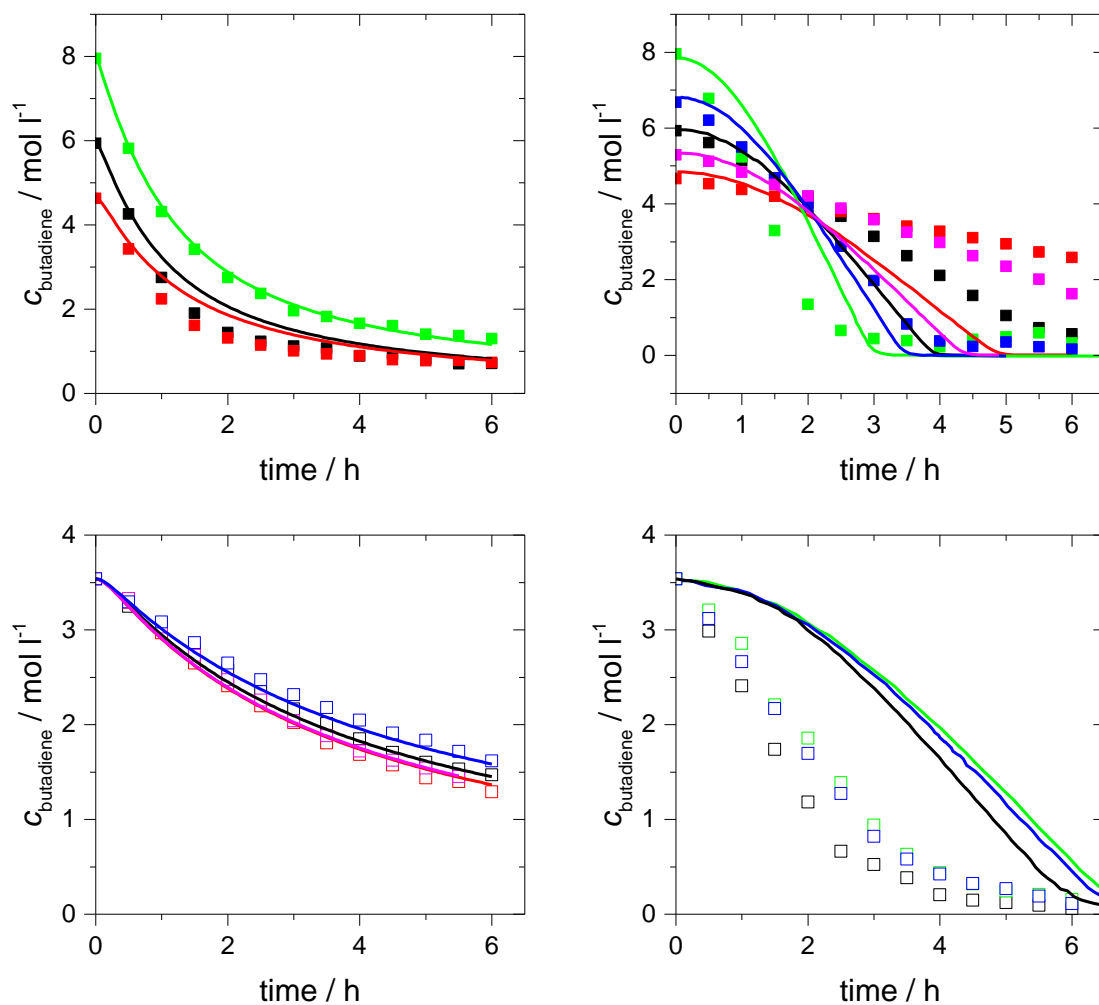
**Figure 32: Results of the parameter estimation applying the kinetic models (lines) derived for the TPP (left) and the IMes (right) modified catalysts with pure butadiene (top) and sCC$_4$ (bottom) compared to the experimental data (symbols) obtained for the variation of the molar ratio of butadiene to methanol (see Chapter 4.2.2.6).**

*Reaction conditions: 70 °C, 15 bar, $n_{butadiene}$:$n_{Pd} = 40,000$, $n_{Lig}$:$n_{Pd} = 4$, $n_{butadiene}$:$n_{base} = 400$, $n_{butadiene}$:$n_{MeOH} = (black = 1:2,$ $red = 1:3,$ $green = 1:1,$ $blue = 1:1.5, pink = 1:2.5).$*

## 4.2.3.1   Deviation of the Pd-IMes catalyst from the known Jolly mechanism

For the Pd-IMes catalyst, the rate equation based on the Jolly mechanism did not describe the experimental data satisfactorily. Based on the experimental data from the previous chapters, it is obvious that either the base or the catalyst concentration affects the Pd-IMes catalyst more than in the case of the Pd-TPP catalyst. Furthermore, the experimental data indicated an overall zero order dependency in butadiene for the IMes based catalyst. In order to gain further detailed kinetic information, a set of experiments with varying base concentration as well as one set with varying butadiene concentration and one with varying methanol concentration were carried out for the Pd-IMes catalyst. For these experiments, all other concentrations were kept constant by using hexane as additional solvent.

### 4.2.3.1.1   Supporting experiments for kinetic modeling

**Variation of the base concentration**

According to the previous experimental results, the reaction kinetics of the Pd-IMes catalyst seems to be strongly influenced by the base KOMe. In order to support these observations a variation of the added amount of base was carried out, all other parameters were kept constant. The results are depicted in Figure 33.

As expected, the reaction rate is strongly dependent on the base concentration. With increasing amount of added base the reaction rate increased. This observation indicates that the nucleophilic attack is the rate determining step of the whole telomerization sequence for the Pd-IMes catalyst. Furthermore, the base is necessary to undergo this nucleophilic attack as shown in previous experiments (see Chapter 4.2.2.2). The selectivities were not influenced strongly lying in the error margin.
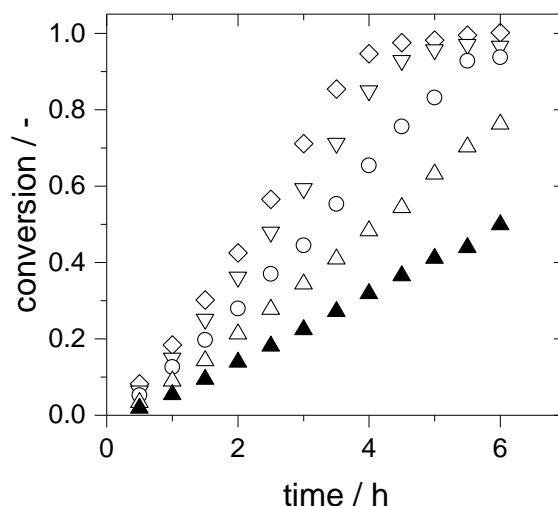
**Figure 33: Variation of the base concentration for the IMes modified catalyst with pure butadiene ($\Diamond$ 3.234 mmol, $\triangledown$ 2.597 mmol, $\bigcirc$ 2.010 mmol, $\triangle$ 1.293 mmol, ▲ 0.668 mmol).**

*Reaction conditions: 70 °C, 15 bar, $V_{reaction} = 140 \, ml$, $n_{butadiene}{:}n_{MeOH} = 0.5$, $n_{butadiene}{:}n_{Pd} = 40,000$, $n_{IMes}{:}n_{Pd} = 4$.*

**Variation of the butadiene concentration**

In order to study the influence of butadiene on the reaction rate, a variation of the butadiene concentration was carried out while all other concentrations were kept constant by adding hexane as additional solvent. By this, the amount of methanol and the amount of base were constant as well. The results of these experiments are shown in Figure 34.

Interestingly, the five experiments showed very similar conversion plots confirming the observed independency of the butadiene concentration. Slight differences were found in the reaction start or activation phase. But this reaction period is very sensitive and also strongly dependent on the temperature. As slight temperature fluctuations might occur especially during the first 20 minutes, the slight differences in the activation phase was probably caused by this. Furthermore, the reaction rate of the catalyst activation seems to be dependent on the butadiene concentration. The selectivities again differed only by around 1 %.

These observations lead to the conclusion that the telomerization reaction with an IMes based catalyst exhibits a reaction order of zero in butadiene.
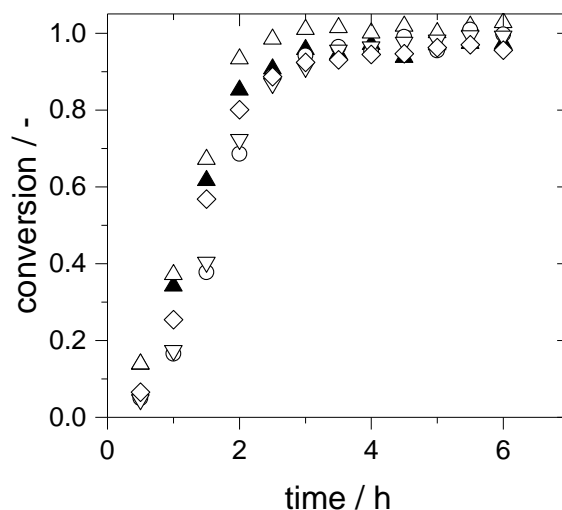
**Figure 34: Variation of the butadiene concentration for the IMes modified catalyst with pure butadiene (▲ 1.099 mol ($n_{butadiene}$:$n_{MeOH}$ = 1:1), △ 0.732 mol (1:1.5), ○ 0.548 mol (1:2), ▽ 0.440 mol (1:2.5), ◇ 0.366 mol (1:3)).**

*Reaction conditions: 70 °C, 15 bar, $V_{reaction}$ = 140 ml, $n_{MeOH}$ = 1.1 mol, $n_{Pd}$ = 0.028 mmol, $n_{IMes}$ = 0.111 mmol, $n_{KOMe}$ = 2.58 mmol, solvent: hexane.*

**Variation of the methanol concentration**

The influence of methanol was studied by varying the methanol concentration. All other concentrations were again kept constant by adding hexane. By this, a lowering of the methanol concentration was compensated by the addition of hexane. The results are presented in Figure 35.

In contrast to the variation of the butadiene concentration, the variation of the methanol concentration strongly influenced the reaction performance. With increasing amount of methanol, the reaction performance decreased although all other concentrations, e.g. catalyst, ligand and base, were kept constant. Low methanol concentrations exhibiting low butadiene to methanol ratios (1:1 and 1.5:1) showed similar results compared to the results of the butadiene variation. Nevertheless, higher concentrations of methanol showed much lower performances compared to their analogues of the butadiene variation experiments. The negative influence might be caused by the dependence of the nucleophilicity of the base on

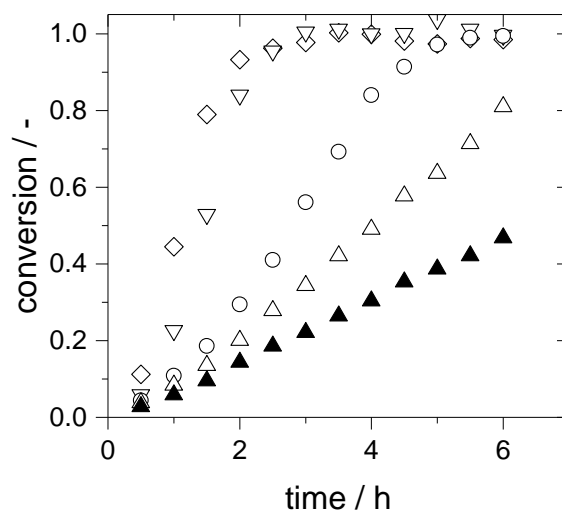the composition of the reaction mixture being higher at lower concentration of the protic solvent methanol.



**Figure 35: Variation of the methanol concentration for the IMes modified catalyst with pure butadiene ($\diamond$ 0.679 mol ($n_{butadiene}$:$n_{MeOH}$ =1:1), $\triangledown$ 1.012 mol (1:1.5), $\bigcirc$ 1.345 mol (1:2), $\triangle$ 1.679 mol (1:2.5), $\blacktriangle$ 2.024 mol (1:3)).**

*Reaction conditions: 70 °C, 15 bar, $V_{reaction} = 140$ ml, $n_{butadiene} = 0.68$ mol, $n_{Pd} = 0.017$ mmol, $n_{IMes} = 0.068$ mmol, $n_{KOMe} = 1.6$ mmol, solvent: hexane.*

As the base seems to be the essential component in the reaction mechanism of the IMes modified catalyst, a lower nucleophilicity decreases the reaction rate.

This observation was further investigated by experiments with constant ratio of methanol to base. The results are shown in Figure 36.

The reaction rates increased compared to their analogues of the methanol variation but still differed among each other. The negative influence of methanol seems to be stronger than the positive influence of the base. This observation indicates that the influence of the protic methanol on the nucleophilicity of the base does not behave in a linear fashion.
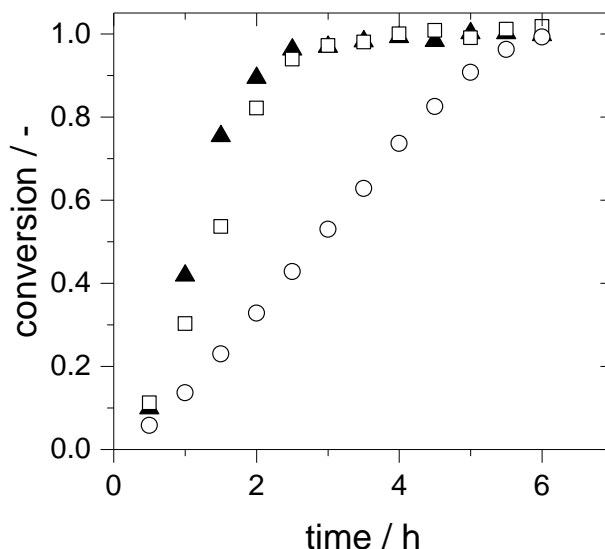
**Figure 36: Variation of the methanol concentration for the IMes modified catalyst with pure butadiene and constant ratio of methanol to base (▲ $n_{MeOH}$ = 0.679 mol and $n_{KOMe}$ = 1.60 mmol,** □ $n_{MeOH}$ = 1.348 mol **and $n_{KOMe}$ = 3.14 mmol, ○ $n_{MeOH}$ = 2.015 mol and $n_{KOMe}$ = 4.75 mmol).**

*Reaction conditions: 70 °C, 15 bar, $V_{reaction}$ = 140 ml, $n_{butadiene}$ = 0.68 mol, $n_{Pd}$ = 0.017 mmol, $n_{IMes}$ = 0.067 mmol, solvent: hexane.*

### 4.2.3.1.2   Kinetic model and new aspects for the Jolly mechanism

Based on the results of the detailed kinetic study, the Jolly mechanism was adapted as shown in Figure 37. The only difference to the original Jolly mechanism postulated for Pd-TPP systems is that the nucleophilic attack at complex **12** takes solely place in the presence and by means of a strong base such as KOMe. The already bound methoxy is assumed to be not strong enough to attack the allyl-group in an intramolecular fashion. Instead, the additional, external methoxide performs an intermolecular nucleophilic attack under release of the bound methoxide. Thus, without a strong base the reaction would stop at this point. It is known from the literature [106] that even for the Pd-TPP system, the addition of a base changes the rate-determining step due to facilitating the nucleophilic attack at complex **12**. To account for the negative influence of the protic solvent methanol, the active concentration of methoxide is represented as a function of methanol.
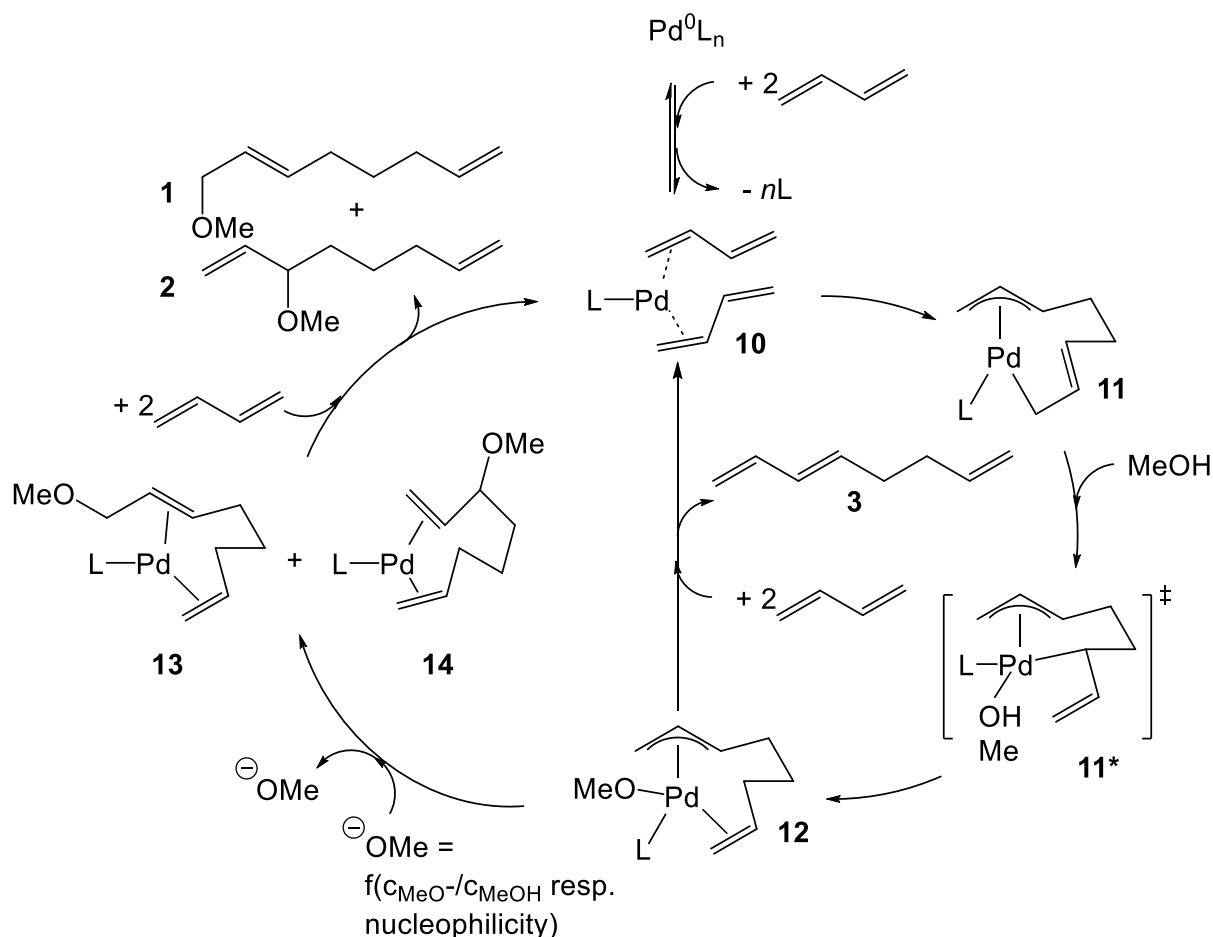
**Figure 37: Adapted Jolly mechanism for the Pd-IMes catalyzed telomerization of butadiene with methanol.**

For the modeling, the influence of the nucleophilicity was added by the creation of a resting state for the methoxide anion which is dependent on the methanol concentration. Based on this adapted Jolly mechanism, the kinetic rate equation were derived in the similar way than for the Pd-TPP catalyst [178].

$$r_{0,\text{IMes}} = K_{0,\text{IMes}} \cdot c_B^2 \cdot c_{\text{Pd,pre}} \tag{7}$$

$$r_{1,\text{IMes}} = c_{\text{cat}} \cdot \frac{K_{1,\text{IMes}} \cdot c_B^2 \cdot c_{\text{KOMe}}}{1 + K_{2,\text{IMes}} \cdot c_B^2 \cdot c_{\text{MeOH}} + K_{3,\text{IMes}} \cdot c_{\text{KOMe}}} \tag{8}$$

With this model, the experimental data can be described quite well, see Figure 38.
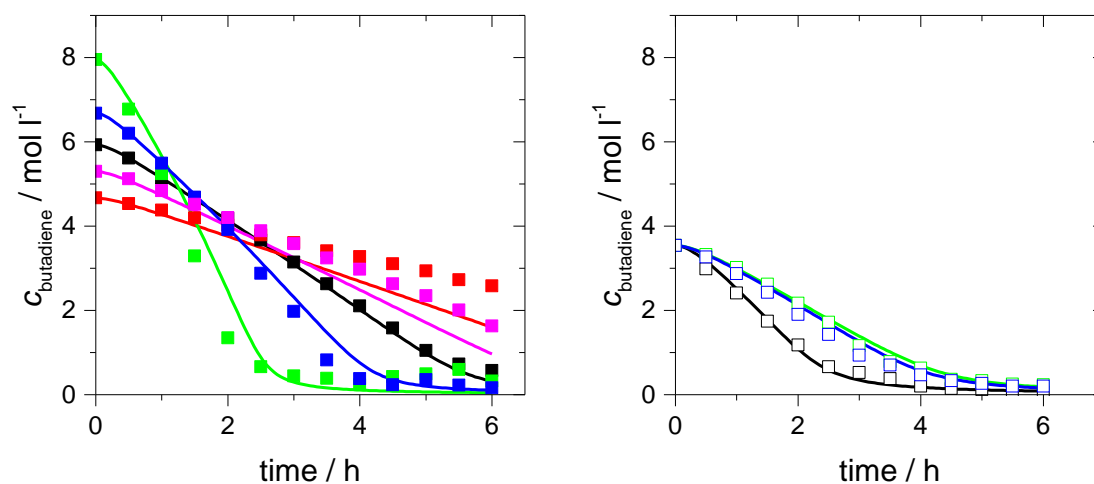
**Figure 38: Results of the parameter estimation applying the kinetic model based on the adapted Jolly mechanism (lines) derived for the IMes modified catalyst with pure butadiene (left) and sCC$_4$ (right) compared to the experimental data (symbols) obtained for the variation of the molar ratio of butadiene to methanol (see Chapter 4.2.2.6).**

*Reaction conditions: 70 °C, 15 bar, $n_{butadiene}$:$n_{Pd}$ = 40,000, $n_{Lig}$:$n_{Pd}$ = 4, $n_{butadiene}$:$n_{base}$ = 400, $n_{butadiene}$:$n_{MeOH}$ = (black = 1:2, red = 1:3, green = 1:1, blue = 1:1.5, pink = 1:2.5).*

At high to moderate concentrations of butadiene, the reaction is of zero order in butadiene. The dependency on the base concentration is described by a reaction order of 1. The negative influence of methanol which is reflected in the nucleophilicity of the base is represented by a negative order of 1 in methanol. Only at very high base concentrations, the reaction is independent of the base concentration. The latter behavior is not relevant at all studied reaction conditions of this thesis.

This kinetic model also explains the observed behavior of the Pd-IMes catalyst with diluted feeds in comparison to pure butadiene as the rate is independent of the butadiene concentration. The rate determining step seems to be the nucleophilic attack of the methoxide anion. A further hint for this assumption is the observation that with a weaker base such as NEt$_3$ only a very low conversion (6 % after 18 h) was obtained.

## 4.2.4 Catalyst screening

For the butadiene telomerization with methanol, the most often used palladium precursors in the literature are either Pd(acac)$_2$ or Pd(OAc)$_2$. In order to study the influence of the palladium source on the four reaction systems, different palladium precursors were tested in this thesis. Furthermore, the effect of different NHC-ligand structures was investigated by the application of well-defined Pd-NHC-complexes which were synthesized within the SYNFLOW project by Anthony Chartoire of the Nolan group, University of St. Andrews.

### 4.2.4.1 Variation of catalyst precursor

Besides the two well-known palladium precursors Pd(acac)$_2$ and Pd(OAc)$_2$, a third one, namely palladium cinnamyl chloride (Pd$_2$(cin)$_2$Cl$_2$), was tested for the evaluation of the effect of palladium source on the telomerization reaction. The three precursors were combined with both feeds under the same reaction conditions. The results of this comparative study are depicted in Figure 39.

For both feeds, the Pd-TPP catalyst did not show a strong dependence on the applied catalyst precursors. With pure butadiene, the activities of Pd(acac)$_2$ and Pd(OAc)$_2$ were observed to be very similar whereas the reaction rate obtained for Pd$_2$(cin)$_2$Cl$_2$ was slightly lower. With sCC$_4$ as feed, the precursors Pd(acac)$_2$ and Pd$_2$(cin)$_2$Cl$_2$ exhibited the same reaction rate while Pd(OAc)$_2$ showed a slightly lower one. For the Pd-TPP catalyst, no clear trend and no crucial difference was found for the different catalyst precursors.

In contrast, the observed differences were larger, especially with pure butadiene, for the Pd-IMes modified reaction systems. For pure butadiene, Pd(acac)$_2$ exhibited the highest activity. The reaction rates observed for Pd(OAc)$_2$ and Pd$_2$(cin)$_2$Cl$_2$ were distinctly lower whereas the one for Pd(OAc)$_2$ was the lowest. Also for the diluted butadiene feed, Pd(acac)$_2$ showed the best performance followed by Pd(OAc)$_2$ and Pd$_2$(cin)$_2$Cl$_2$. However, the difference is distinctively less pronounced compared to pure butadiene. The reason for Pd(acac)$_2$ being the best precursor especially when applying pure butadiene is not clear. An assumption could be that the chelating

acetylacetonate (acac) exhibits a higher potential to protect the palladium center against chelating butadiene.
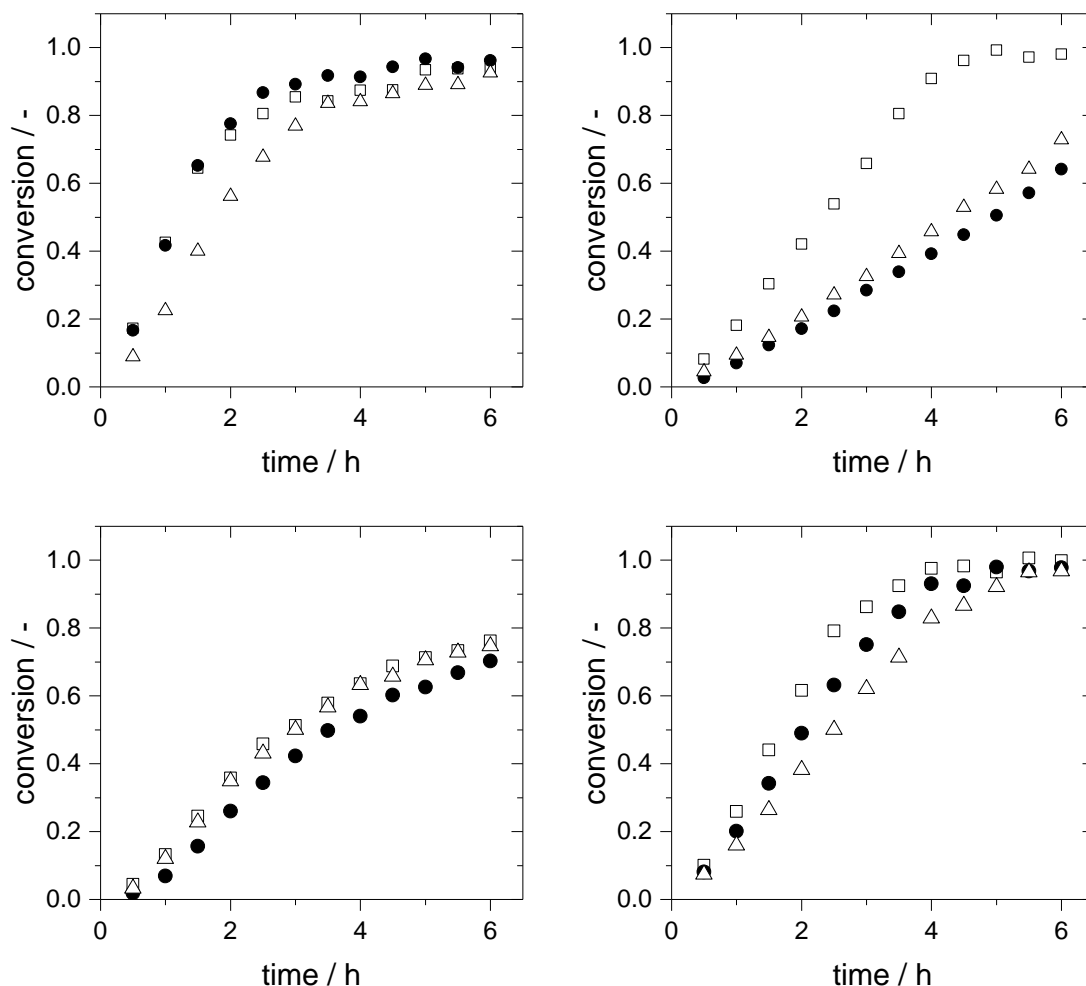


**Figure 39: Influence of different palladium precursors for the TPP (left) and IMes (right) modified catalysts with pure butadiene (top) and sCC$_4$ (bottom) (□ Pd(acac)$_2$, ● Pd(OAc)$_2$, △ Pd$_2$(cin)$_2$Cl$_2$).**

*Reaction conditions: 70 °C, 15 bar, $n_{butadiene}$:$n_{MeOH}$ = 0.5, $n_{butadiene}$:$n_{Pd}$ = 40,000, $n_{Lig}$:$n_{Pd}$ = 4, $n_{butadiene}$:$n_{base}$ = 400.*

The variation of the palladium precursor did not influence the selectivity for both ligands applied. The already discussed changes of selectivities for the Pd-TPP catalyst when using sCC$_4$ instead of pure butadiene were observed consistently for all applied precursors.

As the palladium precursors did not influence the Pd-TPP catalyst strongly and the Pd(acac)$_2$ was observed to be the best for the IMes modified system, Pd(acac)$_2$ was applied as palladium precursor for all further experiments.

### 4.2.4.2  Ex-situ prepared catalyst-ligand-complexes

The influence of different feed compositions on the applied Pd-IMes catalyst was already discussed in detail. Other NHC-ligands were tested in the literature for the butadiene telomerization reaction with methanol but no complete kinetic study comparing the two feeds was found [27; 29]. Therefore, different well-defined Pd-NHC complexes were tested in this thesis. The complexes were synthesized ex-situ by the Nolan group and differed in the leaving group (cin vs. acac) and in the steric demand of the NHC-ligand as summarized in Figure 40. All complexes were investigated applying pure butadiene as well as sCC$_4$. The results are depicted in Figure 41.

For sCC$_4$, the performance of the applied complexes was strongly dependent on the leaving group of the complex. With cinnamyl (cin) the reaction with the IMes complex started instantaneously with a high activity in the same order as the in-situ generated Pd-IMes catalyst. With the acetylacetonate (acac) leaving group, the initial activity was significantly lower. For Pd(IMes)(acac)Cl an activation phase was required to reach a similar activity compared to the complex bearing the cin leaving group.

All these described trends were also observed when applying pure butadiene. The trend regarding the steric demand was reported in literature as well [27; 29]. Furthermore, all tested Pd-NHC complexes seemed to follow the same reaction kinetics as the in-situ generated Pd-IMes catalyst.
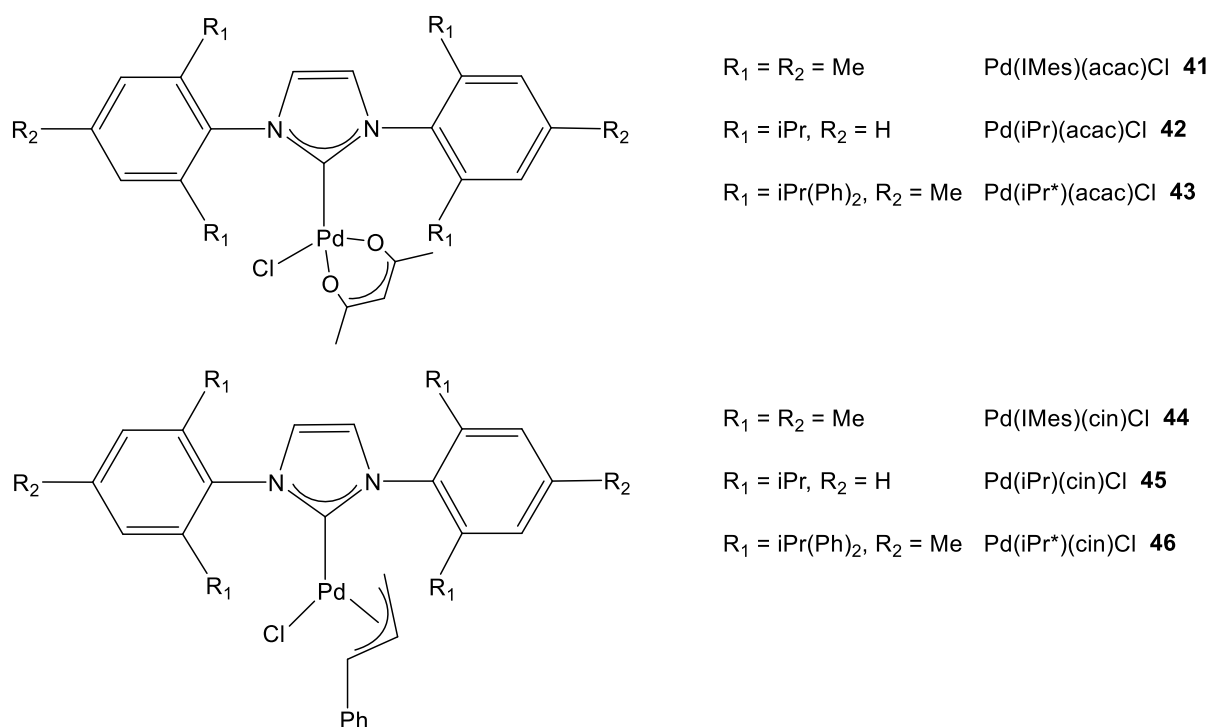
R_1 = R_2 = Me       Pd(IMes)(acac)Cl **41**

R_1 = iPr, R_2 = H       Pd(iPr)(acac)Cl **42**

R_1 = iPr(Ph)_2, R_2 = Me   Pd(iPr*)(acac)Cl **43**

R_1 = R_2 = Me       Pd(IMes)(cin)Cl **44**

R_1 = iPr, R_2 = H       Pd(iPr)(cin)Cl **45**

R_1 = iPr(Ph)_2, R_2 = Me   Pd(iPr*)(cin)Cl **46**

**Figure 40: Studied well-defined Pd-NHC complexes.**
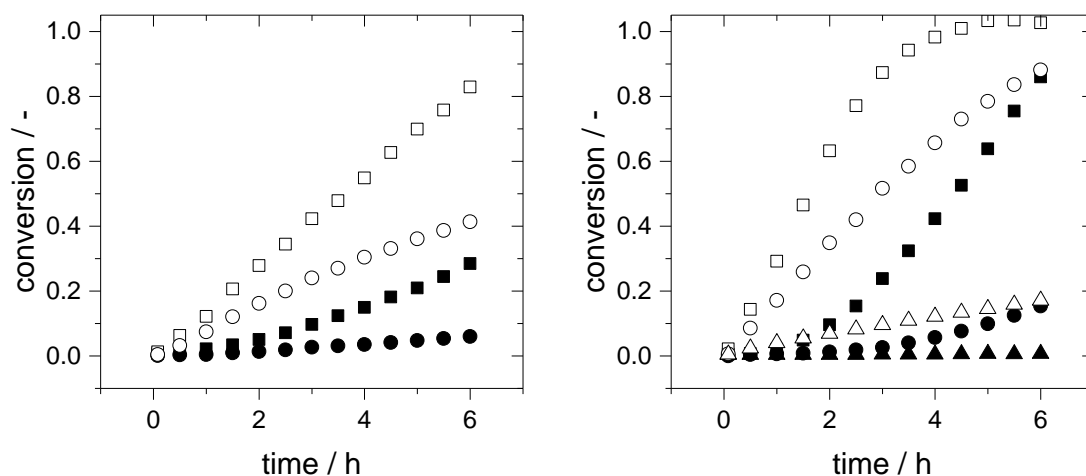


**Figure 41: Influence of different Pd-NHC complexes with pure butadiene (left) and sCC_4 (right) (■ Pd(IMes)(acac)Cl, ● Pd(IPr)(acac)Cl, ▲ Pd(IPr*)(acac)Cl, □ Pd(IMes)(cin)Cl, ○ Pd(IPr)(cin)Cl, △ Pd(IPr*)(cin)Cl).**

*Reaction conditions: 70 °C, 15 bar, $n_{butadiene}$:$n_{MeOH}$ = 0.5, $n_{butadiene}$:$n_{Pd}$ = 40,000, $n_{butadiene}$:$n_{base}$ = 400.*

The screening of different Pd-NHC complexes showed that the IMes ligand is the best of the studied ones. Comparing the reaction performance of the ex-situ and

in-situ generated IMes-complexes, the in-situ generated catalyst showed a slightly higher reaction rate than the ex-situ prepared one. In consequence, the additional effort of preparing well-defined complexes ex-situ is not reflected in a better performance of the reaction.

Comparing the behavior of the leaving groups, acac and cin, for the in-situ formed and ex-situ generated complexes gave opposing trends. For the ex-situ generated complexes, cin showed a better performance than acac while for the in-situ formed catalysts starting with the IMes salt and the palladium precursors, acac exhibited a better performance especially with pure butadiene. The reason for this observation is not known. An assumption could be that the leaving groups offer different binding characteristics in the precursors compared to the well-defined complexes with the already bound NHC-ligands.

As summarized in Table 12, the selectivity toward the main product 1-Mode decreased whereas the formation of 3-Mode and octatriene increased with increasing steric demand of the applied complex. In consequence, also the chemo- as well as the regioselectivity decreased. For pure butadiene, the same trends for the selectivities were observed.

**Table 12: Results for the studied Pd-NHC complexes with pure butadiene and sCC$_4$ after 6 h.**

| complex | feed | $X$ / % | $S_1$ / % | $S_2$ / % | $S_3$ / % | $S_{1+2}$ / % | $n$:$iso$ |
|---|---|---|---|---|---|---|---|
| (IMes)(acac) | sCC$_4$ | 85.9 | 97.8 | 1.5 | 0.4 | 99.3 | 64.1 |
| (IMes)(cin) | sCC$_4$ | 100.0 | 97.8 | 1.6 | 0.4 | 99.4 | 61.3 |
| (iPr)(acac) | sCC$_4$ | 15.4 | 88.0 | 6.6 | 2.0 | 94.6 | 13.3 |
| (iPr)(cin) | sCC$_4$ | 88.1 | 90.2 | 6.7 | 2.2 | 96.9 | 13.4 |
| (iPr*)(acac) | sCC$_4$ | 0.7 | 22.8 | 15.1 | 16.5 | 37.9 | 1.5 |
| (iPr*)(cin) | sCC$_4$ | 17.1 | 36.0 | 29.1 | 32.1 | 65.1 | 1.2 |
| (IMes)(acac) | butadiene | 28.5 | 95.5 | 1.6 | 0.4 | 97.1 | 59.2 |
| (IMes)(cin) | butadiene | 82.8 | 97.4 | 1.6 | 0.4 | 99.1 | 60.4 |
| (iPr)(acac) | butadiene | 6.0 | 85.8 | 7.5 | 2.1 | 93.3 | 11.4 |
| (iPr)(cin) | butadiene | 41.4 | 89.3 | 7.3 | 2.3 | 96.6 | 12.2 |

*Reaction conditions: 70 °C, 15 bar, $n_{butadiene}$:$n_{MeOH} = 0.5$, $n_{butadiene}$:$n_{Pd} = 40,000$, $n_{butadiene}$:$n_{base} = 400$.*

### 4.2.5 Transfer of experiments to another reactor concept

For the biphasic experiments with ionic liquid, a loop reactor was planned and constructed. As explained in Chapter 3.2.2.1, the loop reactor can also be operated in batch mode by bypassing the internal separator. For batch experiments, the reaction volume of the loop reactor is 350 ml. The scale-up from the batch autoclave with a reaction volume of 150 ml to the loop will be introduced in the following chapter. Furthermore, the first continuous operation of the telomerization reaction without catalyst recycling will be discussed.

### 4.2.5.1 Comparison of the reaction systems

The two investigated catalyst systems, Pd-TPP and Pd-IMes, showed a characteristic behavior in combination with the two applied feeds. With these four systems, the transfer and scale-up of the telomerization reaction to the loop reactor was tested. In Figure 42, the results of the four reaction systems conducted at the same reaction conditions and the same molar ratios in the loop reactor are compared with the results obtained in the autoclave.

For the Pd-TPP system, the trends and the studied dilution effect were also observed in the loop reactor. However, the experiments carried out in the loop reactor showed a slightly higher initial activity. For each feed, the same conversion was reached after 6 hours in both reactors.

The Pd-IMes catalyst exhibited the same trend but the difference between autoclave and loop reactor was somewhat larger compared to Pd-TPP. Comparing butadiene and sCC$_4$, the increase of the activity in the loop reactor was in the same range for both. The better performance of the Pd-IMes catalyst with the diluted butadiene feed was also observed in the loop reactor.

Despite the exothermic behavior of the reaction, the loss of heat via the reactor periphery by heat transfer to the environment seems to be higher than the released heat of reaction. Due to its construction, the reaction volume per heat exchange surface is lower in the loop reactor resulting in a better heat supply and thus a better compensation of the heat loss. Furthermore, the feed entering the loop reactor was

preheated whereas in the autoclave, the preheating was carried out only for the methanol solution and butadiene was added having room temperature.
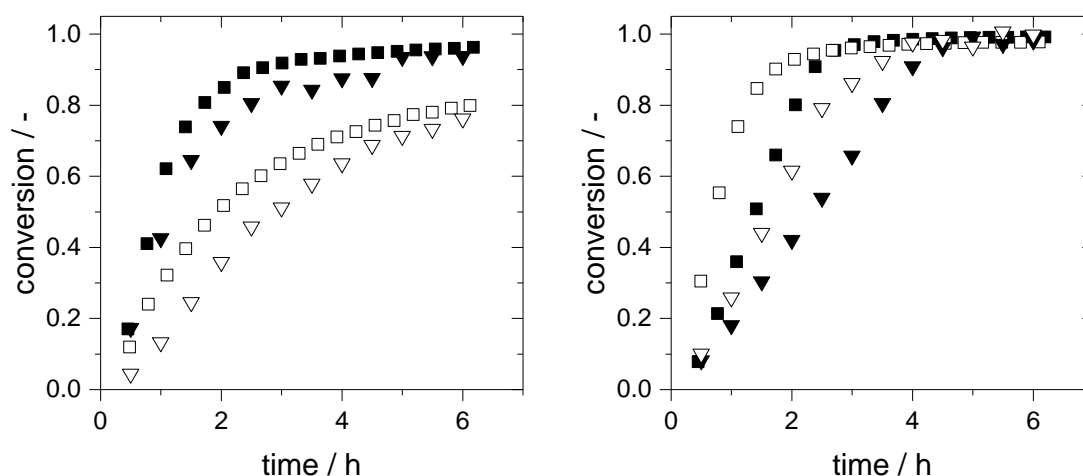


**Figure 42: Transfer and scale-up of the telomerization reaction from the autoclave (AC) to the loop reactor (LR) for the TPP (left) and IMes (right) modified catalysts (■ LR pure butadiene, □ LR sCC₄, ▼ AC pure butadiene, ▽ AC sCC₄).**

*Reaction conditions: 70 °C, 15 bar, $n_{butadiene}:n_{MeOH} = 0.5$, $n_{butadiene}:n_{Pd} = 40,000$, $n_{Lig}:n_{Pd} = 4$, $n_{butadiene}:n_{base} = 400$.*

In Figure 43, the effect of preheating the feed lines on the activity is exemplarily shown for the Pd-IMes catalyst with sCC₄. Here, an experiment with preheating was directly compared with an experiment without preheating for the Pd-IMes catalyst combined with sCC₄. The initial activity observed for the experiment with preheating was slightly higher. But the increase caused by the preheating is not in the same range as it was observed for the comparison of loop reactor and autoclave. This means that the preheating is not the only effect responsible for the increased activity in the loop reactor. Thus, also the better heat supply and compensation of heat loss in the loop reactor itself seems to have a distinct effect.
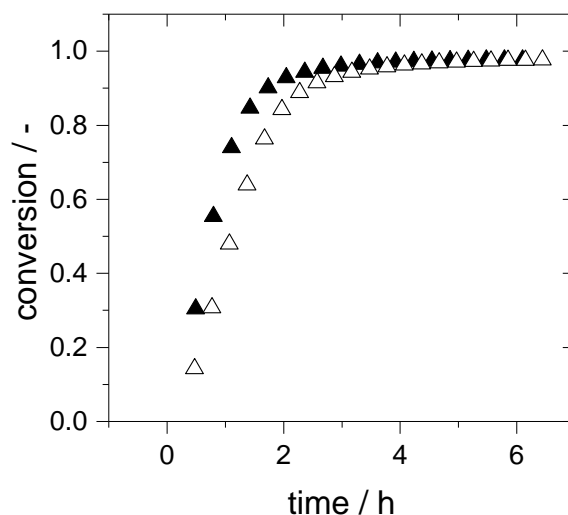
**Figure 43: Effect of preheating the feed lines for the IMes modified catalyst with sCC$_4$ (▲ with preheating, △ without preheating).**

*Reaction conditions: 70 °C, 15 bar, $n_{butadiene}$:$n_{MeOH}$ = 0.5, $n_{butadiene}$:$n_{Pd}$ = 40,000, $n_{Lig}$:$n_{Pd}$ = 4, $n_{butadiene}$:$n_{base}$ = 400.*

As summarized in Table 13, the selectivities exhibited slight but no crucial differences to the values obtained in the batch autoclave (see Figure 23 and Table 7). As already observed in the autoclave for the Pd-TPP catalyst, the selectivity toward 1-Mode was lower with sCC$_4$ than with pure butadiene. For the Pd-IMes system the formation of 1-Mode was lowered slightly with pure butadiene compared to the autoclave.

**Table 13: Results from batch experiments without ionic liquids in the loop reactor for the TPP and IMes modified catalysts with pure butadiene and sCC$_4$.**

| ligand | feed | run time / h | $X$ / % | $S_1$ / % | $S_2$ / % | $S_{3+4}$ / % | $S_{1+2}$ / % | n:iso / - |
|--------|------|-----------|---------|-----------|-----------|---------------|---------------|-----------|
| TPP | butadiene | 6.18 | 96.2 | 86.2 | 7.0 | 7.0 | 93.0 | 12.3 |
| TPP | sCC$_4$ | 6.13 | 78.7 | 84.0 | 6.3 | 10.3 | 90.0 | 13.8 |
| IMes | butadiene | 6.19 | 99.2 | 98.3 | 2.0 | 0.0 | 99.6 | 48.3 |
| IMes | sCC$_4$ | 6.10 | 97.7 | 97.2 | 1.7 | 0.0 | 99.6 | 55.7 |

*Reaction conditions: 70 °C, 15 bar, $n_{butadiene}$:$n_{MeOH}$ = 0.5, $n_{butadiene}$:$n_{Pd}$ = 40,000, $n_{Lig}$:$n_{Pd}$ = 4, $n_{butadiene}$:$n_{base}$ = 400.*

## 4.2.5.2 Continuous flow experiments without catalyst recycling

Before using the loop reactor for the characterization of the continuous process by means of a biphasic reaction system with ionic liquids, first continuous flow experiments were carried out without ionic liquid and without catalyst recycling. Three different feed streams were chosen to study the activation period of the telomerization reaction and the conversions obtained in the steady state. The Pd-TPP catalyst was applied in combination with pure butadiene. A low amount of catalyst and ligand was added to the methanol feed and fed to the loop reactor continuously in order to keep the concentration of catalyst in the reaction mixture constant. The catalyst and ligand concentration in the methanol feed as well as the flow rates of the HPLC pumps were set in a way to keep the molar ratios constant. The circulation pump was set to 1 l·min$^{-1}$ resulting in a reaction mode similar to a CSTR. The reaction performance depending on the circulation speed is presented in Appendix 7.8.1, Figure A 11. The results for the continuous experiments are depicted in Figure 44.

As expected, the conversion was observed to be higher at lower feed streams due to higher residence times. The activation period seemed to be similar for the three experiments and consequently rather independent of the feed streams. After around 2 to 3 hours, the conversion started to become constant getting close to the steady state. The conversion reached in the steady state for the different residence times are consistently lower compared to the conversion of a batch experiment at the corresponding reaction time. Furthermore, the difference in conversion was decreased with increasing residence time respectively reaction time. This was caused by the ideal backmixing in a reactor similar to a CSTR compared to a PFTR-like behavior with time for the batch reactor.
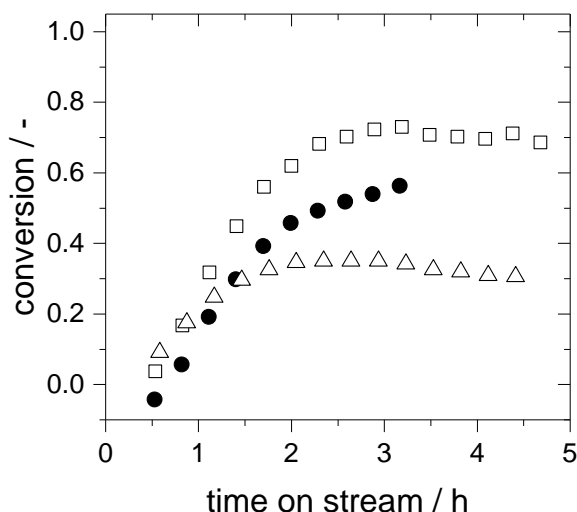
**Figure 44: Results for continuous experiments without catalyst recycling using three different feed streams and the TPP modified catalyst with pure butadiene (□ 2.82 g·min$^{-1}$, ● 5.64 g·min$^{-1}$, △ 11.27 g·min$^{-1}$).**

*Reaction conditions: 70 °C, 15 bar, $n_{Pd}$: 0.064 mmol, $n_{TPP}$: 0.26 mmol, $n_{KOMe}$: 7.27 mmol, $\dot{V}_{circ}$ = 1 l·h$^{-1}$,*
*Flows 2.82 g·min$^{-1}$: MeOH: 1.52 g·min$^{-1}$, butadiene: 1.3 g·min$^{-1}$,*
*Flows 5.64 g·min$^{-1}$: MeOH: 3.05 g·min$^{-1}$, butadiene: 2.59 g·min$^{-1}$,*
*Flows 11.27 g·min$^{-1}$: MeOH: 6.09 g·min$^{-1}$, butadiene: 5.18 g·min$^{-1}$.*

Another reason for the difference between batch and continuous operation could be the age distribution of the catalyst. In the loop reactor, fresh and not yet activated catalyst was continuously added to the reaction mixture whereas in the batch autoclave the activated catalyst remained in the reaction mixture.

A possibility to overcome the age distribution is the transfer of the telomerization reaction to a continuous process with product separation and efficient catalyst recycling. An attempt for this transfer was carried out in this thesis applying a biphasic reaction mode with ionic liquids and will be discussed in detail in the following chapter.

## 4.3 Telomerization in biphasic reaction system with ionic liquids

The last part of this thesis focuses on the immobilization of the investigated catalyst systems in ionic liquids. As the choice of the ionic liquid phase is crucial, the preselection of ionic liquids by a computer based method, COSMO-RS and its experimental validation will be introduced. The selected ionic liquids were tested in the telomerization reaction to study their influence on the reactivity of the system. The best performing systems were then applied in recycle studies before the transfer of these systems to the continuous loop reactor was carried out.

### 4.3.1 Preselection of ionic liquids with COSMO-RS

The selection of an appropriate ionic liquid for the application as catalyst phase in a biphasic reaction system is important. The ionic liquid has to dissolve and immobilize the catalyst. For exhibiting a good extraction efficiency, the formed products should not be miscible with the ionic liquid whereas the reactants should be soluble in the catalyst phase. The solubility properties of reactants and products can be determined a priori by means of computer based methods, e.g. COSMO-RS. By this, the screening of a large amount of different anion-cation combinations is possible with a comparatively small effort in contrast to experimental screenings. With COSMO-RS, the activity coefficient $\gamma_i^{\alpha}$ of a component $i$ at infinite dilution in phase $\alpha$ can be calculated. In case of the telomerization reaction, the activity coefficients of methanol, butadiene and the two main products, 1-Mode and 3-Mode were calculated. As prediction criterion, the solubility selectivity $S_{sol}$ is defined according to Equation (9) whereas a large value for $S_{sol}$ indicates a good extraction efficiency.

$$S_{sol} = \frac{\prod(\gamma_{products})}{\prod(\gamma_{reactants})} \qquad (9)$$

Within this thesis, 960 different anion-cation combinations were screened by this theoretical approach. Cations of three different main groups, imidazolium-based, pyridinium-based and ammonium-based cations were investigated. For the anions,

the following groups were chosen: fluorine-containing, sulfate-, sulfonate-, borate-, cyanate- and halogenide-based anions.

Nearly every combination showed only slightly differing, good solubility properties for the two reactants, methanol and butadiene. For the products, larger differences were observed. In general, the dependence on the used cation was observed to be small. For a lot of combinations, the solubility increased with increasing length of the alkyl chain. Longer alkyl chains exhibit a better solubility for the methoxyoctadienes due to increasing lipophilicity. The anion showed a stronger influence on the solubility properties. Some anions showed good solubility also for the products, e.g. Cl$^-$, Br$^-$, [NTf$_2$]$^-$, [FAP]$^-$ or [BETI]$^-$ and are thus less suitable for the application in the telomerization reaction. Others, e.g. the sulfate- and sulfonate-based anions, exhibited a poor solubility for the products being suitable for the desired application.

This preselection was then validated experimentally. For this, 9 different ionic liquids were chosen. Some of them exhibited a good extraction efficiency, others a poor one. The extraction efficiency of an ionic liquid was tested by determining the amount of ionic liquid required to form a second phase with a common reaction mixture for the telomerization reaction. This reaction mixture consisted of remaining and not converted methanol and the formed products. The better the extraction efficiency, the less amount of ionic liquid would be required. The calculated solvation selectivity for these ionic liquids is shown in Figure 45 and the amount of ionic liquid required to form a second phase with 2 ml of the reaction mixture is presented in Figure 46.

The extraction efficiency predicted by COSMO-RS was determined to be the best for [EMMIM][BF$_4$] followed by [EMMIM][MeSO$_4$], [EMMIM][TOS], [BMMIM][OcSO$_4$], [BMMIM]Cl, [EMMIM]Cl and [BMMIM][BF$_4$], whereas ionic liquids exhibiting the [NTf$_2$]$^-$ anion were predicted to show the worst extraction efficiency.

By the experimental validation, the relative tendency of the predicted results was confirmed very well. Contrary to the prediction, with [BMMIM][OcSO$_4$] no biphasic system could be achieved. But the added amount of ionic liquid was less than for e.g. [EMMIM][MeSO$_4$] or [BMMIM]Cl. For the [NTf$_2$]$^-$ based ionic liquids, no second phase was formed even with a large amount of ionic liquid. This was in agreement with the predictions.
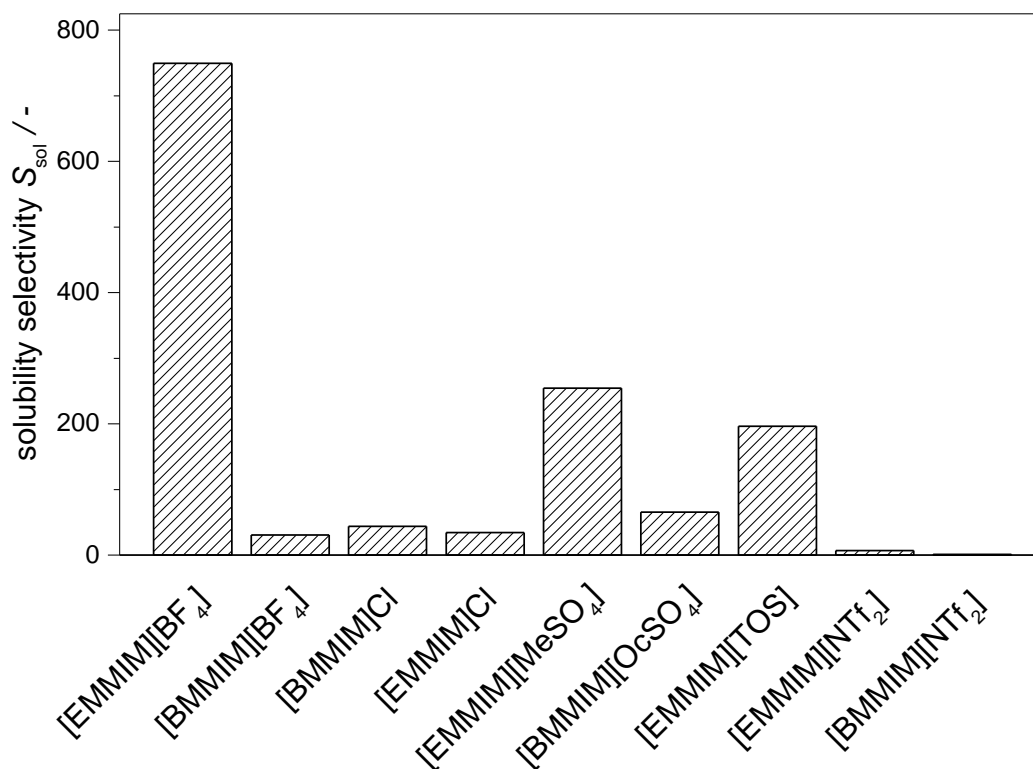
**Figure 45: Predicted solubility selectivity $S_{sol}$ for 9 different ionic liquids.**
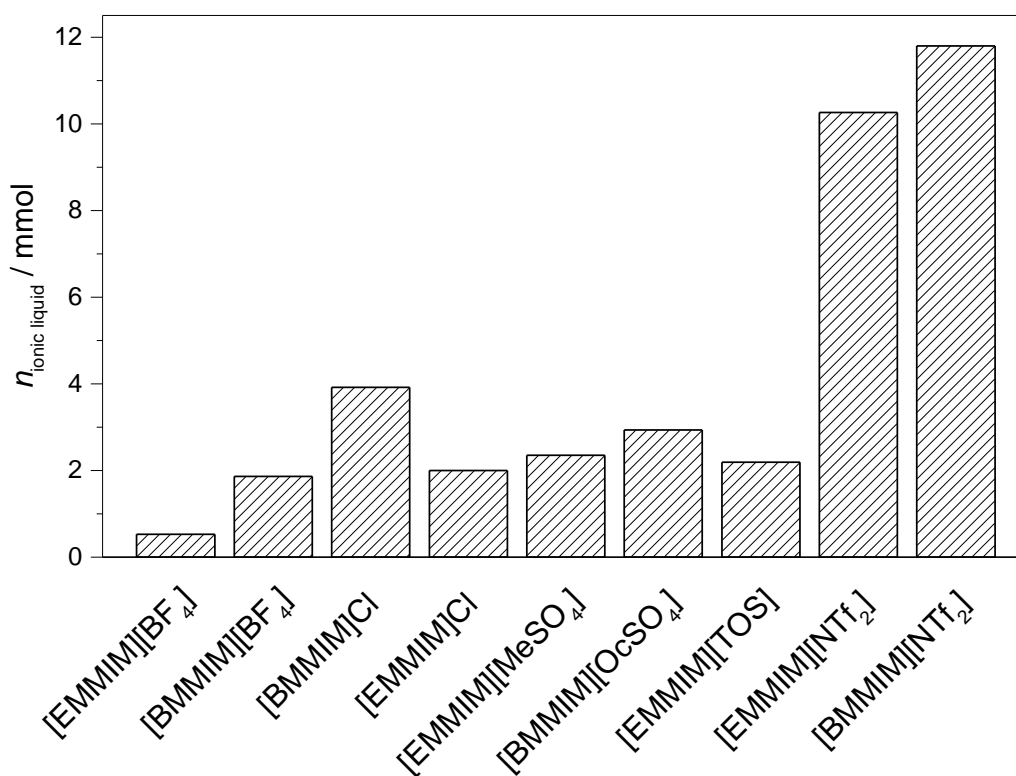


**Figure 46: Required amount of ionic liquid to form a second phase with 2 ml of the reaction mixture (no second phase obtained within the investigated molar amount of ionic liquid for [BMMIM][OcSO$_4$], [EMMIM][NTf$_2$] and [BMMIM][NTf$_2$]).**

Figure 47 illustrates that the extraction efficiency of an ionic liquid does not only indicate whether a second phase is formed or not but also gives information how good the product extracts out of the ionic liquid. For example, the best predicted ionic liquid [EMMIM][BF$_4$] showed a much smaller ionic liquid phase than [BMMIM]Cl meaning that more product was extracted out of the ionic liquid [EMMIM][BF$_4$] into the upper phase. This extraction efficiency and phase formation is an important fact for the desired in-situ extraction in biphasic reaction systems.
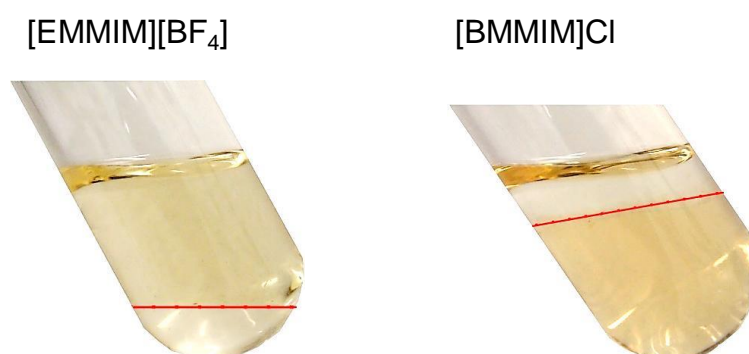
[EMMIM][BF$_4$]                    [BMMIM]Cl



**Figure 47: Extraction efficiency for [EMMIM][BF$_4$] and [BMMIM]Cl (line marks phase boundary)**

However, the application of COSMO-RS as a priori prediction method has also some limitations. COSMO-RS calculates the activity coefficients at infinite dilution as well as in thermodynamic equilibrium. Furthermore, it does not give any information about the state of the ionic liquid which is also important for implementing this ionic liquid in a continuous liquid phase process. In this case, only the two [NTf$_2$]$^-$ based ionic liquids are liquid in pure form, the others are solid at room temperature and some of them also at reaction temperature. COSMO-RS also does not take any chemical reaction or the presence of catalysts and additives, e.g. bases, into account. The activity of the telomerization reaction system with the preselected ionic liquids was tested in a next set of experiments.

## 4.3.2  Batch experiments

Based on the results published by Magna *et al.* [33] first preliminary experiments were performed in order to get information about the reaction system and the reaction conditions. After fixing the reaction conditions, different ionic liquids were screened in combination with different ligands. Besides the already discussed literature known ligands, TPP and IMes, also different sulfonated derivatives of the phosphine based ligand were tested. The Pd-leaching into the organic phase was determined by ICP. The recycling experiments were carried out with three different ionic liquids in combination with one of the sulfonated derivatives of the phosphine ligands.

### 4.3.2.1  Preliminary experiments

According to Magna *et al.* [33] the preliminary experiments with ionic liquids in this thesis were carried out with [BMMIM][NTf$_2$], without the addition of base, with Pd(OAc)$_2$ as catalyst precursor and with TPP as ligand. After 6 hours of reaction time, only a low conversion was observed in the experiments of this thesis. In addition, no biphasic system was observed after the reaction. But the addition of some droplets of hexane resulted in a proper phase separation exhibiting a clear, yellow catalyst/ionic liquid phase and a upper phase containing the formed products. Consequently, hexane was added prior to the reaction in the following experiments resulting in phase separation after 6 hours of reaction time. In a first study, the influence of two different anions as well as cations was determined. The results are depicted in Figure 48.

For the experiment with [BMMIM][NTf$_2$] full conversion was reached. Comparing the alkyl-chain of the cation, the experiment with [BMMIM][NTf$_2$] showed a distinctly better performance than [EMMIM][NTf$_2$]. This behavior is probably caused by the better solubility of the reactant butadiene in the [BMMIM][NTf$_2$] ionic liquid.
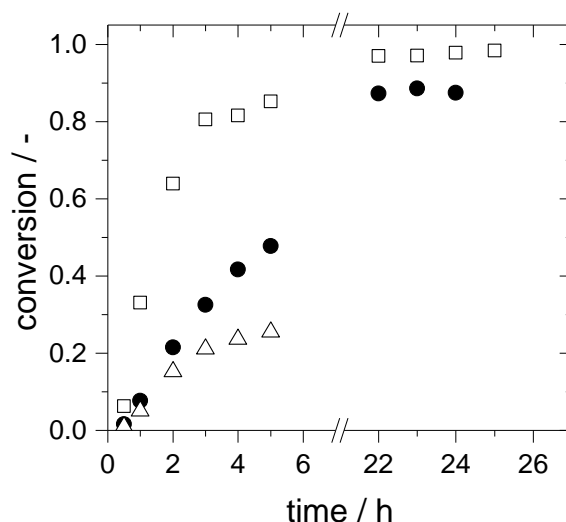
**Figure 48: Influence of different anions and cations on the telomerization reaction with the TPP modified catalyst and pure butadiene (□ [BMMIM][NTf$_2$], ● [EMMIM][TOS], △ [EMMIM][NTf$_2$]).**

*Reaction conditions: 85 °C, 15 bar, $n_{butadiene}$:$n_{MeOH}$ = 1, $n_{butadiene}$:$n_{Pd}$ = 10,000, $n_{TPP}$:$n_{Pd}$ = 3, $n_{butadiene}$:$n_{IL}$ = 30, $n_{MeOH}$:$n_{hexane}$ = 3.22; Precursors: TPP and Pd(OAc)$_2$.*

As Pd(acac)$_2$ was figured out as best catalyst precursor in previous experiments, the influence of catalyst precursor was checked as well in reaction systems with ionic liquids. Furthermore, the accelerating effect of triethylamine (NEt$_3$) was studied. The results are shown in Figure 49.

An increase of the reaction rate was observed with addition of the base NEt$_3$. Interestingly, the influence of NEt$_3$ in combination with the Pd-TPP catalyst is distinctively more pronounced with ionic liquids compared to the homogeneous catalysis without liquid salt. The application of Pd(acac)$_2$ as catalyst precursor resulted in a higher reaction rate compared to Pd(OAc)$_2$. This behavior is contradictory to the experiments without ionic liquids where the TPP modified catalyst system was almost independent of the applied Pd-precursor.

For following experiments, Pd(acac)$_2$ was chosen as catalyst precursor and a base was added to accelerate the activation of the catalyst.
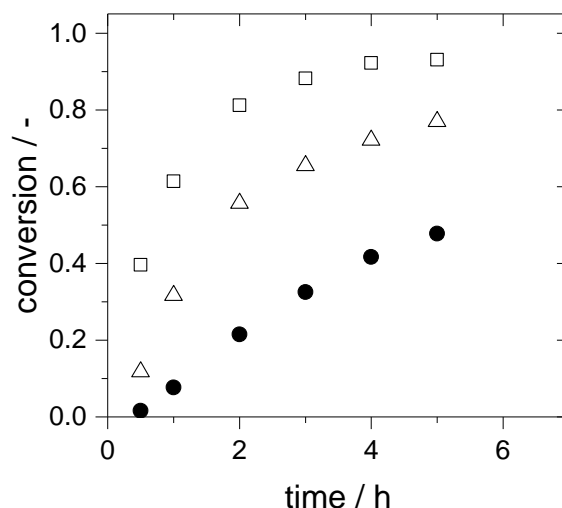
**Figure 49: Influence of catalyst precursor and base on the telomerization reaction with the TPP modified catalyst and pure butadiene using [EMMIM][TOS] as catalyst phase (□ Pd(acac)$_2$ with base, △ Pd(OAc)$_2$ with base, ● Pd(OAc)$_2$ without base).**

*Reaction conditions: 85 °C, 15 bar, $n_{butadiene}$:$n_{MeOH}$ = 1, $n_{butadiene}$:$n_{Pd}$ = 10,000, $n_{TPP}$:$n_{Pd}$ = 3, $n_{butadiene}$:$n_{IL}$ = 30, $n_{butadiene}$:$n_{NEt3}$ = 300, $n_{MeOH}$:$n_{hexane}$ = 3.22; Precursor: TPP, IL: [EMMIM] [TOS].*

## 4.3.2.2  Screening of ionic liquids using different ligands

For the screening experiments, the values for conversion and selectivities were recorded and compared at the end of the reaction. Besides different ionic liquids, also different ligands were screened in these experiments. In order to get a comparison to the reactions without ionic liquid, experiments were carried out with the already discussed ligands TPP and IMes. To increase the solubility in the ionic liquid, also sulfonated derivatives of the phosphine ligand, namely triphenylphosphine monosulfonate (TPPMS) and triphenylphosphine trisulfonate (TPPTS) were tested. By replacing the Na$^+$ of the monosulfonated phosphine ligand (TPPMS) with 1-butyl-2,3-dimethylimidazolium ([BMMIM]$^+$), the solubility of the ligand in the applied ionic liquid should be increased and thus the leaching decreased [173].

The experiments were carried out at 70 °C and hexane was added prior to the reaction in order to induce proper phase separation. For the IMes ligand, KOMe was used as base as this ligand was not active with a weaker base such as NEt$_3$. The

threefold alkylated imidazolium cations were proven to be stable in the presence of KOMe. For the phosphine based ligands, $NEt_3$ was applied as base.

The results of the biphasic telomerization reaction with the TPP ligand are depicted in Figure 51. In all figures for the ionic liquid screening of this chapter, the order of the ionic liquids is structured with decreasing extraction efficiency from left to right.

The selectivity toward 1-Mode as well as the chemoselectivity were very similar for all investigated ionic liquids and seemed to be independent of the applied immobilization phase. Only the chemoselectivity of the experiment using [EMMIM]Cl was slightly higher compared to the others but this might be caused by the very low conversion during the reaction. The reason for the low conversion of the ionic liquid with the $Cl^-$ anion could be the anion itself competing for free coordination sites of the active catalyst. Besides the ionic liquid [EMMIM]Cl also the ionic liquid [EMMIM][$MeSO_4$] exhibited a very low conversion. The reason is not known but again seems to be the anion itself as also the other sulfate anion, namely [$OcSO_4$]$^-$, showed a lower conversion compared to the best ionic liquids tested in these experiments. The remaining ionic liquids showed very similar performances with conversions of about 60 %, except the ionic liquid [BMMIM][$BF_4$] resulting in a conversion of about 80 % after 3 hours. Comparing the two different cations, the [BMMIM]$^+$ showed a higher conversion for both anions [$BF_4$]$^-$ and [$NTf_2$]$^-$. This is probably caused by the better solubility of the reactant butadiene in the ionic liquid with the same alkyl chain length and confirms the results obtained in the preliminary experiments.

Comparing the conversion with the extraction efficiency, no correlation between these two properties was found. Nevertheless, after the opening of the reactor the extraction efficiency of the different ionic liquids was reflected by the phase separation. For the ionic liquid [EMMIM][$BF_4$] a small ionic liquid/catalyst phase and a large upper organic phase resulted. For the ionic liquids containing the [$NTf_2$]$^-$ anion, additional hexane had to be added after the reaction in order to get a clear phase separation. This behavior was observed for all other investigated ligands and will not be discussed in detail for each ligand.
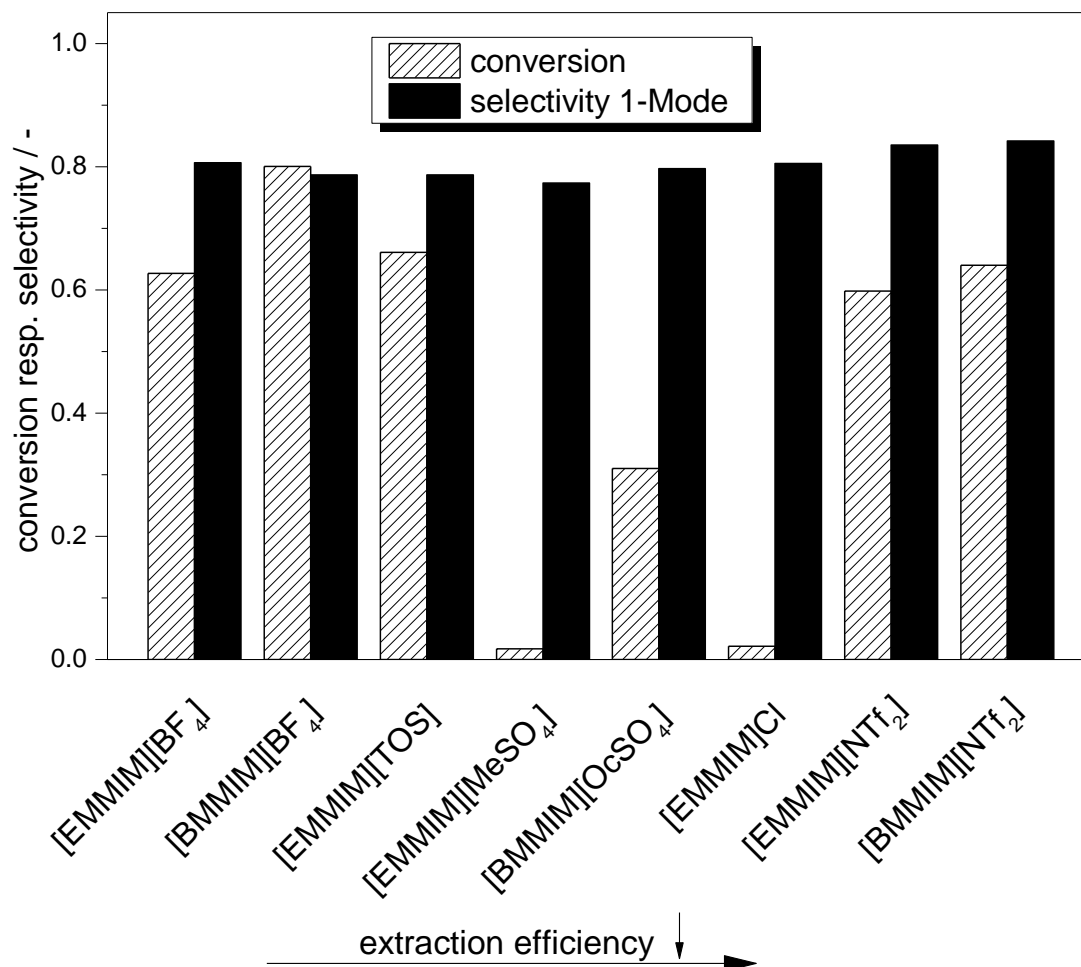
**Figure 50: Conversion and selectivity toward 1-Mode for the screening of different ionic liquids with the TPP modified catalyst and pure butadiene.**

*Reaction conditions: 70 °C, 15 bar, t = 3 h, $n_{butadiene}:n_{MeOH} = 1$, $n_{butadiene}:n_{Pd} = 10,000$, $n_{TPP}:n_{Pd} = 3$, $n_{butadiene}:n_{IL} = 30$, $n_{butadiene}:n_{NEt3} = 300$, $n_{MeOH}:n_{hexane} = 3.22$.*

According to Magna *et al.* [33], the leaching was expected to be quite high as TPP does not exhibit any ionic character and was thus not supposed to be applied in continuous experiments. This was confirmed by the color of the upper organic phase which was slightly yellow.

In Figure 51 the results of the ionic liquid screening in combination with the IMes ligand are presented. Here, only 6 ionic liquids are shown as for the two sulfate based ionic liquids no second phase, even after the addition of further hexane, was achieved. According to the preliminary studies for parameter optimization, see Chapter 4.2.2.5, a palladium to ligand ratio of 1 was chosen for the experiments with IMes.
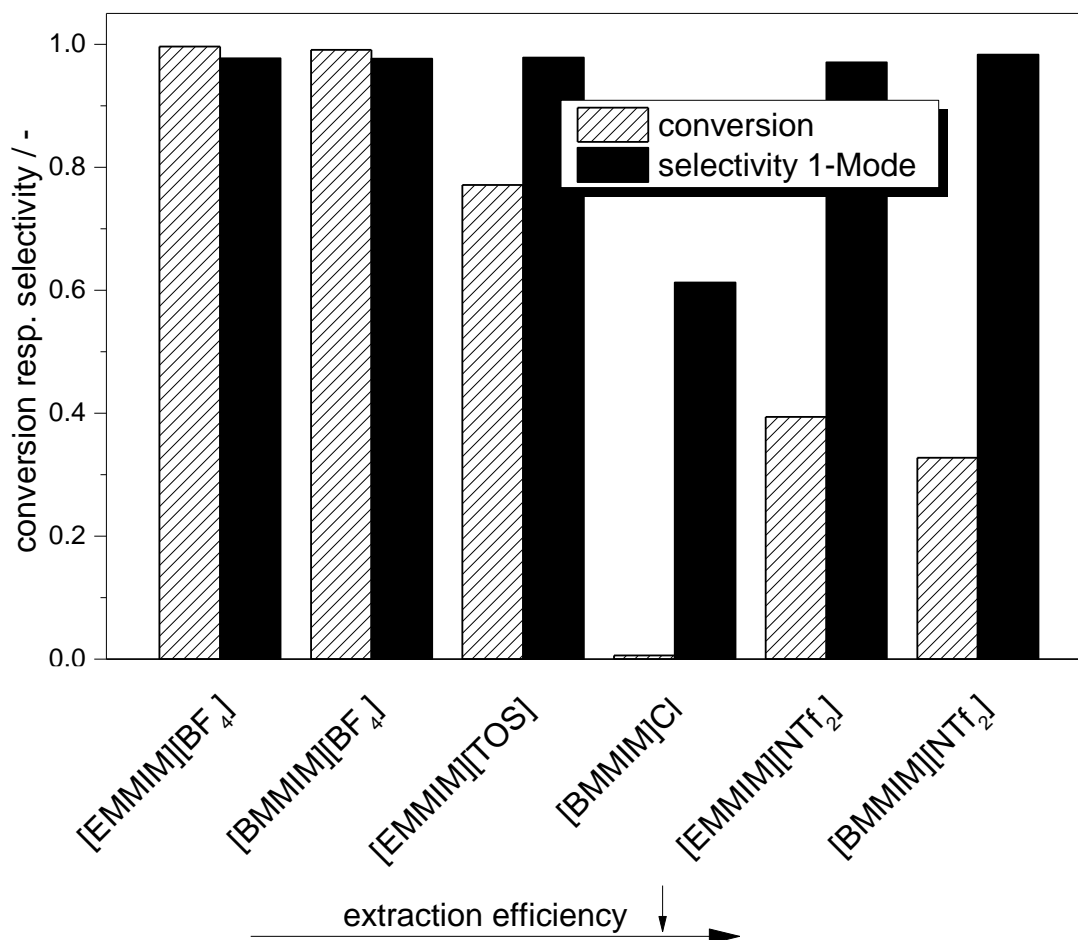
**Figure 51: Conversion and selectivity toward 1-Mode for the screening of different ionic liquids with the IMes modified catalyst and pure butadiene.**

*Reaction conditions: 70 °C, 15 bar, t = 3 h, $n_{butadiene}:n_{MeOH} = 1$, $n_{butadiene}:n_{Pd} = 10,000$, $n_{IMes}:n_{Pd} = 1$, $n_{butadiene}:n_{IL} = 30$, $n_{butadiene}:n_{NEt3} = 300$, $n_{MeOH}:n_{hexane} = 3.22$.*

The reached selectivities were very high for all ionic liquids being in the same range than for the experiments without ionic liquid. Only the selectivity values for the experiment with [BMMIM]Cl were distinctively lower compared to the other investigated ionic liquids. But for this ionic liquid, the conversion was quite low as well. The best ionic liquids reaching almost full conversion were the $[BF_4]^-$ based ones followed by [EMMIM][TOS]. The two $[NTf_2]^-$ based ionic liquids showed only a conversion between 30 and 40 % while the cation $[EMMIM]^+$ showed a slightly higher one. This might probably be caused by a better solubility of the IMes ligand in the $[EMMIM]^+$ based ionic liquid, but the exact reason is not known.

As KOMe was used as base for the experiments with the IMes ligand, a comparison with the TPP ligand is difficult. Nevertheless, the [BF$_4$]$^-$ based ionic liquids showed the best performance with both ligands. Compared to the [BF$_4$]$^-$ based ionic liquids, the performance of the [NTf$_2$]$^-$ based ionic liquids was drastically decreased for the IMes ligand. The different behavior for the two ligands cannot be explained exactly but is probably caused by interaction effects between the ligands or the active species and the used ionic liquids.

As expected, the leaching was high lying in the range of up to 50 % of the initial Pd content which was also confirmed by the resulting yellow to brownish color of the upper, organic phase. As the potential of the application of the TPP as well as the IMes ligand in a continuous process is limited due to their structural character and the resulting high leaching, sulfonated derivatives of the phosphine ligand were tested in the ionic liquid screening as well. By the sulfonation of the TPP ligand, ionic groups are incorporated in the ligand structure resulting in an ionic character and thus in a better solubility in the ionic liquid. The solubility of the ligand respectively the catalyst complex is crucial for a good immobilization behavior.

The results of the ionic liquid screening for the monosulfonated phosphine ligand (TPPMS) are presented in Figure 52.

As the sulfonated phosphine ligands showed an activation period of around 2 hours in experiments without ionic liquids, the experiments were carried out for 6 hours. For the sulfonated phosphine ligands, the results of only 5 ionic liquids are depicted as for the sulfate as well as the chlorine based ionic liquids no second phase resulted.

Again, the selectivities were independent of the applied ionic liquid and similar to those obtained for experiments without ionic liquid. Despite the longer reaction time, the values for the conversion were in the same range as for TPP. The reason is the activation period of the sulfonated phosphine ligands, see Appendix 7.6. Whereas the performance of [EMMIM][TOS] and the [NTf$_2$]$^-$ based ionic liquids was similar to TPP, the performance of the [BF$_4$]$^-$ based ionic liquids dropped drastically. The reason for this drop is not known but might be caused by the ligand itself as the sulfonated ligands are present as hydrates. The [BF$_4$]$^-$ anion might interact with the water forming HF which could decelerate or partly deactivate the catalyst.
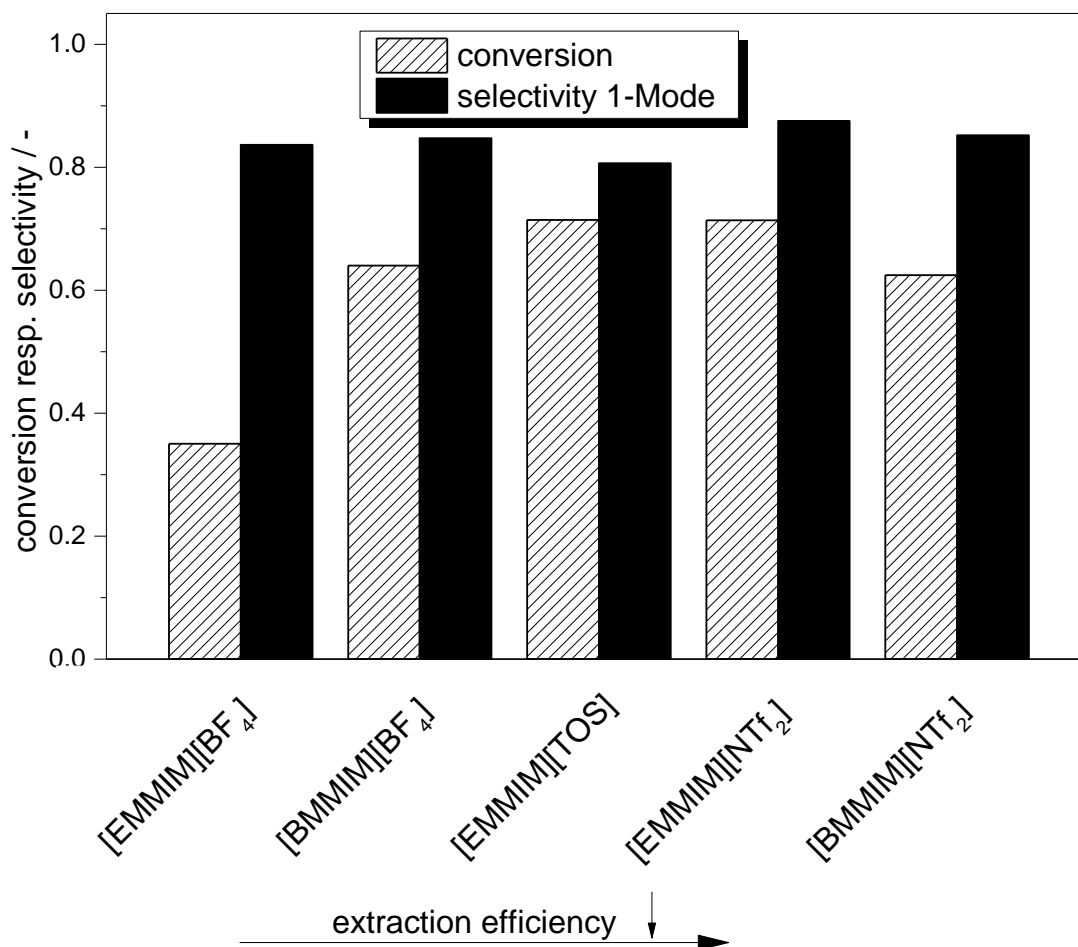
**Figure 52: Conversion and selectivity toward 1-Mode for the screening of different ionic liquids with the TPPMS modified catalyst and pure butadiene.**

*Reaction conditions: 70 °C, 15 bar, t = 3 h, $n_{butadiene}$:$n_{MeOH}$ = 1, $n_{butadiene}$:$n_{Pd}$ = 10,000, $n_{TPPMS}$:$n_{Pd}$ = 3, $n_{butadiene}$:$n_{IL}$ = 30, $n_{butadiene}$:$n_{NEt3}$ = 300, $n_{MeOH}$:$n_{hexane}$ = 3.22.*

For the [NTf$_2$]$^-$ based ionic liquids, the behavior changed as [EMMIM]$^+$ showed a slightly higher conversion. This is probably caused by the better solubility of the ligand in the ionic liquid with the shorter alkyl chain [9; 173].

For the two other sulfonated ligands, TPPTS and [BMMIM]-TPPMS, the performance and the behavior of the different ionic liquids was quite similar to TPPMS. The performance especially of [EMMIM][BF$_4$] dropped drastically whereas the other ionic liquids showed similar conversions. The selectivities, again, were not strongly dependent on the applied ionic liquid. For TPPTS, the selectivity toward 1-Mode and thus the chemoselectivity were slightly lower for all ionic liquids compared to TPPMS and [BMMIM]-TPPMS whereas more octatriene was formed. This might be caused

by the degree of oxidation of around 10 to 15 % lowering the available unoxidized ligand for catalysis. This should be considered for application in continuous experiments. Comparing [BMMIM]-TPPMS with TPPMS, a similar amount of 1-Mode was formed while with [BMMIM]-TPPMS a slightly higher amount of 3-Mode and consequently a slightly lower amount of octatriene was observed.

The main drawback of the synthesized ligand [BMMIM]-TPPMS was that it did not seem to be able to stabilize the catalyst as after the reaction a large amount of palladium-black was observed which was distributed between the two phases. Detailed results for these two ligands are shown in Appendix 7.7.

Regarding conversion and selectivities, an influence of the degree of sulfonation between TPPMS and TPPTS was not observed. However, the degree of sulfonation influenced the Pd-leaching strongly. The determined Pd-leaching is comparatively shown for the ligands TPPMS and TPPTS in Figure 53.

The Pd-leaching for the experiments carried out with TPPTS as ligand was at least four times lower than with TPPMS. This is due to the higher degree of sulfonation causing better solubility in the ionic liquids and lower solubility in methanol.

For both ligands, the lowest leaching was observed for [EMMIM][TOS] followed by [EMMIM][NTf$_2$] and [BMMIM][BF$_4$]. The highest leaching was found with [BMMIM][NTf$_2$] and [EMMIM][BF$_4$].
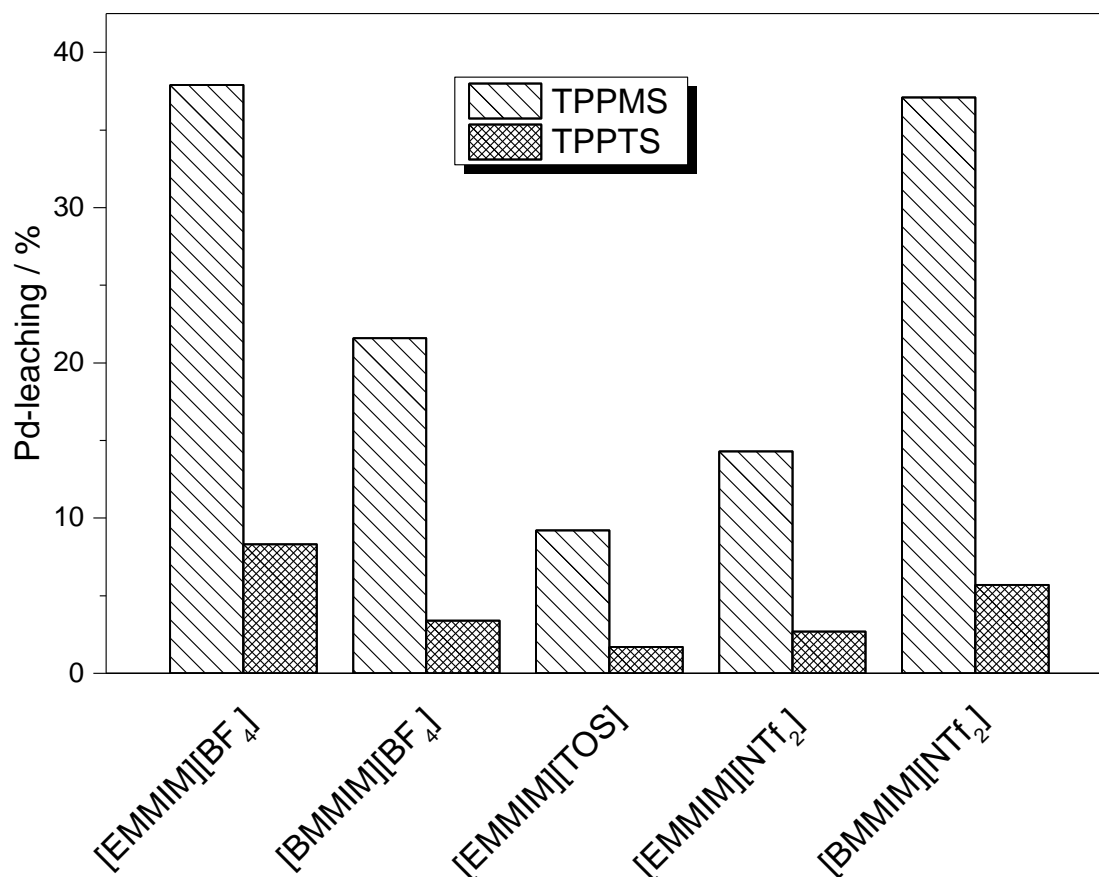
**Figure 53: Pd-leaching determined by ICP for the ligands TPPMS and TPPTS with different ionic liquids.**

### 4.3.3 Recycle experiments

With the following experiments, the recyclability of the catalyst phase was studied. In a first attempt, the same reaction conditions as applied for the screening experiments were used. The recycling experiments were carried out with three different ionic liquids and Pd-TPP as catalyst. For the studied systems containing the ionic liquids [EMMIM][BF$_4$], [EMMIM][TOS] and [BMMIM][NTf$_2$], the conversion decreased drastically after the initial run. Also the second as well as the third recycle showed further decreasing conversion values. The strong decrease in conversion indicates a high loss of palladium due to leaching into the organic phase. This is in accordance with the observations in the screening experiments where a high leaching of the

Pd-TPP catalyst was expected. A change of the ligand from TPP to TPPMS showed no distinct improvement regarding the recyclability.

The conclusion of this first recycling attempt was that the reaction parameters have to be optimized in order to lower the Pd-leaching. It was known from the literature [33] and from the screening experiments that the degree of sulfonation influences the leaching strongly. However, as the threefold sulfonated ligand is also about three times more expensive, the optimization experiments toward the best working system were carried out with TPPMS first. The reactant methanol acts as good solvent and this is also the challenging problem of the biphasic telomerization reaction as the catalyst is also highly soluble in methanol. Unreacted methanol accumulates in the catalyst phase, the cross-solubility into the product phase increases and consequently methanol will be removed from the reactor via the exit stream of a continuous process. In consequence, catalyst dissolved in methanol will be leached out of the reactor. For a continuous process, the methanol accumulation in the catalyst phase also leads to a slightly different ratio of butadiene to methanol as it was initially adjusted in the reactant streams. Thus, the amount of remaining unreacted methanol should be kept low by increasing the ratio of butadiene to methanol to a stoichiometric one. Furthermore, the amount of the extraction solvent hexane was increased in order to reduce the cross-solubility of methanol and its removal out of the catalyst phase. In addition, the temperature as well as the catalyst amount were increased for accelerating the reaction in order to get higher conversion and thus keeping the methanol concentration low.

Again, three ionic liquids based on the anions $[NTf_2]^-$, $[BF_4]^-$ and $[TOS]^-$ were tested. The results for [BMMIM][NTf$_2$] as catalyst phase are shown in Figure 54.

In the initial experiment a conversion of 75 % and a selectivity toward 1-Mode of 77.5 % were achieved. The regioselectivity was decreased compared to the screening experiments. This is known from the literature [95] and caused by the lower amount of methanol present in the reaction as well as the elevated reaction temperature of 85 °C. The Pd-leaching was distinctively decreased compared to the screening experiments and showed a value of 1.9 %. Magna *et al.* [33] determined the same value for the Pd-leaching under these reaction conditions. In the first recycle of the initial experiments, the conversion was regained. The selectivity to the main product 1-Mode was slightly decreased while the regioselectivity was increased. The increase of the regioselectivity is caused by the larger amount of

methanol present in the reaction mixture compared to the initial experiment. The same amount of methanol was added for each experiment but unreacted methanol dissolved in the catalyst phase was not removed from the reactor resulting in an increase of the methanol concentration. The Pd-leaching increased to 4.4 %. After the initial experiment and its recycle, no palladium-black was observed in the reaction vessel.
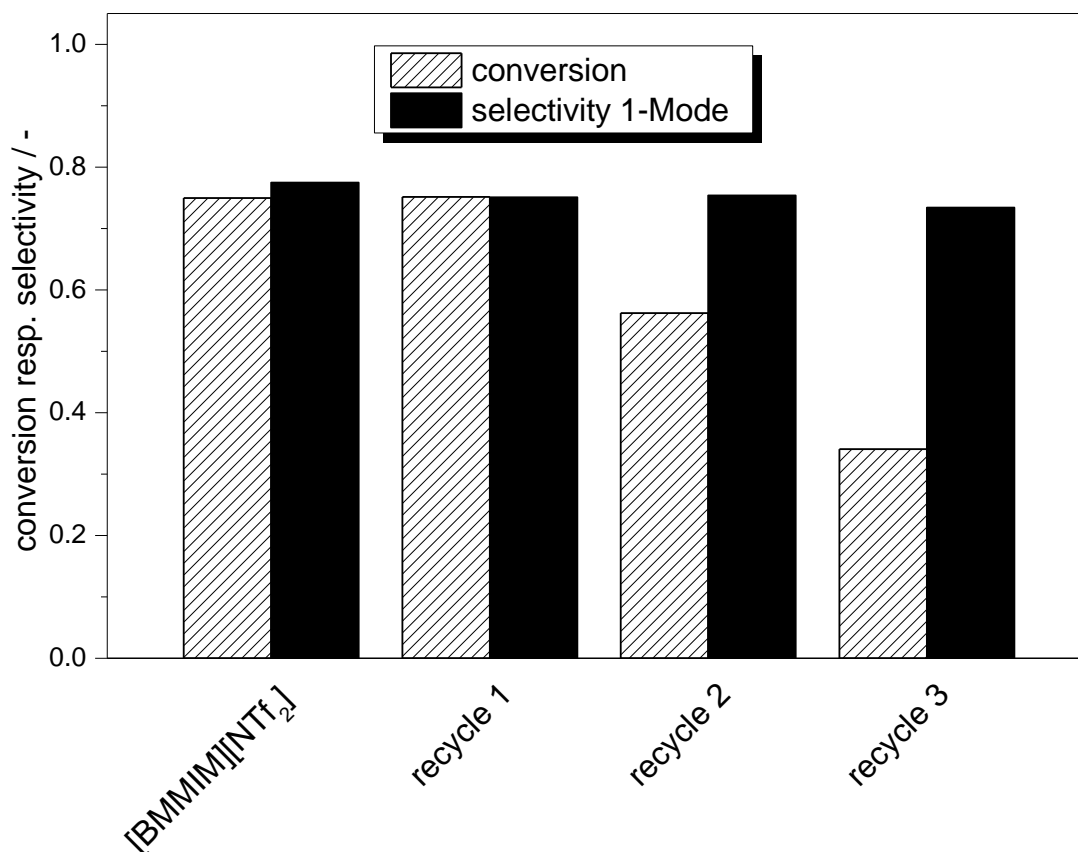


**Figure 54: Conversion and selectivity toward 1-Mode for the recycling study with the TPPMS modified catalyst, pure butadiene and [BMMIM][NTf$_2$] as catalyst phase.**

*Reaction conditions: 85 °C, 15 bar, t = 3 h, $n_{butadiene}$:$n_{MeOH}$ = 0.5, $n_{butadiene}$:$n_{Pd}$ = 5,500, $n_{TPPMS}$:$n_{Pd}$ = 3, $n_{butadiene}$:$n_{IL}$ = 30, $n_{butadiene}$:$n_{NEt3}$ = 300, $n_{MeOH}$:$n_{hexane}$ = 2.45.*

After the first two experiments, the catalyst phase had to be stored over night. The organic phase was removed and the catalyst phase was kept in the autoclave. The autoclave was pressurized with argon in order to store the catalyst phase under inert

atmosphere. In the next morning, the second recycle was started. A strong drop of conversion was observed and Pd-black was found in the reaction mixture after the experiment. The decrease in conversion and the amount of Pd-black was even stronger for the third recycle.

A possible explanation for this observation is the deactivation by oxygen over night. Despite treating everything under argon, it was probably not possible to guarantee 100 % inert atmosphere during the opening of the reactor. Another explanation might be the removal and lack of butadiene over night as butadiene is incorporated in the active catalyst species. The lack of butadiene might cause the deactivation of the catalyst species. In addition, Pd respectively small amounts of the catalyst phase might also get lost during decantation of the product phase.

In a continuous process, these problems would not occur as the reactor will not be opened for catalyst recycling and butadiene will be continuously fed to the reactor.

With [BMMIM][BF$_4$], the observed behavior was quite similar to [BMMIM][NTf$_2$]. The conversion of the initial experiments was regained with the first recycle while the second recycle showed a strong drop in conversion of around 50 %.

The same recycling studies were carried out for [EMMIM][TOS]. The results are presented in Figure 55.

The conversion of the first recycle was slightly increased compared to the initial experiment but was in the error margin of the experiments. Again, the selectivity toward 1-Mode decreased slightly and the regioselectivity increased due to the increasing amount of methanol. In the second and the third recycle, the conversion dropped compared to the initial experiment and the first recycle. For this ionic liquid, the determined Pd-leaching was the lowest confirming the results of the screening experiments.

The main limitation of this ionic liquid was that it was not liquid at reaction conditions and thus required methanol to be dissolved. The lack of methanol due to the selected reaction conditions of the recycling study caused some precipitation of the ionic liquid. The recycling became difficult and some solid precipitates of the ionic liquid were distributed in both phases. In consequence, the precipitate in the organic phase was removed from the catalyst phase lowering the amount of ionic liquid and catalyst present for the next recycle experiment. Therefore, the ionic liquid [EMMIM][TOS] is, despite its good performance and immobilization behavior, not suitable for a continuous process.

In summary, all studied ionic liquids showed the same behavior. The conversion of the initial experiment was regained but the second and third recycle showed a strong decrease in conversion. The problem seems to be the storage over night, the opening of the reactor without 100 % exclusion of oxygen and the removal of butadiene from the catalyst. All these facts indicate the relevance and potential of transferring the biphasic telomerization reaction to a continuous process where all these issues are solved by the reactor concept.
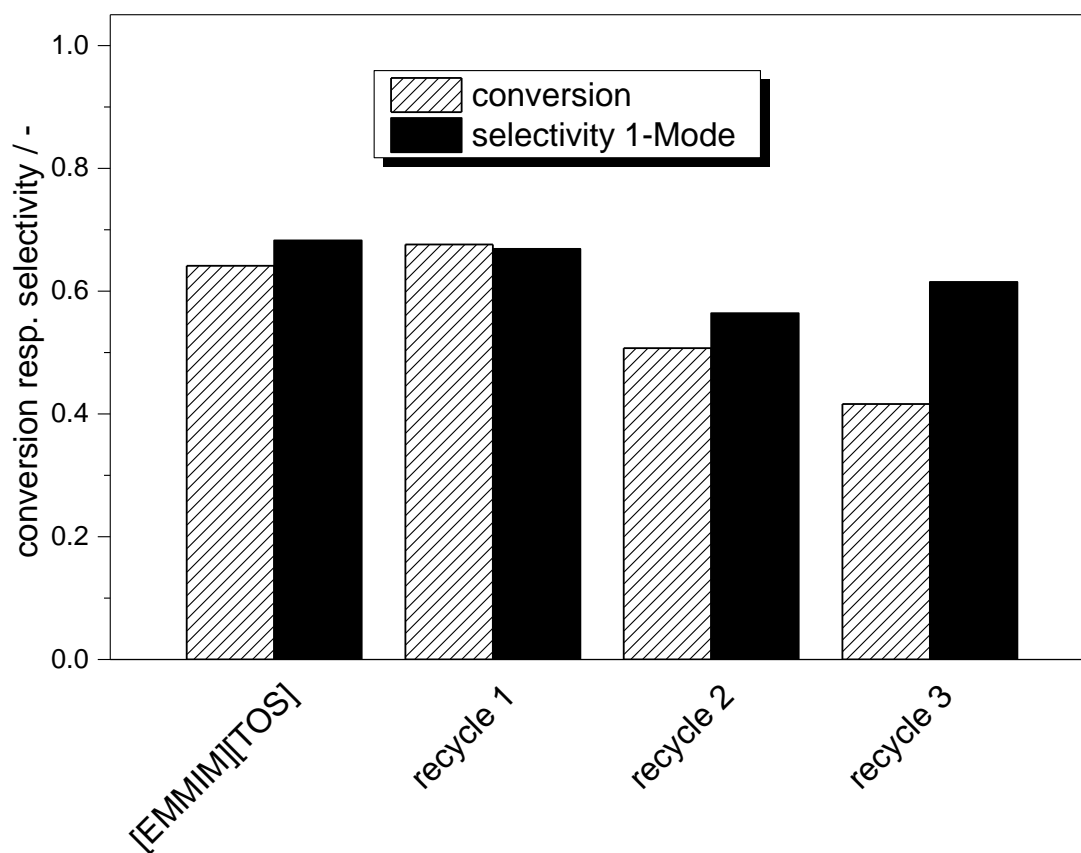


**Figure 55: Conversion and selectivity toward 1-Mode for the recycling study with the TPPMS modified catalyst, pure butadiene and [EMMIM][TOS] as catalyst phase.**

*Reaction conditions: 85 °C, 15 bar, $t = 3$ h, $n_{butadiene}:n_{MeOH} = 0.5$, $n_{butadiene}:n_{Pd} = 5,500$, $n_{TPPMS}:n_{Pd} = 3$, $n_{butadiene}:n_{IL} = 30$, $n_{butadiene}:n_{NEt3} = 300$, $n_{MeOH}:n_{hexane} = 2.45$.*

## 4.3.4 Continuous operation

The optimization of the continuous process by means of a biphasic reaction system was carried out stepwise. As a starting point, [BMMIM][NTF$_2$] and TPPMS were applied and a reaction temperature of 70 °C was adjusted.

The necessity of a stoichiometric ratio of the reactants (butadiene:MeOH = 2:1) was already shown in the first attempts of the recycle experiments. This was proven for the continuous process as well. A ratio of butadiene to methanol of 1:1 in the feed streams led to a drop in conversion from 80 % to around 15 % after 20 hours.

The change to a stoichiometric ratio increased the performance of the reaction system. The results of this experiment are depicted in Figure 56.
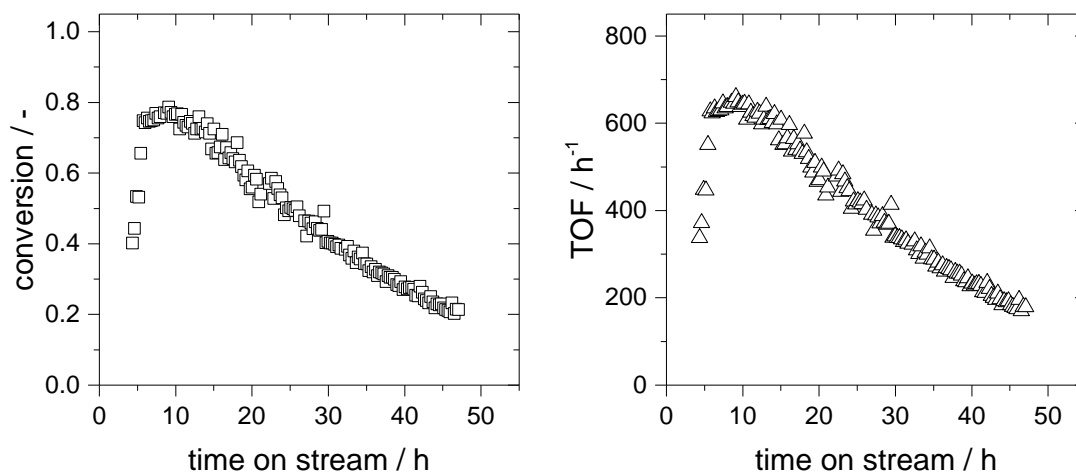


**Figure 56: Conversion (left) and TOF (right) for the continuous operation with the TPPMS modified catalyst, pure butadiene, [BMMIM][NTf$_2$] as catalyst phase and a stoichiometric ratio of the reactants.**

*Reaction conditions: 70 °C, 18 bar, $n_{Pd}$: 1 mmol, $n_{TPPMS}$: 3 mmol, $n_{NEt3}$: 14 mmol, [BMMIM][NTf$_2$]: 175.4 mmol resp. 76 g, $\dot{V}_{circ} = 0.25\ l \cdot h^{-1}$,*
*Flows: MeOH: 7.22 mmol·min$^{-1}$ resp. 0.231 g·min$^{-1}$, hexane: 4.86 mmol·min$^{-1}$ resp. 0.419 g·min$^{-1}$, butadiene: 14.46 mmol·min$^{-1}$ resp. 0.782 g·min$^{-1}$.*

The conversion increased within the first 10 hours until a maximum conversion of around 80 % was reached. Afterwards, the conversion decreased steadily with around 20 % per 10 hours. After 47 hours of reaction time, the conversion exhibited a value of around 20 %. Despite a sufficient phase separation with only one clear phase leaving the reactor, no steady state was reached throughout the reaction time.

The constant decrease in conversion was probably caused by the leaching of the Pd catalyst. The latter was determined by ICP measurements. As shown in Table 14, around 0.3 – 0.7 mg of the initial Pd leached out of the reactor per hour correlating to 1,000 – 2,400 $ppm \cdot h^{-1}$ of the initial Pd inventory. After a run time of 21.5 hours around 3.5 % of the starting amount of Pd was leached out of the reactor. In total, between 9 and 10 % of the initial Pd content left the reactor at the end of reaction after 47 hours time on stream (TOS).

**Table 14: ICP data of Pd-leaching for the continuous operation with the TPPMS modified catalyst, pure butadiene, [BMMIM][NTf$_2$] as catalyst phase and a stoichiometric ratio of the reactants.**

| TOS / h | $Pd_{initial}$ / g | Pd-leaching[1] / $ppm \cdot h^{-1}$ of $Pd_{initial}$ | Total Pd-leaching[2] / % of $Pd_{initial}$ | $Pd_{exit\ stream}$[3] / ppm |
|---|---|---|---|---|
| 1.5 – 2.5 | 0.3046 | 997.0 | 0.2 | 9.5 |
| 2.5 – 3.5 | 0.3046 | 978.4 | 0.3 | 9.3 |
| 3.5 – 4.5 | 0.3046 | 1,629.1 | 0.5 | 15.6 |
| 4.5 – 5.5 | 0.3046 | 1,740.1 | 3.1 | 16.6 |
| 19.5 – 20.5 | 0.3046 | 2,416.9 | 3.4 | 23.1 |
| 20.5 – 21.5 | 0.3046 | 1,194.3 | 3.5 | 11.4 |
| 47 | 0.3046 | - | 9.6* | - |

*Reaction conditions: 70 °C, 18 bar, $n_{Pd}$: 1 mmol, $n_{TPPMS}$: 3 mmol, $n_{NEt3}$: 14 mmol, [BMMIM][NTf$_2$]: 175.4 mmol resp. 76 g, $\dot{V}_{circ} = 0.25\ l \cdot h^{-1}$,*
*Flows: MeOH: 7.22 $mmol \cdot min^{-1}$ resp. 0.231 $g \cdot min^{-1}$, hexane: 4.86 $mmol \cdot min^{-1}$ resp. 0.419 $g \cdot min^{-1}$, butadiene: 14.46 $mmol \cdot min^{-1}$ resp. 0.782 $g \cdot min^{-1}$.*
[1] *Pd-leaching of the initial Pd inventory determined in ppm per hour.*
[2] *Cumulative Pd-leaching related to the initial Pd inventory and the corresp. TOS.*
[3] *Pd content of the exit stream related to the total molar amount of the exit stream.*
*\* Value of Pd-leaching at the end of the continuous run, extrapolated using the last determined ICP value.*

In addition, the steady decrease in conversion due to the Pd-leaching led to an accumulation of unreacted methanol in the reaction mixture. Excess methanol consequently dissolved into the product phase increasing additionally the leaching of the Pd catalyst as the latter is highly soluble in methanol as well.

The continuous operation started with a turn over frequency (TOF) of 650 $h^{-1}$ at the achieved maximum in conversion after 10 hours. Afterwards, the TOF decreased steadily as well reaching a value of around 200 $h^{-1}$ after 47 hours.

The obtained selectivities were constant over the reaction time exhibiting values of around 80 % toward 1-Mode, 5 % toward 3-Mode, 12 % toward octatriene and 3 % toward vinylcyclohexene.

### 4.3.4.1  Influence of feeding velocity

The residence time in the loop reactor depends on the feeding velocity of the reactants. With a higher residence time, the conversion should be increased. By increasing the conversion, the accumulation of unreacted methanol should be suppressed and the leaching of the Pd catalyst should be decreased. As a consequence, the achieved time on stream should increase.

In order to increase the residence time, the feeding velocities were lowered to 1/3 of the initial values from the previous experiment. The results are shown in Figure 57 and the obtained selectivities are presented in Figure 58.
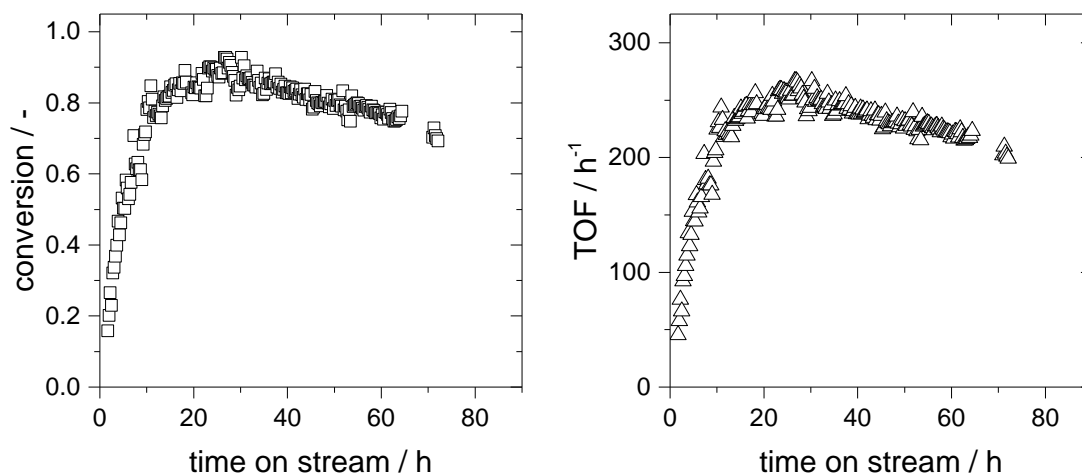


**Figure 57: Conversion (left) and TOF (right) for the continuous operation with the TPPMS modified catalyst, pure butadiene, [BMMIM][NTf$_2$] as catalyst phase and lowered feeding velocities.**

*Reaction conditions: 70 °C, 18 bar, $n_{Pd}$: 1 mmol, $n_{TPPMS}$: 3 mmol, $n_{NEt3}$: 14 mmol, [BMMIM][NTf$_2$]: 175.4 mmol resp. 76 g, $\dot{V}_{circ}$ = 0.25 l·h$^{-1}$,*
*Flows: MeOH: 2.41 mmol·min$^{-1}$ resp. 0.077 g·min$^{-1}$, hexane: 1.67 mmol·min$^{-1}$ resp. 0.144 g·min$^{-1}$, butadiene: 4.86 mmol·min$^{-1}$ resp. 0.263 g·min$^{-1}$.*
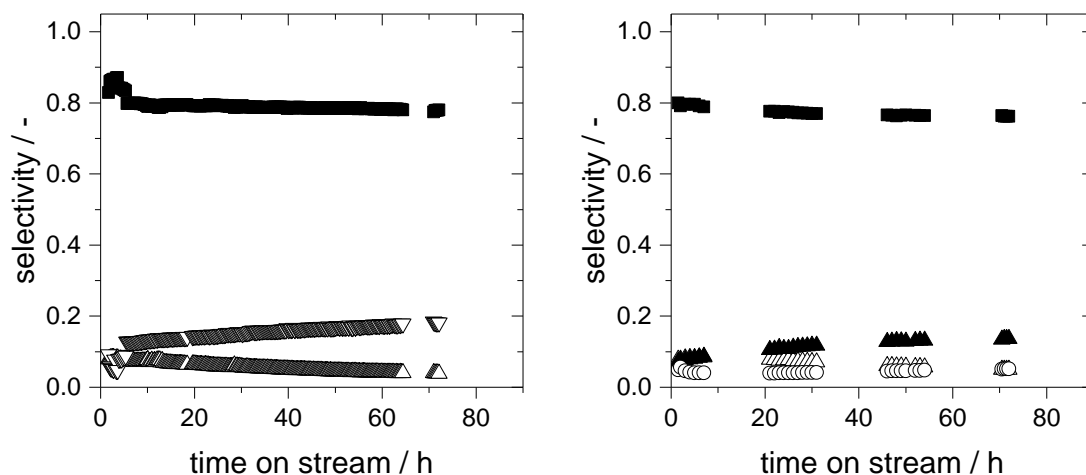
**Figure 58: Selectivities for the continuous operation with the TPPMS modified catalyst, pure butadiene, [BMMIM][NTf₂] as catalyst phase and lowered feeding velocities determined by online GC (left) and offline GC (right) (■ 1-Mode, △ 3-Mode,       ▽ octatriene + vinylcyclohexene,       ▲ octatriene, ○ vinylcyclohexene).**

*Reaction conditions: 70 °C, 18 bar, $n_{Pd}$: 1 mmol, $n_{TPPMS}$: 3 mmol, $n_{NEt3}$: 14 mmol, [BMMIM][NTf₂]: 175.4 mmol resp. 76 g, $\dot{V}_{circ} = 0.25\ l \cdot h^{-1}$,*
*Flows: MeOH: 2.41 mmol·min⁻¹ resp. 0.077 g·min⁻¹, hexane: 1.67 mmol·min⁻¹ resp. 0.144 g·min⁻¹, butadiene: 4.86 mmol·min⁻¹ resp. 0.263 g·min⁻¹.*

The lowering of the feeding velocities led to a higher maximum conversion of around 93 % which was reached within a time period of around 20 hours. Afterwards, the conversion, again, decreased steadily. The decrease in conversion with around 10 % per 20 hours was smaller compared to the previous experiment and was even smaller than 1/3 of its conversion drop (40 % in 20 h). This confirms the postulation of improved immobilization by lowering the accumulating methanol. After 72 hours time on stream, a conversion of around 70 % was reached. This improvement is probably partly caused by the lower Pd-leaching per hour because of the lower feeding velocities and thus lower velocity of the exit stream. Nevertheless, if the improvement would be only caused by the lower feeding velocities, the Pd-leaching per hour should be 1/3 of the leaching from the previous experiment. Especially in the first hours the leaching is slightly lower than 1/3 (see Table 15) but this might also lie in the margin of error of the ICP measurement and the corresponding sample treatment. A further hint for lower Pd-leaching is the lower conversion drop

(0.5 %·h$^{-1}$ < 1/3 · 2 %·h$^{-1}$).This observation indicates that an increase of the methanol conversion was advantageously for the Pd immobilization.

**Table 15: ICP data of Pd-leaching for the continuous operation with the TPPMS modified catalyst, pure butadiene, [BMMIM][NTf$_2$] as catalyst phase and lowered feeding velocities.**

| TOS / h | Pd$_{initial}$ / g | Pd-leaching[1] / ppm·h$^{-1}$ of Pd$_{initial}$ | Total Pd-leaching[2] / % of Pd$_{initial}$ | Pd$_{exit\ stream}$[3] / ppm |
|---|---|---|---|---|
| 5 – 6 | 0.3046 | 278.3 | 0.2 | 2.7 |
| 29 – 30 | 0.3046 | 444.8 | 1.2 | 4.2 |
| 50 – 51 | 0.3046 | 1,571.1 | 4.5 | 15.0 |
| 72 | 0.3046 | - | 7.8* | - |

*Reaction conditions: 70 °C, 18 bar, $n_{Pd}$: 1 mmol, $n_{TPPMS}$: 3 mmol, $n_{NEt3}$: 14 mmol, [BMMIM][NTf$_2$]: 175.4 mmol resp. 76 g, $\dot{V}_{circ}$ = 0.25 l·h$^{-1}$,*
*Flows: MeOH: 2.41 mmol·min$^{-1}$ resp. 0.077 g·min$^{-1}$, hexane: 1.67 mmol·min$^{-1}$ resp. 0.144 g·min$^{-1}$, butadiene: 4.86 mmol·min$^{-1}$ resp. 0.263 g·min$^{-1}$.*
*[1] Pd-leaching of the initial Pd inventory determined in ppm per hour.*
*[2] Cumulative Pd-leaching related to the initial Pd inventory and the corresp. TOS.*
*[3] Pd content of the exit stream related to the total molar amount of the exit stream.*
*\* Value of Pd-leaching at the end of the continuous run, extrapolated using the last determined ICP value.*

The TOF was lower compared to the previous experiment due to the lower flow rate in as well as out of the reactor. Starting with a maximum value of 260 h$^{-1}$, the TOF decreased to a value of around 200 h$^{-1}$ during the 72 hours time on stream.

The selectivity toward the desired product 1-Mode is rather constant exhibiting a value of around 80 %. The formation of 3-Mode decreased throughout the reaction in favor of the formation of octatriene. In the online GC, the peaks for octatriene and vinylcyclohexene were detected with a very similar retention time whereas the offline GC was able to separate these two components.

### 4.3.4.2   Influence of ionic liquid

In the preliminary batch studies, [EMMIM][NTf$_2$] was identified as more suitable ionic liquid compared to its [BMMIM]$^+$ based analogue due to lower leaching values as well as slightly higher achievable conversion values. The results of the experiment with

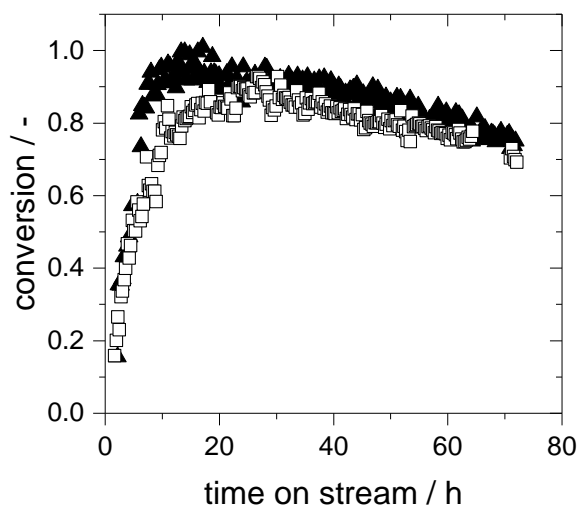the changed ionic liquid as well as of the previous experiment are depicted comparatively in Figure 59.



**Figure 59: Comparative study of continuous experiments with the TPPMS modified catalyst, pure butadiene, [BMMIM][NTf$_2$] (□) and [EMMIM][NTf$_2$] (▲) as catalyst phase.**

*Reaction conditions: 70 °C, 18 bar, $n_{Pd}$: 1 mmol, $n_{TPPMS}$: 3 mmol, $n_{NEt3}$: 14 mmol, [EMMIM][NTf$_2$]: 175.4 mmol resp. 68.7 g, [BMMIM][NTf$_2$]: 175.4 mmol resp. 76 g, $\dot{V}_{circ} = 0.25\ l\cdot h^{-1}$,*
*Flows: MeOH: 2.41 mmol·min$^{-1}$ resp. 0.077 g·min$^{-1}$, hexane: 1.67 mmol·min$^{-1}$ resp. 0.144 g·min$^{-1}$, butadiene: 4.86 mmol·min$^{-1}$ resp. 0.263 g·min$^{-1}$.*

The starting period of the two experiments differed slightly. With [EMMIM][NTf$_2$] full conversion was reached around 5 hours earlier compared to the maximum with [BMMIM][NTf$_2$]. In the following, the conversion level of the [EMMIM]$^+$ based ionic liquid was slightly superior (around 5 %). However, the trend of slowly decreasing conversion with time is the same for both experiments. After 72 hours, the continuous experiment with [EMMIM][NTf$_2$] achieved a conversion of around 75 % whereas the one with [BMMIM][NTf$_2$] reached 69 %. These observations confirmed the obtained results and the claimed statement from the preliminary batch study that the [EMMIM]$^+$ based ionic liquid exhibits higher activity.

Similar to the conversion, the TOF started at a slightly higher value (275 h$^{-1}$ vs. 260 h$^{-1}$) and reached a value of 215 h$^{-1}$ after 72 hours time on stream compared to 200 h$^{-1}$.

The absolute drop in conversion throughout the progress of these two experiments was the same for both ionic liquids only proceeding on different levels. Nevertheless, the determined ICP values (see Table 15 and Table 16) showed lower leaching for the ionic liquid [EMMIM][NTf$_2$] especially at advanced process time confirming the results from the preliminary batch experiments.

**Table 16: ICP data of Pd-leaching for the continuous operation with the TPPMS modified catalyst, pure butadiene and [EMMIM][NTf$_2$] as catalyst phase.**

| TOS / h | Pd$_{initial}$ / g | Pd-leaching[1] / ppm·h$^{-1}$ of Pd$_{initial}$ | Total Pd-leaching[2] / % of Pd$_{initial}$ | Pd$_{exit\ stream}$[3] / ppm |
|---|---|---|---|---|
| 5 – 6 | 0.3046 | 8.0 | 0.0 | 0.1 |
| 25 – 26 | 0.3046 | 691.5 | 1.4 | 6.6 |
| 29 – 30 | 0.3046 | 722.7 | 1.7 | 6.9 |
| 53 – 54 | 0.3046 | 725.2 | 3.4 | 6.9 |
| 72 | 0.3046 | - | 4.7* | - |

*Reaction conditions: 70 °C, 18 bar, $n_{Pd}$: 1 mmol, $n_{TPPMS}$: 3 mmol, $n_{NEt3}$: 14 mmol, [EMMIM][NTf$_2$]: 175.4 mmol resp. 68.7 g, $\dot{V}_{circ}$ = 0.25 l·h$^{-1}$,*
*Flows: MeOH: 2.41 mmol·min$^{-1}$ resp. 0.077 g·min$^{-1}$, hexane: 1.67 mmol·min$^{-1}$ resp. 0.144 g·min$^{-1}$, butadiene: 4.86 mmol·min$^{-1}$ resp. 0.263 g·min$^{-1}$.*
*[1] Pd-leaching of the initial Pd inventory determined in ppm per hour.*
*[2] Cumulative Pd-leaching related to the initial Pd inventory and the corresp. TOS.*
*[3] Pd content of the exit stream related to the total molar amount of the exit stream.*
*\* Value of Pd-leaching at the end of the continuous run, extrapolated using the last determined ICP value.*

The selectivities behaved quite similar compared to the previous experiment with [BMMIM][NTf$_2$] showing a rather constant formation of 1-Mode and vinylcyclohexene, a decreasing formation of 3-Mode and an increasing formation of octatriene.

### 4.3.4.3  Influence of ligand

From the preliminary batch studies, the threefold sulfonated phosphine ligand TPPTS was known to be superior to the monosulfonated one regarding the leaching of the Pd catalyst. The leaching was shown to be at least 1/4 lower with TPPTS than with TPPMS. However, the activation of the TPPTS based catalyst was observed to be slower than for TPPMS. Furthermore, the achieved performance was slightly lower

as well (see Appendix 7.6). Nevertheless, the application of the TPPTS ligand in the continuous process was tested as a next optimization step and the results are presented in Figure 60.
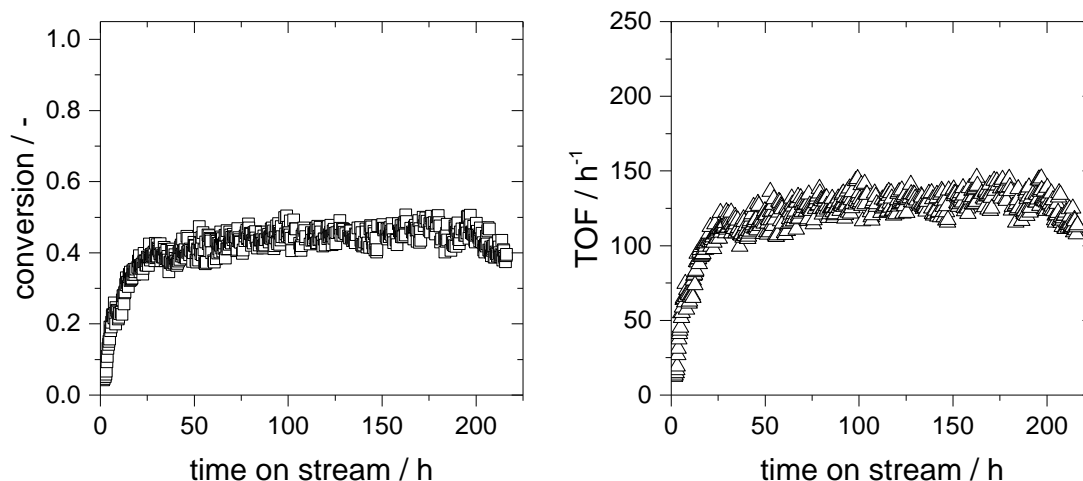


**Figure 60: Conversion (left) and TOF (right) for the continuous operation with the TPPTS modified catalyst, pure butadiene and [EMMIM][NTf$_2$] as catalyst phase.**

*Reaction conditions: 70 °C, 18 bar, $n_{Pd}$: 1 mmol, $n_{TPPTS}$: 3.2 mmol, $n_{NEt3}$: 14 mmol, [EMMIM][NTf$_2$]: 175.4 mmol resp. 68.7 g, $\dot{V}_{circ}$ = 0.25 l·h$^{-1}$,*
*Flows: MeOH: 2.41 mmol·min$^{-1}$ resp. 0.077 g·min$^{-1}$, hexane: 1.67 mmol·min$^{-1}$ resp. 0.144 g·min$^{-1}$, butadiene: 4.86 mmol·min$^{-1}$ resp. 0.263 g·min$^{-1}$.*

The conversion is much lower compared to the previous experiments. After around 23 hours, a conversion of 40 % was achieved. This strong difference was not observed in the batch experiment and might be caused by the difference in the residence time (2.2 hours) and the reaction time of the batch experiments (6 hours). In addition, the solubility of the ligand TPPTS in methanol is limited drastically. This might be followed by mass transport limitations of the reactants to the active species. Despite the low activity of the system, the maximum conversion of around 45 % was kept constant for around 200 hours time on stream. Afterwards, the conversion started to decrease slowly. After 216 hours, a conversion of around 40 % was reached. This long stability of the catalytic system probably originated from the low leaching values that are presented in Table 17.

**Table 17: ICP data of Pd-leaching for the continuous operation with the TPPTS modified catalyst, pure butadiene and [EMMIM][NTf$_2$] as catalyst phase.**

| TOS / h | Pd$_{initial}$ / g | Pd-leaching[1] / ppm·h$^{-1}$ of Pd$_{initial}$ | Total Pd-leaching[2] / % of Pd$_{initial}$ | Pd$_{exit\ stream}$[3] / ppm |
|---|---|---|---|---|
| 4 – 6 | 0.3046 | 19.7 | 0.0 | 0.2 |
| 28 – 30 | 0.3046 | 86.8 | 0.2 | 0.8 |
| 52 – 54 | 0.3046 | 185.0 | 0.7 | 1.8 |
| 76 – 78 | 0.3046 | 178.6 | 1.1 | 1.9 |
| 98 – 100 | 0.3046 | 123.4 | 1.4 | 1.2 |
| 120 – 122 | 0.3046 | 120.5 | 1.6 | 1.1 |
| 216 | 0.3046 | - | 2.8 | - |

*Reaction conditions: 70 ℃, 18 bar, $n_{Pd}$: 1 mmol, $n_{TPPTS}$: 3.2 mmol, $n_{NEt3}$: 14 mmol, [EMMIM][NTf$_2$]: 175.4 mmol resp. 68.7 g, $\dot{V}_{circ}$ = 0.25 l·h$^{-1}$,*
*Flows: MeOH: 2.41 mmol·min$^{-1}$ resp. 0.077 g·min$^{-1}$, hexane: 1.67 mmol·min$^{-1}$ resp. 0.144 g·min$^{-1}$, butadiene: 4.86 mmol·min$^{-1}$ resp. 0.263 g·min$^{-1}$.*
[1] *Pd-leaching of the initial Pd inventory determined in ppm per hour.*
[2] *Cumulative Pd-leaching related to the initial Pd inventory and the corresp. TOS.*
[3] *Pd content of the exit stream related to the total molar amount of the exit stream.*
*\* Value of Pd-leaching at the end of the continuous run, extrapolated using the last determined ICP value.*

Between 20 and 200 ppm of the initial Pd content were leached out of the reactor per hour. This is a very low value meaning that after around 100 hours time on stream only around 1.5 % of the initial Pd left the reactor. The Pd content in the exit stream amounted to 1 – 2 ppm which is distinctively lower as the reported value of 50 ppm by Dehn [30] who carried out the continuous telomerization of butadiene with methanol using an aqueous biphasic system for catalyst immobilization.

Due to the low leaching, the slight decrease in conversion after a reaction time of around 200 hours might also be caused by slowly deactivating catalyst. The limited stability is known for phosphine based catalysts. An indication for this assumption was the observation of low amounts of Pd-black in the catalyst phase after shutting down and emptying the loop reactor.

The obtained TOF in the steady state varied between 120 und 140 h$^{-1}$. Nevertheless, throughout the reaction time of 216 hours around 1.5 kg of the desired product 1-Mode were formed, a total TON of around 25,000 and a productivity of 65.3 (g·1-Mode)·(g·Pd)$^{-1}$·h$^{-1}$ were reached.

The selectivity over time for this continuous experiment is depicted in Figure 61.
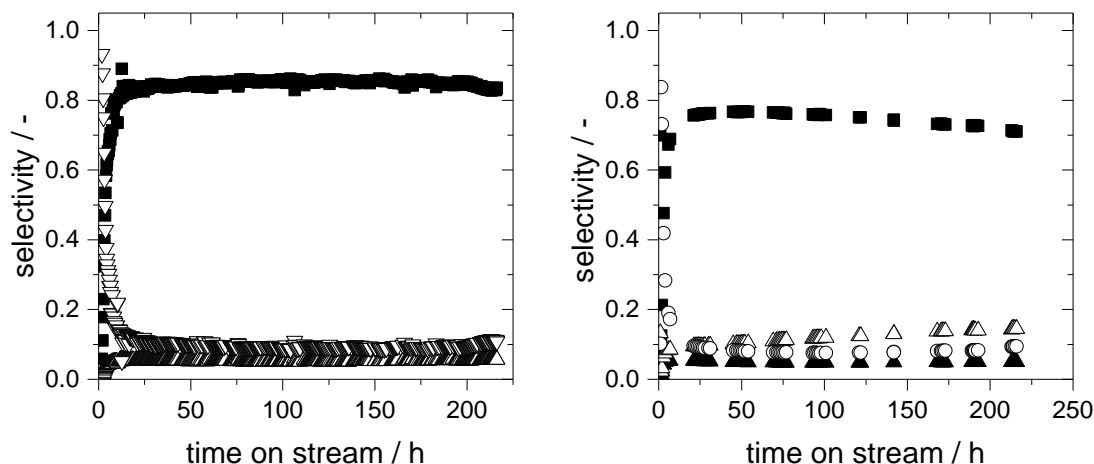
**Figure 61: Selectivities for the continuous operation with the TPPTS modified catalyst, pure butadiene and [EMMIM][NTf₂] as catalyst phase determined by online GC (left) and offline GC (right) (■ 1-Mode, △ 3-Mode, ▽ octatriene + vinylcyclohexene, ▲ octatriene, ○ vinylcyclohexene).**

*Reaction conditions: 70 °C, 18 bar, $n_{Pd}$: 1 mmol, $n_{TPPTS}$: 3.2 mmol, $n_{NEt3}$: 14 mmol, [EMMIM][NTf₂]: 175.4 mmol resp. 68.7 g, $\dot{V}_{circ}$ = 0.25 l·h⁻¹,*
*Flows: MeOH: 2.41 mmol·min⁻¹ resp. 0.077 g·min⁻¹, hexane: 1.67 mmol·min⁻¹ resp. 0.144 g·min⁻¹, butadiene: 4.86 mmol·min⁻¹ resp. 0.263 g·min⁻¹.*

Due to the special temperature conditions in the laboratory during this experiment (room temperature of around 40 °C due to hot summer days), the selectivities determined by online and offline GC differed slightly. The determination of the selectivity via the online GC resulted in a constant 1-Mode formation showing a selectivity of around 83 %. In contrast, the offline GC exhibited lower values for the 1-Mode formation as well as a slight decrease of around 4 to 5 %. The decrease in 1-Mode was in favor of the formation of octatriene as well as vinylcyclohexene. The formation of vinylcyclohexene is known to be an uncatalyzed reaction which is induced at higher temperatures. While the online GC determined the composition right after the exit of the reactor, the offline samples were not measured immediately so that further vinylcyclohexene as well as octatriene might be formed due to the elevated room temperature. Furthermore, the exact addition of a small amount of the external standard dibutylether which is very volatile is more complicated at elevated room temperatures.

## 4.3.4.4  Influence of temperature and circulation speed

At elevated temperatures, the activity of a reaction system should increase according to the Arrhenius law. For the TPP modified catalyst, the preliminary batch experiments showed that an increase in temperature from 70 to 90 °C exhibited a negative effect due to catalyst deactivation and formation of Pd-black, see Chapter 4.2.2.3. The continuous operation was carried out at 80 °C in order to check if an increase of the activity would be possible. In addition, the circulation speed was increased to 1 l·h$^{-1}$. After 75 hours, the feeding velocities of the reactants were decreased. The results of this combined optimization step is shown in Figure 62.
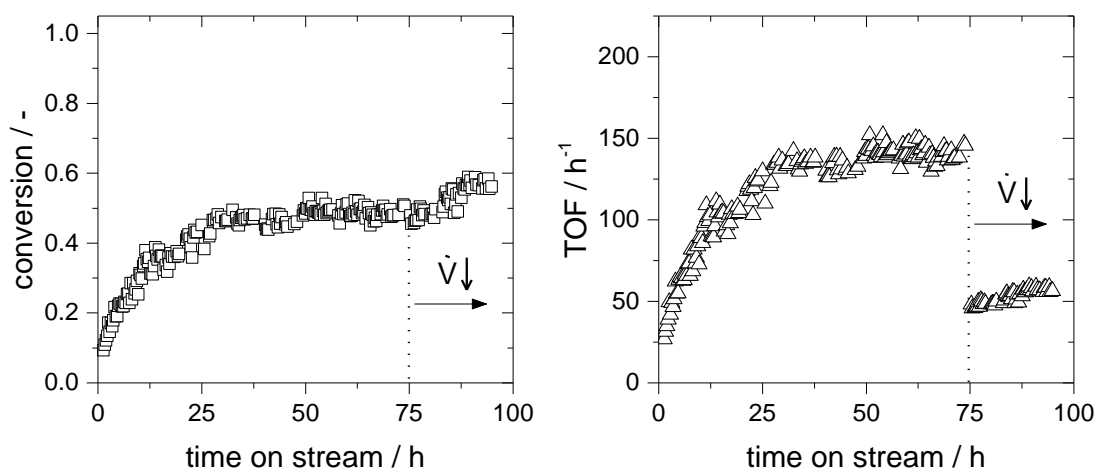


**Figure 62: Conversion (left) and TOF (right) for the continuous operation at 80 °C and increased circulation speed (1 l·h$^{-1}$ vs 0.25 l·h$^{-1}$ in previous experiments) with the TPPTS modified catalyst, pure butadiene and [EMMIM][NTf$_2$] as catalyst phase (lowering of feeding velocities after 75 h).**

*Reaction conditions: 80 °C, 18 bar, $n_{Pd}$: 1 mmol, $n_{TPPTS}$: 3.2 mmol, $n_{NEt3}$: 14 mmol, [EMMIM][NTf$_2$]: 175.4 mmol resp. 68.7 g, $\dot{V}_{circ}$ = 1 l·h$^{-1}$,*
*Flows: MeOH: 2.41 mmol·min$^{-1}$ resp. 0.077 g·min$^{-1}$, hexane: 1.67 mmol·min$^{-1}$ resp. 0.144 g·min$^{-1}$, butadiene: 4.86 mmol·min$^{-1}$ resp. 0.263 g·min$^{-1}$,*
*Flows after 75 h: MeOH: 0.82 mmol·min$^{-1}$ resp. 0.026 g·min$^{-1}$, hexane: 0.58 mmol·min$^{-1}$ resp. 0.05 g·min$^{-1}$, butadiene: 1.70 mmol·min$^{-1}$ resp. 0.09 g·min$^{-1}$.*

The maximum conversion of around 50 % was reached after around 26 hours. A steady state was obtained. As the expected increase in conversion was only around 5 %, another attempt to increase the activity was carried out after 75 hours time on

stream. The feed velocities were again lowered to 1/3 of the starting velocities in order to increase the residence time. However, the increase of conversion was only around 10 %. After 93 hours the conversion started to get constant again at a value of around 58 to 60 %. This low increase is probably caused by the only minor difference in the achieved residence times (133.6 min vs 135.2 min according to the determination of the residence time presented in Appendix 7.8.2).

In the first steady state, a TOF of around 130 to 145 h$^{-1}$ was obtained. The TOF reached in the second steady state at lowered feed rates exhibited a value of around 50 to 60 h$^{-1}$.

The influence of the temperature increase and the increase of the circulation speed on the selectivity is presented in Figure 63.
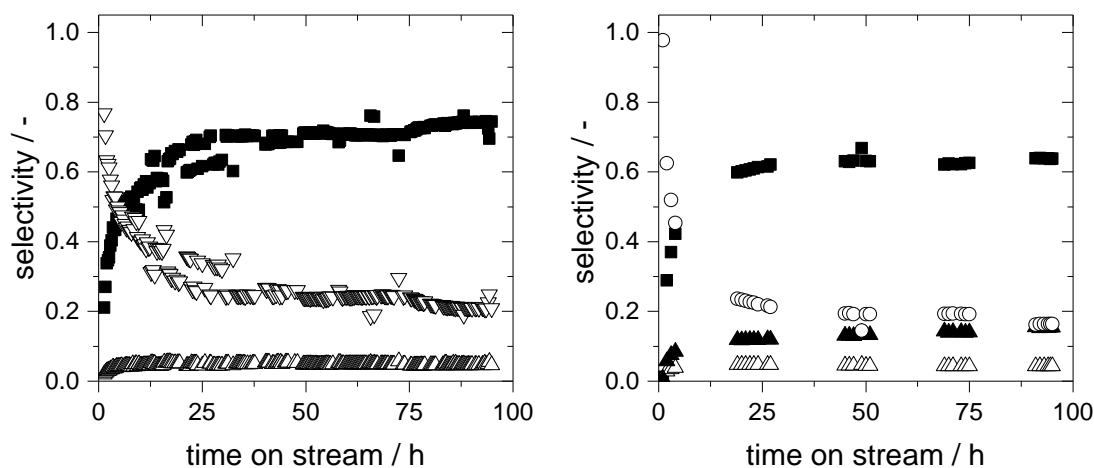


**Figure 63: Selectivities for the continuous operation at 80 °C and increased circulation speed with the TPPTS modified catalyst, pure butadiene and [EMMIM][NTf₂] as catalyst phase (lowering of feeding velocities after 75 h) determined by online GC (left) and offline GC (right) (■ 1-Mode, △ 3-Mode, ▽ octatriene + vinylcyclohexene, ▲ octatriene, ○ vinylcyclohexene).**

*Reaction conditions: 70 °C, 18 bar, $n_{Pd}$: 1 mmol, $n_{TPPTS}$: 3.2 mmol, $n_{NEt3}$: 14 mmol, [EMMIM][NTf₂]: 175.4 mmol resp. 68.7 g, $\dot{V}_{circ} = 1\ l \cdot h^{-1}$,*
*Flows: MeOH: 2.41 mmol·min$^{-1}$ resp. 0.077 g·min$^{-1}$, hexane: 1.67 mmol·min$^{-1}$ resp. 0.144 g·min$^{-1}$, butadiene: 4.86 mmol·min$^{-1}$ resp. 0.263 g·min$^{-1}$,*
*Flows after 75 h: MeOH: 0.82 mmol·min$^{-1}$ resp. 0.026 g·min$^{-1}$, hexane: 0.58 mmol·min$^{-1}$ resp. 0.05 g·min$^{-1}$, butadiene: 1.70 mmol·min$^{-1}$ resp. 0.09 g·min$^{-1}$.*

Interestingly, the selectivity toward 1-Mode is decreased compared to the previous continuous experiments. With the online GC, a selectivity of around 70 % was determined whereas even a lower selectivity of around 62 to 64 % was obtained with the offline GC. The selectivity toward 3-Mode was the same for both determination methods lying at around 4 to 5 %. For vinylcyclohexene as well as octatriene, a very high selectivity was observed compared to the previous experiments: around 20 to 23 % for both determined by the online GC and around 20 % for vinylcyclohexene respectively around 13 % for octatriene determined by the offline measurement. This high selectivity for octatriene and vinylcyclohexene to the disadvantage of 1-Mode is probably caused by the higher reaction temperature. Elevated temperatures are known to influence the selectivity negatively. The differences between online and offline GC were again caused by the elevated room temperature during hot summer days and the not immediate measurement of the offline samples as well as the inaccurate addition of the volatile external standard dibutylether.

In sum, the slight increase in activity by increasing the temperature as well as the circulation speed was followed by a strong decrease in selectivity. Thus, the change of these two parameters did not constitute an optimization of the process.

In addition, a twofold increase of the ionic liquid amount as well as the active cooling of the phase separator to 10 °C did not improve the process performance.

# 5  Summary

The basic aim of this thesis was the development of a continuous process for the telomerization reaction of butadiene with methanol applying ionic liquids in a biphasic reaction system. Besides this aim, the applicability of NIR spectroscopy for determination of concentrations in reaction mixtures of a homogeneously catalyzed reaction was tested. Furthermore, its applicability in ionic liquid mixtures was studied. The thesis was divided into three parts. The first part comprised the study of NIR spectroscopy in mixtures of the investigated telomerization reaction. In the second part, the telomerization of butadiene with methanol was examined without ionic liquids. The immobilization of the catalyst in the ionic liquid phase and the transfer from batch to conti were studied in the last part.

The NIR spectrometer was integrated in a bypass of the loop reactor so that the NIR studies were all carried out with experiments in the loop reactor. For the development of a calibration model, different strategies regarding the applied feed were carried out. These strategies are depicted in Table 18.

**Table 18: Different strategies for the development of a NIR calibration model.**

| Determination in monophasic system – calibration model based on experiments with: | | |
|---|---|---|
| Feed: butadiene | Feed: $sCC_4$ | Combination of both |

| Determination in biphasic system – calibration model based on experiments with: | |
|---|---|
| Feed: $sCC_4$<br><br>Ionic liquid: none | Feed: combination butadiene + $sCC_4$<br><br>Ionic liquid: none |
| Feed: butadiene<br><br>Ionic liquid: [EMMIM][NTf$_2$] | Feed: combination butadiene + $sCC_4$<br><br>Ionic liquid: [EMMIM][NTf$_2$] |

For the NIR-determination in monophasic reaction mixtures, one calibration model was constructed by using only experiments carried out with either butadiene or $sCC_4$ as well as the combination of experiments with both feeds. During the experiments, NIR spectra were recorded and reference values were determined by online GC. For the development of a calibration model, the spectra were divided into a calibration and a test set. With the test set, the calibration model was validated resulting in true-predicted plots comparing the true values (reference values) with the values
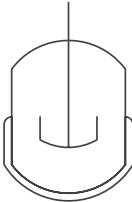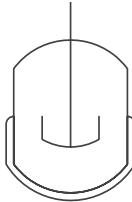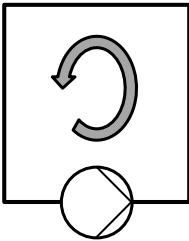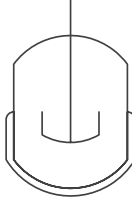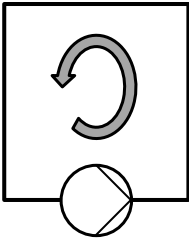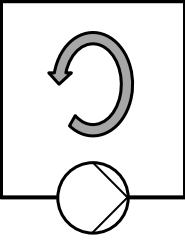
predicted by the calibration model. These plots showed that the concentration of 1-Mode, butadiene and methanol were determined with a very high accuracy. However, the applicability of NIR spectroscopy is limited for components which are present in the reaction mixture only at very low concentrations, e.g. 3-Mode.

An independent validation of the calibration model was carried out by additional experiments which were not used for the calibration. The predicted concentrations were compared to the concentrations determined by GC analysis. These plots showed very good alignment of both determination methods for the components 1-Mode, butadiene and methanol. Again, the accuracy for the determination of 3-Mode was low. Nevertheless, the qualitative progress of the reaction was also represented for 3-Mode.

The feasibility and applicability of NIR spectroscopy for the telomerization reaction was shown in this thesis. In addition, NIR spectroscopy seems to be very promising for other liquid phase reactions. Furthermore, the applicability of NIR spectroscopy in reaction mixtures with ionic liquids was tested. For this, the calibration models using experiments with $sCC_4$ and the combination of experiments with butadiene and $sCC_4$ were applied. Moreover, a separate calibration with ionic liquid experiments was developed as well as a combinatory calibration of ionic liquid experiments and $sCC_4$ experiments. With those four calibration models, the reaction progress was presented in high accuracy. Also the quantitative determination of the mass fraction was successful. However, the best applied calibration model differed depending on the determined component. For instance, for 1-Mode the best calibration was the combinatory model with ionic liquid and $sCC_4$ whereas for butadiene, the best results were obtained with the calibration models without ionic liquid. This was probably caused by insufficient calibration for the components. The calibration with ionic liquid did not obtain enough information about butadiene whereas it showed highly accurate information for 1-Mode. In order to overcome these differences, a sufficient calibration with all involved components in the complete concentration range of interest has to be developed.

In the second and third part of this thesis, a variety of telomerization experiments were conducted. Table 19 provides an overview of the studied reaction systems and the applied reaction mode.

**Table 19: Overview of the studied reaction systems in this thesis.**

| Monophasic experiments | Biphasic experiments |
|---|---|
| • **Batch** | • **Batch** |
| <u>Pd-Precursor</u>: Pd(acac)$_2$, Pd(OAc)$_2$, Pd$_2$(cin)$_2$Cl$_2$, NHC-complexes <br> <u>Ligand-Precursors</u>: [IMes][MeSO$_3$], TPP <br> <u>Feeds</u>: pure butadiene, sCC$_4$ <br> $T_{reaction}$ = 50 – 90 °C <br> $n_{Buta}$:$n_{Pd}$ = 20,000 – 60,000 <br> $n_{Lig}$:$n_{Pd}$ = 1:5 – 10:1 <br> $n_{Buta}$:$n_{MeOH}$ = 2:1 – 1:5 <br> $n_{KOMe}$ = 0.668 – 3.234 mmol | <u>Pd-Precursor</u>: Pd(acac)$_2$, Pd(OAc)$_2$, <br> <u>Ligand-Precursors</u>: [IMes][MeSO$_3$], TPP, TPPMS, TPPTS, [BMMIM]TPPMS <br> <u>Feeds</u>: pure butadiene <br> $T_{reaction}$ = 70 – 85 °C <br> $n_{Buta}$:$n_{Pd}$ = 10,000 <br> $n_{Lig}$:$n_{Pd}$ = 1:1 – 3:1 <br> $n_{Buta}$:$n_{MeOH}$ = 1:1 <br> $n_{Buta}$:$n_{IL}$ = 30 <br> $n_{MeOH}$:$n_{hexane}$ = 3.22 <br> <u>Ionic liquids</u>: [EMMIM][BF$_4$], [BMMIM][BF$_4$], [EMMIM][TOS], [EMMIM][MeSO$_4$], [BMMIM][OcSO$_4$], [EMMIM]Cl, [EMMIM][NTf$_2$], [BMMIM][NTf$_2$] |
| • **Batch** | • **Recycling** |
| <u>Pd-Precursor</u>: Pd(acac)$_2$ <br> <u>Ligand-Precursors</u>: [IMes][MeSO$_3$], TPP <br> <u>Feeds</u>: pure butadiene, sCC$_4$ <br> $T_{reaction}$ = 70 °C <br> $n_{Buta}$:$n_{Pd}$ = 40,000 <br> $n_{Lig}$:$n_{Pd}$ = 4:1 <br> $n_{Buta}$:$n_{MeOH}$ = 1:2 | <u>Pd-Precursor</u>: Pd(acac)$_2$ <br> <u>Ligand-Precursors</u>: TPPMS <br> <u>Feeds</u>: pure butadiene <br> $T_{reaction}$ = 85 °C <br> $n_{Buta}$:$n_{Pd}$ = 5,500 <br> $n_{Lig}$:$n_{Pd}$ = 3:1 <br> $n_{Buta}$:$n_{MeOH}$ = 2:1 – 1:1 <br> $n_{Buta}$:$n_{IL}$ = 30 <br> $n_{MeOH}$:$n_{hexane}$ = 2.45 <br> <u>Ionic liquids</u>: [BMMIM][BF$_4$], [EMMIM][TOS], [BMMIM][NTf$_2$] |
| • **Conti** | • **Conti** |
| <u>Pd-Precursor</u>: Pd(acac)$_2$ <br> <u>Ligand-Precursors</u>: TPP <br> <u>Feeds</u>: pure butadiene <br> $T_{reaction}$ = 70 °C <br> $n_{Buta}$:$n_{Pd}$ = 40,000 <br> $n_{Lig}$:$n_{Pd}$ = 4:1 <br> $n_{Buta}$:$n_{MeOH}$ = 1:2 | <u>Pd-Precursor</u>: Pd(acac)$_2$ <br> <u>Ligand-Precursors</u>: TPPMS, TPPTS <br> <u>Feeds</u>: pure butadiene <br> $T_{reaction}$ = 70 - 80 °C <br> $n_{Pd}$ = 1 mmol <br> $n_{Lig}$ = 3 mmol <br> $n_{IL}$ = 175 - 350 mmol <br> $\dot{V}_{MeOH}$ = 7.22 - 2.41 mmol·min$^{-1}$ <br> $\dot{V}_{Buta}$ = 14.46 - 4.86 mmol·min$^{-1}$ <br> $\dot{V}_{hexane}$ = 4.86 – 1.67 mmol·min$^{-1}$ <br> <u>Ionic liquids</u>: [BMMIM][NTf$_2$], [EMMIM][NTf$_2$] |

The experiments without ionic liquid were carried out in order to compare the two literature known ligands, namely TPP and IMes, in combination with pure butadiene and the technical, diluted butadiene feed ($sCC_4$). In addition, the influence of different reaction parameters was studied in order to optimize the reaction conditions for each ligand. The optimum reaction conditions for each reaction system are summarized in Table 20.

**Table 20: Optimized reaction conditions for the monophasic reaction systems.**

| General:<br>• No oxygen<br>• $Pd(acac)_2$ | TPP | IMes |
|---|---|---|
| Butadiene | $T_{reaction}$ = 70 °C<br>$n_{Buta}$:$n_{Pd}$ = 20,000<br>$n_{Buta}$:$n_{Lig}$ = 4:1<br>$n_{Buta}$:$n_{MeOH}$ = 1:1.5 resp. 1:2 | $T_{reaction}$ = 90 °C<br>$n_{Buta}$:$n_{Pd}$ = 20,000<br>$n_{Lig}$:$n_{Pd}$ = 4:1<br>$n_{Buta}$:$n_{MeOH}$ = 2:1 |
| $sCC_4$ | $T_{reaction}$ = 70 °C<br>$n_{Buta}$:$n_{Pd}$ = 20,000<br>$n_{Lig}$:$n_{Pd}$ = 4:1 resp. 10:1<br>$n_{Buta}$:$n_{MeOH}$ = 1:5 | $T_{reaction}$ = 90 °C<br>$n_{Buta}$:$n_{Pd}$ = 20,000<br>$n_{Lig}$:$n_{Pd}$ = 1:1<br>$n_{Buta}$:$n_{MeOH}$ = 1:2 |

At the same reaction conditions, the two ligands showed a completely different behavior in combination with both feeds. The Pd-TPP catalyst exhibited a higher reaction rate with pure butadiene than with the diluted feed, $sCC_4$. The components of the technical feed, mainly butenes and butanes, were proven to be inert in the telomerization reaction. Thus, the observed behavior for the TPP based catalyst was caused by the expected dilution effect of inert components.

In contrast, the Pd-IMes catalyst showed higher conversion values in combination with the diluted feed. The reaction rate was observed to be similar for both feeds resembling an overall reaction of zero order in butadiene. This differing behavior of TPP and IMes was found for all following experiments of this thesis.

Studies with the Pd-TPP catalyst showed the oxygen sensitivity of the telomerization reaction but the application of technical methanol did not disturb the reaction.

The influence of the base strength differs strongly for the two applied catalyst complexes. Whereas the Pd-TPP catalyst did not show a strong dependency on the base strength and would not need a base at all to promote the telomerization reaction, the Pd-IMes catalyst was observed to require a strong base such as KOMe. With weaker bases, the IMes based catalyst was not active in the telomerization reaction, even at elevated reaction temperatures and reaction times.

A temperature variation between 50 °C and 90 °C showed a deactivation of the Pd-TPP catalyst at 90 °C and a decelerated reaction rate at 50 °C. The temperature dependence of the IMes based catalyst was observed to be in accordance with the Arrhenius law showing an increase in reaction rate with increasing temperature. The behavior of both ligands was obtained in combination with both feeds. For the Pd-IMes catalyst, the selectivities remained almost constant whereas an increase of formed octatriene at elevated temperatures was observed for the TPP based catalyst.

A variation of the butadiene to catalyst ratio showed an expected increasing reaction rate with increasing catalyst amount. The selectivities of 1-Mode decreased mainly in favor of the formation of 3-Mode. The reason was not exactly known.

By the variation of the molar ratio of ligand to catalyst, an optimum ratio was achieved for both ligands. For Pd-TPP, the optimum ratio was at 4:1 with pure butadiene whereas with the diluted feed, the ratios 4:1 and 10:1 showed very similar results. With both feeds, the worst performance was obtained with an excess of catalyst. These observations underlined literature reports stating that phosphine based catalysts require an excess of ligand in order to stabilize the catalyst [95; 176]. Similar to the Pd-TPP catalyst, the IMes based catalyst showed the worst performance with an excess of palladium. With pure butadiene, the optimum ratio was 4:1 whereas with $sCC_4$ the ratio of 1:1 showed the best performance. Obviously, the optimum ratio depends on the applied ligand but also on the applied feed. Vollmüller [95] reported a strong dependence of the selectivities on the amount of the used ligand as well as on the ligand itself. For Pd-TPP, an increase of ligand leads to a decrease in the formation of the *n*-telomer in favor of the *iso*-telomer. For a ligand with a higher steric demand such as the IMes ligand, the increase of the ligand amount does not affect the selectivity. For both ligands in combination with both feeds, the experimental results of this thesis were in accordance with Vollmüller.

The influence of the reactants butadiene and methanol on activity and selectivity of the studied system was investigated by the variation of the molar ratio of butadiene to methanol. The influence of this variation differed strongly dependent on the applied system. For Pd-TPP no large difference in the performance was observed within the ratio range of 1:1 to 1:3. With a large excess of methanol, an activation phase of around 1.5 to 2 hours was achieved whereas a negative influence was obtained applying a stoichiometric ratio of butadiene to methanol of 2:1. With $sCC_4$, the performance of the Pd-TPP catalyst increased with increasing methanol concentration. This was probably caused by solubility effects of the catalyst and ligand in hydrocarbons. The regio- as well as the chemoselectivity increased with increasing amount of methanol. This trend is in accordance with literature reports [95] and independent of the applied feed. For the Pd-IMes catalyst in combination with pure butadiene, an increase of the reaction rate with decreasing methanol concentration was observed whereas an optimum ratio of 1:2 was found in combination with $sCC_4$. The latter was probably the result of the combination of increasing reaction rate with increasing butadiene and the contrary effect of better solubility of the catalyst complex when adding more methanol.

Based on these observations, a kinetic model was derived on the basis of the Jolly mechanism in cooperation with the SYNFLOW partner RWTH Aachen. For the TPP based catalyst, a reaction order of 2 in butadiene and 1 in methanol was found. For the IMes based catalyst, no kinetic model based on the Jolly mechanism was found which fit the experimental data. Further kinetic experiments showed that the IMes based catalyst is independent of the butadiene concentration but strongly dependent on the base concentration. Methanol has a negative effect on the reaction which might be explained by the influence of this protic solvent on the nucleophilicity of the base. With this knowledge, the Jolly mechanism was adapted and a kinetic model could be derived.

A screening of different in-situ as well as ex-situ prepared catalyst complexes showed that $Pd(acac)_2$ was the most effective catalyst precursor and that the performance of different Pd-NHC complexes decreased with increasing steric demand. The latter behavior was found to be in accordance with the literature [177]. The NHC-ligand IMes exhibited the best results. Also with the ex-situ prepared Pd-NHC complexes as well as all studied catalyst precursors in combination with IMes, the obtained conversion values with pure butadiene were lower than with $sCC_4$.

The transfer from the batch autoclave to the loop reactor and the commissioning of the latter were successfully carried out for monophasic experiments. The performance in the loop reactor was slightly higher for both catalyst systems and both feeds probably due to a better heat supply and compensation of heat loss in the loop reactor. First continuous experiments without catalyst recycling using the TPP based catalyst in combination with pure butadiene were carried out at 3 different residence times. The experiments passed a start-up phase of around 3 hours before reaching a steady state. The conversion obtained in this steady state decreased, as expected, with decreasing residence times.

The next step for the development of a continuous process was the study of the telomerization reaction in a biphasic reaction system. Here, the choice of the ionic liquid is crucial due to the exhibited extraction efficiency. For a preselection of ionic liquids, a screening of 960 different anion-cation combinations with the computational tool COSMO-RS was carried out. By experimental validation of 9 ionic liquids, the trends of the predicted extraction efficiencies were proven to be in accordance with the experimental obtained tendencies.

The activity of these ionic liquids in the telomerization reaction was studied by a screening of 8 different ionic liquids in combination with a screening of different ligands. The extraction efficiency and the activity in the telomerization reaction were observed to be completely independent. The leaching of the Pd-TPP and Pd-IMes catalyst into the organic phase was too high due to the missing ionic groups. Consequently, sulfonated derivatives of the phosphine ligand were tested as well. The activities of the three tested ligands, namely TPPMS, TPPTS and [BMMIM]-TPPMS, were very similar but the determined leaching values differed strongly. By applying the threefold sulfonated phosphine ligand (TPPTS), the leaching was drastically reduced compared to the monosulfonated one (TPPMS). The most active systems with these ligands were obtained with the ionic liquids [EMMIM][TOS], [EMMIM][NTf$_2$] followed by [BMMIM][NTf$_2$] and [BMMIM][BF$_4$] whereas [EMMIM][BF$_4$] showed distinctively lower conversion values after the same reaction time.

The stability of the catalyst was studied in recycling experiments using three different ionic liquids based on the three anions [TOS]$^-$, [NTf$_2$]$^-$ and [BF$_4$]$^-$ whereas the [NTf$_2$]$^-$ based ionic liquid is the only liquid one in pure form at room temperature. In these experiments, the catalyst phase was recycled a first time with the conversion

regained for all three studied systems. After the first recycle (the second experiment of 3 hours), however, the catalyst phase was stored over night under argon. Nevertheless, the catalyst seemed to be deactivated by this storage by either oxygen traces or the removal of butadiene which is inserted in the active catalyst species or even a combination of both. In the second and third recycle, the conversion dropped. This was again observed for all three systems. This deactivation could be prevented by transferring the reaction system to the continuously operating loop reactor.

The transfer to the loop reactor was carried out using the Pd-TPPMS catalyst and the ionic liquid [BMMIM][NTf$_2$]. The optimization process was carried out stepwise and is summarized in Figure 64.
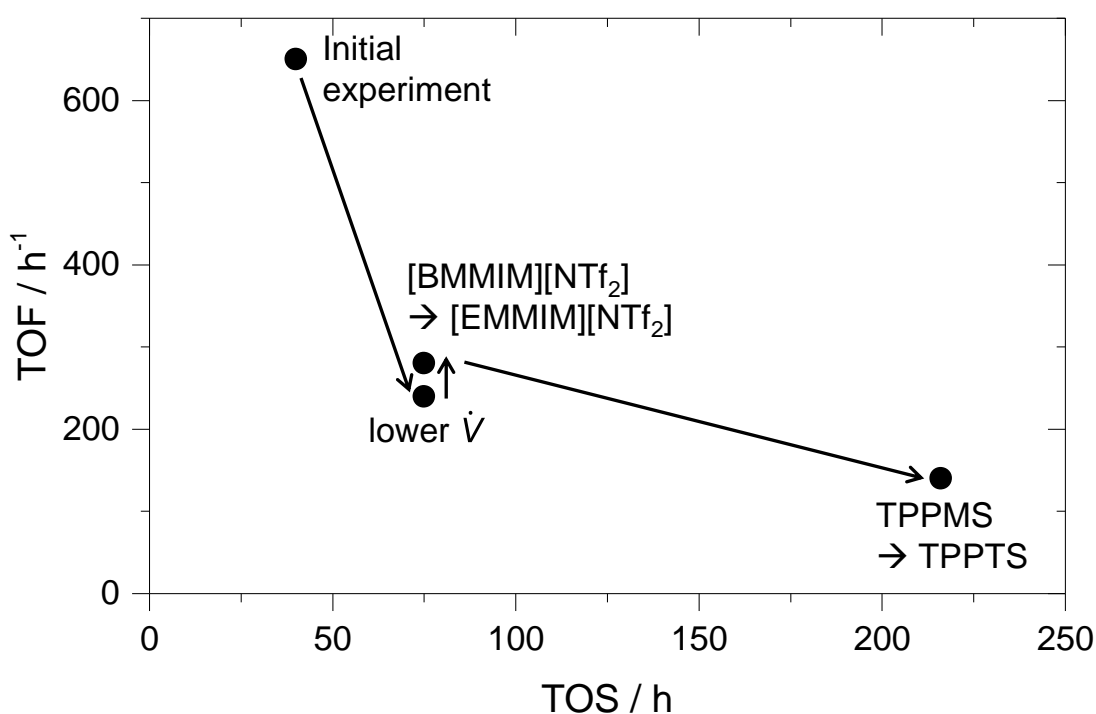


**Figure 64: Way of stepwise optimization for the continuous process with ionic liquids.**

The need of stoichiometric ratios was again shown in the loop reactor. An experiment with a ratio of butadiene to methanol of 1:1 led to a drastic drop in conversion during 20 hours (80 % to 15 %). The change of the ratios to a stoichiometric one ($n_{butadiene}$:$n_{MeOH}$ = 2:1) led to a more stable continuous process with a time on stream of 47 hours. During these 47 hours, the conversion decreased from initially 80 to

20 % probably due to the Pd-leaching into the product stream. Leaching values were determined to lie between 1,000 and 2,400 ppm per hour resulting in 9.6 % of the initial palladium concentration after 47 hours. The TOF started with a value of 650 $h^{-1}$ and decreased throughout the process to 200 $h^{-1}$. The obtained selectivities were constant and similar to those of the preliminary biphasic batch experiment with around 80 % 1-Mode, 5 % 3-Mode, 12 % octatriene and 3 % vinylcyclohexene.

The lowering of the feeding velocities to 1/3 of the previous continuous run resulted in an increase of the achieved time on stream (72 h) as well as of the maximum obtained conversion (93 %). The decrease in conversion was slower reaching around 70 % after 72 hours. This improvement was probably caused by the lower leaching of the Pd catalyst due to the lower flow rates. The selectivities were similar to the previous experiment and constant over the time on stream. Due to the lower flow rates, the activity of the catalytic system was lower as well ($TOF_{max} = 260$ $h^{-1}$).

The change of the ionic liquid from [BMMIM][$NTf_2$] to [EMMIM][$NTf_2$] did not show an obvious influence on the stability of the system due to lower leaching as it was expected from the preliminary batch study. The slightly higher activity obtained with the [EMMIM]$^+$ based ionic liquid in the batch experiments was also achieved in the continuous process. The conversion level was around 5 % higher. Also the TOF was slightly higher compared to the experiment with [BMMIM][$NTf_2$]. The change of the ionic liquid did not show any influence on the selectivity.

The most efficient optimization step was the change of the ligand from the monosulfonated to the threefold sulfonated phosphine ligand. Although the activity was distinctly lower compared to the continuous runs with the TPPMS modified catalyst, the time on stream increased significantly. The maximum conversion of around 45 % was kept constant for around 200 hours. The leaching values were reduced drastically to around 50 to 200 ppm per hour. After 200 hours time on stream, the conversion started slowly to decrease (40 % at 216 h) probably due to catalyst deactivation as well as slight leaching of the Pd catalyst. The TOF obtained in the steady state varied slightly between 120 and 140 $h^{-1}$. Despite the relatively low activity, in total 1.5 kg of the desired product 1-Mode were formed throughout this continuous run. A cumulative TON of around 25,000 was achieved. The selectivities were again comparable to those obtained in the batch experiments exhibiting a value of around 83 % toward the main product 1-Mode.

Further optimization attempts regarding reaction temperature, circulation speed or applied amount of ionic liquid did not show distinct improvements.

The challenge of the catalyst immobilization concerning the reactant methanol was met by applying a biphasic reaction system with ionic liquids in combination with ionic ligands. A continuous process which yielded constant activity over 200 h time on stream was successfully established. Thus, the basic aim of this thesis to develop a continuous process for the telomerization of butadiene with methanol was achieved.

# 6 Zusammenfassung / Kurzfassung

Ziel dieser Arbeit war die Entwicklung eines kontinuierlichen Prozesses für die Telomerisation von Butadien mit Methanol unter Verwendung eines zweiphasigen Reaktionssystems mit ionischen Flüssigkeiten. Ein weiteres Ziel war es, die Konzentrationsbestimmung online mit Hilfe der NIR-Spektroskopie sowohl in einphasig homogen katalysierten Reaktionen als auch in Reaktionsgemischen mit ionischen Flüssigkeiten zu testen. Aufgrund dieser Aufgabenstellung wurde die vorliegende Arbeit in drei Hauptteile unterteilt. Im ersten Teil wurde die Anwendung der NIR-Spektroskopie untersucht. Der zweite Teil beinhaltete grundlegende Untersuchungen der Telomerisation von Butadien mit Methanol ohne den Einsatz von ionischen Flüssigkeiten. Die Übertragung der Telomerisation in ein zweiphasiges Reaktionssystem mit ionischen Flüssigkeiten und der Transfer vom Batch- zum kontinuierlichen Betrieb wurden im dritten Teil thematisiert.

Die NIR-Experimente wurden alle in einem Schlaufenreaktor durchgeführt, bei dem in einem Bypass das NIR-Spektrometer installiert war. Für die Entwicklung eines Kalibriermodells wurden verschiedene Ansätze basierend auf der Wahl der verwendeten Butadien-Quelle getestet und evaluiert. Die verschiedenen Ansätze sind in Tabelle 1 zusammengefasst.

**Tabelle 1: Verwendete Ansätze zur Entwicklung eines Kalibriermodells für die NIR-Spektroskopie**

| Einphasige Experimente – Kalibriermodell basierend auf Experimenten mit: | | |
|---|---|---|
| Edukt: Butadien | Edukt: $sCC_4$ | Kombination aus beiden Varianten |
| Zweiphasige Experimente – Kalibriermodell basierend auf Experimenten mit: | | |
| Edukt: $sCC_4$<br>Ionische Flüssigkeit: keine | | Edukt: Kombination Butadien + $sCC_4$<br>Ionische Flüssigkeit: keine |
| Edukt: Butadien<br>Ionische Flüssigkeit: [EMMIM][NTf$_2$] | | Edukt: Kombination Butadien + $sCC_4$<br>Ionische Flüssigkeit: [EMMIM][NTf$_2$] |

Für die Anwendung in einphasigen Reaktionsmischungen wurde jeweils ein Kalibriermodell auf Basis von Experimenten mit Butadien und mit $sCC_4$, einem Gasgemisch aus ca. 45 mol% Butadien und 55 mol% Butenen und Butanen, erstellt.

Zusätzlich wurde ein Modell aus der Kombination dieser Experimente entwickelt. Während dieser Experimente wurden NIR Spektren aufgenommen und gleichzeitig Referenzwerte mit Hilfe eines online GCs bestimmt. Für die Erstellung der Kalibriermodelle wurden die aufgenommenen Spektren in ein Kalibrier-Set und ein Test-Set aufgeteilt. Die Validierung der Kalibriermodelle erfolgte zunächst mit den Spektren des Test-Sets durch einen Vergleich der mit NIR bestimmten Werte mit den Referenzwerten in Paritätsdiagrammen. Die Konzentrationen von 1-Mode, Butadien und Methanol konnten mit einer sehr großen Genauigkeit bestimmt werden. Dennoch konnte auch gezeigt werden, dass die Anwendung der NIR-Spektroskopie Grenzen aufweist. Die Bestimmung von Komponenten, die nur in sehr geringer Konzentration vorliegen, wie beispielsweise das Nebenprodukt 3-Mode, war deutlich ungenauer.

Zur weiteren Validierung wurden unabhängige Experimente durchgeführt. Die Konzentrationen wurden mit NIR aufgezeichnet und mit parallel detektierten Referenzwerten verglichen. Wieder konnten die Konzentrationen der Hauptkomponenten 1-Mode, Butadien und Methanol sehr genau bestimmt werden. Obwohl eine exakte quantitative Bestimmung der Konzentration von 3-Mode nicht möglich war, konnte der qualitative Reaktionsverlauf sehr gut wiedergegeben werden.

Die Anwendung der NIR-Spektroskopie konnte in dieser Arbeit erfolgreich gezeigt werden. Die NIR-Spektroskopie ist auch zur Konzentrationsbestimmung in anderen Flüssigphasenreaktionen eine vielversprechende Methode. Des Weiteren wurde im Rahmen dieser Arbeit auch die Anwendbarkeit der NIR-Spektroskopie in Mischungen mit ionischen Flüssigkeiten gezeigt. Hierfür wurden wieder verschiedene Ansätze für die Erstellung des Kalibriermodells getestet. Neben den schon für die einphasigen Versuche verwendeten Kalibriermodellen aus Experimenten mit entweder reinem Butadien oder $sCC_4$ wurden zusätzliche Spektren mit ionischer Flüssigkeit aufgenommen. Ein viertes Kalibriermodell wurde aus einer Kombination der Spektren auf Basis von ionischer Flüssigkeit und $sCC_4$ erstellt. Mit diesen Kalibriermodellen konnten sowohl der Reaktionsverlauf als auch die quantitativen Konzentrationswerte sehr genau bestimmt werden. Abhängig von der zu detektierenden Komponente erwiesen sich unterschiedliche Kalibriermodelle als das jeweils Beste für die entsprechende Komponente. Für 1-Mode zeichnete sich das kombinatorische Modell aus ionischer Flüssigkeit und $sCC_4$ als das mit der größten Genauigkeit ab, für Butadien hingegen waren es die beiden Modelle ohne ionische Flüssigkeit, die auch

schon bei den einphasigen Reaktionssystemen verwendet wurden. Letzteres lässt sich vermutlich dadurch erklären, dass die Kalibrierungen mit ionischer Flüssigkeit zu wenige Informationen über die Komponente Butadien enthielten. Dieses Problem könnte allerdings durch eine ausreichende Kalibrierung mit allen Komponenten in allen Konzentrationsbereichen behoben werden.

Im zweiten und dritten Teil dieser Arbeit wurden verschiedene Systeme und Reaktionsbedingungen untersucht, die in Tabelle 2 thematisch zusammengefasst sind.

Die Versuche ohne ionische Flüssigkeit wurden durchgeführt, um die beiden literaturbekannten Liganden TPP und IMes mit reinem Butadien und $sCC_4$ zu vergleichen. Des Weiteren wurden verschiedene Reaktionsparameter variiert, um die optimalen Reaktionsbedingungen für jedes einzelne Reaktionssystem zu erarbeiten. Die erhaltenen optimalen Reaktionsbedingungen sind in Tabelle 3 zusammengefasst.

Bei gleichen Reaktionsbedingungen zeigten die beiden Liganden ein deutlich unterschiedliches Verhalten. Für den Pd-TPP Katalysator wurde mit reinem Butadien eine deutlich höhere Reaktionsrate erreicht als mit $sCC_4$. Durch weitere Versuche wurde gezeigt, dass alle zusätzlichen Komponenten im $sCC_4$ (Butene und Butane) inerten Charakter in der Telomerisation aufwiesen. Demzufolge lag der Grund für die erwähnte geringere Reaktionsrate mit dem Butadiengemisch in einem Verdünnungseffekt durch die inerten Komponenten.

Im Gegensatz zum Pd-TPP System zeigte der Pd-IMes Katalysator ein umgekehrtes Verhalten. Mit reinem Butadien lag der Umsatzverlauf unter dem mit $sCC_4$. Ein Vergleich der Reaktionsraten zeigte, dass diese bis zum jeweiligen Vollumsatz nahezu gleich waren. Der lineare Verlauf der Reaktionsraten deutete darauf hin, dass die Telomerisation für den Pd-IMes Katalysator eine Gesamtreaktionsordnung von 0 aufweist. Dieses beschriebene, unterschiedliche Verhalten der beiden Katalysatorsysteme wurde in allen folgenden Versuchen zur Reaktionsoptimierung beobachtet.

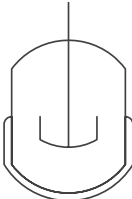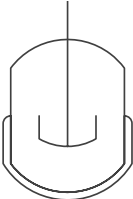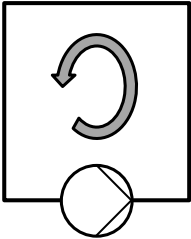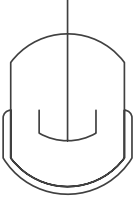**Tabelle 2: Überblick über die durchgeführten Versuche, die verwendeten Systeme und Reaktionsbedingungen.**
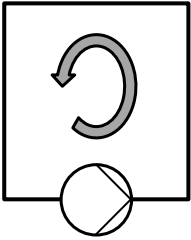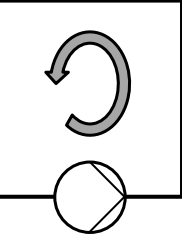
| Einphasige Versuche | Zweiphasige Versuche |
|---|---|
| • **Batch** | • **Batch** |
| <u>Pd-Präkursoren</u>: Pd(acac)$_2$, Pd(OAc)$_2$, Pd$_2$(cin)$_2$Cl$_2$, NHC-Komplexe<br><u>Ligand-Präkursoren</u>: [IMes][MeSO$_3$], TPP<br><u>Edukte</u>: reines Butadien, sCC$_4$<br>$T_{\text{Reaktion}}$ = 50 – 90 °C<br>$n_{\text{Buta}}$:$n_{\text{Pd}}$ = 20000 – 60000<br>$n_{Lig}$:$n_{\text{Pd}}$ = 1:5 – 10:1<br>$n_{\text{Buta}}$:$n_{\text{MeOH}}$ = 2:1 – 1:5<br>$n_{\text{KOMe}}$ = 0,668 – 3,234 mmol | <u>Pd-Präkursoren</u>: Pd(acac)$_2$, Pd(OAc)$_2$,<br><u>Ligand-Präkursoren</u>: [IMes][MeSO$_3$], TPP, TPPMS, TPPTS, [BMMIM]TPPMS<br><u>Edukte</u>: reines Butadien<br>$T_{\text{Reaktion}}$ = 70 – 85 °C<br>$n_{\text{Buta}}$:$n_{\text{Pd}}$ = 10000<br>$n_{Lig}$:$n_{\text{Pd}}$ = 1:1 – 3:1<br>$n_{\text{Buta}}$:$n_{\text{MeOH}}$ = 1:1<br>$n_{\text{Buta}}$:$n_{\text{IL}}$ = 30<br>$n_{\text{MeOH}}$:$n_{\text{Hexan}}$ = 3,22<br><u>Ionische Flüssigkeiten</u>:<br>[EMMIM][BF$_4$], [BMMIM][BF$_4$], [EMMIM][TOS], [EMMIM][MeSO$_4$], [BMMIM][OcSO$_4$], [EMMIM]Cl, [EMMIM][NTf$_2$], [BMMIM][NTf$_2$] |
| • **Batch** | • **Rezyklierung** |
| <u>Pd-Präkursoren</u>: Pd(acac)$_2$<br><u>Ligand-Präkursoren</u>: [IMes][MeSO$_3$], TPP<br><u>Edukte</u>: reines Butadien, sCC$_4$<br>$T_{\text{Reaktion}}$ = 70 °C<br>$n_{\text{Buta}}$:$n_{\text{Pd}}$ = 40000<br>$n_{Lig}$:$n_{\text{Pd}}$ = 4:1<br>$n_{\text{Buta}}$:$n_{\text{MeOH}}$ = 1:2 | <u>Pd-Präkursoren</u>: Pd(acac)$_2$<br><u>Ligand-Präkursoren</u>: TPPMS<br><u>Edukte</u>: reines Butadien<br>$T_{\text{Reaktion}}$ = 85 °C<br>$n_{\text{Buta}}$:$n_{\text{Pd}}$ = 5500<br>$n_{Lig}$:$n_{\text{Pd}}$ = 3:1<br>$n_{\text{Buta}}$:$n_{\text{MeOH}}$ = 2:1 – 1:1<br>$n_{\text{Buta}}$:$n_{\text{IL}}$ = 30<br>$n_{\text{MeOH}}$:$n_{\text{Hexan}}$ = 2,45<br><u>Ionische Flüssigkeiten</u>:<br>[BMMIM][BF$_4$], [EMMIM][TOS], [BMMIM][NTf$_2$] |
| • **Konti** | • **Konti** |
| <u>Pd-Präkursoren</u>: Pd(acac)$_2$<br><u>Ligand-Präkursoren</u>: TPP<br><u>Edukte</u>: reines Butadien<br>$T_{\text{Reaktion}}$ = 70 °C<br>$n_{\text{Buta}}$:$n_{\text{Pd}}$ = 40000<br>$n_{Lig}$:$n_{\text{Pd}}$ = 4:1<br>$n_{\text{Buta}}$:$n_{\text{MeOH}}$ = 1:2 | <u>Pd-Präkursor</u>: Pd(acac)$_2$<br><u>Ligand-Precursors</u>: TPPMS, TPPTS<br><u>Edukte</u>: reines Butadien<br>$T_{\text{Reaktion}}$ = 70 - 80 °C<br>$n_{\text{Pd}}$ = 1 mmol<br>$n_{Lig}$ = 3 mmol<br>$n_{\text{IL}}$ = 175 - 350 mmol<br>$\dot{V}_{\text{MeOH}}$ = 7,22 – 2,41 mmol·min$^{-1}$<br>$\dot{V}_{\text{Buta}}$ = 14,46 – 4,86 mmol·min$^{-1}$<br>$\dot{V}_{\text{Hexan}}$ = 4,86 – 1,67 mmol·min$^{-1}$<br><u>Ionische Flüssigkeiten</u>:<br>[BMMIM][NTf$_2$], [EMMIM][NTf$_2$] |

**Tabelle 3: Optimierte Reaktionsbedingungen der einphasigen Reaktionssysteme.**

| Allgemein:<br>• Kein Sauerstoff<br>• Pd(acac)$_2$ | TPP | IMes |
|---|---|---|
| Butadien | $T_{\text{Reaktion}} = 70\ °C$<br>$n_{\text{Buta}}:n_{\text{Pd}} = 20000$<br>$n_{\text{Buta}}:n_{\text{Lig}} = 4:1$<br>$n_{\text{Buta}}:n_{\text{MeOH}} = 1:1,5$ bzw. $1:2$ | $T_{\text{Reaktion}} = 90\ °C$<br>$n_{\text{Buta}}:n_{\text{Pd}} = 20000$<br>$n_{Lig}:n_{\text{Pd}} = 4:1$<br>$n_{\text{Buta}}:n_{\text{MeOH}} = 2:1$ |
| sCC$_4$ | $T_{\text{Reaktion}} = 70\ °C$<br>$n_{\text{Buta}}:n_{\text{Pd}} = 20000$<br>$n_{Lig}:n_{\text{Pd}} = 4:1$ bzw. $10:1$<br>$n_{\text{Buta}}:n_{\text{MeOH}} = 1:5$ | $T_{\text{Reaktion}} = 90\ °C$<br>$n_{\text{Buta}}:n_{\text{Pd}} = 20000$<br>$n_{Lig}:n_{\text{Pd}} = 1:1$<br>$n_{\text{Buta}}:n_{\text{MeOH}} = 1:2$ |

In Versuchen mit dem Pd-TPP Katalysator konnte gezeigt werden, dass die Reaktion sauerstoffempfindlich ist. Die Verwendung von technischem Methanol hingegen stellte kein Problem dar und hatte auch keinen Einfluss auf die erzielte Selektivität. Die beiden Katalysatorsysteme wiesen eine unterschiedliche Abhängigkeit von der Basenstärke auf. Der Pd-TPP Katalysator war kaum abhängig von der Basenstärke und konnte auch ohne den Einsatz einer Base aktiviert werden. Hingegen konnte der Pd-IMes Katalysator nur mit der starken Base Kaliummethanolat (KOMe) aktiviert werden. Mit allen anderen, schwächeren Basen zeigte das Pd-IMes System auch bei höheren Temperaturen und längeren Reaktionszeiten kaum Aktivität.

Der Pd-TPP Katalysator deaktivierte bei höheren Temperaturen (90 °C) und erwies sich somit als instabil. Die Bildung des Hauptproduktes nahm zu Gunsten des Nebenproduktes Octatrien ab. Bei einer Reaktionstemperatur von 50 °C wurde die Reaktionsgeschwindigkeit verlangsamt. Die Reaktionsgeschwindigkeit des Pd-IMes Katalysators stieg mit steigender Temperatur entsprechend dem Arrhenius Gesetz. Die Selektivitäten des Pd-IMes Systems blieben durch die Temperaturvariation unbeeinflusst.

Für beide Katalysatorsysteme führte eine Variation des Verhältnisses von Butadien zu Palladium mit steigender Palladiumkonzentration zu einer erhöhten

Reaktionsgeschwindigkeit. Die Selektivität von 1-Mode nahm ab, wobei verstärkt 3-Mode gebildet wurde.

Für das Pd-TPP System wurde mit Butadien ein optimales Verhältnis von Ligand zu Palladium von 4:1 gefunden. Mit $sCC_4$ zeigten die Verhältnisse 4:1 und 10:1 sehr ähnliche Umsatzverläufe. Die schlechteste Katalysatoraktivität stellte sich für beide Edukte bei einem Überschuss an Palladium ein. Diese Beobachtung stimmt mit der Literatur überein [95]. Phosphinbasierte Katalysatoren benötigen einen Ligandenüberschuss, um den Katalysator effizient stabilisieren zu können [95; 176]. Auch der Pd-IMes Katalysator zeigte die schlechteste Aktivität mit einem Überschuss an Katalysator. Mit reinem Butadien erreichte der IMes modifizierte Katalysator ein Optimum bei einem Verhältnis von 4:1, mit $sCC_4$ bei 1:1. Vollmüller *et al.* [95] berichteten eine starke Abhängigkeit der Selektivität zum einen vom Liganden und zum anderen vom Verhältnis Ligand zu Katalysator. Generell erreichte der Pd-IMes Katalysator deutlich höhere Selektivitäten zum Hauptprodukt (~ 97 %) als das Pd-TPP System (~ 85 %). Des Weiteren nahm die Selektivität zum Hauptprodukt für das TPP modifizierte System mit steigendem Verhältnis Ligand zu Katalysator ab, wobei verstärkt das *iso*-Telomer 3-Mode gebildet wurde. Aufgrund des großen sterischen Anspruchs des IMes-Liganden hatte die Variation des Ligand zu Katalysator Verhältnisses beim IMes modifizierten Katalysator keinen Einfluss auf die Selektivitäten [95].

Eine Variation des Verhältnisses von Butadien zu Methanol hatte im Bereich von 1:1 zu 1:3 kaum Einfluss auf den Pd-TPP Katalysator mit reinem Butadien. Ein Überschuss an Methanol führte zu einer Aktivierungsphase von ca.1,5 bis 2 Stunden, wohingegen ein stöchiometrisches Verhältnis (2:1) eine deutliche Abnahme der Aktivität verursachte. Ein deutlicher Trend wurde für den phosphinbasierten Katalysator in Kombination mit $sCC_4$ gefunden. Eine Zunahme der Methanolkonzentration hatte eine Zunahme der Reaktionsgeschwindigkeit zur Folge. Dies könnte durch die Verbesserung der Löslichkeit des Katalysatorkomplexes begründet werden. Für beide Edukte nahmen sowohl die Regio- als auch die Chemoselektivität mit steigender Methanolkonzentration zu. Dies wurde auch durch Vollmüller *et al.* [95] beobachtet. Mit reinem Butadien führte eine Steigerung der Butadienkonzentration beim IMes modifizierten Katalysator zu einer Steigerung der Aktivität, wohingegen mit $sCC_4$ ein Optimum bei einem Verhältnis von 1:2 erreicht wurde. Dies könnte durch einen gegenläufigen Effekt der abnehmenden

Katalysatorlöslichkeit und der zunehmenden Aktivität mit steigendem Butadienanteil begründet werden.

Basierend auf diesen Ergebnissen wurden in Zusammenarbeit mit dem SYNFLOW Partner RWTH Aachen kinetische Modelle für die beiden Katalysatorsysteme erstellt. Die Modellierung wurde auf Basis des Jolly Mechanismus durchgeführt. Hierbei wurden für das Pd-TPP System Reaktionsordnungen von 2 in Butadien und 1 in Methanol ermittelt. Die Herleitung eines kinetischen Modells für den Pd-IMes Katalysator war auf Basis des Jolly Mechanismus nicht möglich. Weitere kinetische Untersuchungen zeigten, dass der Pd-IMes Katalysator unabhängig von der Butadienkonzentration ist, allerdings eine starke Abhängigkeit von der Base sowie ein negativer Einfluss durch Methanol vorliegt. Dieser negative Einfluss des Methanols ist wahrscheinlich begründet im Einfluss des protischen Lösungsmittels auf die Nukleophilität der Base. Mit diesem Wissen konnte der Jolly Mechanismus angepasst und ein kinetisches Modell hergeleitet werden, welches die experimentellen Daten sehr gut wiedergibt.

Durch ein Screening verschiedener Katalysatorpräkursoren stellte sich der Präkursor Pd(acac)$_2$ als aktivster Katalysator heraus. Neben diesem in-situ Katalysatorscreening wurden auch ex-situ generierte NHC-Katalysatoren getestet. Hier zeigte sich, dass eine Erhöhung des sterischen Anspruchs des NHC-Liganden eine Erniedrigung der Aktivität zur Folge hatte, was ebenfalls literaturbekannt ist [177]. Des Weiteren konnte gezeigt werden, dass die charakteristische Kinetik des IMes-Liganden auch für die untersuchten NHC-Liganden gilt.

Die Inbetriebnahme des Schlaufenreaktors erfolgte durch den Transfer der einphasigen Experimente. Hierbei wurde eine geringe Erhöhung der Reaktionsgeschwindigkeit aller Systeme beobachtet. Dies konnte durch die bessere Wärmezufuhr und den besseren Ausgleich der Wärmeverluste im Schlaufenreaktor begründet werden. Erste kontinuierliche Experimente ohne Katalysatorrezyklierung bei drei verschiedenen Verweilzeiten zeigten eine Anfahrphase von ca. 3 Stunden. Anschließend wurde ein stationäres Verhalten erreicht, wobei der stationär erreichte Umsatz mit steigender Verweilzeit stieg.

Für die Anwendung eines zweiphasigen Reaktionssystems als Immobilisierungskonzept ist die Wahl der Katalysatorphase wichtig. Diese sollte eine gute Extraktionseigenschaft für die entstehenden Produkte aufweisen. Um eine Vorauswahl der ionischen Flüssigkeit zu treffen, wurde ein Screening von 960

verschiedenen Anion-Kation Kombinationen mit Hilfe der computerbasierten Methode COSMO-RS durchgeführt. Die vorhergesagten Trends der Extraktionseigenschaften wurden im Anschluss mit 9 ionischen Flüssigkeiten erfolgreich validiert.

Neben der Extraktionseffizienz einer ionischen Flüssigkeit sollte diese keinen negativen Einfluss auf die katalysierte Reaktion aufweisen. Um den Einfluss auf die Aktivität zu testen, wurden 8 ionische Flüssigkeiten mit verschiedenen Liganden untersucht. Hierbei wurde beobachtet, dass die Extraktionseffizienz und der Einfluss auf die Aktivität unabhängig waren. Da die mit den Liganden TPP und IMes modifizierten Katalysatorkomplexe keine ionischen Gruppen aufweisen, war der Immobilisierungseffekt der ionischen Flüssigkeit nicht ausreichend. Deshalb wurden auch sulfonierte Phosphinliganden, TPPMS, TPPTS und [BMMIM]-TPPMS, getestet. Die Aktivitäten der phosphinbasierten Liganden waren sehr ähnlich, allerdings unterschieden sie sich stark in ihrer Immobilisierungseffektivität. Hierbei wies der dreifach sulfonierte Ligand (TPPTS) einen mindestens 4-fach kleineren Wert für den Palladiumaustrag auf als der einfach sulfonierte Ligand (TPPMS). Die aktivsten Systeme mit den sulfonierten Liganden wurden mit den ionischen Flüssigkeiten [EMMIM][TOS], [EMMIM][NTf$_2$], [BMMIM][NTf$_2$] und [BMMIM][BF$_4$] erreicht.

Die Katalysatorstabilität wurde mit Hilfe von Rezyklierstudien untersucht. Drei ionische Flüssigkeiten, basierend auf den Anionen [TOS], [NTf$_2$] und [BF$_4$], wurden untersucht, wobei nur die [NTf$_2$]-basierte ionische Flüssigkeit bei Raumtemperatur und in reiner Form flüssig vorlag. Mit allen drei ionischen Flüssigkeiten konnte in der ersten Rezyklierung der Umsatz des ursprünglichen Startexperiments wieder erreicht werden. Nach dem ursprünglichen Experiment und der ersten Rezyklierung (Versuchsdauer jeweils 3 Stunden) musste die Katalysatorphase über Nacht aufbewahrt werden. Dies wurde unter Argonatmosphäre im Autoklaven durchgeführt. Nichtsdestotrotz scheint der Katalysator über Nacht seine Aktivität verloren zu haben, da zwei weitere Rezyklierversuche nicht erfolgreich waren. Die Katalysatordeaktivierung könnte dadurch begründet werden, dass entweder Sauerstoffspuren nicht vermieden werden konnten oder das Ablassen des Butadiens die aktive Spezies, in der Butadien koordiniert ist, zerstört hat. Diese genannten Ursachen könnten in einem kontinuierlichen Prozess vermieden werden.

Für den Transfer zum kontinuierlichen Betrieb wurde der TPPMS modifizierte Katalysator und die ionische Flüssigkeit [BMMIM][NTf$_2$] verwendet. Der darauf

folgende Optimierungsprozess wurde schrittweise durchgeführt und ist in Abbildung 1 zusammengefasst.
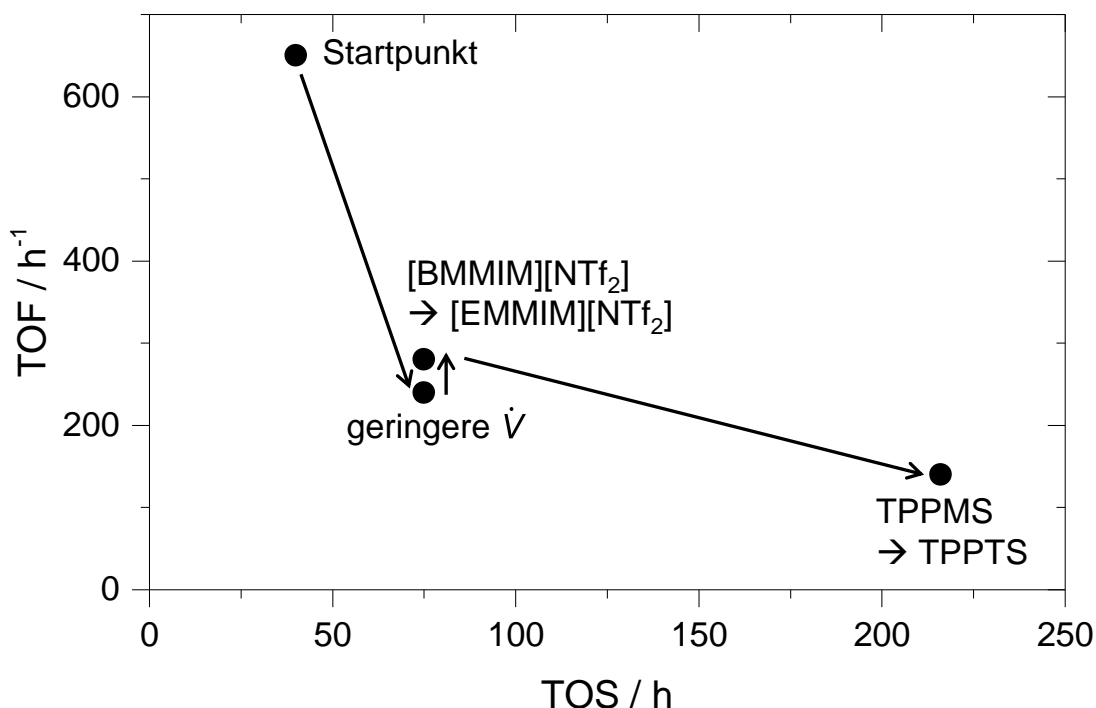


**Abbildung 1: Schrittweise Optimierung des kontinuierlichen Prozesses.**

Auch im Schlaufenreaktor konnte gezeigt werden, dass ein stöchiometrisches Verhältnis der Edukte (Butadien:MeOH = 2:1) notwendig ist, um die Menge an Methanol im System gering zu halten und somit den Katalysatoraustrag zu verringern. Ein kontinuierlicher Versuch mit einem Verhältnis von 1:1 führte zu einem starken Abfall des Umsatzes von 80 auf 15 % innerhalb von 20 Stunden. Durch die Verwendung eines stöchiometrischen Verhältnisses der Edukte konnte die Stabilität des Reaktionssystems auf 47 Stunden Laufzeit gesteigert werden. Während dieser Zeit fiel der Umsatz von 80 auf 20 % ab. Die Werte für den Palladiumaustrag lagen zwischen 1000 und 2400 ppm pro Stunde. Auch die TOF sank von 650 auf 200 h$^{-1}$. Die erzielten Selektivitäten lagen bei 80 % für 1-Mode, 5 % für 3-Mode, 12 % für Octatrien und 3 % für Vinylcyclohexen und waren vergleichbar mit den zweiphasigen Batch-Versuchen.

Eine weitere Steigerung der Stabilität konnte durch die Verringerung der Eduktströme erzielt werden. Der maximal erreichte Umsatz stieg auf 93 % und der

Umsatz bei einer Reaktionslaufzeit von 72 Stunden betrug noch 70 %. Diese Verbesserung konnte durch den geringeren Palladiumaustrag aufgrund der geringeren Volumenströme und des höheren Methanolumsatzes begründet werden. Die Selektivitäten blieben durch die Veränderung der Ströme unverändert und waren vergleichbar mit dem vorhergehenden kontinuierlichen Versuch. Aufgrund der geringeren Volumenströme war die Aktivität mit einer maximalen TOF von 260 $h^{-1}$ deutlich geringer.

Die Experimente im Autoklaven zeigten für die ionische Flüssigkeit [EMMIM][NTf$_2$] eine geringfügig bessere Immobilisierungseffizienz sowie Aktivität verglichen mit [BMMIM][NTf$_2$]. Ein Vergleich im kontinuierlichen Prozess konnte nur die etwas höhere Aktivität (5 % höherer Umsatzverlauf) bestätigen. Die ICP Messungen zeigten zwar einen geringeren Pd Austrag, eine bessere Immobilisierungseffizienz und somit ein stabileres Reaktionssystem wurden allerdings nicht beobachtet. Die Selektivitäten waren unbeeinflusst von der Variation der ionischen Flüssigkeit.

Der effizienteste Optimierungsschritt war die Variation des Liganden von TPPMS auf TPPTS. Obwohl die Aktivität deutlich geringer war als mit TPPMS, konnte mit dem TPPTS modifizierten Katalysatorsystem ein langzeitstabiles System entwickelt werden. Der maximale Umsatz von 45 % war ca. 200 Stunden konstant. Im Anschluss nahm der Umsatz leicht ab und erreichte nach 216 Stunden 40 %. Diese Abnahme konnte durch die beginnende Deaktivierung des phosphinbasierten Katalysator als auch den geringfügigen Katalysatoraustrag von 100 bis 200 ppm·$h^{-1}$ begründet werden. Im konstanten Bereich der Reaktion wurde eine TOF zwischen 120 und 140 $h^{-1}$ erreicht. Trotz der geringen Aktivität wurden während diesem Versuch 1,5 kg 1-Mode gebildet und eine TON von 25000 erreicht. Die Selektivitäten waren vergleichbar zu den vorhergehenden kontinuierlichen Versuchen.

Weitere Optimierungsansätze wie die Erhöhung der Reaktionstemperatur, Variation der Umlaufgeschwindigkeit oder Erhöhung der Menge an ionischer Flüssigkeit zeigten keine Verbesserungen des Prozesses.

Das Ziel dieser Arbeit einen kontinuierlichen Prozess für die Telomerisation von Butadien mit Methanol zu entwickeln wurde auf Basis eines zweiphasigen Reaktionssystems mit ionischen Flüssigkeiten erfolgreich erreicht.

# 7  Appendix

## 7.1  Chemicals

The chemicals used within this work are listed in Table A 1. If not noted otherwise, all chemicals were used without further purification. The applied ionic liquids are specified in Table A 2.

**Table A 1: Used chemicals for experiments and analysis.**

| Application | Chemical | Origin | Purity |
|---|---|---|---|
| reactant | 1,3-butadiene | Linde AG | > 99.9 % |
| reactant | synthetic crack-$C_4$ | Evonik | - |
| reactant/solvent | methanol | Merck KGaH | ≥ 99.9 % |
| reactant/solvent | methanol | VWR Int. GmbH | ≥ 99.9 % |
| catalyst precursor | palladium(II) acetylacetonate | Merck KGaH | ≥ 98.0 % |
| catalyst precursor | palladium(II) acetate | Merck KGaH | ≥ 98.0 % |
| catalyst precursor | palladium(π-cinnamyl) chloride dimer | Sigma Aldrich | ≥ 97.0 % |
| ligand | triphenylphosphine | Merck KGaH | ≥ 99.0 % |
| ligand | 1,3-dimesityl-imidazol-3-ium methanesulfonate | Evonik | ≥ 95.0 % |
| ligand | sodium triphenylphosphine monosulfonate | TCI GmbH | ≥ 90.0 % |
| ligand | sodium triphenylphosphine trisulfonate | Strem Chemicals | ≥ 85.0 % |
| base | potassium methoxide 30-35 % solution in methanol | Merck KGaH | ≥ 99.9 % |
| base | triethylamine | Merck KGaH | ≥ 99.0 % |
| base | methylimidazole | Sigma Aldrich | ≥ 99.0 % |
| internal standard | di-*n*-butylether | Merck KGaH | ≥ 99.0 % |
| solvent | toluene | VWR Int. GmbH | ≥ 98.0 % |
| solvent | hexane | Merck KGaH | ≥ 98.0 % |

| solvent | hexane | | VWR Int. GmbH | ≥ 99.0 % |
|---|---|---|---|---|
| solvent | *o*-xylene | | VWR Int. GmBH | ≥ 99.0 % |
| $C_4$ component | 1-butene | | Linde AG | ≥ 99.5 % |
| $C_4$ component | *iso*-butene | | Linde AG | ≥ 99.5 % |
| NMR solvent | chloroform-$d_1$ | | Deutero GmbH | ≥ 99.8 % |
| NMR solvent | methanol-$d_1$ | | Deutero GmbH | ≥ 99.8 % |
| inert gas | argon 4.6 | | Linde AG | ≥ 99.9 % |

**Table A 2: Used ionic liquids.**

| Ionic liquid | Origin | Purity |
|---|---|---|
| [BMMIM][BF$_4$] | IoLiTec GmbH | ≥ 99,0 % |
| [EMMIM][BF$_4$] | Merck KGaH | - |
| [BMMIM]Cl | Solvent Innovation | ≥ 99,0 % |
| [EMMIM]Cl | Merck KGaH | - |
| [EMMIM][MeSO$_4$] | Merck KGaH | - |
| [BMMIM][NTf$_2$] | IoLiTec GmbH | ≥ 99,0 % |
| [EMMIM][NTf$_2$] | IoLiTec GmbH | ≥ 99,0 % |
| [BMMIM][OcSO$_4$] | Merck KGaH | - |
| [EMMIM][TOS] | Merck KGaH | - |

## 7.2 Characterization of [BMMIM]-TPPMS

NMR spectra were measured with a JEOL ECX + 400 spectrometer ([1]H: 400 MHz, [13]C: 100 MHz, [31]P: 162 MHz) with DMSO-D$_6$ as solvent. The listed data present the chemical shifts which are given in parts per million (ppm).

### 1-Butyl-2,3-dimethylimidazolium Diphenyl(3-sulfonatophenyl)phosphine ([BMMIM]-TPPMS)

^{1}H-NMR (400MHz, DMSO-D$_6$, [ppm]) δ = 0.84 (3H, t, -C$_3$H$_6$-$CH_3$), 1.16-1.30 (2H, m, -C$_2$H$_4$-$CH_2$-CH$_3$), 1.55-1.74 (2H, m, -CH$_2$-$CH_2$-C$_2$H$_5$), 2.52 (3H, s, N-C($CH_3$)-N), 3.69 (3H, s, N-$CH_3$), 4.00-4.11 (2H, m, -$CH_2$-C$_3$H$_7$), 7.10-7.52 (14H, m, -$Ph_2$PC$_6$$H_4$SO$_3$), 7.53-7.63 (2H, m, N-$CH=CH$-N).

^{13}C-NMR (100MHz, DMSO-D$_6$, [ppm]) δ = 10.0 (-C$_3$H$_6$-$CH_3$), 10.3 (-N-C($CH_3$)-N), 19.3 (N-C$_2$H$_4$-$CH_2$-CH$_3$), 31.5 (N-CH$_2$-$CH_2$-C$_2$H$_5$), 34.5 (N-CH$_3$), 48.8 (N-$CH_2$-C$_3$H$_7$), 121.2 (N-$CH=$CH-N), 124.1 (N-CH=$CH$-N), 126.8 (p-C$_6$H$_4$SO$_3$), 127.0 (m-C$_6$H$_5$), 128.8 (C$_6$H$_4$SO$_3$), 129.1 ( p-C$_6$H$_5$), 131.8 (o-$C$CSO$_3$), 133.7 (o-C$_6$H$_5$), 133.9 (o-C$_6$H$_4$SO$_3$), 137.1 (ipso-C$_6$H$_4$SO$_3$), 138.6 (ipso-C$_6$H$_5$), 143.3 (N-C-N), 147.4 (CSO$_3$).

^{31}P-NMR (162MHz, DMSO-D$_6$, [ppm]) δ = -5.73 ($P$(Ph$_2$)(PhSO$_3$)).

## 7.3 Formula and definitions

The offline as well as the inline GC were calibrated with the internal standard dibutylether. With the knowledge of the exact mass of dibutylether in the reaction, the masses of all other components could be determined according to Equation (10).

$$m_i = \frac{A_i \cdot m_{STD}}{A_{STD}} \cdot C_i \qquad (10)$$

Here, $m_i$ and $m_{STD}$ are masses of the component $i$ and the internal standard, $A_i$ and $A_{STD}$ are the corresponding peak areas and $C_i$ is the correction factor determined by calibration.

Within this work, conversion, yield and selectivity were all referred, if not mentioned otherwise, to the reactant butadiene.

The conversion $X_i$ (see Equation (11)) describes the amount of converted reactant $n_i$ related to the used amount of reactant $n_{i0}$ at the start of reaction.

$$X_i = \frac{n_{i0} - n_i}{n_{i0}} \tag{11}$$

The yield $Y_p$ (see Equation (12)) represents the amount of formed product related to the used amount of reactant $n_{i0}$ at the start of reaction and the stoichiometric coefficients $\vartheta_i$ and $\vartheta_p$.

$$Y_p = \frac{n_p - n_{p0}}{n_{i0}} \cdot \frac{\vartheta_i}{\vartheta_p} \tag{12}$$

The selectivity $S_{ip}$ (see Equation (13)) describes the amount of reactant $i$ that has been converted to the desired product $p$.

$$S_{pi} = \frac{n_p - n_{p0}}{n_{i0} - n_i} \cdot \frac{\vartheta_i}{\vartheta_p} \tag{13}$$

Within this work, also the chemo- and regioselectivity are important.

The chemoselectivity $S_c$ (see Equation (14)) describes the amount of butadiene that has been converted to either 1-Mode or 3-Mode.

$$S_c = \frac{Y_{\text{1-Mode}} + Y_{\text{3-Mode}}}{X_{\text{butadiene}}} \tag{14}$$

Regioisomerism is a form of constitutional isomerism. In the telomerization of butadiene with methanol, regioisomers are formed by the attack of the methoxide anion which can occur in C1 or C3 position. In this work, regioselectivity describes the ratio of *n*-telomer (1-Mode) to *iso*-telomer (3-Mode) according to Equation (15).

$$n{:}iso = \frac{Y_{\text{1-Mode}}\,Y_{\text{3-Mode}}}{Y_{\text{3-Mode}}} \tag{15}$$

The turn over number (*TON*, see Equation (16)) describes the amount of converted reactant molecules per catalyst molecule and quantifies the catalyst stability.

$$TON = \frac{n_{\text{butadiene,0}} - n_{\text{butadiene}}}{n_{\text{Pd}}} \tag{16}$$

The turnover frequency (*TOF*, see Equation (17)) represents the amount of converted reactant molecules per palladium molecule and reaction time and quantifies the catalyst activity.

$$TOF = \frac{n_{\text{butadiene,0}} - n_{\text{butadiene}}}{n_{\text{Pd}} \cdot t} \tag{17}$$

The space time yield (*STY*, see Equation (18)) describes the amount of formed product per time and reaction volume.

$$STY = \frac{n_p - n_{p0}}{V_{\text{reactor}} \cdot t} \tag{18}$$

Due to the degassing of butadiene during sampling, all samples which were analyzed with the offline GC only contained information on the product composition. Thus, the amount of converted butadiene was calculated by the amount of all formed products according to Equation (19).

$$n_{\text{butadiene}} = 2 \cdot \sum n_p \tag{19}$$

For the characterization of the newly built loop reactor, also the residence time distribution was determined. In the following, the equations used in this thesis are introduced in detail. For further information, refer to [1; 183; 184].

The exit age distribution $E(t)$ describes the distribution of the volume elements which left the reactor at the time $t$ and is defined by Equation (20).

$$E(t) = \frac{\dot{n}(t)}{n_0} = \frac{\dot{V} \cdot c(t)}{\int_0^\infty \dot{V} \cdot c(t) dt} = \frac{c(t)}{\int_0^\infty c(t) dt} \qquad (20)$$

The integration of $E(t)$ over time results in the sum of all volume elements which left the reactor at time $t$, see Equation (21).

$$F(t) = \int_0^t E(t) dt \qquad (21)$$

For comparison of different experiments, the dimensionless time $\theta$ is defined according to Equation (22).

$$\theta = \frac{t}{\tau} \text{ respectively } \theta = \frac{t}{\bar{t}} \qquad (22)$$

The residence time $\tau$ describes the ideal case, for real cases the effective residence time $\bar{t}$ the real cases applied and can be calculated according to Equation (23) for $E(t)$ and Equation (24) for $F(t)$.

$$\bar{t} \approx \frac{\sum_i t_i \cdot c_i \cdot \Delta t_i}{\sum_i c_i \cdot \Delta t_i} \qquad (23)$$

$$\bar{t} \approx \sum_i (1 - F_i) \cdot \Delta t_i \qquad (24)$$

$E(t)$ and $F(t)$ can be expressed with the dimensionless time $\theta$.

$$E(t) = \frac{1}{\tau} E(\theta) \text{ and } F(t) = F(\theta) \qquad (25)$$

The residence time distribution can experimentally be determined by either a pulse or a step experiment. For a pulse experiment, a defined small amount of a concentrated tracer is added instantaneously to the inlet stream and the concentration of this tracer is recorded in the exit stream resulting in the exit age distribution $E(t)$. For a step experiment, the inlet stream is marked with a tracer and permanently fed to the reactor. The concentration is again determined in the outlet stream and normalized to the concentration $c_0$. The step experiment results in the summation function $F(t)$.

In this thesis, the determination of the residence time was carried out with a step experiment. The reactor was filled with ethanol and replaced by dibutylether. The concentration change was recorded by GC samples. The summation function can be expressed according to Equation (26).

$$F(\theta) = 1 - \exp(-\theta) \tag{26}$$

The residence time $\tau$ can be determined graphically using the summation function $F(t)$ by Equation (27).

$$\tau = \int_0^1 t\, dF(t) \tag{27}$$

## 7.4 Additional results of NIR spectroscopy



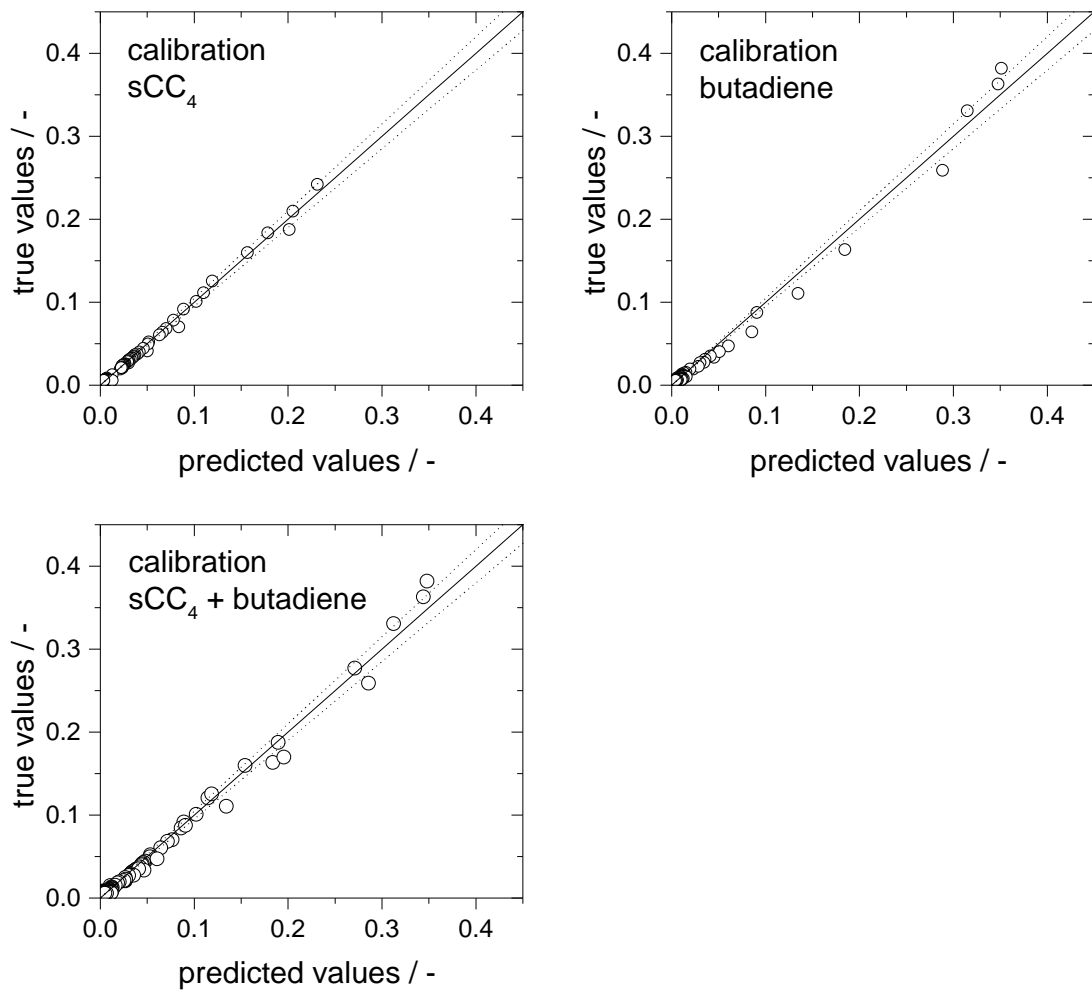**Figure A 1: Validation of the NIR calibration models for 1-Mode with the spectra of the test set presented in true-predicted plots (○ 1,3-butadiene, ― bisecting line, --- 5 % deviation).**

**Figure A 2: Additional validation of the calibration models determining the mass fraction of methanol using independently conducted experiments for the Pd-IMes system with sCC$_4$ (▲ NIR, ○ GC).**

**Figure A 3: Additional validation of the calibration models determining the mass fraction of 1-Mode using independently conducted experiments for the Pd-TPP system with sCC$_4$ (▲ NIR, ○ GC).**

**Figure A 4: Additional validation of the calibration models determining the mass fraction of 3-Mode using independently conducted experiments for the Pd-TPP system with sCC$_4$ (▲ NIR, ○ GC).**
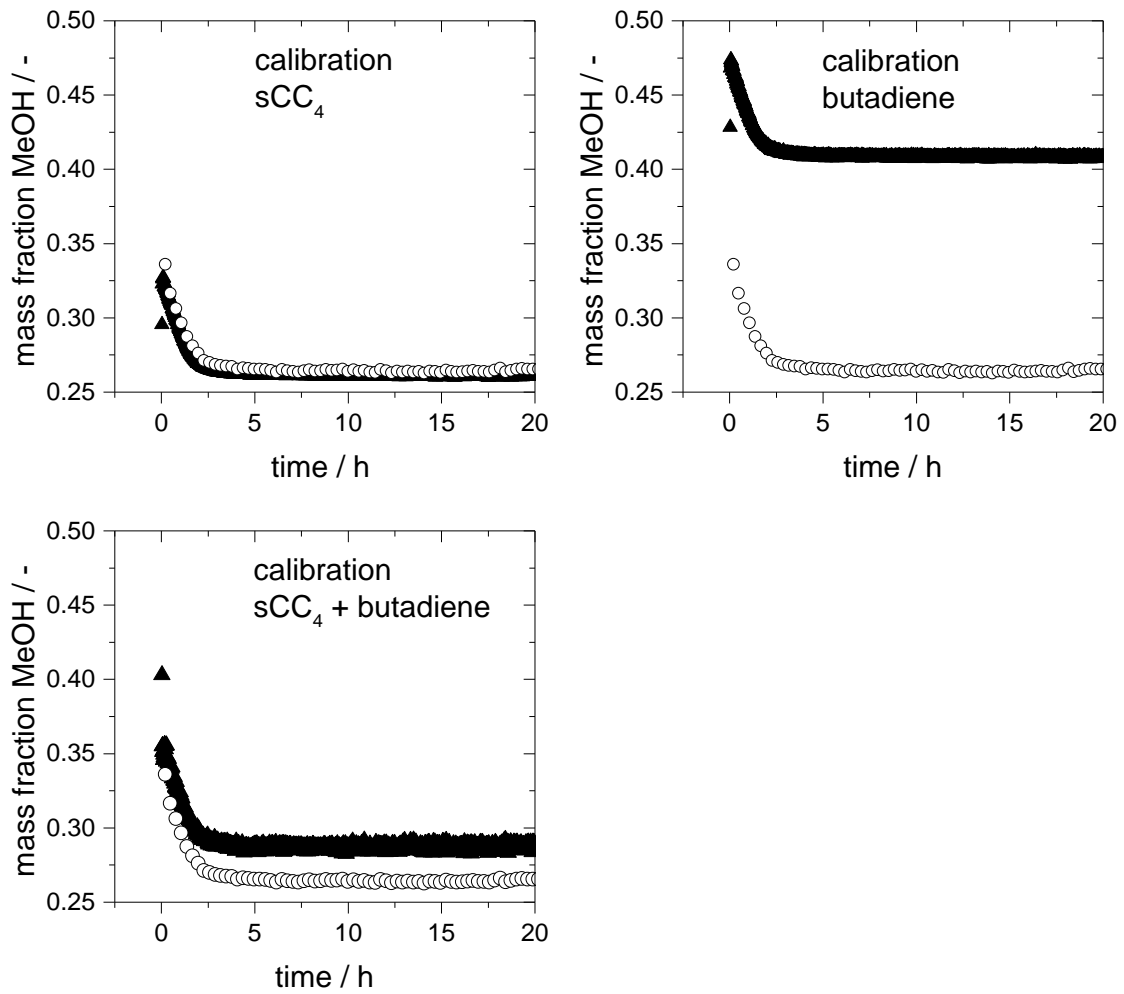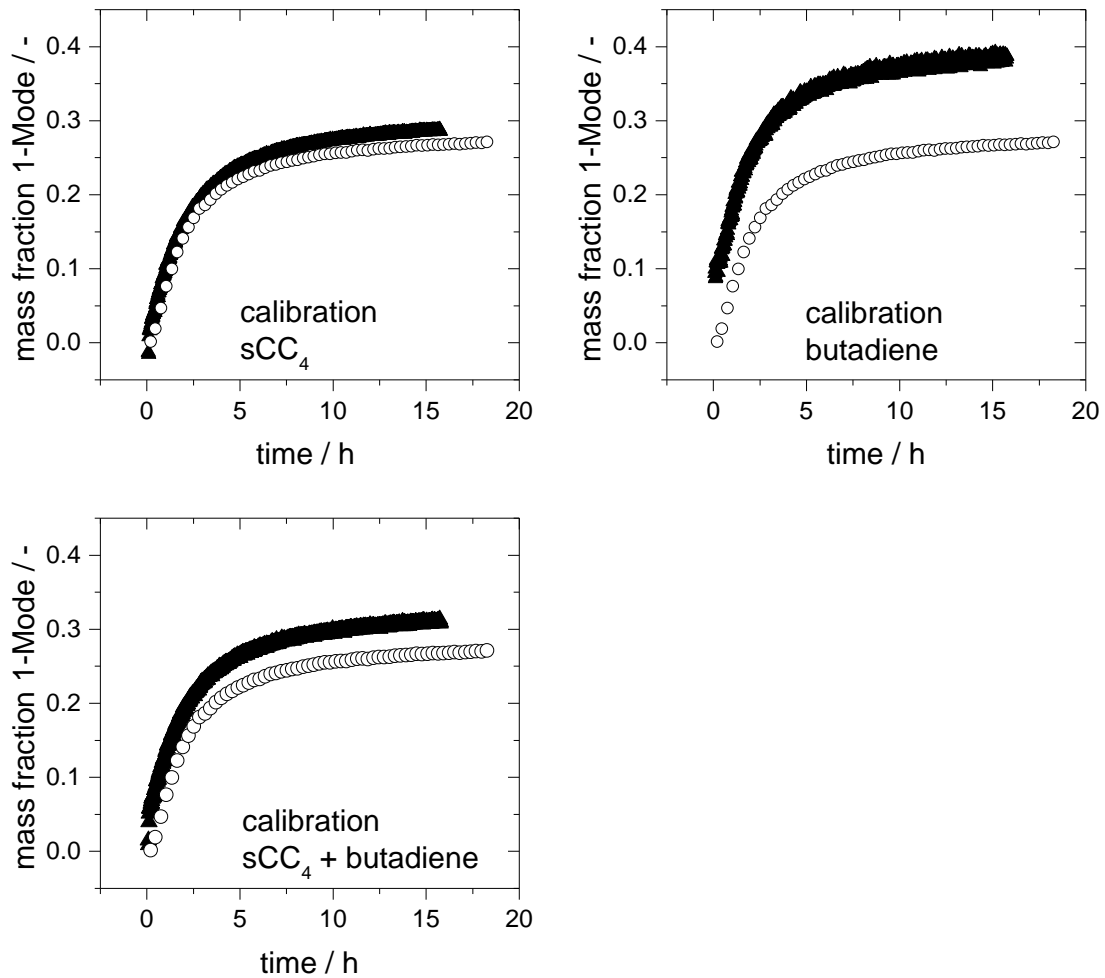
**Figure A 5: Additional validation of the calibration models determining the mass fraction of methanol using independently conducted experiments for the Pd-TPP system with sCC$_4$ (▲ NIR, ○ GC).**
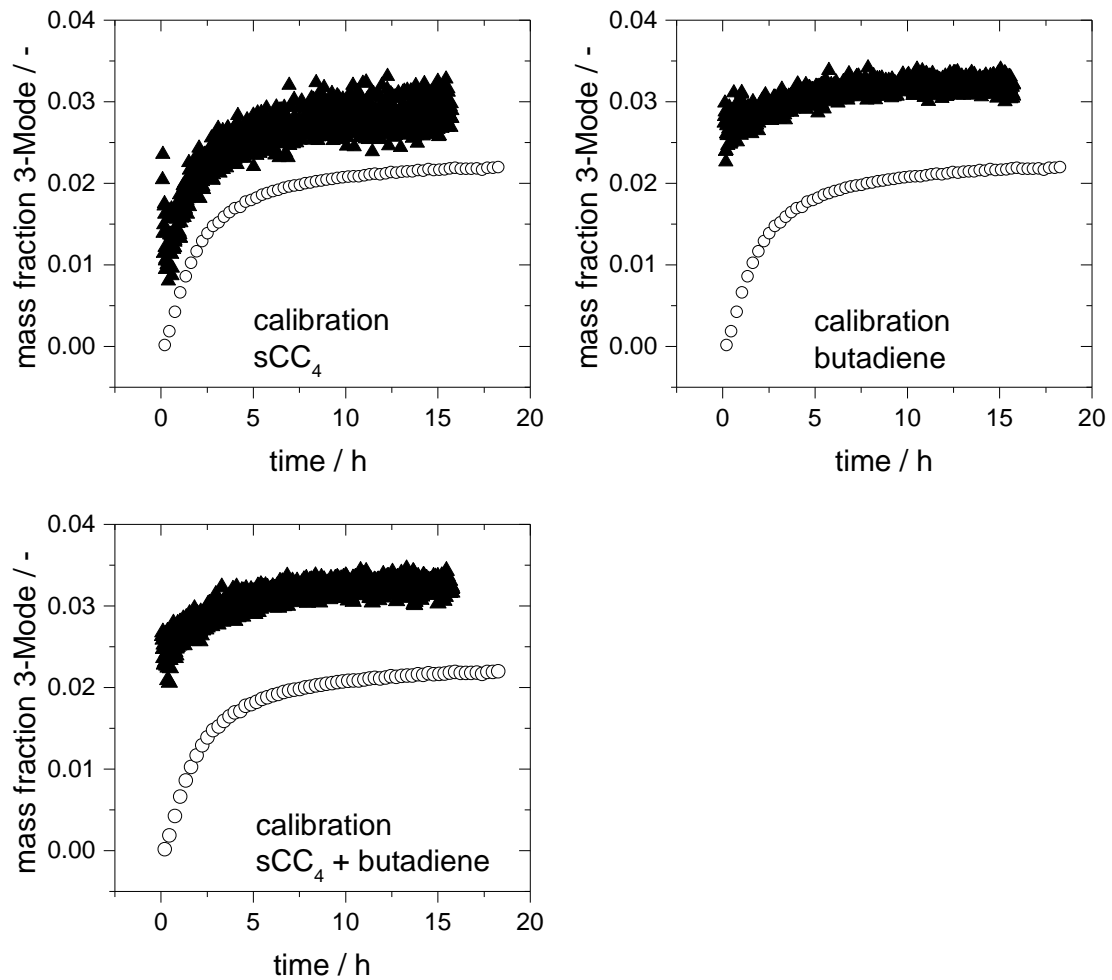
**Figure A 6: Additional validation of the calibration models determining the mass fraction of 1,3-butadiene using independently conducted experiments for the Pd-TPP system with sCC$_4$ (▲ NIR, ○ GC).**
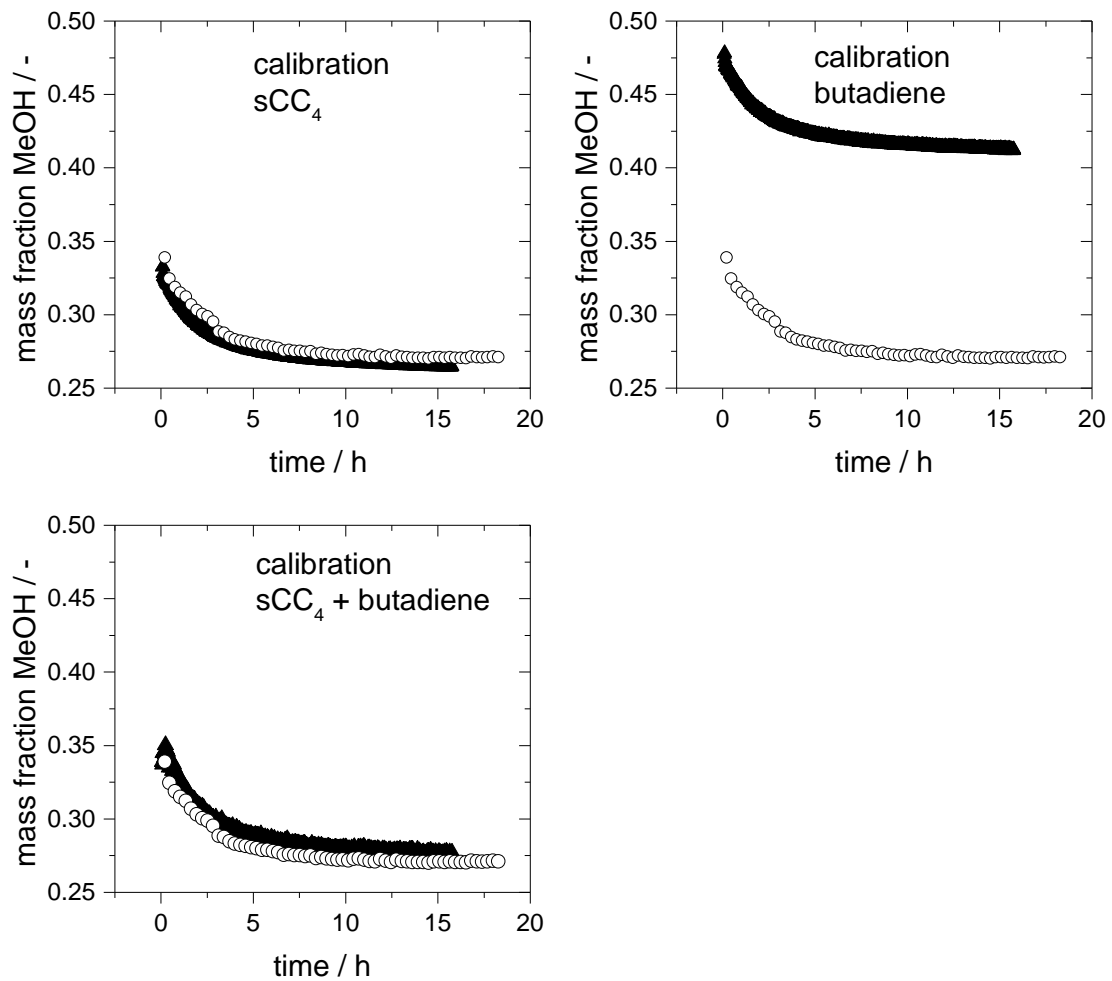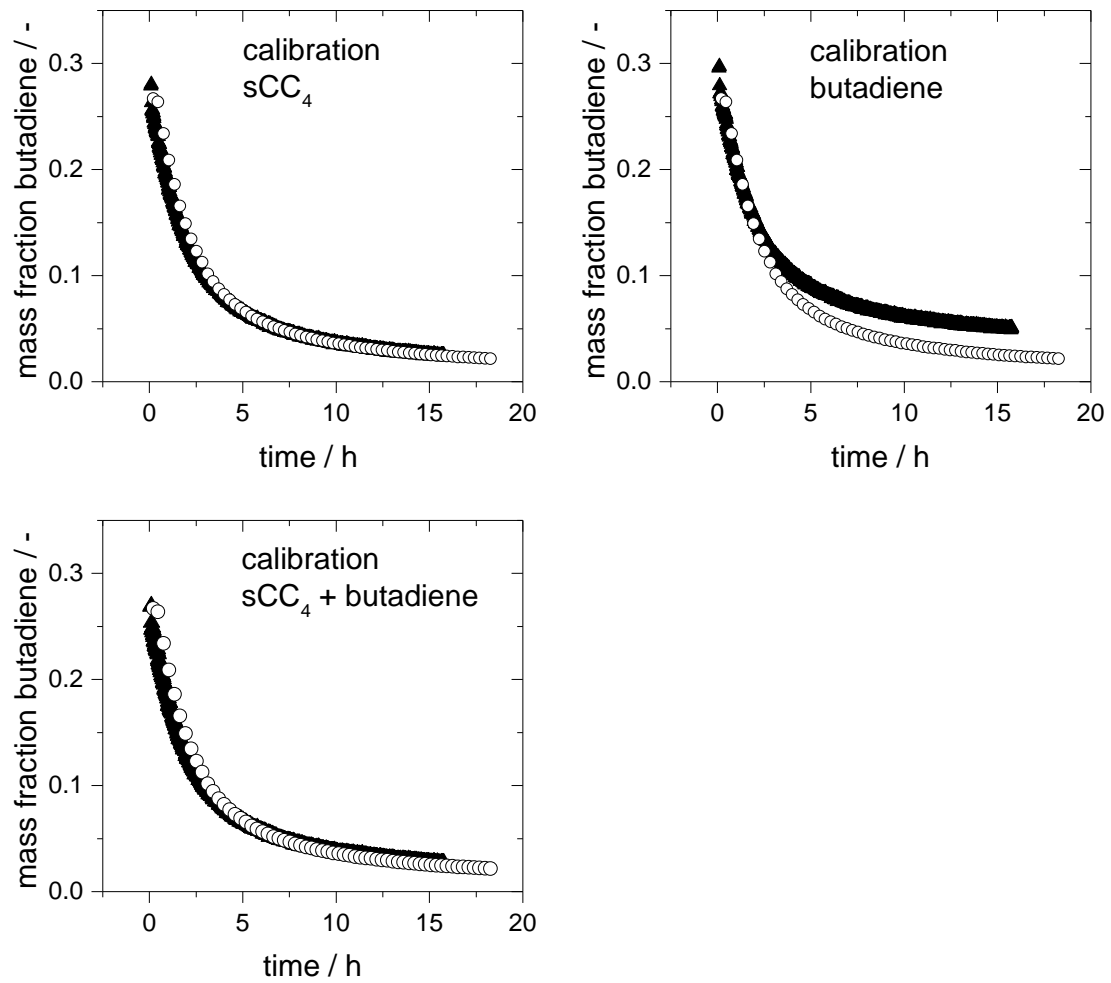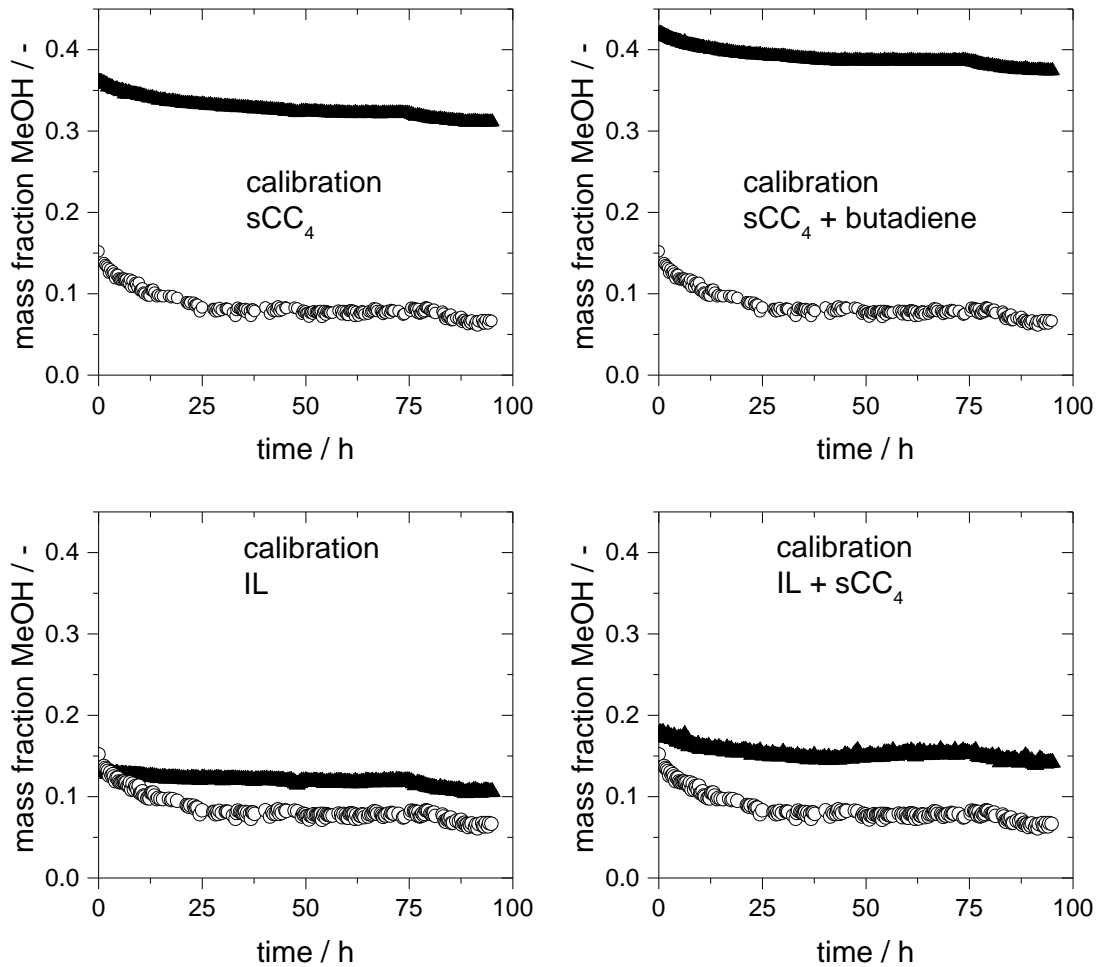
**Figure A 7: Comparison of the mass fractions obtained for methanol by GC analysis and four different NIR calibration models for a continuous experiment biphasic experiment with ionic liquid (▲ NIR, ○ GC).**

## 7.5   Selectivities for the variation of the molar ratio of the reactants

**Table A 3: Results at different molar ratios of butadiene to MeOH for the TPP modified and the IMes modified catalysts with butadiene and sCC$_4$ after 6 h.**

| ratio butadiene:MeOH | ligand | feed | $X$ / % | $S_1$ / % | $S_2$ / % | $S_3$ / % | $S_{1+2}$ / % | $n$:$iso$ |
|---|---|---|---|---|---|---|---|---|
| 2:1 | TPP | butadiene | 58.6 | 74.1 | 8.9 | 14.7 | 83.0 | 8.3 |
| 1:1 | TPP | butadiene | 83.6 | 84.0 | 9.2 | 6.5 | 93.2 | 9.1 |
| 1:1.5 | TPP | butadiene | 86.8 | 86.4 | 8.8 | 4.4 | 95.2 | 9.8 |
| 1:2 | TPP | butadiene | 88.0 | 88.3 | 7.8 | 3.5 | 96.0 | 11.3 |
| 1:2.5 | TPP | butadiene | 89.6 | 89.4 | 6.9 | 3.1 | 96.3 | 12.9 |
| 1:3 | TPP | butadiene | 84.1 | 90.4 | 6.6 | 2.6 | 97.0 | 13.7 |
| 1:5 | TPP | butadiene | 86.7 | 89.2 | 7.0 | 2.9 | 96.2 | 12.8 |
| 2:1 | TPP | sCC$_4$ | 14.0 | 60.6 | 5.0 | 31.7 | 65.6 | 12.1 |
| 1:1 | TPP | sCC$_4$ | 31.2 | 78.7 | 6.0 | 14.6 | 84.7 | 13.2 |
| 1:1.5 | TPP | sCC$_4$ | 54.3 | 81.4 | 5.8 | 9.1 | 87.2 | 14.0 |
| 1:2 | TPP | sCC$_4$ | 58.4 | 85.0 | 5.8 | 7.6 | 90.8 | 14.5 |
| 1:2.5 | TPP | sCC$_4$ | 63.0 | 88.5 | 5.2 | 6.1 | 93.7 | 16.9 |
| 1:3 | TPP | sCC$_4$ | 63.5 | 88.5 | 5.1 | 5.5 | 93.6 | 17.3 |
| 1:5 | TPP | sCC$_4$ | 76.9 | 91.9 | 4.2 | 3.8 | 96.1 | 22.1 |
| 2:1 | IMes | butadiene | 100 | 90.9 | 2.7 | 5.3 | 93.7 | 33.4 |
| 1:1 | IMes | butadiene | 95.9 | 97.4 | 1.6 | 0.4 | 99.0 | 62.0 |
| 1:1.5 | IMes | butadiene | 97.5 | 97.7 | 1.6 | 0.3 | 99.3 | 62.8 |
| 1:2 | IMes | butadiene | 90.4 | 97.7 | 1.5 | 0.3 | 99.3 | 63.1 |
| 1:2.5 | IMes | butadiene | 69.3 | 97.5 | 1.5 | 0.3 | 99.0 | 64.4 |
| 1:3 | IMes | butadiene | 44.6 | 96.2 | 1.5 | 0.3 | 97.7 | 63.2 |
| 1:5 | IMes | butadiene | 19.9 | 97.8 | 1.6 | 0.4 | 99.4 | 60.5 |
| 2:1 | IMes | sCC$_4$ | 84.8 | 95.2 | 2.0 | 2.7 | 97.2 | 47.4 |
| 1:1 | IMes | sCC$_4$ | 95.7 | 97.5 | 1.6 | 0.5 | 99.2 | 60.6 |
| 1:1.5 | IMes | sCC$_4$ | 96.8 | 97.1 | 1.6 | 0.3 | 98.7 | 62.6 |
| 1:2 | IMes | sCC$_4$ | 98.4 | 97.9 | 1.5 | 0.3 | 99.3 | 67.5 |
| 1:2.5 | IMes | sCC$_4$ | 94.3 | 98.0 | 1.5 | 0.3 | 99.5 | 67.2 |
| 1:3 | IMes | sCC$_4$ | 93.3 | 97.6 | 1.5 | 0.3 | 99.1 | 65.6 |
| 1:5 | IMes | sCC$_4$ | 65.3 | 98.2 | 1.5 | 0.3 | 99.7 | 67.0 |

## 7.6   Activation of phosphine-based catalysts without ionic liquids



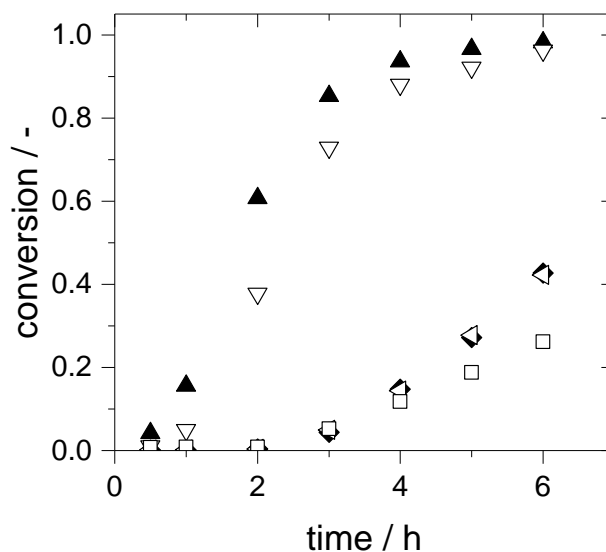**Figure A 8: Obtained conversion for different phosphine-based catalysts with NEt$_3$ as base and without base in the telomerization with pure butadiene (▲ TPP with NEt$_3$, ▽ TPP without base, ◆ TPPMS with NEt$_3$, ◁ TPPMS without base, □ TPPTS with NEt$_3$).**

*Reaction conditions: 70 °C, 15 bar, $n_{butadiene}$:$n_{MeOH}$ = 0.5, $n_{butadiene}$:$n_{Pd}$ = 40,000, $n_{Lig}$:$n_{Pd}$ = 4, $n_{butadiene}$:$n_{NEt3}$ = 300.*

## 7.7 Ionic liquid screening with the ligands TPPTS and [BMMIM]-TPPMS
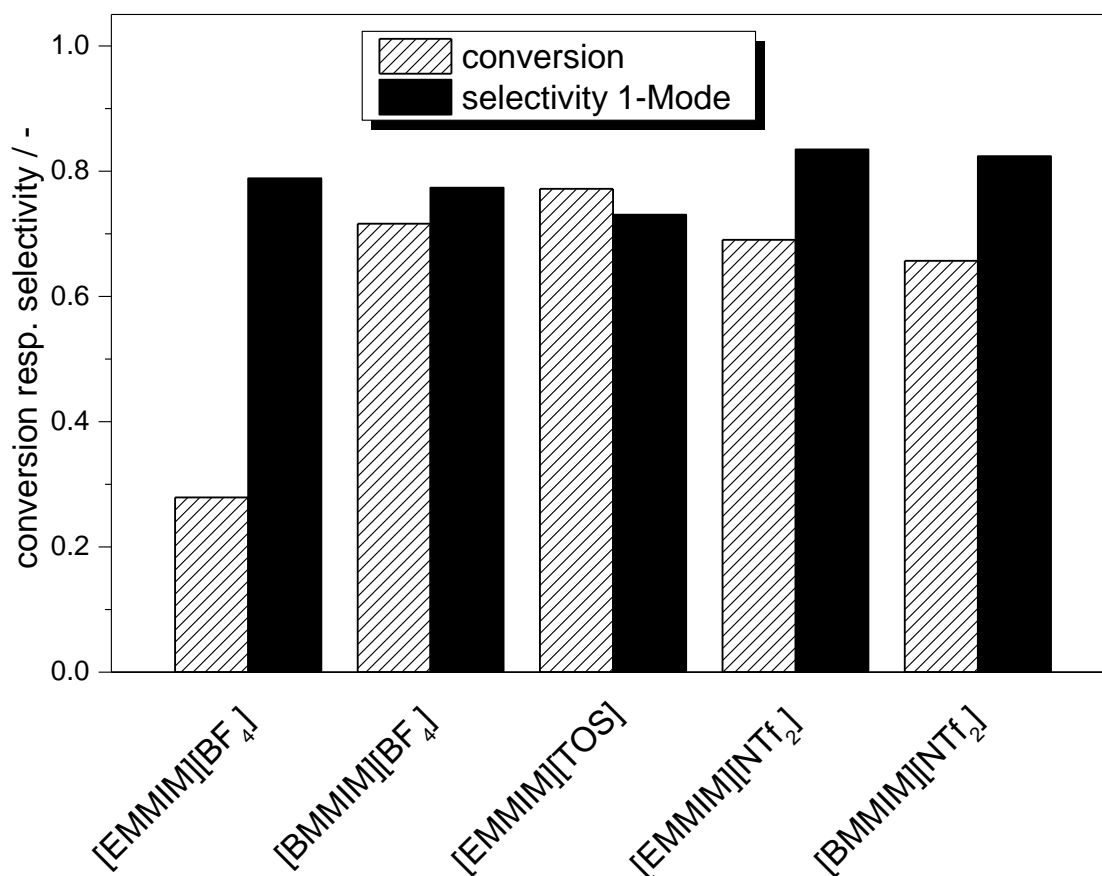


**Figure A 9: Obtained conversion and selectivity toward 1-Mode for the screening of different ionic liquids with the TPPTS modified catalyst and pure butadiene.**

*Reaction conditions: 70 °C, 15 bar, $t = 3$ h, $n_{butadiene}:n_{MeOH} = 1$, $n_{butadiene}:n_{Pd} = 10,000$, $n_{TPPTS}:n_{Pd} = 3$, $n_{butadiene}:n_{IL} = 30$, $n_{butadiene}:n_{NEt3} = 300$, $n_{MeOH}:n_{hexane} = 3.22$.*

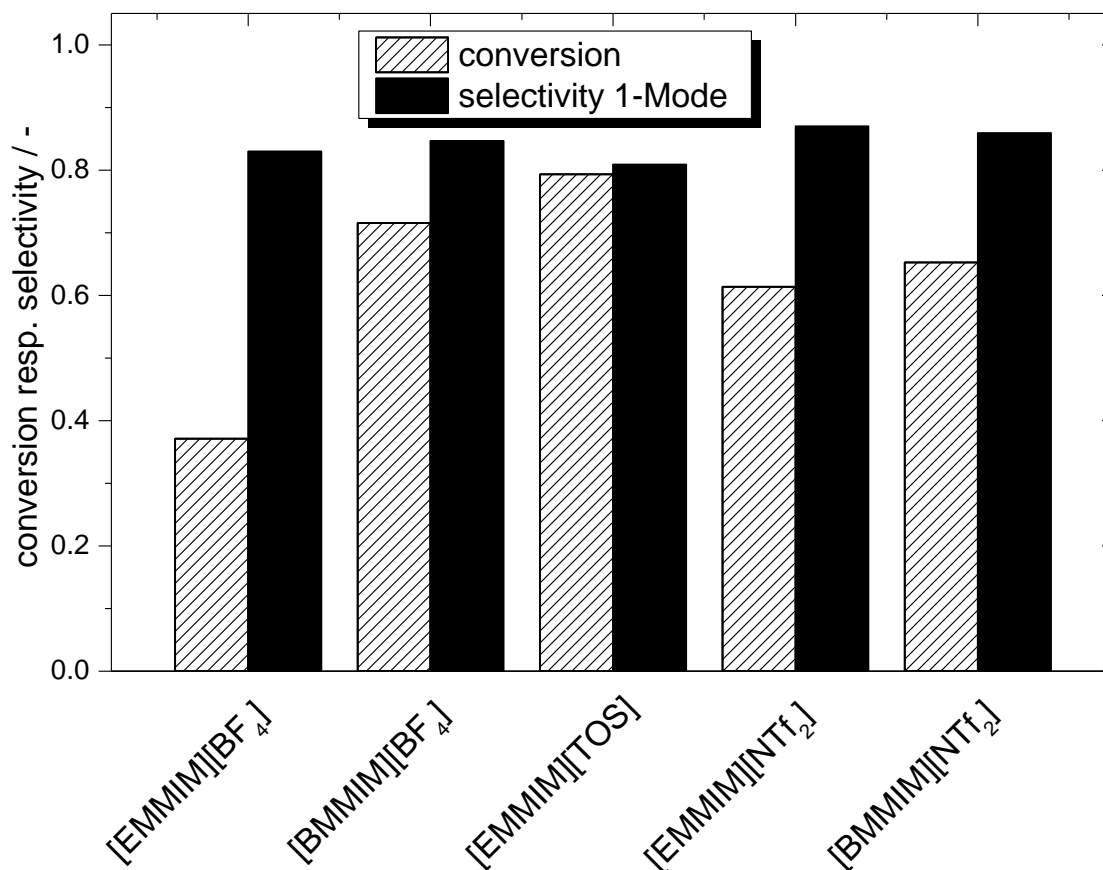**Figure A 10: Obtained conversion and selectivity toward 1-Mode for the screening of different ionic liquids with the [BMMIM]-TPPMS modified catalyst and pure butadiene.**

*Reaction conditions: 70 °C, 15 bar, t = 3 h, $n_{butadiene}:n_{MeOH} = 1$, $n_{butadiene}:n_{Pd} = 10,000$, $n_{[BMMIM]\text{-}TPPMS}:n_{Pd} = 3$, $n_{butadiene}:n_{IL} = 30$, $n_{butadiene}:n_{NEt3} = 300$, $n_{MeOH}:n_{hexane} = 3.22$.*

## 7.8   Characterization of the loop reactor

### 7.8.1   Influence of circulation speed



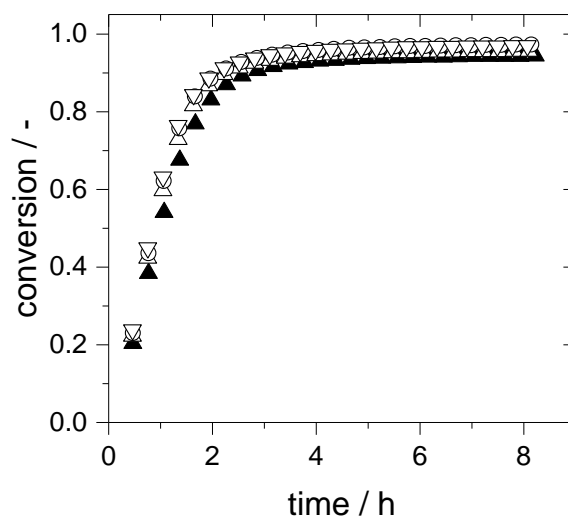**Figure A 11: Influence of circulation speed on the obtained conversion for the Pd-IMes catalyst with sCC$_4$ in the loop reactor (▲ 0.25 l·min$^{-1}$, △ 0.5 l·min$^{-1}$, ○ 1.0 l·min$^{-1}$, ▽ 3.0 l·min$^{-1}$).**

*Reaction conditions: 70 °C, 15 bar, $n_{butadiene}$:$n_{MeOH}$ = 0.5, $n_{butadiene}$:$n_{Pd}$ = 40,000, $n_{Lig}$:$n_{Pd}$ = 4, $n_{butadiene}$:$n_{base}$ = 400.*

## 7.8.2 Determination of the residence time
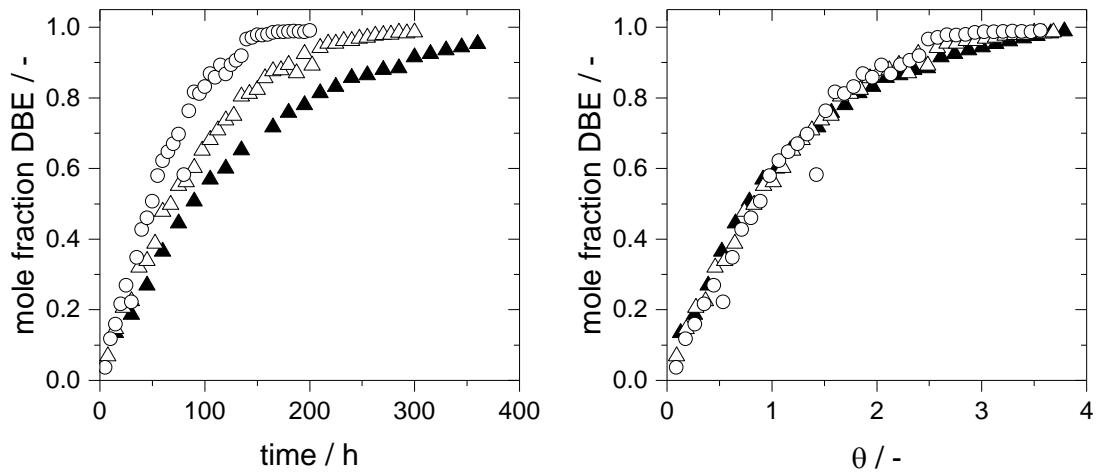


**Figure A 12: Results of the step experiment using dibutylether (DBE) depending on the recorded time *t* (left) and the dimensionless time *θ* (right) for the replacement of ethanol for three different feeding velocities, a circulation speed of 1.0 l·min$^{-1}$ and an opening pressure of 18 bar (▲ 8.2 ml·min$^{-1}$, △ 16.5 ml·min$^{-1}$, ○ 24.7 ml·min$^{-1}$).**



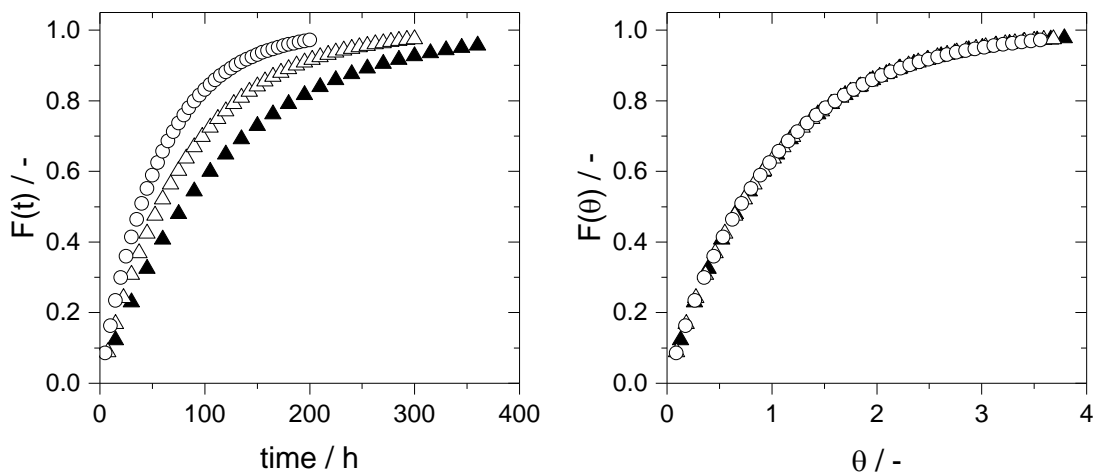**Figure A 13: Calculated summation function according to Equation (26) depending on the recorded time *t* (left) and the dimensionless time *θ* (right) based on the step experiment using dibutylether (DBE) for the replacement of ethanol for three different feeding velocities, a circulation speed of 1.0 l·min$^{-1}$ and an opening pressure of 18 bar (▲ 8.2 ml·min$^{-1}$, △ 16.5 ml·min$^{-1}$, ○ 24.7 ml·min$^{-1}$).**

# 8   References

[1]     A. Jess, P. Wasserscheid, Chemical Technology: An Integral Textbook, 1st ed., Wiley-VCH Verlag GmbH, Weinheim, Germany, **2013**.

[2]     C.C. Tzschucke, C. Markert, W. Bannwarth, S. Roller, A. Hebel, R. Haag, *Angewandte Chemie International Edition*, 41, 3964-4000, **2002**.

[3]     W. Keim, *Angewandte Chemie International Edition*, 29, 235-244, **1990**.

[4]     W. Keim, M. Vogt, P. Wasserscheid, B. Drießen-Hölscher, *Journal of Molecular Catalysis A: Chemical*, 139, 171-175, **1999**.

[5]     I.T. Horváth, J. Rábai, *Science*, 266, 72-75, **1994**.

[6]     B. Cornils, *Angewandte Chemie*, 107, 1709-1711, **1995**.

[7]     B. Cornils, *Angewandte Chemie*, 109, 2147-2149, **1997**.

[8]     R.A. Brown, P. Pollet, E. McKoon, C.A. Eckert, C.L. Liotta, P.G. Jessop, *Journal of the American Chemical Society*, 123, 1254-1255, **2001**.

[9]     M.F. Sellin, P.B. Webb, D.J. Cole-Hamilton, *Chemical Communications*, 781-782, **2001**.

[10]    A. Bösmann, G. Franciò, E. Janssen, M. Solinas, W. Leitner, P. Wasserscheid, *Angewandte Chemie International Edition*, 40, 2697-2699, **2001**.

[11]    Y. Chauvin, B. Gilbert, I. Guibard, *Journal of the Chemical Society, Chemical Communications*, 1715-1716, **1990**.

[12]    H. Olivier, *Journal of Molecular Catalysis A: Chemical*, 146, 285-289, **1999**.

[13]    P. Wasserscheid, W. Keim, *Angewandte Chemie International Edition*, 39, 3772-3789, **2000**.

[14]    P. Wasserscheid, T. Welton, Ionic Liquids in Synthesis, 2nd ed., Wiley-VCH Verlag GmbH, Weinheim, Germany, **2007**.

[15]    W. Keim, *Green Chemistry*, 5, 105-111, **2003**.

[16]    W.A. Herrmann, C.W. Kohlpaintner, *Angewandte Chemie*, 105, 1588-1609, **1993**.

[17]    E. Wiebus, B. Cornils, *Chemie Ingenieur Technik*, 66, 916-923, **1994**.

[18]    C.W. Kohlpaintner, R.W. Fischer, B. Cornils, *Applied Catalysis A: General*, 221, 219-225, **2001**.

[19]    E. Kuntz, Verfahren zur Herstellung von Aldehyden, Rhône-Poulenc Industries, Paris, DE2627354 A1, **1976**.

[20]    B. Cornils, W. Konkol, H. Bach, G. Daembkes, W. Gick, E. Wiebus, H. Bahrmann, Verfahren zur Herstellung von Aldehyden, Ruhrchemie AG, Oberhausen, DE3415968 A1, **1985**.

[21]    R.C. Bohley, G.B. Jacobsen, H.L. Pelt, B.J. Schaart, M. Schenk, D.A. Van Oeffelen, Process for Producing 1-Octene, Dow Benelux N.V., WO 1992010450 A1, **1992**.

[22]    G.B. Jacobsen, H.L. Pelt, B.J. Schaart, Continuous Process for the Telomerization of Conjugated Dienes, Dow Benelux N.V., WO1991009822 A1, **1991**.

[23]    A. Behr, M. Becker, T. Beckmann, L. Johnen, J. Leschinski, S. Reyer, *Angewandte Chemie International Edition*, 48, 3598-3614, **2009**.

[24]    M.J.L. Tschan, E.J. García-Suárez, Z. Freixa, H. Launay, H. Hagen, J. Benet-Buchholz, P.W.N.M. van Leeuwen, *Journal of the American Chemical Society*, 132, 6463-6473, **2010**.

[25]    M.J.L. Tschan, H. Launay, H. Hagen, J. Benet-Buchholz, P.W.N.M. van Leeuwen, *Chemistry – A European Journal*, 17, 8922-8928, **2011**.

[26]    J.R. Briggs, H. Hagen, S. Julka, J.T. Patton, *Journal of Organometallic Chemistry*, 696, 1677-1686, **2011**.

[27]    R. Jackstell, M. Gómez Andreu, A. Frisch, K. Selvakumar, A. Zapf, H. Klein, A. Spannenberg, D. Röttger, O. Briel, R. Karch, M. Beller, *Angewandte Chemie International Edition*, 41, 986-989, **2002**.

[28]    R. Jackstell, A. Frisch, M. Beller, D. Röttger, M. Malaun, B. Bildstein, *Journal of Molecular Catalysis A: Chemical*, 185, 105-112, **2002**.

[29]    R. Jackstell, S. Harkal, H. Jiao, A. Spannenberg, C. Borgmann, D. Röttger, F. Nierlich, M. Elliot, S. Niven, K. Cavell, O. Navarro, M.S. Viciu, S.P. Nolan, M. Beller, *Chemistry – A European Journal*, 10, 3891-3900, **2004**.

[30]    D. Dehn, TU Dortmund, PhD Thesis, **2006**.

[31]    A. Behr, D. Dehn, *Chemie Ingenieur Technik*, 80, 1509-1517, **2008**.

[32]    A. Behr, D. Dehn, *Chemie Ingenieur Technik*, 80, 1775-1783, **2008**.

[33]    L. Magna, Y. Chauvin, G.P. Niccolai, J.-M. Basset, *Organometallics*, 22, 4418-4425, **2003**.

[34]    B.I. Lee, K.H. Lee, J.S. Lee, *Journal of Molecular Catalysis A: Chemical*, 156, 283-287, **2000**.

[35]    B. Blanco, M. Brissart, M. Moreno-Manas, R. Pleixats, A. Mehdi, C. Reyé, S. Bouquillon, F. Hénin, J. Muzart, *Applied Catalysis A: General*, 297, 117-124, **2006**.

[36]    B. Estrine, R. Soler, C. Damez, S. Bouquillon, F. Hénin, J. Muzart, *Green Chemistry*, 5, 686-689, **2003**.

[37]    A.N. Parvulescu, P.J.C. Hausoul, P.C.A. Bruijnincx, S.T. Korhonen, C. Teodorescu, R.J.M. Klein Gebbink, B.M. Weckhuysen, *ACS Catalysis*, 1, 526-536, **2011**.

[38]    F. Benvenuti, C. Carlini, A.M. Raspolli Galletti, G. Sbrana, M. Marchionna, R. Patrini, *Journal of Molecular Catalysis A: Chemical*, 137, 49-63, **1999**.

[39]    F. Benvenuti, C. Carlini, M. Marchionna, R. Patrini, A.M. Raspolli Galletti, G. Sbrana, *Journal of Molecular Catalysis A: Chemical*, 139, 177-187, **1999**.

[40]    B. Estrine, B. Blanco, S. Bouquillon, F. Hénin, M. Moreno-Manas, J. Muzart, C. Pena, R. Pleixats, *Tetrahedron Letters*, 42, 7055-7057, **2001**.

[41]    A. Behr, M. Becker, T. Beckmann, L. Johnen, J. Leschinski, S. Reyer, *Angewandte Chemie*, 121, 3652-3669, **2009**.

[42]    A. Behr, Telomerization of Dienes by Homogeneous Transition Metal Catalysts, in: Aspects of Homogeneous Catalysis, R. Ugo (Ed.), Springer Netherlands, 3-73, **1984**.

[43]    A. Behr, Application of Telomerization and Dimerization to the Synthesis of Fine Chemicals, in: Industrial Applications of Homogeneous Catalysis, A. Mortreux, F. Petit (Eds.), Springer Netherlands, 141-175, **1987**.

[44]    S. Takahashi, T. Shibano, N. Hagihara, *Tetrahedron Letters*, 8, 2451-2453, **1967**.

[45]    E.J. Smutny, *Journal of the American Chemical Society*, 89, 6793-6794, **1967**.

[46]    T.C. Shields, W.E. Walker, *Journal of the Chemical Society D: Chemical Communications*, 193-194, **1971**.

[47]    J. Beger, C. Duschek, H. Reichel, *Journal für Praktische Chemie*, 315, 1077-1089, **1973**.

[48]    J. Beger, H. Reichel, *Journal für Praktische Chemie*, 315, 1067-1076, **1973**.

[49]    R. Palkovits, A.N. Parvulescu, P.J.C. Hausoul, C.A. Kruithof, R.J.M. Klein Gebbink, B.M. Weckhuysen, *Green Chemistry*, 11, 1155-1160, **2009**.

[50]    E. Monflier, P. Bourdauducq, J.-L. Couturier, J. Kervennal, I. Suisse, A. Mortreux, *Catalysis Letters*, 34, 201-212, **1995**.

[51]   E. Monflier, P. Bourdauducq, J.-L. Couturier, J. Kervennal, A. Mortreux, *Journal of Molecular Catalysis A: Chemical*, 97, 29-33, **1995**.

[52]   A. Behr, W. Keim, *Chemische Berichte*, 116, 862-873, **1983**.

[53]   E. Monflier, P. Bourdauducq, J.-L. Couturier, J. Kervennal, A. Mortreux, *Applied Catalysis A: General*, 131, 167-178, **1995**.

[54]   B.I. Lee, K.H. Lee, J.S. Lee, *Journal of Molecular Catalysis A: Chemical*, 166, 233-242, **2001**.

[55]   A. Behr, M. Heite, *Chemical Engineering & Technology*, 23, 952-955, **2000**.

[56]   A. Behr, M. Becker, *Dalton Transactions*, 4607-4613, **2006**.

[57]   A. Behr, K.-D. Juszak, *Journal of Organometallic Chemistry*, 255, 263-268, **1983**.

[58]   W.E. Walker, R.M. Manyik, K.E. Atkins, M.L. Farmer, *Tetrahedron Letters*, 11, 3817-3820, **1970**.

[59]   D. Rose, H. Lepper, *Journal of Organometallic Chemistry*, 49, 473-476, **1973**.

[60]   A. Behr, T. Beckmann, P. Schwach, *Journal of Organometallic Chemistry*, 693, 3097-3102, **2008**.

[61]   J. Beger, F. Meier, *Journal für Praktische Chemie*, 322, 69-80, **1980**.

[62]   A.M. Lazutkin, A.I. Lazutkina, *Reaction Kinetics and Catalysis Letters*, 8, 263-268, **1978**.

[63]   S.M. Maddock, M.G. Finn, *Organometallics*, 19, 2684-2689, **2000**.

[64]   K. Kaneda, H. Kurosaki, M. Terasawa, T. Imanaka, S. Teranishi, *The Journal of Organic Chemistry*, 46, 2356-2362, **1981**.

[65]   A. Grotevendt, M. Bartolome, D.J. Nielsen, A. Spannenberg, R. Jackstell, K.J. Cavell, L.A. Oro, M. Beller, *Tetrahedron Letters*, 48, 9203-9207, **2007**.

[66]   K. Hill, B. Gruber, K.J. Weese, *Tetrahedron Letters*, 35, 4541-4542, **1994**.

[67]   A. Bessmertnykh, F. Hénin, J. Muzart, *Journal of Molecular Catalysis A: Chemical*, 238, 199-206, **2005**.

[68]   C. Hadad, C. Damez, S. Bouquillon, B. Estrine, F. Hénin, J. Muzart, I. Pezron, L. Komunjer, *Carbohydrate Research*, 341, 1938-1944, **2006**.

[69]   J. Mesnager, C. Quettier, A. Lambin, F. Rataboul, C. Pinel, *ChemSusChem*, 2, 1125-1129, **2009**.

[70]   N. Yoshimura, T. Masuhiko, Process for Producing Normal-Octanol, Kuraray Company, Ltd., CA1174246 A1, **1984**.

[71]   P.M. Fritz, H.V. Bölt, *Linde Technology*, 40-47, **2004**.

[72]   W. Kaminsky, M. Arndt-Rosenau, Reactions of Unsaturated Compounds, in: Applied Homogeneous Catalysis with Organometallic Compounds, 2nd ed., B. Cornils, W.A. Herrmann (Eds.), Wiley-VCH Verlag GmbH, Weinheim, Germany, 213-385, **2008**.

[73]   H.A. Wittcoff, B.G. Reuben, J.S. Plotkin, Chemicals and Polymers from Ethylene, in: Industrial Organic Chemicals, 3rd ed., John Wiley & Sons, Inc., Hoboken, NJ, USA, 139-209, **2012**.

[74]   E. Burridge, P. Massoth, *ICIS Chemical Business*, **2007**.

[75]   P.W.N.M. van Leeuwen, M. Tschan, Z. Freixa, H. Hagen, Novel Phosphine-Based Catalysts Suitable for Butadiene Telomerization, Dow Global Technologies LLC, USA, WO2011101504 A1, **2011**.

[76]   A. Behr, P. Neubert, Applied Homogeneous Catalysis, 1st ed., Wiley-VCH Verlag GmbH, Weinheim, Germany, **2012**.

[77]   C. Zörlein, *Linde Technology*, 44-47, **2011**.

[78]   P.W.N.M. van Leeuwen, N.D. Clément, M.J.L. Tschan, *Coordination Chemistry Reviews*, 255, 1499-1517, **2011**.

[79]   A. Bollmann, K. Blann, J.T. Dixon, F.M. Hess, E. Killian, H. Maumela, D.S. McGuinness, D.H. Morgan, A. Neveling, S. Otto, M. Overett, A.M.Z. Slawin, P. Wasserscheid, S. Kuhlmann, *Journal of the American Chemical Society*, 126, 14712-14713, **2004**.

[80]   M.J. Overett, K. Blann, A. Bollmann, J.T. Dixon, D. Haasbroek, E. Killian, H. Maumela, D.S. McGuinness, D.H. Morgan, *Journal of the American Chemical Society*, 127, 10723-10730, **2005**.

[81]   M.J. Overett, K. Blann, A. Bollmann, J.T. Dixon, F. Hess, E. Killian, H. Maumela, D.H. Morgan, A. Neveling, S. Otto, *Chemical Communications*, 622-624, **2005**.

[82]   A.J. Rucklidge, D.S. McGuinness, R.P. Tooze, A.M.Z. Slawin, J.D.A. Pelletier, M.J. Hanton, P.B. Webb, *Organometallics*, 26, 2782-2787, **2007**.

[83]   D.S. McGuinness, M. Overett, R.P. Tooze, K. Blann, J.T. Dixon, A.M.Z. Slawin, *Organometallics*, 26, 1108-1111, **2007**.

[84]   D.S. McGuinness, *Organometallics*, 28, 244-248, **2008**.

[85]   S. Kuhlmann, J.T. Dixon, M. Haumann, D.H. Morgan, J. Ofili, O. Spuhl, N. Taccardi, P. Wasserscheid, *Advanced Synthesis & Catalysis*, 348, 1200-1206, **2006**.

[86]   S. Kuhlmann, C. Paetz, C. Hägele, K. Blann, R. Walsh, J.T. Dixon, J. Scholz, M. Haumann, P. Wasserscheid, *Journal of Catalysis*, 262, 83-91, **2009**.

[87]   J. Botha, C. De Bruyn, E. De Wet, J. Reynhardt, Method of Increasing the Carbon Chain Length of Olefinic Compounds, Sasol Technology, WO2003024910A1, **2005**.

[88]   O. Diels, K. Alder, *Justus Liebigs Annalen der Chemie*, 460, 98-122, **1928**.

[89]   W. Keim, *Angewandte Chemie*, 80, 968-969, **1968**.

[90]   A. Behr, G.V. Ilsemann, W. Keim, C. Krueger, Y.H. Tsay, *Organometallics*, 5, 514-518, **1986**.

[91]   R. Benn, P.W. Jolly, R. Mynott, B. Raspel, G. Schenker, K.P. Schick, G. Schroth, *Organometallics*, 4, 1945-1953, **1985**.

[92]   P.W. Jolly, *Angewandte Chemie*, 97, 279-291, **1985**.

[93]   P.W. Jolly, R. Mynott, B. Raspel, K.P. Schick, *Organometallics*, 5, 473-481, **1986**.

[94]   R. Benn, P.W. Jolly, R. Mynott, G. Schenker, *Organometallics*, 4, 1136-1138, **1985**.

[95]   F. Vollmüller, J. Krause, S. Klein, W. Mägerlein, M. Beller, *European Journal of Inorganic Chemistry*, 1825-1832, **2000**.

[96]   B. Aakermark, S. Hansson, B. Krakenberger, A. Vitagliano, K. Zetterberg, *Organometallics*, 3, 679-682, **1984**.

[97]   B. Aakermark, A. Vitagliano, *Organometallics*, 4, 1275-1283, **1985**.

[98]   J. Krause, G. Cestaric, K.-J. Haack, K. Seevogel, W. Storm, K.-R. Pörschke, *Journal of the American Chemical Society*, 121, 9807-9823, **1999**.

[99]   S.E. Denmark, R.C. Smith, *Synlett*, 18, 2921-2928, **2006**.

[100]  S. Baba, T. Ogura, S. Kawaguchi, *Bulletin of the Chemical Society of Japan*, 47, 665-668, **1974**.

[101]  A.M. Trzeciak, J.J. Ziółkowski, *Coordination Chemistry Reviews*, 249, 2308-2322, **2005**.

[102]  F. Vollmüller, W. Mägerlein, S. Klein, J. Krause, M. Beller, *Advanced Synthesis & Catalysis*, 343, 29-33, **2001**.

[103]  J. Tsuji, *Accounts of Chemical Research*, 6, 8-15, **1973**.

[104]  E.J. Smutny, *Annals of the New York Academy of Sciences*, 214, 125-142, **1973**.

[105]  C.-F. Huo, R. Jackstell, M. Beller, H. Jiao, *Journal of Molecular Modeling*, 16, 431-436, **2010**.

[106]  A. Jabri, P.H.M. Budzelaar, *Organometallics*, 30, 1374-1381, **2011**.

[107]  M. Viciu, S. Nolan, The Use of N-Heterocyclic Carbenes as Ligands in Palladium-Mediated Catalysis, in: Palladium in Organic Synthesis, J. Tsuji (Ed.), Springer Berlin Heidelberg, 241-278, **2005**.

[108]  J. Tsuji, Palladium Reagents and Catalysts: Innovations in Organic Synthesis, John Wiley & Sons, Inc., Chichester, UK, **1995**.

[109]  M.J.L. Tschan, J.-M. López-Valbuena, Z. Freixa, H. Launay, H. Hagen, J. Benet-Buchholz, P.W.N.M. van Leeuwen, *Organometallics*, 30, 792-799, **2011**.

[110]  M. Basato, L. Crociani, F. Benvenuti, A.M. Raspolli Galletti, G. Sbrana, *Journal of Molecular Catalysis A: Chemical*, 145, 313-316, **1999**.

[111]  F. Benvenuti, C. Carlini, M. Lami, M. Marchionna, R. Patrini, A.M. Raspolli Galletti, G. Sbrana, *Journal of Molecular Catalysis A: Chemical*, 144, 27-40, **1999**.

[112]  F. Benvenuti, C. Carlini, M. Marchionna, R. Patrini, A.M. Raspolli Galletti, G. Sbrana, *Journal of Molecular Catalysis A: Chemical*, 140, 139-155, **1999**.

[113]  L. Crociani, G. Bandoli, A. Dolmella, M. Basato, B. Corain, *European Journal of Inorganic Chemistry*, 1811-1820, **1998**.

[114]  M. Camargo, P. Dani, J. Dupont, R.F. de Souza, M. Pfeffer, I. Tkatchenko, *Journal of Molecular Catalysis A: Chemical*, 109, 127-131, **1996**.

[115]  F. Bouachir, P. Grenouillet, D. Neibecker, J. Poirier, I. Tkatchenko, *Journal of Organometallic Chemistry*, 569, 203-215, **1998**.

[116]  H.W. Wanzlick, E. Schikora, *Angewandte Chemie*, 72, 494, **1960**.

[117]  H.W. Wanzlick, H.J. Kleiner, *Angewandte Chemie*, 73, 493, **1961**.

[118]  H.-J. Schönherr, H.-W. Wanzlick, *Justus Liebigs Annalen der Chemie*, 731, 176-179, **1970**.

[119]  W.A. Herrmann, L.J. Goossen, C. Köcher, G.R.J. Artus, *Angewandte Chemie International Edition*, 35, 2805-2807, **1996**.

[120]  H. Kücükbay, B. Cetinkaya, S. Guesmi, P.H. Dixneuf, *Organometallics*, 15, 2434-2439, **1996**.

[121]  H.M. Lee, T. Jiang, E.D. Stevens, S.P. Nolan, *Organometallics*, 20, 1255-1258, **2001**.

[122]  L.D. Vazquez-Serrano, B.T. Owens, J.M. Buriak, *Chemical Communications*, 2518-2519, **2002**.

[123]  S. Díez-González, N. Marion, S.P. Nolan, *Chemical Reviews*, 109, 3612-3676, **2009**.

[124]  M. Moreno-Mañas, R. Pleixats, J. Spengler, C. Chevrin, B. Estrine, S. Bouquillon, F. Hénin, J. Muzart, A. Pla-Quintana, A. Roglans, *European Journal of Organic Chemistry*, 274-283, **2003**.

[125]  B. Cornils, W.A. Herrmann, I.T. Horváth, W. Leitner, S. Mecking, H. Olivier-Bourbigou, D. Vogt, Wiley-VCH Verlag GmbH, Weinheim, Germany, **2005**.

[126]  F. Liu, M.B. Abrams, R.T. Baker, W. Tumas, *Chemical Communications*, 433-434, **2001**.

[127]  A. Behr, M. Urschey, *Journal of Molecular Catalysis A: Chemical*, 197, 101-113, **2003**.

[128]  A. Behr, M. Urschey, V.A. Brehme, *Green Chemistry*, 5, 198-204, **2003**.

[129]  A. Behr, M. Urschey, *Advanced Synthesis & Catalysis*, 345, 1242-1246, **2003**.

[130]  A. Behr, J. Leschinski, *Green Chemistry*, 11, 609-613, **2009**.

[131]  E. Kuntz, Telomerization Process Using Sulfonated Triarylphosphine and Transition Metal, Rhône-Poulenc Industries, Paris, US4142060 A, **1979**.

[132] E. Kuntz, Telomerization Process, Rhône-Poulenc Industries, Paris, US4219677 A, **1980**.

[133] J. Mesnager, E. Kuntz, C. Pinel, *Journal of Organometallic Chemistry*, 694, 2513-2518, **2009**.

[134] R.E. Baltus, R.M. Counce, B.H. Culbertson, H. Luo, D.W. DePaoli, S. Dai, D.C. Duckworth, *Separation Science and Technology*, 40, 525-541, **2005**.

[135] P. Scovazzo, J. Kieft, D.A. Finan, C. Koval, D. DuBois, R. Noble, *Journal of Membrane Science*, 238, 57-63, **2004**.

[136] J. Dupont, R.F. de Souza, P.A.Z. Suarez, *Chemical Reviews* 102, 3667-3692, **2002**.

[137] N. Kaftzik, S. Neumann, M.-R. Kula, U. Kragl, Enzymatic Condensation Reactions in Ionic Liquids, in: Ionic Liquids as Green Solvents, R.D. Rogers, K.R. Seddon (Eds.), American Chemical Society, 206-211, **2003**.

[138] S.H. Schöfer, N. Kaftzik, P. Wasserscheid, U. Kragl, *Chemical Communications*, 425-426, **2001**.

[139] H.K. Farag, F. Endres, *Journal of Materials Chemistry*, 18, 442-449, **2008**.

[140] N. Birbilis, P.C. Howlett, D.R. MacFarlane, M. Forsyth, *Surface and Coatings Technology*, 201, 4496-4504, **2007**.

[141] T. Fukushima, T. Aida, *Chemistry – A European Journal*, 13, 5048-5058, **2007**.

[142] H. Wang, Q. Lu, C. Ye, W. Liu, Z. Cui, *Wear*, 256, 44-48, **2004**.

[143] D. Wei, A. Ivaska, *Analytica Chimica Acta*, 607, 126-135, **2008**.

[144] P.A.Z. Suarez, V.M. Selbach, J.E.L. Dullius, S. Einloft, C.M.S. Piatnicki, D.S. Azambuja, R.F. de Souza, J. Dupont, *Electrochimica Acta*, 42, 2533-2535, **1997**.

[145] D.R. MacFarlane, M. Forsyth, P.C. Howlett, J.M. Pringle, J. Sun, G. Annat, W. Neil, E.I. Izgorodina, *Accounts of Chemical Research*, 40, 1165-1173, **2007**.

[146] J.E.L. Dullius, P.A.Z. Suarez, S. Einloft, R.F. de Souza, J. Dupont, J. Fischer, A. De Cian, *Organometallics*, 17, 815-819, **1998**.

[147] G. Santos Fonseca, R.F. de Souza, J. Dupont, *Catalysis Communications*, 3, 377-380, **2002**.

[148] A. Klamt, G. Schuurmann, *Journal of the Chemical Society, Perkin Transactions 2*, 799-805, **1993**.

[149] M. Diedenhofen, A. Klamt, *Fluid Phase Equilibria*, 294, 31-38, **2010**.

[150] A. Klamt, F. Eckert, *Fluid Phase Equilibria*, 172, 43-72, **2000**.

[151] A. Klamt, Cosmo-Rs: From Quantum Chemistry to Fluid Phasethermodynamics and Drug Design, Elsevier, Amsterdam, Netherlands, **2005**.

[152] C. Jork, C. Kristen, D. Pieraccini, A. Stark, C. Chiappe, Y.A. Beste, W. Arlt, *The Journal of Chemical Thermodynamics*, 37, 537-558, **2005**.

[153] M. Blanco, I. Villarroya, *TrAC Trends in Analytical Chemistry*, 21, 240-250, **2002**.

[154] Y. Roggo, P. Chalus, L. Maurer, C. Lema-Martinez, A.I. Edmond, N. Jent, *Journal of Pharmaceutical and Biomedical Analysis*, 44, 683-700, **2007**.

[155] D.A. Burns, E.W. Ciurczak, Handbook of near-Infrared Analysis, 3rd ed., CRC Press, **2007**.

[156] H. Günzler, H.-U. Gremlich, Ir Spectroscopy - an Introduction, 1st ed., Wiley-VCH Verlag GmbH, Weinheim, Germany, **2002**.

[157] P. Geladi, *Spectrochimica Acta Part B: Atomic Spectroscopy*, 58, 767-782, **2003**.

[158] P. Geladi, B. Sethson, J. Nyström, T. Lillhonga, T. Lestander, J. Burger, *Spectrochimica Acta Part B: Atomic Spectroscopy*, 59, 1347-1357, **2004**.

[159] M. Otto, Chemometrics - Statistics and Computer Application in Analytical Chemistry, 2nd ed., Wiley-VCH Verlag GmbH, Weinheim, Germany, **2007**.

[160] R.G. Brereton, Chemometrics Data Analysis for the Laboratory and Chemical Plant, John Wiley & Sons, Inc., Chichester, UK, **2003**.

[161] D.L. Massart, B.G.M. Vandeginste, S.M. Deming, Y. Michotte, L. Kaufmann, Chemometrics: A Textbook, Elsevier, Amsterdam, Netherlands, **2003**.

[162] E.D. Yalvac, M.B. Seasholtz, M.A. Beach, S.R. Crouch, *Journal of Applied Spectroscopy*, 51, 1565-1578, **1997**.

[163] M. Blanco, S. Maspoch, I. Villarroya, X. Peralta, J.M. González, J. Torres, *Analytica Chimica Acta*, 434, 133-141, **2001**.

[164] A.F. Parisi, L. Nogueiras, H. Prieto, *Analytica Chimica Acta*, 238, 95-100, **1990**.

[165] R. Guchardi, P.A. da Costa Filho, R. Poppi, C. Pasquini, *Journal of Near Infrared Spectroscopy*, 6, 333-339, **1998**.

[166] G. Bohács, Z. Ovád, A. Salgó, *Journal of Near Infrared Spectroscopy*, 6, 341-348, **1998**.

[167] C. Pasquini, A.F. Bueno, *Fuel*, 86, 1927-1934, **2007**.

[168] S. Pinzi, F. Alonso, J. García Olmo, M.P. Dorado, *Fuel*, 92, 354-359, **2012**.

[169] M.H.M. Killner, J.J.R. Rohwedder, C. Pasquini, *Fuel*, 90, 3268-3273, **2011**.

[170] S.M. de Lima, B.F.A. Silva, D.V. Pontes, C.F. Pereira, L. Stragevitch, M.F. Pimentel, *Fuel*, 115, 46-53, **2014**.

[171] J.L. Hopewell, G.A. George, D.J.T. Hill, *Polymer*, 41, 8221-8229, **2000**.

[172] M.J. Strauss, N.M. Prinsloo, *Applied Catalysis A: General*, 320, 16-23, **2007**.

[173] P.B. Webb, M.F. Sellin, T.E. Kunene, S. Williamson, A.M.Z. Slawin, D.J. Cole-Hamilton, *Journal of the American Chemical Society*, 125, 15577-15588, **2003**.

[174] M. Eichmann, RWTH Aachen, PhD Thesis, **1999**.

[175] P. Wasserscheid, M. Eichmann, *Catalysis Today*, 66, 309-316, **2001**.

[176] R.H. Crabtree, The Organometallic Chemistry of the Transition Metals, 4th ed., John Wiley & Sons, Inc., Hoboken, NJ, USA, **2005**.

[177] L. Torrente-Murciano, A. Lapkin, D.J. Nielsen, I. Fallis, K.J. Cavell, *Green Chemistry*, 12, 866-869, **2010**.

[178] L. Hopf, S. Recker, D. Maschmeyer, A. Chartoire, S.P. Nolan, W. Marquardt, M. Haumann, P. Wasserscheid, *in preparation*, **2015**.

[179] D.G. Blackmond, *Angewandte Chemie International Edition*, 44, 4302-4320, **2005**.

[180] J.-M. Chern, F.G. Helfferich, *AIChE Journal*, 36, 1200-1208, **1990**.

[181] K.A.P. McLean, K.B. McAuley, *The Canadian Journal of Chemical Engineering*, 90, 351-366, **2012**.

[182] T. Quaiser, M. Mönnigmann, *BMC Systems Biology*, 3, 50, **2009**.

[183] O. Levenspiel, Chemical Reaction Engineering, Wiley VCH Verlag GmbH, Weinheim, Germany, **1999**.

[184] M. Baerns, A. Behr, A. Brehm, J. Gmehling, H. Hofmann, U. Onken, A. Renken, K.O. Hinrichsen, R. Palkovits, Technische Chemie, Wiley VCH Verlag GmbH, Weinheim, Germany, **2013**.